DEVELOPMENT AND DEPLOYMENT OF A FAECAL MATTER SENSOR FOR MARINE AND FRESHWATER ENVIRONMENTS

by

Ciprian Briciu-Burghina BSc.

Supervisor: Prof. Fiona Regan

School of Chemical Sciences

Dublin City University

Thesis Submitted for the Degree of Doctor of Philosophy

January 2016

DECLARATION

I hereby certify that this material, which I now submit for assessment on the programme of study leading to the award of PhD, is entirely my own work, that I have exercised reasonable care to ensure that the work is original, and does not to the best of my knowledge breach any law of copyright, and has not been taken from the work of others save and to the extent that such work has been cited and acknowledged within the text of my work.

Signed:_____

ID No.:_____

Date:_____

Ciprian Briciu-Burghina BSc.

For my parents and Raul

"We can use our scientific knowledge to improve and beautify the earth, or we can use it to ...poison the air, corrupt the waters, blacken the face of the country, and harass our souls with loud and discordant noises, [or]...we can use it to mitigate or abolish all these things."

~ John Burroughs

ACKNOWLEDGEMENTS

Firstly I would like to thank my supervisor Professor Fiona Regan for her consistent support and guidance that she has given me throughout my project and for the many opportunities she has afforded me. For believing in me and for being a great mentor.

I thank the ATWARM Marie-Curie actions Research Fellowship Programme without which I would not have been able to pursue my research and to all the ATWARM and QUESTOR fellows.

I would like to thank everyone in the School of Chemical Sciences in DCU, especially the technical staff, who were always helpful and accommodating. I would like to thank everyone in the Water Research Group in DCU especially those in X154 and X152 for the continued support and for putting up with me.

I must say a huge thank you to all my postgrad friends for all the support during my time in DCU, Louise, Lisa, Dian, Tim, James, Niall, Alan, Gillian, Maria, Jaime, Ivan, thank you all guys. Thanks for being there throughout the highs and lows.

Special thanks to Larisa for being a great friend.

Special thanks to Brendan, for the 4 a.m. field trips, for being a great friend and for being an engineer.

I would also like to thank my family for their support and encouragement.

Finally, and most importantly, I would like to thank Saorla for love, patience, support, and for constantly believing in me.

CONTENTS

LIST OF TABLES

LIST OF FIGURES

LIST OF ABBREVIATIONS AND ACRONYMS

- **3-CU:** 7-hydroxyxoumarin-3-carboxylic acid
- **3-CUG**: 3-carboxy-umbelliferyl-β-D-glucuronide
- **4-MU:** 4-methyl umbelliferone
- **4-MUG:** 4-methyl-umbelliferyl-β-D-glucuronide
- **6-CMU:** 6-chloro-4-methyl-umbelliferone
- **6-CMUG:** 6-chloro-4-methyl-umbelliferyl-β-D-glucuronide
- **AWACCS:** Automated Water Analyser Computer Supported System
- **AWISS:** Autonomous Wireless In-Situ Sensor
- **BB:** Bug Buster® protein extraction reagent
- **CL:** CellLytic^{TM} B Cell Lysis Reagent
- **BWD:** Bathing Water Directive
- **DMSO:** Dimethyl Sulfoxide
- **DTT:** 1,4- dithiothreitol
- **DWD:** Drinking Water Directive
- **EIA:** Enzyme ImmunoAssay
- **EIS:** Electrochemical Impedance Spectroscopy
- **EPA:** Environmental Protection Agency
- **ESP:** Environmental Sample Processor
- **FC:** Faecal Coliforms
- **FIB**: Faecal Indicator Bacteria
- **FISH:** Flouresent In-Situ Hybridisation
- **FPEDD:** Flouresent Paired Emitter Detector
- **FS:** Faecal Streptococci
- **GC:** Gas Chromatography
- **GPRS:** General Packet Radio Service
- **GSM:** Global System for Mobile communications
- **GUS :** β-D-Glucoronidase
- **HPC:** Hetrotrophic Plate-Count
- **IFA:** ImmunoFluorescence Assay
- **LTP**: Lauryl- Tryptose Broth
- **MALS:** Multi-Angle Light Scattering
- **MEMS:** Micro Electro-Mechanical Machines

- **MF:** Microfiltration
- **MPN:** Most Probable Number
- **MS:** Mass Spectrometry
- **MST:** Microbial Source Tracking
- **MTF:** Multiple Tube Fermentation
- **MUD:** 4-Methylumbelliferyl β-D-Galactopyranoside
- **NDSB:** Non Detergent Sulfobetaine 201
- **OB:** Optical Brightener
- **ONGP**: Ortho-nitrophenyl-b-D-galactopyranoside
- **P-40:** Nonidet® P-40 Substitute
- **PCR:** Polymerase Chain Reaction
- **PELB:** Bacterial PE LB™
- **PFGE**:Pulse-Field Gel Electrophoresis
- **PES**: Polyethersulfonate
- **QD**: Quantum Dot
- **RIANA:** River ANAlyser
- **SFCA:** Corning® syringe filters with cellulose acetate surfactant free membrane
- **SPR:** Surface Plasmon Resonance
- **TC:** Total Coliforms
- **TSA**: Tripyicase Soy Agar
- **TTC:** Thermo-Tolerant Coliforms
- **UHF:** Ultra High Frequency
- **USEPA:** United States EPA
- **VBNC:** Viable But Not Culturable
- **VC:** Viable Culturable
- **WFD:** Water Framework Directive
- **WIMAX:** Worldwide Interoperability for Microwave Access

ABSTRACT

Development and deployment of a faecal matter sensor for marine and freshwater environments

Ciprian Briciu-Burghina

There is currently great interest in monitoring the microbiological quality of bathing waters and ensuring the safety of users. The European Bathing Water Directive 2006/7/EC which came into place in 2011 sets strict new standards for the classification of bathing waters. Ability to rapidly test microbiological quality of bathing waters is a powerful tool for meeting water quality standards and guidelines, risk assessment and management systems. Real-time and on-line monitoring are key factors for consideration in current method developments for continuous indicator organism assessment to meet early warning requirements and water safety plans. The aim of this work is to address the need for tests capable of rapid *on-site* and *in-situ* assessment of microbiological water quality. To achieve an active management of bathing areas and to reduce the risk associated with the presence of faecal pollution, such tests are essential.

In the 1st part of this thesis, commercial *in-situ* sensors are used to collect continuous high frequency water quality data for a period of 7 months in Dublin Port. These data are used to identify pollution hot-spots at the site and coupled with data collected from discrete samples it is shown that continuous monitoring can be used as a decision support tool.

In the 2nd part, the thesis looks at developing a rationale for monitoring water for biological contamination and follows by establishing a proposed sensor technology based on a bacterial marker enzyme and fluorescence optical detection. A novel protocol for the recovery and detection of faecal pollution indicator bacteria, *E. coli*, using β-glucuronidase (GUS) activity is developed. The developed protocol involves two main steps: sample preparation and GUS activity measurement and has a time–to-result of less than 75 min.

1 INTRODUCTION

1.1 Faecal pollution

Water pollution is a major problem worldwide and has great negative and far reaching consequences for human health as well as aquatic and terrestrial life. In the recent years, the quality of both drinking and bathing/recreational waters constitutes one of the major concerns for governments in the world, in part due to frequent contamination of coastal and inland water resources by waterborne bacterial, viral and protozoan pathogens. Waterborne diseases result from the ingestion of water contaminated by faecal material or urine (especially of mammalian origin) that contains pathogenic microorganisms, such as *Bacillus dysenteriae*, *Giardia sp.*, *Cryptosporidium sp.*, *Campylobacter*, *Salmonella*, *Shigella*, *Yersinia*, *Aeromonas*, *Pasteurella*, *Francisella*, *Leptospira*, Vibrio, some protozoa and several virus groups [1-3]. This faecal material can originate from point source discharges such as raw sewage, storm water, effluent from wastewater treatment plants and other agricultural, industrial and municipality wastes [1, 4].

Annually, waterborne diseases like cholera, dysentery, typhoid and shigellosis affect and even kill millions of people, making faecal pollution one of the biggest threats to human health [5-7]. Aggravating such outbreaks is the lack of efficient continuous water monitoring methods, overloaded wastewater treatment systems, and expensive and laborious methods of detection for the supposedly early warning system. In these conditions, faecal pollution remains a major challenge for public service providers, both in developing and developed countries, but also for the scientific community, where great deal of research is done towards the development of real-time detection and efficient routine early warning systems for faecal pollution.

Since the pathogens causing waterborne diseases appear intermittently in natural waters at low concentrations, detection and quantification of each pathogenic bacterium will be highly labour-intensive, time-consuming and hard to perform for most cases. In this respect, water analyses for faecal pollution are based on detection of conventional (microbiological) and alternative (chemical, physical) faecal indicators.

1.2 Indicators of Faecal Pollution

The majority of pathogens responsible for faecal pollution require long periods of time for the detection (up to weeks) [8, 9], by which time the water would already have been used. Therefore, in order to provide more efficient detection methods and prevent health hazards, indicator parameters for faecal pollution are employed. Although in the past years these parameters were overwhelmingly based on indicator organisms, currently alternative indicators including chemical and physical parameters are used [1]. The ideal indicator for faecal pollution should be in direct relationship with the faecal pollution and must be rapidly, easily, reliably and cheaply detectable. Although the reality of such an ideal indicator is questionable, new molecular-based techniques have shown that by combining the use of conventional and alternative indicators for faecal pollution, increases in both the detection sensitivity and specificity of faecal pollution and associated pathogens are obtained [1].

The following sections present the most commonly used surrogates employed for identifying sources of faecal contamination, as such microbiological, chemical and physical indicators. A short description of each indicator class is provided, along with some particular examples, advantages and disadvantages of each class.

1.2.1 Microbiological Indicators

Organizations associated with environmental protection like the Environmental Protection Agency (EPA), The World Health Organization (WHO) and many other governing agencies identified several microorganisms, commonly referred to as indicator organisms, to use as markers for the possibility of pathogen presence. Indicator microorganisms are routinely used for the assessment of the potential presence/absence of pathogens in water for several reasons. First, they are more numerous in the faecal material than are the pathogens, making them an easier target. Second they are more time and cost-effective to measure because they serve as surrogates for measurement of many different bacterial, viral and protist pathogens known to cause waterborne illness. Moreover, indicator organisms are easier to detect when compared with some pathogens, such as the virus causing hepatitis (Hepatitis A virus) [10, 11].

An ideal indicator organism for faecal contamination must be present whenever enteric pathogens are present and should be at least as resistant as the pathogens to environmental conditions and to disinfection. In addition, it should be a member of the intestinal microflora of warm-blooded animals, should present inability to multiply outside the intestinal tract and allow simple, trustworthy and cheap detection methodologies [2, 12, 13]. Because of such properties, when these indicators are detected they signal the potential presence of pathogens and consequently a health hazard.

However, the ecological and survival characteristics of bacterial, viral and parasitic pathogens might vary significantly under different environmental conditions. This is an indication that no single indicator organism can predict the presence of all enteric pathogens for all types of waters and different host-associated faecal pollution. For this reason, various types of indicator organisms are used which vary in specificity and suitability for different environments.

Some of the most widely employed faecal indicators are shown below:

1.2.1.1 Total coliforms (TC)

Total coliforms are a subset of the family Enterobacteriaceae within which species like *E. coli, C. freundii and K. pneumoniae* are found [3].The coliform group is made up of aerobic and facultative anaerobic, gram-negative, non-spore forming, rod-shaped bacteria that produce gas upon lactose fermentation within 48 hours at 35 °C [3]. Coliforms come from the same sources as pathogenic organisms but are easier to identify, as they are usually present in larger numbers than more dangerous pathogens. Moreover, total coliforms respond to the environment, wastewater treatment, and water treatment similarly to many pathogens. As a result, the number of total coliforms has been a widely accepted as an indicator system. Nevertheless, the TC method presents several limitations. Most members of the coliform group regrow on natural surface and drinking water distribution systems and their concentration depend on the physio-chemical conditions of the water environment [14].Thus, eutrophic tropical waters will contain high concentrations of coliform bacteria. Although used as an indicator, mainly for drinking water, TC are not specific for faecal pollution.

1.2.1.2 Faecal coliforms (FC)

Faecal coliforms are the group of the total coliforms that are considered to be present specifically in the gut and faeces of warm-blooded animals. Because the origins of faecal coliforms are more specific than the origins of the more general total coliform group of bacteria, faecal coliforms are considered a more accurate indication of animal or human waste than the total coliforms. Studies have not shown a relationship between Faecal coliforms (including *Klebsiella* as well as *Escherichia*) and gastrointestinal illnesses [10, 11].Thus, depending on the on local conditions, alternative more specific indicators may be required.

1.2.1.3 *Escherichia coli* (*E. coli*)

Escherichia coli are gram-negative, thermo-tolerant, coliform bacterium commonly found in the lower intestine of warm-blooded animals. Its optimal growth temperature is 39 °C; however, it has been shown to reproduce in temperatures reaching 49 °C [15]. *E. coli* is rod-shaped and is commonly about 1.5 – 2.0 μm long (Fig. 1-1) and weight approximately 1.2 x 10^{-12} g, of which approximately 70% is water.

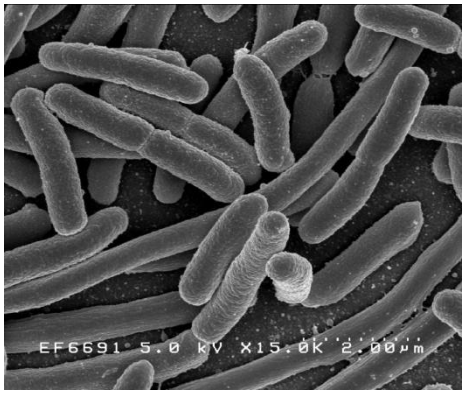

Figure 1-1 Scanning electron microscopy image of *E. coli*. Reproduced from Rocky Mountain Laboratories – Images collection, NIAID, NIH.

Dissolved within the bacteria are nucleic acids like deoxyribonucleic acid (DNA) and ribonucleic acid (RNA) as well as thousands of different proteins. A complex, multi-layered structure shown in Fig. 1-2 serves to protect the dissolved solutes and to add shape and rigidity to *E. coli* cell [16]. The first layer is a phospholipid bilayer called the cytoplasmic membrane, which serves as a highly selective permeability barrier. The purpose of this membrane is to keep the dissolved ions in and unwanted solutes out. Within the cytoplasmic membrane are integral membrane proteins, which either serve as enzymes involved in bioenergetic functions or as transporters of substances in and out of the shell. Outside the cytoplasmic membrane is a layer of peptidoglycan that forms the rigid portion of the cell wall. Surrounding the peptidoglycan in gram-negative cells is the periplasm, which often houses proteins including hydrolytic enzymes. Finally, on the exterior of the gram-negative cell is a semi-permeable outer membrane. The lipid-polysaccharide (LPS) based outer membrane is attached to the periplasm with the lipoprotein complex. Although the primary function of the outer membrane is structural, it also serves to pass small molecules into the cell through proteins known as porins [16].

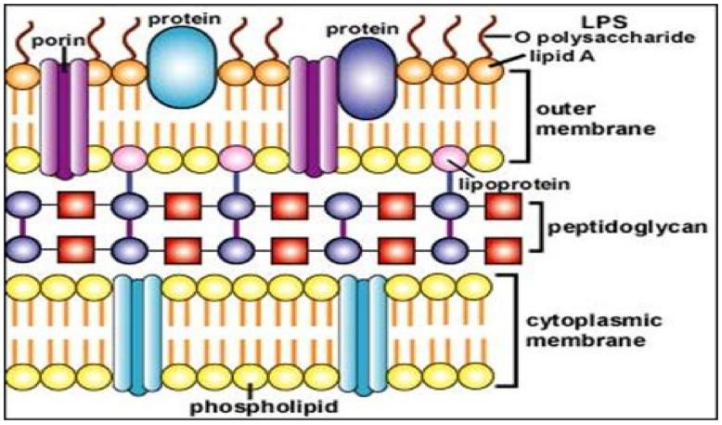

Figure 1-2 Diagram of a gram-negative bacteria cell wall which is typical of *E. coli* cells. Reproduced from [16].

E. coli is the major species in the faecal coliform group. Of the five general groups of bacteria that comprise the total coliforms, only *E. coli* is generally not found growing and reproducing in the environment. Consequently, *E. coli* is considered by many environmental organizations to be the species of coliform bacteria that is the best indicator of faecal pollution and the possible presence of pathogens. Although the majority of *E. coli* strains are harmless, some like the O157:H7 strain, produce Shiga-like toxins, which can lead to illness or death [3].

1.2.1.4 Faecal streptococci (FS)

Faecal streptococci (FS) are gram-positive, catalase-negative cocci, belonging to the genera *Streptococcus* and *Enterococcus*. These bacteria are spherical and grow in chains. They are primarily found only in the faeces of warm-blooded animals but it is now under- stood that some subtypes of this group might be associated with insects. They are now little used as indicator bacteria. The recognition that the faecal streptococci numbers in animal faeces was considerably higher than that for faecal coliforms, caused the presumption that the ratio of their numbers relative to each other (FC/FS) in a water sample would be an indication of the source of faecal contamination (human vs animal) [17, 18]. It has since been abandoned because of the recognition that the die-off rate of the various species and sub-species of faecal streptococci are quite different, some being even greater than that of the faecal coliforms.

1.2.1.5 Enterococci

Enterococci are a subgroup of faecal *Streptococcus* and they are gram-positive cocci. They survive in salt water and are more human specific than the rest of the Faecal *Streptococcus* group. They are recommended by the US EPA and European EPA for use as a faecal indicator in recreational salt-waters and can also be used in freshwater.

1.2.1.6 Clostridium perfringens

Clostridium perfringens are anaerobic sulphite-reducing spore-forming gram-positive rods. They originate exclusively from faeces where they are present in lower numbers than faecal coliforms or faecal enterococci [1, 19]. However, *Clostridium perfringens* survive longer in water than *E. coli* or Streptococci. If they can be cultured from a water sample, but faecal coliforms and faecal enterococci cannot be, its presence indicates: either "remote" faecal pollution, i.e. pollution that has occurred at some point in the past but since then FC and Enterococci have died, but not the spores of *Clostridium perfringens*; or faecal pollution in the presence of industrial wastewater toxins which killed or inhibited faecal coliforms and faecal enterococci, but not the spores of *Clostridium perfringens*. Thus, in general *Clostridium perfringens* are used only when FC or faecal enterococci cannot be detected or when industrial wastes are present [19]. However, they are not useful indicators for the determination of faecal pollution in recreational waters as they can be re-suspended from sediments causing false positives in detection long after a pollution event.

1.2.1.7 Bifidobacteria

Bifidobacteria are gram-positive anaerobic rods found in human and animal faeces. They are considered useful indicators in the tropics as they won't multiply outside the gut. They are not widely used as they have a short survival time in the environment and are difficult to detect [1].

1.2.1.8 Rhodococcus

Rhodococcus is an anaerobic bacteria sourced exclusively in farm animal faeces. It survives longer in water than other indicators. It has been used as an indicator of farm animal pollution but it is slow to detect taking 17-18 days to obtain a result [1].

1.2.1.9 Clostridium Heterotrophic Plate Count Bacteria

Heterotrophic plate count (HPC) bacteria are aerobic or facultative anaerobic gram-negative bacteria. They are non-specific as they can arise in vegetation as-well as sewage and can multiply in the environment. Therefore they are not a direct indicator of faecal pollution but can be used as an indicator of water quality [1, 20].

Alternative faecal indicators such as faecal anaerobes (e.g. *Bacteroides*), viruses (e.g. *B. fragilis* phage, coliphages (e.g. FRNA phage)), Enteroviruses, *Pseudomonas aeruginosa*, *Candida albicans* have also been proposed [1, 20]. However, their use is of small extent and they have not been implemented as indicators in any legislations related with water quality.

1.2.2 Chemical Indicators

Currently, the quality of drinking and recreational waters is estimated through the measurement of faecal bacteria such as *Escherichia coli* and Enterococci. However, since it takes time for the microorganisms to grow and be detected, their utility as indicators of human faecal contamination and their ability to minimize contact with contaminated waters is limited (by the time you get results, people will have long been in contact with the contaminated water). Moreover, most microbial indicators are not suitable for monitoring faecal pollution in some tropical and temperate regions because they could multiply or be part of the natural flora [1]. In these conditions, more flexible and reliable techniques are required [21]. Therefore, certain chemical indicators associated with faecal pollution have been proposed:

1.2.2.1 Faecal Sterols

Faecal sterols could be used as alternative indicators of faecal contamination [22-24]. Animal faeces contain considerable amount of faecal sterols. From these, coprostanol is one of the major faecal sterols excreted by humans and animals. Under aerobic conditions coprostanol could be microbially degraded in water column having half-lives of less than 10 days at 20 °C [23]. Based on this, presence of coprostanol in aquatic environments suggests the presence of relatively fresh faecal pollution. Thus, the coprostanol measurement has been proposed as a powerful tool for monitoring fresh faecal pollution in tropical regions of Japan, Malaysia and Vietnam [23, 25]. Detection

however requires analysis by a gas chromatography – mass spectrometry (GC–MS), an expensive and complex technique [23].

1.2.2.2 Urobilins

Urobilins are a product of intestinal microflora, specific to mammals. Detection requires high performance liquid chromatography (HPLC) a complex technique which limits their usefulness as an indicator [20].

1.2.2.3 Hydrogen sulfide (H2S)

Hydrogen sulfide is produced by faecal bacteria including: *Citrobacter, Enterobacter, Salmonella, Clostridium perfringens* and can be detectable using simple inexpensive colour-change chemistry [26, 27]. H_2S production is detected by formation of black iron sulphide precipitate on the strips or in the medium where the samples are incubated (18-24 h). Different versions and media for H_2S tests exist and the method is not standardised world-wide. The H_2S paper strip test is popular especially in locations with poorly resourced nations as its cost are a lot less expensive that of standard coliform tests. The H_2S tests can be used for qualitative detection (presence/absence (P/A)), or semi quantitatively by measuring the time taken to change colour. Accuracy and specificity are variable. However, the time of analysis between 18 and 24 h does not allow the required early warning system. In addition, the method is not specific to human coliforms and therefore unreliable when used in other water bodies that have other sources of coliforms e.g. decomposing organic matter [27].

1.2.2.4 Other chemical indicators

Other chemical indicators from a variety of classes, such as those which are produced and excreted by humans (bile acids and aminoacetone [28]), those which are ingested nearly exclusively by humans (certain pharmaceuticals (Chlorpropamide, Phensuximide and Carbamazepine, Seiler *et al.*. 1999), caffeine, nicotine), and those which can enter the human waste stream (surfactants, fluorescent whitening agents, musks) have all been individually suggested for use as chemical indicators of human faecal contamination [1]. Most of the published studies did not investigate if there were a relationship between the concentrations of the compounds and illnesses caused by human faecal material, or even to compare the concentrations of the chemical indicators to the microbial ones, so there is no measure of the utility of the compounds to act as

indicators. Detection methods for chemical indicators rely mostly on expensive techniques such as GC-MS and HPLC [29-31].

1.2.3 Physical and optical indicators

At present, traditional methods used to monitor the concentrations of faecal-indicator bacteria (such as *E. coli* and faecal coliforms) in the water take at least 18 hours to obtain results. The elapsed time between the occurrence of elevated faecal-indicator bacteria concentrations in recreational waters and their detection is too long to assess water quality and take adequate control measures. This is especially true in rivers and other complex environments like estuaries, where decay, dilution, dispersion, and transport of faecal-indicator bacteria can cause concentrations to change greatly over short periods of time. In these conditions, a number of physical and optical parameters can be used to infer the presence of pollution in water, but not necessarily identify it. These can be used to monitor conditions and trigger more specific testing to identify and or quantify the pollution.

1.2.3.1 Turbidity

From these parameters, turbidity has attracted major attention and has been employed as an early indicative system of faecal pollution. Turbidity is a simple and direct optical measurement, which quantifies particulate matter suspended in water. Several predictive models based on turbidity and rainfall measurements have been developed [32, 33]. It was found that for particular water environments, turbidity measurements, although not entirely specific to faecal pollution, might be able to provide reliable results of the current day's faecal-indicator bacteria concentrations (Fig. 1-3). Moreover, it was found that when compared to the traditional method of determining the current day's conditions based on the previous day's bacterial count, turbidity model predicted conditions correctly more often: 77 percent compared to 74 percent of the time for the traditional method. Although the specificity of the model was lower than that of the traditional method, the sensitivity of the turbidity model was greater, demonstrating that the model could be successfully used for predicting water quality especially in the case of rivers or recreational waters [33]. Turbidity can be used to detect a change in the environment but not to quantify pollution.

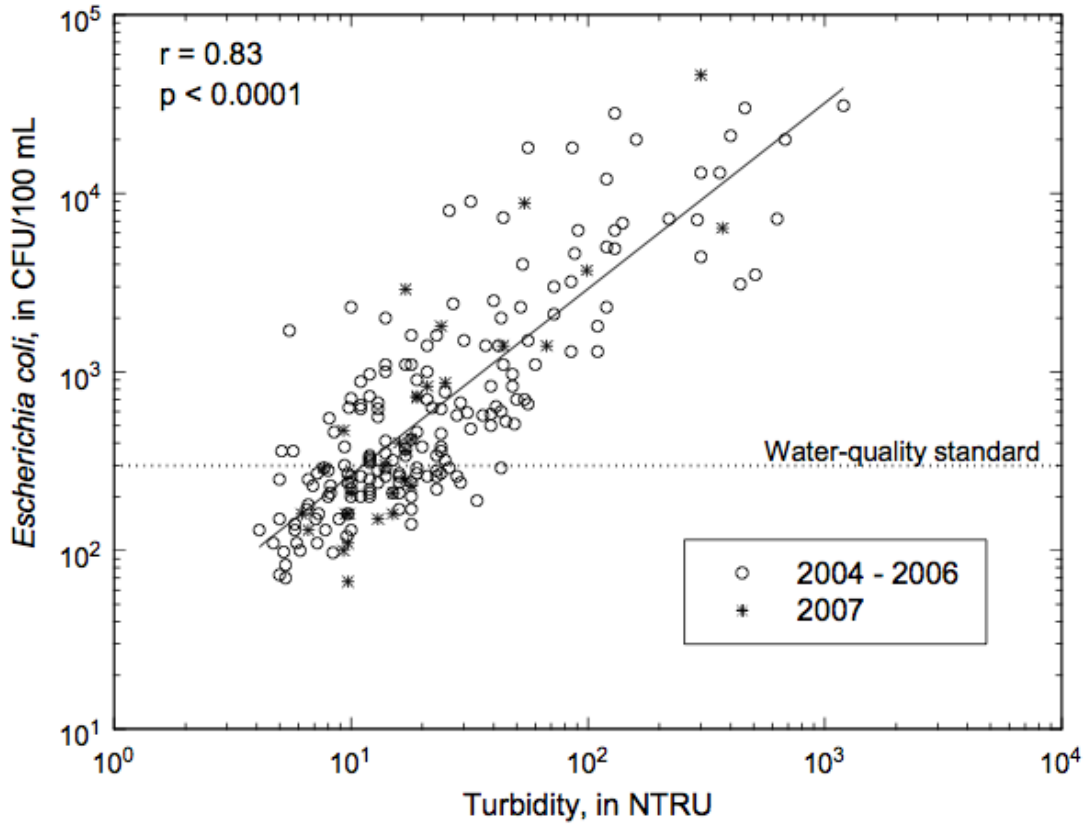

Figure 1-3 Relationship between *Escherichia coli* concentrations and turbidity obtained at Jaite, Cuyahoga Valley National Park, Ohio, during the recreational seasons (May through August) of 2004 through 2007. The solid line indicates the best-fit line. [r = Pearson's correlation coefficient; p = significance of the relation; CFU/100 mL = colony-forming units per 100 milliliters; NTRU = nephelometric turbidity ratio units]. Reproduced from [33].

1.3 Detection Methods for *E. coli*

As mentioned before, *E. coli* is considered by many legislation organisms, dealing with water quality, to be the best indicator for faecal pollution. A variety of techniques for the determination and quantification of *E. coli* indicator organisms exist. These techniques can be subdivided into cultural, molecular, and enzymatic methods [3, 34]. These classes tend to overlap as improvements have led to combinations of methods from different classes to increase the sensitivity, and reduce the amount of labour and time required for water sample analyses. In recent years a new category, biosensors, has attracted major attention, developed in the attempt of producing rapid, cost-effective and automated detection of faecal pollution indicators.

1.3.1 Culture-based Methods

Membrane filtration (MF) and multiple tube fermentation (MTF) or the most probable number (MPN) techniques are the commonly used culture based methods.

1.3.1.1 Membrane filtration (MF)

Membrane filtration (MF) or culture and colony-count consist of filtering a water sample through a sterile filter with a 0.45 μm pore size to concentrate and entrap bacteria. The membrane filter is then layered on selective agar, incubated at 35 to 37 °C for total coliforms to grow. The coliform colonies are observed after 18 – 24 h (Brenner *et al.* 1993, 3534-3544; Grabow 1996, 193-202; Van Poucke and Nelis 2000, 233-244). The counting of typical colonies formed on the filter is done using ocular methods. Turbid samples may prevent filtration of large volumes of water leading to limited sensitivity and sample volumes to be analysed.

1.3.1.2 Multiple tube fermentation (MTF)

The technique of enumerating coliforms by means of multiple-tube fermentation (MTF) has been used for over 80 years as a water quality monitoring method. In the MTF technique, tubes with media (e.g. lactose broth, lauryl sulphate broth), or with additional selective compounds for coliforms (e.g. sodium azide, cefsulodin and bile acids) are inoculated with appropriate decimal dilutions of the water sample [3]. Production of gas, acid formation or abundant growth in the test tubes after 48 h of incubation at 35 °C constitutes a positive presumptive reaction. The results of the MTF technique are expressed in terms of the most probable number (MPN) of micro-organisms present. This number is a statistical estimate of the mean number of coliforms in the sample. As a consequence, this technique offers a semi-quantitative enumeration of coliforms. Nevertheless, the precision of the estimation is low and depends on the number of tubes used for the analysis. The disadvantage of the MTF technique, as opposed to MF, is that it does not allow for the analysis of large volumes of water and sample numbers. The method can become very tedious, time-consuming (at least 48 hours required for a positive result) and labour-intensive since many dilutions have to be processed for each water sample. However, this technique remains useful, especially when the conditions do not allow the use of the membrane filter technique, such as turbid or coloured waters.

1.3.1.2.1 Limitations

Although culturing techniques are very sensitive and selective [3], they might underestimate microbial counts since they cannot detect viable but non culturable (VBNC) cells. Cells become non-culturable or fail to grow due to stress induced by lack of nutrients in most water bodies and injury suffered during treatment [3, 35]. Another important drawback is the long time required for sample analysis, mostly due to the fact that microbial growth cannot be accelerated during culturing. Consequently, retrospective results are inevitable when using these methods. This presents a health hazard, since the water would already have been used before the microbial quality is established. Thus the need for efficient and timely techniques for the detection of faecal pollution in aquatic environments is crucial [3].

1.3.2 Molecular based methods

Molecular methods have been developed to increase the rapidity of analysis through the elimination of the time-consuming culturing/growth step. Some of these methods permit the detection of specific culturable and/or non-culturable bacteria within hours, instead of the days required with the traditional methods. Molecular methods can be classified into immunological and nucleic acid (NA)-based methods. Several molecular methods applied to the specific detection of coliforms in waters are discussed here.

Immunological-based methods take advantage of the specificity of antibody-antigen interactions in techniques such as enzyme linked immunosorbent assay (ELISA), immunofluorescent assay (IFA) and immunoblotting. Nucleic acid based methods comprise NA hybridisation, polymerase chain reaction (PCR) and the use of genetically modified bacteriophages [that express genes (e.g. *lux*) in specific hosts in the environment] [3, 36-38].

1.3.2.1 Immunological-based techniques

Immunological methods are based on the specific recognition between antibodies and antigens and the high affinity that is characteristic of this recognition reaction. Consequently, the properties of the antigen-antibody complex can be used to perform an immunocapture of cells or antigens by enzyme-linked immunosorbent assay (IMS or ELISA), or to detect targeted cells by immunofluorescence assay (IFA) or immuno-enzyme assay (IEA). Various forms of ELISA namely: direct [direct labelled antibody

(Ab)/antigen (Ag)]; indirect; sandwich (direct/direct); competition (direct/indirect Ab competition and direct/indirect Ag competition) together with multiple variations of each method have been demonstrated [39]. As an example, the principle of direct labelled Ab ELISA is illustrated in Fig. 1-4. In this approach, enzyme-labelled antibodies are bound to the antigen immobilized to a support material and will remain attached to the antigen during washing of the unbound antibodies. When the chromogenic/fluorogenic substrate is added to the experimental sample, the enzymes will catalyze the breakdown of the substrates and occurrence of colour or fluorescence indicates the presence of the microorganism in question [39].

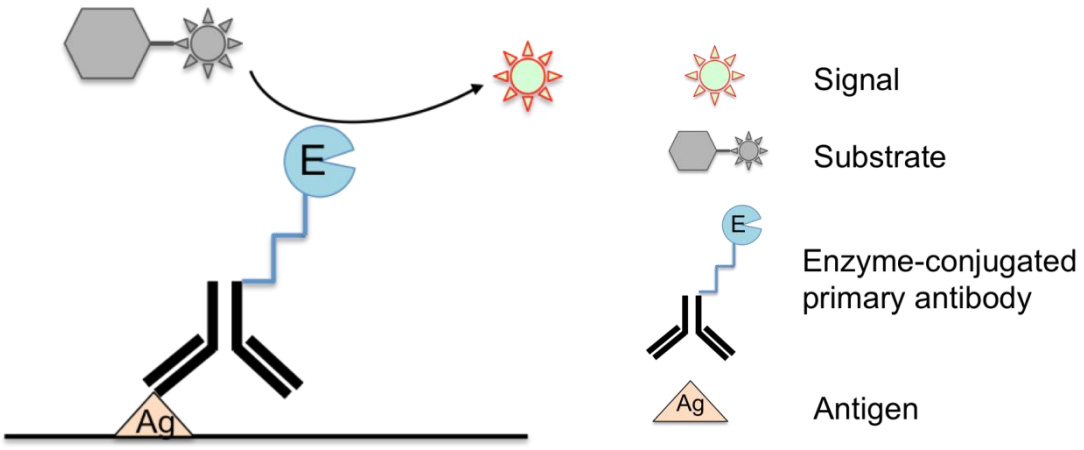

Figure 1-4 Illustration of a direct labelled antibody ELISA.

The specific antigens can be immobilized on a variety of supports ranging from conventional well plates to magnetic beads [40], filter-membranes [41], capillary columns [42], or directly on the transducer‘s surface [41] while the end product can be detected through optical absorbance [40, 42], surface plasmon resonance [40], chemiluminescence [40, 43], or amperometry [44]. The variety of immunological-based methods and their modifications/improvements is however overwhelming and beyond the purpose of this literature review.

Specific enzyme-linked immunosorbent assays have been developed for *Escherichia coli* O157:H7, food born pathogen [42, 45, 46]. A particular example is shown in Fig. 1-

5, where an array of antibodies was immobilized inside micro-capillary reactors. Using this approach, the detection limits of *E. coli* O157:H7, combined with the ELISA and Cy5 label-based immunoassays were determined to be 3 and 230 cells respectively.

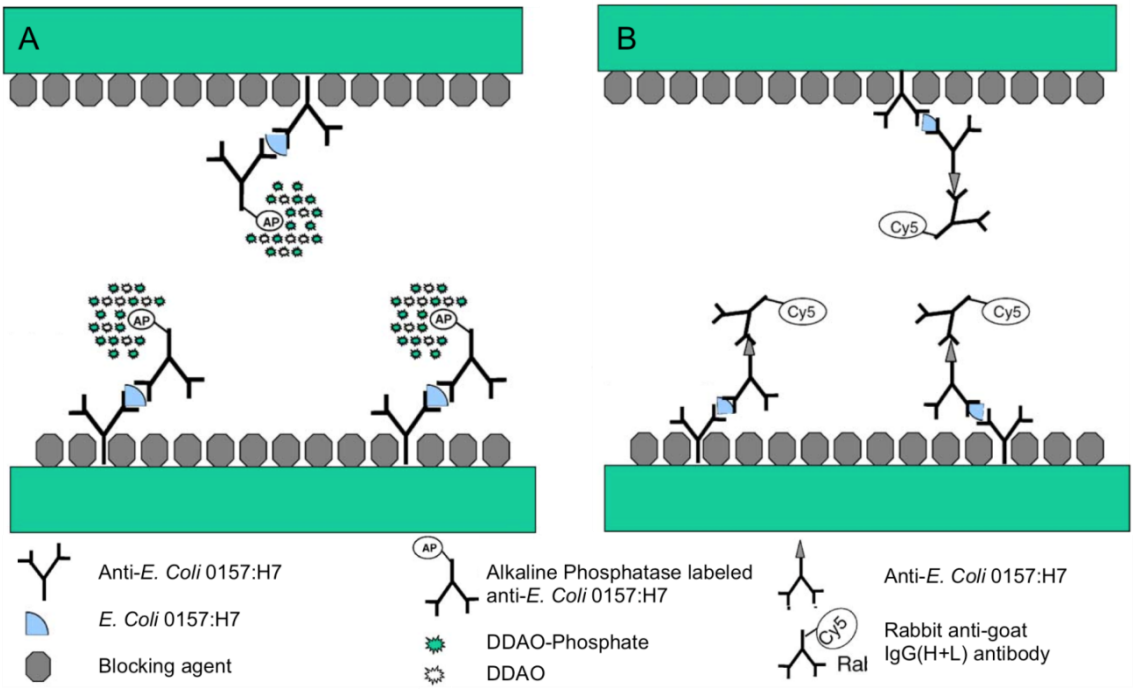

Figure 1-5 Schematic diagram of the ELISA (A) and Cy5 dye-labelled sandwich immunoassay (B) performed in capillary reactors for the detection of *E. coli* O157:H7. Adapted from [42].

However, assay limitations are often associated with the specificity of the antibody used and although antibodies specific to different *E. coli* strains have been presented, real polyvalent antibodies targeted against all environmental strains of *E. coli* do not exist at this time [3].

Immunological-based methods are advantageous, over culturing based methods, as they can be used to detect the toxins of interest [9, 47]. However, disadvantages of immunological methods include limitations due to the concentration of both antibody and antigen and the type of reaction solution used, cross-reactivity that can lead to false positive results and susceptibility to background interference under low microbial populations. Moreover, immunological-based methods are not feasible for real-time detection [47]

1.3.2.2 Nucleic acid-based methods

Most of the nucleic acid (NA) methods use molecular hybridization properties, which involve sequence recognition between a nucleic probe and a nucleic target.

The more frequently used nucleic-acid-based methods are the polymerase chain reaction (PCR – Fig. 1-6) and the *in-situ* hybridization (ISH) methods and they have been used for the detection of coliforms in water samples.

Polymerase chain reaction (PCR) involves the amplification of target fragments of DNA through cycling replication. The technique gives high specificity by amplifying a target gene to detectable levels and low response times, in the order of a few hours [3].

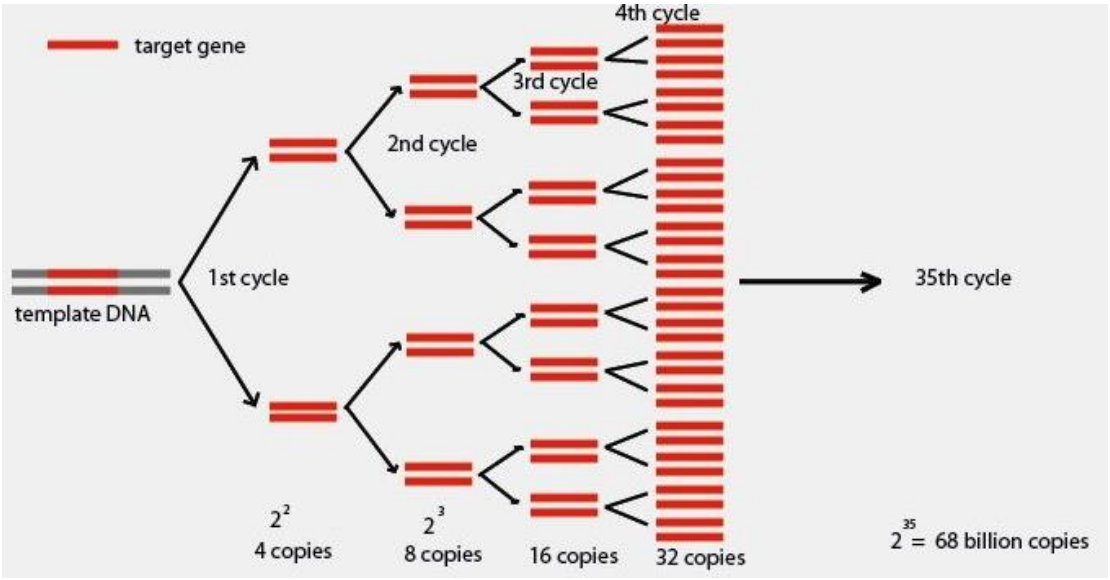

Figure 1-6 PCR gene replication reproduced from [48].

Advantages of using NA methods include the ability to detect genes from VBNC bacteria and the detection of GUS negative *E. coli* O157:H7 (that contains the *uidA* sequence) [49-51]. In addition, NA methods are as sensitive as improved culturing methods when PCR is used [50, 52]. However, NA methods can give both false positive and negative results. Fricker *et al.* [50] showed that strains of *Hafnia alvei* and *Serratia odorifera* have the *uidA* sequence that is used as a target sequence in the detection of *E. coli*. While Bej *et al*. [53] noted that *Shigella* species might interfered with *E. coli* detection. Therefore, in the presence of such strains and absence of *E. coli*, false

positive results would be expected. Moreover, PCR is susceptible to inhibition by (and give false positive results due to) environmental contaminants [3, 47]. Thus, environmental samples will require purification before analyses.

In these conditions, at present, molecular based methods remain undesirable for routine use because they require skilled manpower, are costly and demand dedicated laboratory space and equipment [3, 6, 47]. In addition, these methods are not feasible for real-time monitoring in the environment with contaminated samples.

1.3.2.3 Enzyme-based Methods

The use of microbial enzyme profiles to detect indicator bacteria is an attractive alternative to classical methods. Enzymatic reactions can be group-, genus- or species-specific, depending on the enzyme targeted. Moreover, reactions are rapid and sensitive. Thus, the possibility of detecting and enumerating coliforms through specific enzymatic activities has been under investigation for many years now.

The most used enzymes used for the determination of faecal pollution are: β-glucuronidase (GUS) - a marker enzyme for *E. coli* and β-D-galactosidase (GAL) –a marker enzyme used for total coliforms [3, 8, 54, 55].

1.3.3 Biosensors

The need for rapid, automated, real-time seen many attempts to develop biosensors for indicator microorganisms [47, 56]. A biosensor can be defined as an integrated receptor transducer device, which is capable of providing selective quantitative or semi-quantitative analytical information using a biological recognition element [56]. Biosensor detection entails the conversion of a signal (e.g. microbial growth, enzyme activity or antibody-antigen reaction) to a measurable output. The measured signals can be optical, mass, thermal or electrochemical. Fig. 1-7 shows a schematic of the general principles of a biosensor [47, 56].

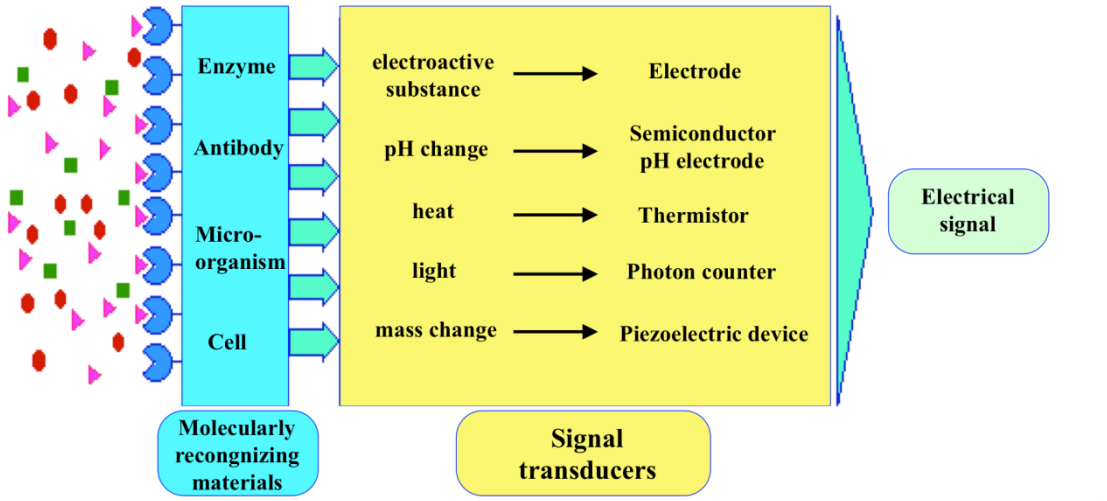

Figure 1-7 Principles of biosensors; reproduced from [57].

1.3.4 Predictive models

The lack of cheap and reliable methods for the detection of faecal indicators has pushed municipalities towards the use of predictive modelling programs to protect their population from exposure to faecal matter. Typically regression analysis of large volumes of historical data (e.g. rainfall, land-usage, turbidity, wind speed and direction, wave height, tidal period, chlorophyll, amount of sunshine etc.) is carried out to develop the model.

According to Jamieson *et al.* [58] a complete watershed scale microbial water quality model should include subroutines that characterize the production and distribution of waste and associated microorganisms, simulate the transport of microorganisms from the land surface to receiving streams, and route microorganisms through stream networks. A model developed and tested included the estimation of pathogen loading from: modelling the decay rate of the bacteria, human and livestock sources, watershed data and hydrology, overland transport of bacteria, movement of the pathogens through the soil, and the channel routing and sedimentation of free and attached microorganisms [59, 60]. A study conducted on four beaches along southern Lake Michigan (USA) during the summer of 2004 reported that waves, outfalls of bacteria from an adjacent stream, sunshine, temperature, and time of day (morning versus afternoon) turned out to be the most useful and consistent predictive variables for log *E. coli* concentrations. Additional analyses, using 99% confidence intervals on predicted log *E. coli* concentrations, indicated that in extreme cases of high or low health threat, model

predictions are likely to be accurate about 90% of the time [61]. Another model for *E. coli* concentrations was conducted using the following parameters: rainfall, wind speed and direction, wave height, tidal period, lake chlorophyll and turbidity. The authors reported a good correlation between the model and actual *E. coli* counts on days when the wind was blowing onshore, but a poor correlation (R^2 = 0.32, N = 124) when the wind was blowing offshore [62]. A strong correlation between *E. coli* concentrations and wave height, turbidity and bird count has also been found [63]. Francy *et al*, developed predictive models for 13 sites, and the most predictive variables were rainfall, wind direction and speed, turbidity, and water temperature. At three sites, the model resulted in increased correct responses, sensitivities, and specificities compared to use of the previous day's *E. coli* concentration. Drought conditions during the validation year precluded being able to adequately assess model performance at most of the other sites [64]. Shibata *et al.* used membrane filtration, qPCR and Enterolert® to quantify Enterococci concentrations in bathing waters. They found a positive correlation between Enterococci (as quantified by all the 3 methods) turbidity and tidal height and a negative correlation between Enterococci (as quantified by the culture based methods) and solar radiation [65]. A recent study used [66] neural artificial network-based models to successfully predict *E. coli* and Enterococci concentrations from readily measurable variables including temperature, conductivity, pH, turbidity, channel water flow, rainfall, and/or time lapse after a rainstorm.

In Ireland the SmartCoasts project between University College Dublin (UCD) and University of Aberystwyth promises, "The real-time prediction of coastal water quality ensuring the protection of public health in Wales and Ireland". The project involves monitoring of *E. coli*, Enterococci and microbial source tracking (which allows for the identification of both the biological and geographical origin of faecal contamination) and modelling against rainfall and land use.

Compared to Europe in US a wide range of predictive models for faecal pollution assessment have been developed and assessed in the past years. Although they have been shown to work well at some beaches and are becoming more widely accepted, there are several roadblocks to their widespread implementation. Continuous funding is needed to maintain and renew models. Not all agencies have the technical expertise to

develop and maintain models or the management capability to ensure that models are used for beach advisory or closure decisions [67].

Most current models report the ability to predict current conditions more accurately than reading a sample taken 24 hours prior. A major drawback, however, is their inability to account for sudden changes in conditions or unexpected events. Additionally, in order to be accurate, the models need to be adjusted to the individual water being monitored and years of data are needed for an accurate regression analysis. Any changes to the monitored waters, requires additional data collection to adjust the model.

1.4 Legislative drivers

In 2000 the EU adopted the Water Framework Directive (WFD) [68] to manage and protect European water supplies. A river basin approach to management is used rather than national management of water resources. The WFD sets out an action plan aimed at achieving quality water throughout Europe by 2015.

The 2006 Bathing Water Directive 2006/7/EC (BWD) [69] replaced the Bathing Water Directive of 1976 and proscribes monitoring of bathing waters with a new classification into: Poor, Sufficient, Good or Excellent. The 2006/7/EC BWD has reduced the number of investigated water quality parameters for faecal indicator bacteria from 19 to 2 main faecal indicators: *Escherichia coli* and Intestinal *Enterococcus*. The Objectives of 2006/7/EC BWD are to:

i. Set more stringent water quality standards and also puts a stronger emphasis on beach management;

ii. Ensure the quality of bathing waters and protecting health and the environment;

iii. Provide high quality and up-to-date information to the public about the quality of their bathing waters;

iv. Work in tandem with the WFD to protect (rivers, lakes, ground waters and coastal waters);

v. Ensure sampling for faecal bacteria is carried out during peak tourist season.

Waters must be classed at the very least "sufficient" to be compliant with the regulations set out in the 2006/7/EC BWD. All bathing waters must be classed sufficient or above by 2015 and will be assessed by the EPAs Office of Environmental Assessment (OEA). If the waters fall into the category "Poor" remedial action will have to be put in place and if the quality of the water does not increase the Office of Environmental Enforcement (OEE) have the power to issue fines and to take the water authority responsible to court if improvements aren't made. The Directive also sets out the sampling regulations for the determination *E. coli* and Enterococci under the headings:

- Sampling Point
- Sterilisation of Sample Bottles

- Sampling – The volume of water to be collected and the types of apparatus to be used
- Storage and Transport

The 2006/7/EC BWD was transposed into Irish law in 2008 as the Bathing Water Regulations 2008 (S.I. No. 79 of 2008) and the following (Tables 1-1 and 1-2) are the standards dictated for inland coastal waters as well as the recommended analysis methods.

Table 1-1 Bathing water standards for inland waters.

Inland waters					
	Parameter	Excellent quality	Good quality	Sufficient quality	Reference methods of analysis
1	Intestinal Enterococci (cfu/100mL)	200(*)	400(*)	330(*)	ISO 7899-1 or ISO 7899-2
2	*Escherichia coli* (cfu/100mL)	500(*)	1,000(*)	900(**)	ISO 9308-3 or ISO 9308-1

(*) Based upon a 95-percentile evaluation, (**) Based on a 90-percentile evaluation.

Table 1-2 Bathing water standards for coastal and transitional waters.

Coastal and transitional waters					
	Parameter	Excellent quality	Good quality	Sufficient quality	Reference methods of analysis
1	Intestinal Enterococci (cfu/100 mL)	100(*)	200(*)	185(*)	ISO 7899-1 or ISO 7899-2
2	*Escherichia coli* (cfu/100mL)	250(*)	500(*)	500(**)	ISO 9308-3 or ISO 9308-1

(*) Based upon a 95-percentile evaluation, (**) Based on a 90-percentile evaluation.

1.5 β-glucuronidase

β-glucuronidase is an enzyme which catalyzes the hydrolysis of β-D-glucopyranosiduronic derivatives into their corresponding aglycons and D-glucuronic acid and it was discovered first in *E. coli*. β-glucuronidase is a globular protein, active as a homotetramer and made up of 68 kDa monomers of 603 amino acids [70]. The active site residues of the enzyme are highly conserved. β-glucuronidase enzyme retains the anomeric configuration of the glucuronic acid and is appropriately termed a retaining hydrolase [71]. The enzyme has three important residues that participate in the breaking down of the glucuronides. It breaks down the O-glycosyl bond by nucleophilic attack with the nucleophilic residue being E504 or Glu504 (equivalent to Glu540 in humans). The acid-base residue is Glu413 (equivalent to human Glu451) while the residue Tyr468 (Tyr504 in humans) has been proven important but its role is not clear [71, 72]. Matsumura and Ellington [73] modelled the *E. coli* GUS against the human crystal structure and proposed that seven conserved residues (Asp163, Tyr468, Glu504, Tyr549, Arg562, Asn566 and Lys568) form eight-intermolecular hydrogen bonds with the substrate. This bonding is thought to confer the typical specificity of GUS to β-D-glucuronide based substrates.

β-glucuronidase presents good specificity for *E. coli*. When tested, β-glucuronidase-positive reactions were observed in 94-96% of *E. coli* isolates [74-76].

1.5.1 Mechanism of catalysis

The actual mechanism of GUS catalysis entails a two-step process, glucuronylation and deglucuronylation steps as illustrated in Fig. 1-8. The first step involves nucleophilic attack by one of the carboxylates on the sugar anomeric centre. General acid catalysis from the other carboxyl group aids in the departure of the aglycon to form an α-D-glycosyl-enzyme intermediate. In the second step, the intermediate is hydrolyzed by general base-catalyzed attack of water at the anomeric centre, resulting in cleavage of the glycosidic bond with net retention of the anomeric configuration. Formation and hydrolysis of the glycosyl-enzyme intermediate proceed via transition states with substantial oxocarbenium ion character (Fig. 1-8) [72].

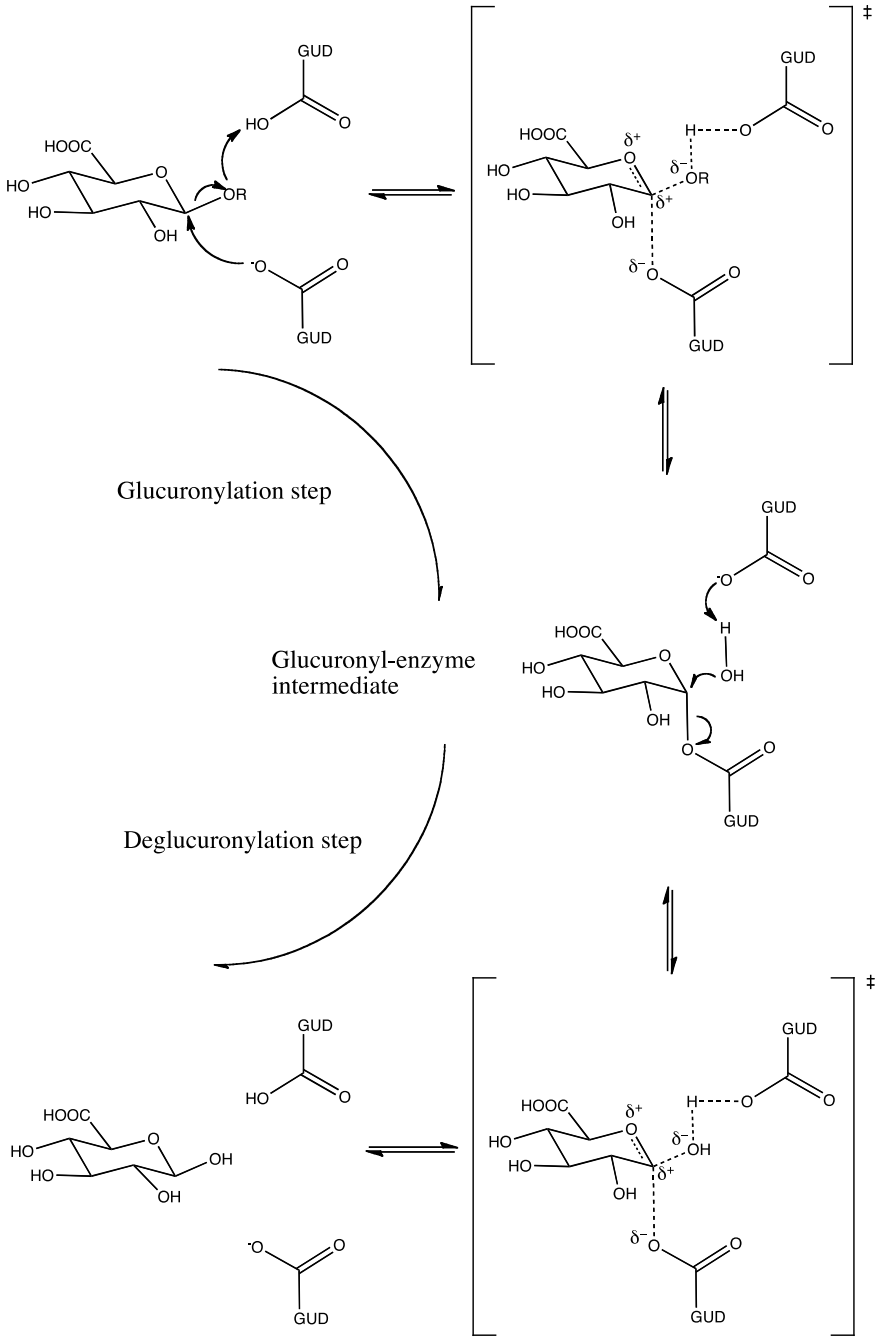

Figure 1-8 Proposed mechanism for a retaining β-glucuronidase (GUS = β-glucuronidase). Reproduced from [72].

1.5.2 Synthetic substrates

Substrates made up of glucuronides linked to a chromophore or fluorophore have been designed for the detection of GUS [34]. The use of enzymatic reactions to detect *E. coli* can provide a rapid, sensitive and less expensive alternative to the more time consuming traditional methods. Enzyme substrates can be added to the samples in question and incubated under optimum conditions for maximum enzyme activity. Colour formation or fluorescence due to the hydrolysis of the synthetic substrates can be recorded (Fig. 1-9). In general, chromogenic substrates are phenol-based, water soluble, heat stable and specific and occur in a wide range of different colours [34]. Most of the chromogenic/ fluorogenic substrates produce the characteristic colour/fluorescence only under optimum pH conditions. The fluorogenic substrates that will be further used in Chapter 3 for the detection of β-glucuronidase and their hydrolysis products are shown in Fig. 1-9.

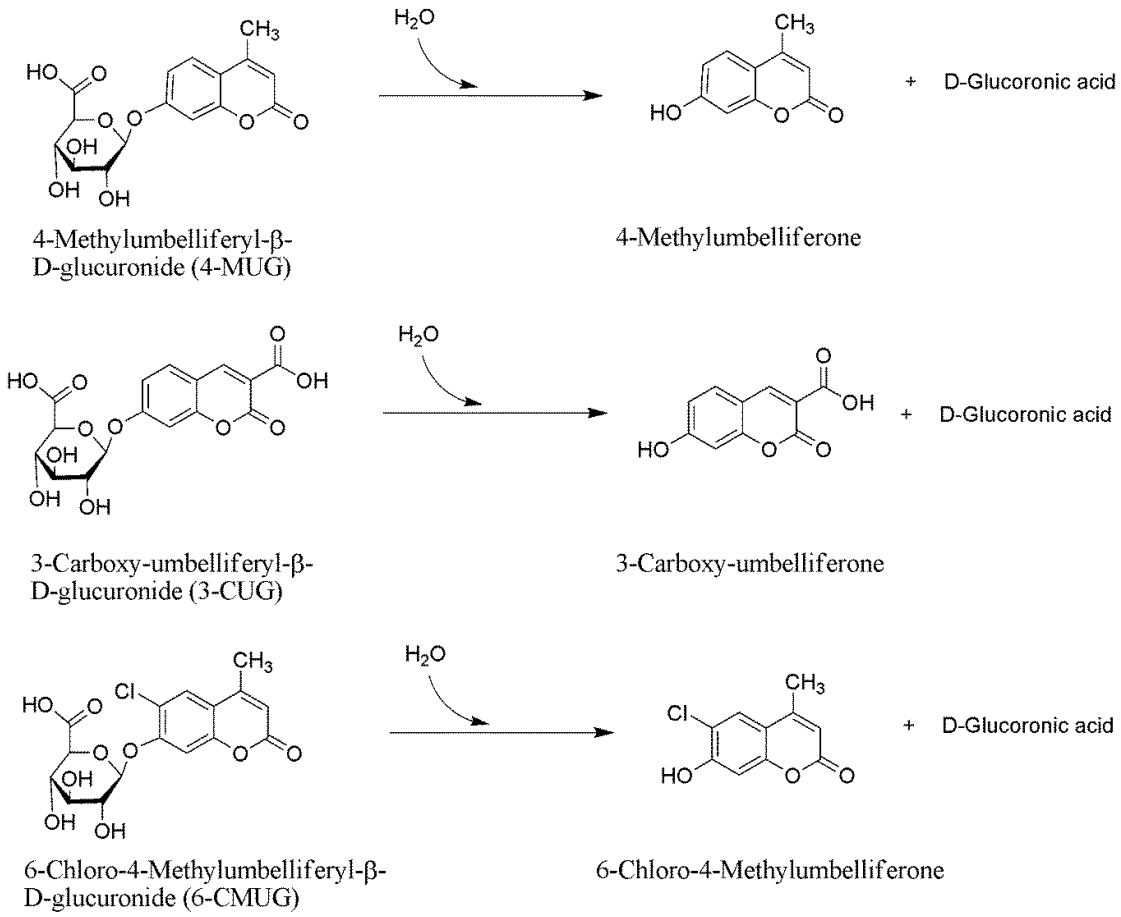

Figure 1-9 Examples of synthetic fluorogenic substrates for GUS and their fluorescent breakdown products.

1.6 Fluorescence spectroscopy overview

Optical based fluorometric techniques are more sensitive than the absorbance methods, because the fluorescence comparison is made in the complete absence of light in the presence of the fluorophore. As a consequence they are the preferred optical detection technique. In this method, a fluorescent molecule, or fluorophore, acts as the aglycon attached via glycosidic bond to the ß-glucuronide. Due to increased stability, the glucuronide bound fluorophore does not fluoresce in the near-UV spectrum. However, when EC synthesized GUS catalyzes the hydrolysis of the glycosidic bond, the fluorescent molecule is released.

Fluorescence is a process that occurs in three stages: excitation; excited state lifetime; and fluorescence emission. The first step is excitation of a molecule due to absorption of a photon from an external source. This creates an excited electronic singlet state, lasting for a defined amount of time, usually only nanoseconds. Once a molecule has absorbed energy, there are a number of routes by which it can return to the ground state. If the photon emission occurs between states of the same spin state (e.g. S1- S0) this is called fluorescence. If the spin state of the initial and final energy levels are different (e.g. T1-S0), the emission is called phosphorescence [77]. Three nonradiative processes are also significant: internal conversion (IC), intersystem crossing (ISC) and vibrational relaxation (VR). Internal conversion is the radiationless transition between energy states of the same spin state. Intersystem crossing is a radiationless transition between different spin states. Of these three processes, vibrational relaxation occurs most frequently for many molecules. This occurs very quickly ($< 1 \times 10^{-12}$ s) and is due to interactions with other intra and intermolecular degrees of freedom. When fluorescence occurs a photon is emitted returning a molecule to its ground state, the energy of this photon is lower than the excitation and therefore of longer wavelength. The fluorescence emission spectrum is spectrally close to the absorption spectrum and they tend to mirror each other. The difference in energy or wavelength between the maximum of the absorption spectra and the maximum of the emission spectra is defined as the Stokes' shift. This difference is characteristic of all complex molecules [77].

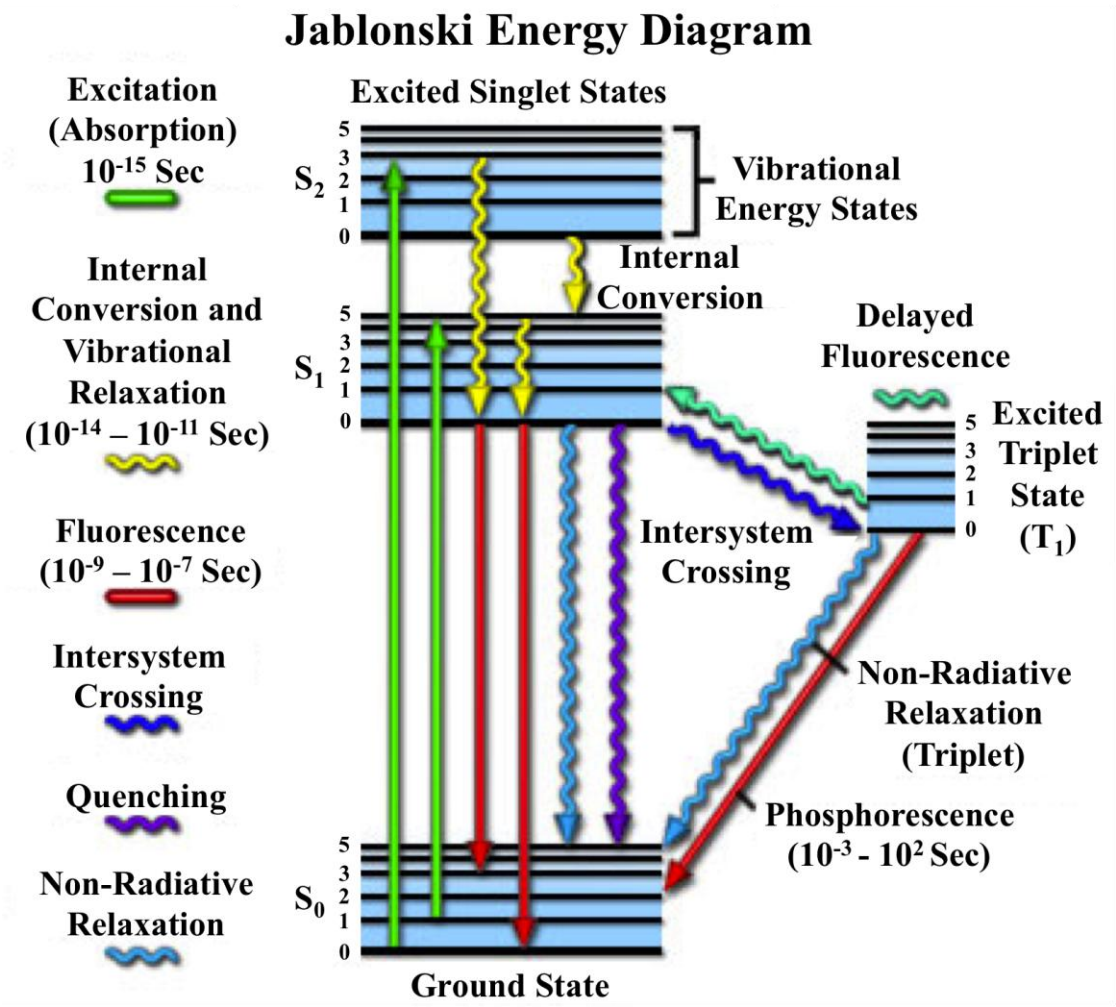

Figure 1-10 Energy levels involved in the absorption and emission of light by a fluorophore. Reproduced from [78].

Environmental factors may affect the rate of fluorescence of a given fluorophore by competing with light emission in the deactivation of the lowest excited singlet state. Excited molecules present in (S1) may return to the ground state (S_0) through intersystem crossing and internal conversion rather than fluorescence decreasing the rate of fluorescence. The solvent in which the fluorescent molecule resides influences electronic spectra primarily through electrostatic properties. Quenching, which is the decrease or elimination of quantum yield, can occur due to interactions between the fluorophore and solvent or interactions between the fluorophore and other species in the solvent. Excited molecules can release energy through rotational or vibration wasting due to interactions with other species. Additionally, quenching occurs when the

fluorophore in the ground state complexes with another species and the resulting conjugate is not luminescent. A decrease in quantum yield also occurs when dissolved and/or suspended solids absorb or scatter incident and fluorescent light waves [79], [80].

1.7 Conclusions

Based on the literature survey it was concluded that the best indicator for faecal pollution assessment of environmental waters is *E. coli*. The already available methods based on the detection of GUS activity from *E. coli* cells can potentially be implemented into an opto-chemical sensor able to perform remotely and continuously into the environment. A review on rapid methods for *E. coli* detection using GUS activity as a marker concluded that rapid assays can be useful for early warning of faecal contamination in water, and represent an alternative indicator concept since GUS activities are more persistent to environmental stress than the culturability of *E. coli* [81].

An integrated sensing platform containing a suite of sensors (like turbidity and *E. coli*) should be more reliable in estimating risks associated with faecal contamination. The high resolution continuous monitoring of turbidity using a relatively cheap probe, could inform the sampling times for the *E. coli* platform. By doing this the reagent and energy consumption of the microbial sensor as well as the deployment period can be minimised and the performance increased. Turbidity thresholds can be designated based on historical data and imbedded into the software, and when a certain turbidity value is reached the system can trigger sampling for bacteriological analysis. Although predictive models have included different input variables to estimate faecal indicator concentrations, no model has looked at ship traffic as a possible input variable for these predictive models.

1.8 Aim of this work

The ultimate objective of this work is to develop a new warning system for the assessment of faecal pollution contamination of recreational waters. This is accomplished by addressing the broad specific objectives which are to:

1. Assess the benefits of using *in-situ* sensors for the collection of continuous water quality data and the challenges associated with collecting reliable data in rough aquatic environments (e.g. biofouling, data management).
2. Assess the potential of continuous, high resolution water quality data to detect sporadic pollution events and to inform sampling times for more complex sampling regimes.
3. Develop a novel rapid method, for the estimation of faecal pollution in environmental waters using GUS as a marker for *E. coli* presence, which has the potential for both automation and on-line monitoring.
4. Test the developed method on environmental water samples, and asses the accuracy, limit of detection and the limitations associated with the method for detecting *E. coli* concentrations.

2 CONTINUOUS HIGH FREQUENCY MONITORING OF ESTUARINE WATER QUALITY AS A DECISION SUPPORT TOOL: A DUBLIN PORT CASE STUDY.

ABSTRACT

High-frequency, continuous monitoring using *in-situ* sensors offers a comprehensive and improved insight into the temporal and spatial variability of any water body. In this paper, we describe a 7-month exploratory monitoring programme in Dublin Port, demonstrating the value of high-frequency data in enhancing knowledge of processes, informing discrete sampling and ultimately increasing the efficiency of port and environmental management. Kruskal-Wallis and Mann-Whitney tests were used to show that shipping operating in Dublin Port has a small-medium effect on turbidity readings collected by *in-situ* sensors. Turbidity events are largely related to vessel activity in Dublin Port, caused by re-suspension of sediments by vessel propulsion systems. The magnitudes of such events are strongly related to water level and tidal state at vessel arrival times. Crucially, measurements of *Escherichia coli* and Enterococci contamination from discrete samples taken at key periods related to detected turbidity events were up to 9 times higher after vessel arrival than prior to disturbance. Daily *in-situ* turbidity patterns revealed time-dependent water quality "hot spots" during a 24 h period. We demonstrate conclusively that if representative environmental assessment of water quality is to be performed at such sites, sampling times, informed by continuous monitoring data, should take into account these daily variations. This work outlines the potential of sensor technologies and continuous monitoring, to act as a decision support tool in both environmental and port management.

Keywords: Water monitoring, Sensors, Turbidity, Ship Traffic, Faecal coliforms.

2.1 Introduction

Marine and coastal resources play a major role in sustaining the economic and social development of society. Today, about 80 % of all international trade is carried by sea [82]. According to some sources, by the year 2020, about 75 % of the world's population will live within 60 km of sea coasts and estuaries [82]. In Ireland, 99.5 % of foreign trade is facilitated through ports, of which 42 % of the gross domestic product (GDP) is exported through Dublin Port [83]. The continual population increase in coastal areas and the ever increasing density of marine transport combined with a limited number of convenient anchorages results in an dense concentration of both cargo and passenger traffic in certain coastal areas [84]. Such areas are of particular concern because of their dynamic and continuously changing state, posing a serious challenge when it comes to environmental monitoring. In this case, conventional discrete grab-sampling regimes are unlikely to provide representative results on temporal and spatial distribution of physicochemical parameters, and thus do not reflect the general matrix behaviours and properties throughout the entire water body [85, 86].

The estuarine environment is a complex blend of continuously changing habitats categorised as the zone where fresh and salt water meet and mix, bounded at its mouth by the ocean and at its head by the upper limit of tides [87]. These estuaries are transitional zones where constantly changing water depths generate rapidly reversing currents and transport vast quantities of salt, heat and sediments on a daily basis [88]. Owing to the constant balance between up-estuary saltwater movement and down-estuary fresh water flow, estuaries are lengthy retention areas for pollutants and upstream contaminated sediments. The physicochemical parameters of water vary considerably both spatially and temporally due to tidal flushing, basin shape, surrounding topography, regional climate and human activity. The hydrology of an estuary together with its anthropogenic activity makes each estuary unique. The establishment of high quality monitoring is the key for taking reactive remedial action. Poolbeg Marina located in Dublin Port illustrates such a complex site were frequent temporal variability is present within the psychochemical and biological parameters.

Recent advances in communication and sensor technology have catalysed progress in remote monitoring capabilities for water quality [89]; [90]; [91]. As a result, the ability

to characterise dynamic hydrological properties at adequate temporal and spatial scales has greatly improved [92]. Emerging sensor technologies have the capability to provide additional information on variability of pollutants present and concentrations, as well as early detection of extraordinary events. Recent monitoring programs trend towards integration of continuous data collection by *in-situ* detectors. Data can be accessed on-site or remotely, the latter having the advantage that constant, perhaps automated, surveillance can be carried out to detect changes in critical indicators and provide early information to assist decision makers.

Ship traffic is a factor that affects the complexity of an estuarine water body. Such traffic may interact with the aquatic environment through a variety of mechanisms including, emissions and exhaust [93], propeller contact [94], turbulence from the propulsion system, waves produced by movement [95], noise [96], and movement itself. Each of these impacting mechanisms may have multiple effects on the aquatic ecosystem. Sediment re-suspension [97], resulting in increased turbidity [98], water pollution, disturbance of fish and wildlife [99], destruction of aquatic plants [99], and shoreline erosion [84] are all major concerns.

Turbidity is generally defined as a decrease in the transparency of a solution owing to the presence of suspended and some dissolved substances that causes incident light to be scattered, reflected, and attenuated rather than transmitted in straight lines. The major sources of turbidity typically include: phytoplankton, particulates from shoreline erosion, re-suspended bed sediments, organic detritus from streams, and excessive algae growth. Although turbidity is a background quality of an aquatic system, increased turbidity can be caused by natural events like storms or heavy rains but also by anthropogenic events like dredging or ship traffic. The negative impacts of increased turbidity on the ecosystem are numerous and well defined in the literature [100]. Limited light penetration owing to absorption and attenuation leads to reduction of phytoplankton production, macroalgae and other photosynthesizing organisms. High and sustained levels of suspended sediment may cause permanent alterations in community structure, diversity, density, biomass, growth, and rates of reproduction along with mortality. Impacts on aquatic individuals, populations, and communities are expressed through alterations in local food webs and habitat. These changes at trophic level translate into reductions in energy output for the next trophic level [101]. The

short-term impact of ship traffic on turbidity owing to re-suspension of sediments has been investigated in the past from different perspectives. Bed sediments can be a significant source of organic pollutants (pesticides, PAHs, PCBs [102, 103]), heavy metals (lead, mercury or zinc [104], nutrients (especially phosphorus [105] and faecal coliforms [106] [107].

The aim of study this was to utilise high frequency (sub-hourly) water quality data from *in-situ* sensors to demonstrate improved understanding of dynamic estuarine processes and to outline the usefulness of collected data in both port and environmental management. More specifically the project was designed to investigate the following key questions:

-Is there a consistent relationship between ship traffic type and turbidity levels over an extended time frame in Dublin Bay?

-Does ship traffic influence re-suspension of bottom sediments and faecal indicator bacteria (FIBs), particularly *Escherichia coli* and Enterococci*?*

-Does exploratory monitoring using continuous data collection provide the potential to predict and indicate appropriate grab sampling times for further intensive monitoring?

2.2 Materials and Methods

2.2.1 Site Description

Poolbeg Marina (latitude: 53° 20' 39", longitude: -6° 12' 59 ") located on the lower Liffey Estuary is a busy port environment with a diverse ecosystem that includes benthic communities [108], fish and shellfish, marine bird populations and some marine mammals [109] [108]. The site forms a zone of passage for salmon and sea trout migrating from feeding areas in the sea, to spawning areas in the River Liffey system and for juveniles migrating from the river to the sea [110]. Anthropogenic activities involve heavy port use, marine transportation, aquaculture and recreation. The estuary is macro-tidal with strong salinity gradients, having a mean tidal range of 2.75 m and average mean spring tides of 3.6 m and 1.9 m respectively [111]. The topography of the estuary has been greatly modified, and is constrained by walls (North and South Walls) for its whole length and is regularly dredged to remove accumulated sediments. The Liffey Estuary covers a wide area of 5 km^2 with the main freshwater inflow into the Estuary coming from the Liffey River. The river is regulated by an upstream hydro-electric plant and dam resulting in a smoothly varying inflow of freshwater (approx. 12.42 m^3/s) with considerable attenuation of its floods [111]. The river is tidal all the way through the City of Dublin up to distance of 10.5 km upstream from the monitoring site.

The working site is located in the upper part of the Estuary, where the ship traffic is less intense (Fig. 2-1).

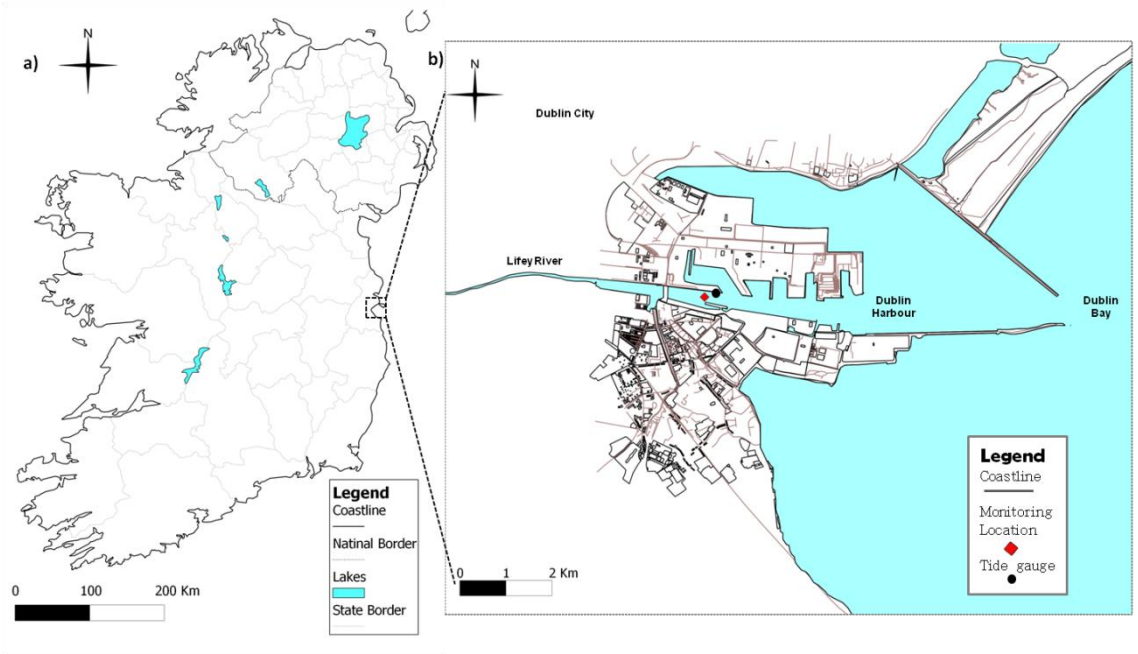

Figure 2-1 Map showing the location of Dublin Bay in relation to Ireland (a) and the monitoring location in the context of the lower Liffey Estuary and Dublin Port, including the location of the nearest national tide gauge (b) [112].

Water depth in the area is approximately 8 m and channel width is approximately 260 m. Water column stratification occurs due to denser, higher salinity water underlying low salinity surface waters at the surface but also due to seasonal heating or cooling which in turn causes a differential event where warm water (summer) or cold water (winter) in the surface layer is isolated from the bottom layer. Fig. 2-2 shows vertical profiles of the water column for salinity, temperature, dissolved oxygen (DO) and pH collected during the cold season. The sediments in Dublin bay at the lower limit of the estuary are predominantly sand. Muddy sediments are present starting with Poolbeg and upstream and are confined to the channel. Sediment samples collected at the site were black and anoxic which is consistent with previous studies [113]. Anthropogenic disturbances include input of pollutants (runoff, storm drains, discharges from sewage treatment plant, industrial discharges, port activity and recreational boating) and the modification of flow (upstream dam releases). All these episodic changes dictate the chemical, physical and biological parameters at the site and thus increase its complexity.

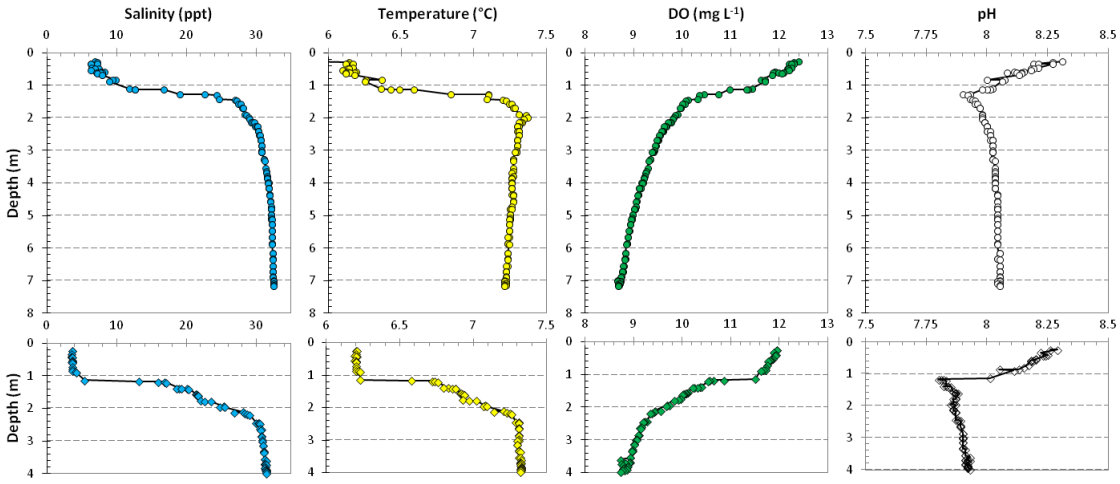

Figure 2-2 Water column vertical profiles collected at the site on high (top) and low (bottom) tide in the month of January [112].

2.2.2 Monitoring port activity

Ship arrival and departure logs were obtained from the Dublin Port Authority, and observations on ships manoeuvring were made during site visits. Large commercial vessels, including cargo ships, freighters, cruise ships, passenger ferries and recreational boats are all active in Dublin Port. The deployment site is located close (c. 230 m) to docking and berthing facilities of cross-channel ferries that service Dublin daily. These vessels operate throughout Dublin Port and have scheduled daily arrival and departure timetables; the 1st vessel arrives between 04:00 and 7:00 (departs between 08:00-11:00), the 2nd one arrives between 10:00 and 14:00 (departs between 14:00-17:00) and the 3rd one arrives between 16:00 and 19:00 (departs between 19:00-21:00). The decision to intensively monitor these particular vessels was made owing to (a) the timetables of arrivals and departures being relatively predictable and constant, (b) that berthing and turning manoeuvres of these vessels are close to a floating dock suitable for deployment of multi-parameter sonde and (c) draughts and propulsion systems of these vessels are potentially large enough to influence turbidity dynamics in the estuary. The effects of small (often recreational) vessels in the area were discounted since mean water depth at this site is circa 7-8 m, and it has been shown previously in other estuaries that small vessels do not generally have large influences on turbidity levels in water of this depth [97]. Other vessels travelling upstream could influence turbidity levels, but the

frequency of this traffic is lower and temporally and spatially random, and thus patterns would be inherently difficult to detect.

2.2.3 Continuous Monitoring of Water Quality

A multi-parameter sonde (YSI 6600EDS V2-2), equipped with telemetry (EcoNet) and sensors to measure turbidity (NTU), optical dissolved oxygen (mg L^{-1}), temperature (°C), conductivity (mS cm^{-1}) and depth was purchased from YSI Hydrodata UK. The sonde was deployed at a depth of 2.5 m from the water surface, and data was collected from 1st of October 2010 until 1st of May 2011(sampling interval = 15 min). The unit was powered with a 12 VDC external battery and data recorded to an internal logger, before transmission via GPS to a web-based server, where it was visualized in real-time and made available for download.

2.2.3.1 Maintenance Protocols

Sensor function and power status were reviewed daily. Onsite visits were performed frequently for cleaning, calibration, and validation purposes. Temperature, DO and salinity were checked using a ProPlus® handheld multi-parameter instrument (YSI UK) and turbidity was validated using a portable turbidity meter Turb® 430 IR (VWR Ireland) calibrated prior to each site visit. Site visit frequency (fortnightly in winter and weekly during spring) was generally governed by fouling rates of sensors, and in a few cases by malfunction of the telemetry system. Copper tape and mechanical wipers were used to limit the extent of biofouling. A protocol for the operation and maintenance of a continuous water quality monitor at sites with rapidly changing conditions was adapted from [114]. Briefly on arrival at the site, the following steps were performed: 1) readings and time were recorded from both the sonde and the lab calibrated meters; 2) an insulated bucket was filled with ambient water and both the sonde and the calibrated meter were placed inside allowing the two systems to run in parallel and record data; 3) the sonde and the sensors were cleaned and step 2 was repeated; 4) the sonde was removed rinsed thoroughly and the sensors calibration was checked in calibration standards and readings recorded; 5) in case the calibration criterion was breached, recalibration was performed. For the turbidity sensor pre-cleaning measurements were made in a bucket of tap water to account for the variable nature of turbidity. Calibration

criterion was: Temperature ±0.2 °C; DO ±0.3 mgL^{-1}; Specific Conductance ±3% of the measured value; Turbidity ±5% of the measured value.

2.2.4 Rainfall data

Daily average rainfall measurements were collected from the Irish Meteorological Service (Met Éireann) from all the meteorological stations in Dublin area. Five stations were selected based on proximity to the monitoring location and the data obtain from each of them was averaged to compute a single daily mean.

2.2.5 Tide data

The Marine Institute, responsible for the Irish National Tide Gauge Network, supplied tidal height data from a site close to the sonde location. This data was supplied at 5 min intervals and was averaged over 15 min to correspond with the sampling frequency of the deployed sonde.

2.2.6 Discrete Sampling

Water samples for total suspended solids (TSS) and faecal indicator bacteria (FIB) were collected in the months of August and September 2012. All the samples were collected in triplicates using a Wheaton grab sampler, and were transported to the lab on ice. Discrete samples were collected before, immediately after the arrival and 45 min after the arrival of the morning vessel to investigate for possible effects of ship traffic on *E. coli* and Enterococci levels. To determine the vertical distribution of measured parameters within the water column and to understand any mixing effects, samples were collected from different depths of 0.5 m, 2.5 m and 4.5 m. A detailed procedure used for the sample collection is presented in Fig. 2-3.

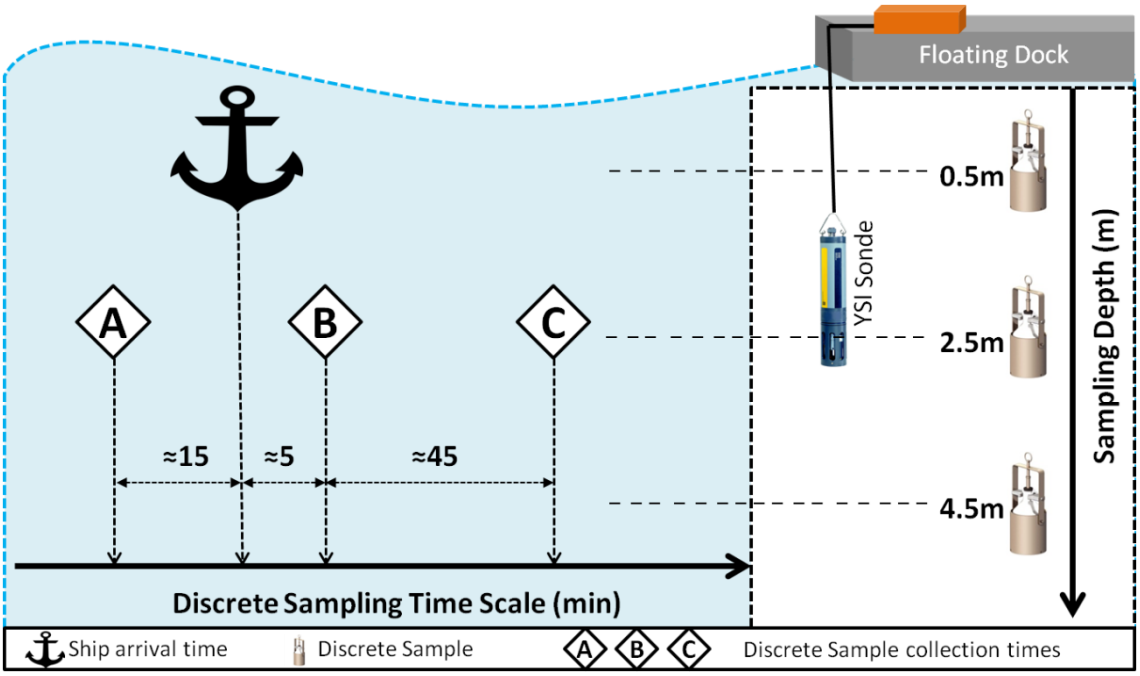

Figure 2-3 Discrete sampling procedure used for temporal and spatial collection of samples before and after ship arrival. A, B and C represent sampling collection times in relation to the ship arrival time. Ship arrival time is defined as the time at which the ship has finished the turnover manoeuvre and has docked. 0.5 m, 2.5 m and 4.5 m represent the sampling depths at which samples were collected [112].

2.2.6.1 Microbial analysis of water samples

Water samples were collected in sterile 500 mL high density polypropylene (HDPP) bottles. Samples were transported to the lab on ice within 2 h and inoculated within 4 h after collection. The Colilert-18®/Quanti-Tray 2000® system (IDEXX Laboratories) was used for the enumeration of coliforms and *Escherichia coli* and Enterolert®/Quanti-Tray 2000® system (IDEXX Laboratories) was used for the enumeration of Enterococci. The enumeration protocol was followed in accordance with manufacturer's instructions. Aliquots of 10 mL from original water samples were diluted 1:10 with sterile deionised into 100 mL bottles. After the addition of Colilert-18 and Enterolert, samples were inoculated into Quanti-Trays and sealed. For *E. coli* and coliform enumeration, samples were incubated at 37.0 °C for 18 to 20 h. Following

incubation the Quanti-Tray wells were read visually for yellow colour indicating the presence of coliforms and for blue fluorescence indicating the presence of *E. coli.* For Enterococci enumeration samples were incubated at 41.0 °C for 24 to 28 h after which the blue fluorescent wells were counted as positive. The number of positive wells was recorded for both tests and converted to most probable number (MPN) estimations using tables provided by the manufacturer. For quality control, replicates of positive controls of *E. coli* ATCC 11775 and *Enterococcus faecalis* ATCC 19433, negative controls and laboratory reagent blank were analysed for each sample batch.

2.2.6.2 Microbial analysis of sediment samples

For sediment analysis, samples were collected in sterile containers, stored on ice and analysed within 4 h of sampling. For the separation of microorganisms from sediments, micro-organisms were elutriated by vortexing for 2 min, 2 g of sediment sample and 35 mL of sterile deionised water in a 50 mL centrifuge tube [115]. After standing for 2 min, the suspension was serially diluted to 100 mL and bacteria enumeration was performed as previously described for water samples. To determine moisture content of sediment samples and express counts per gram dry weight (GDW), fresh samples were dried at 103-105° for 24 h and reweighed.

2.2.6.3 Total suspended solids (TSS) analysis

Samples for TSS determination were collected in 500 mL HDPP bottles, transported to the lab on ice and analysed on the same day. Samples were processed as described in Standard Method 2540 D [116]. Briefly, glass microfibre filters (pore size: 1.2 µm and 47 mm diameter) were washed in DI water, placed in aluminium dishes and dried at 103-105 °C in the oven. After removal dishes were weighed and labelled. Aliquots consisting of 250 mL of water sample were vacuum filtered after which the filters were dried at 103-105 °C for 1 h and re-weighed.

2.2.7 Data management and Statistical Analysis

2.2.7.1 Consideration of errors

Collected data were subjected to rigorous quality assurance (QA) and quality control (QC) procedures before use to ensure removal of anomalous and spurious data [114]. Guidelines and standard procedures for correcting errors in continuous water quality

data streams are provided by Wagner *et al*., [114] and [117] give examples of raw data containing errors that have to be corrected. In the present study, out of range values were short-lived (no more than one sensor value) and were corrected manually by interpolating adjacent values. Anomalous data are represented by values within the measurement range of a particular variable but significantly different than adjacent data values in time series. Anomalies can be short-lived or long-lived and evaluating them requires expertise in both the functioning of the sensor and the process that drives the sensor response [117]. Anomalies were present mostly in the turbidity data set and the short-lived ones were corrected the same way as the out of range values. Longer time scale of questionable reliability (at least 2 consecutive sensor values) were investigated by looking at time series with all the measured parameters, ship traffic, water level and rainfall after which a decision was taken regarding inclusion of the data. Data deemed unreliable were removed from the continuous data set. Sensor drift due to biofouling between service dates were corrected as described by Wagner *et al*. Data correction was applied only when the combine absolute value for calibration and fouling error exceeded the following criterion: Temperature ±0.2 °C; DO ±0.3 mgL^{-1}; Specific Conductance ±3% of the measured value; Turbidity ±5% of the measured value. Sensor drift is assumed to occur at a constant rate throughout the correction, with fouling commencing as soon as the sonde is deployed in the aquatic environment. Thus a zero correction is applied at the start of the interval, the full correction at the end of it and between the two dates, the data is linearly interpolated. Equation (1) [117] was used in this case for linear drift correction, where:

$$V_c=V+(V_f-V_s)[(T_f-T)/T_f] \quad \textbf{(1)}$$

V_c is the drift corrected value, V is the original measured value, V_f is the response of the sensor immediately before cleaning and validation at the end of the correction interval; V_s is the response of the sensor after cleaning and calibration; T_f is the total time interval for which the correction is applied and T is the time between the end of deployment and the measured value. Data was processed and analysed using SPSS® (SPSS Statistics 17.0, SPSS Inc., Chicago, IL, USA), AQUARIUS® (AQUARIUS 3.0.1032 Standard, Aquatic Informatics, Vancouver, Canada) and Excel 2007®.

2.2.7.2 Statistical methods and analysis

During the 7-month deployment period, 20401 individual sensor readings were collected generating 81404 data points. Descriptive statistics of the entire data set are presented in Table 2-1.

To verify if the collected data is parametric, the measured variables were tested for the assumption of normal distribution and homogeneity of variance [118]. For the assumption of normally distributed data the Kolmogorov-Smirnov test [118] was used, turbidity, $D(20401) = 0.15$, $p < 0.01$, salinity, $D(20401) = 0.21$, $p < 0.01$, DO, $D(20401) = 0.15$, $p < 0.01$ and temperature, $D(20401) = 0.11$, $p < 0.01$ were all significantly non-normal. As a consequence all of the four measured parameters have violated the assumption of parametrical statistical analysis.

Table 2-1 Descriptive statistics of the measured parameters. N = sample size. Specific Conductance (μScm^{-1}), Conductivity ($mScm^{-1}$), Depth (m) and DO saturation (DO %) are not shown in the table.

Parameter (units)	N	Range	Minimum	Maximum	Mean	Median	Std. Deviation	Variance
Temperature(°C)	20401	11.90	3.20	15.10	8.62	7.83	2.870	8.237
ODO (mgL^{-1})	20401	9.03	5.16	14.19	9.56	9.78	0.698	0.488
Turbidity(NTU)	20401	95.00	0.20	95.20	5.38	4.4	3.771	14.227
Salinity (ppt)	20401	14.05	16.95	31.00	30.35	30.52	0.706	0.499
Total	81604							

Bivariate correlation analysis measures the inter-relationship between 2 variables in terms of correlation coefficient [119] Spearmen's correlation coefficient, R, is a non-parametric statistic test, and so can be used when the data have violated the parametric assumption. Data collected from the *in-situ* sensors were computed to obtain daily means and compared with the daily rainfall data. It was found that there is a significant correlation ($p < 0.01$) between the monitored parameters and rainfall data with the exception of DO ($p > 0.5$) Table 2-2. The strongest correlation is between DO and temperature ($R = -0.751$, $p < 0.01$) and rainfall is moderately correlated with turbidity levels ($R = 0.387$, $p < 0.01$).

Table 2-2 Spearman's correlation coefficient matrix for the daily averaged data.

Parameters		ODO(mgL^{-1})	Temperature (°C)	Rainfall (mm)	Salinity (ppt)	Turbidity (NTU)
ODO(mgL^{-1})	Spearman's rho	1.000	-.751**	.022	-.285**	.209**
	Sig. (1-tailed)	.	.000	.377	.000	.001
	N (sample size)	213	213	213	213	213
Temperature (°C)	Spearman's rho	-.751**	1.000	-.167**	.363**	-.358**
	Sig. (1-tailed)	.000	.	.007	.000	.000
	N (sample size)	213	213	213	213	213
Rainfall Data (mm)	Spearman's rho	.022	-.167**	1.000	-.197**	.387**
	Sig. (1-tailed)	.377	.007	.	.002	.000
	N (sample size)	213	213	213	213	213
Salinity (ppt)	Spearman's rho	-.285**	.363**	-.197**	1.000	-.490**
	Sig. (1-tailed)	.000	.000	.002	.	.000
	N (sample size)	213	213	213	213	213
Turbidity (NTU)	Spearman's rho	.209**	-.358**	.387**	-.490**	1.000
	Sig. (1-tailed)	.001	.000	.000	.000	.
	N (sample size)	213	213	213	213	213

2.3 Results and Discussion

2.3.1 Temporal scale variability between monitored parameters

Plotting time-series data can give insights into seasonal trends, patterns, changes and sudden events more quickly than other data exploration tools. An event in time series is characterised by an interval of measurements that differs significantly from some underlying baseline threshold. The difficulty in identifying these events is that one must distinguish between events that could have occurred by chance and events that are statistically significant [120].

For an improved understanding of the trends arising from temporal variations, measured parameters were averaged for each day (over 24 h, 96 data points) and a plot of turbidity, salinity, DO and tidal heights is shown in Fig. 2-4. The temperature and DO profiles match the seasonal variation, with the first one decreasing during the cold season and the second one increasing (Fig. 2-4b). The inverse relationship between DO and temperature is a natural process since the solubility of oxygen in water is temperature dependent. As a result, warmer water bodies become more easily saturated with oxygen and can hold less DO.

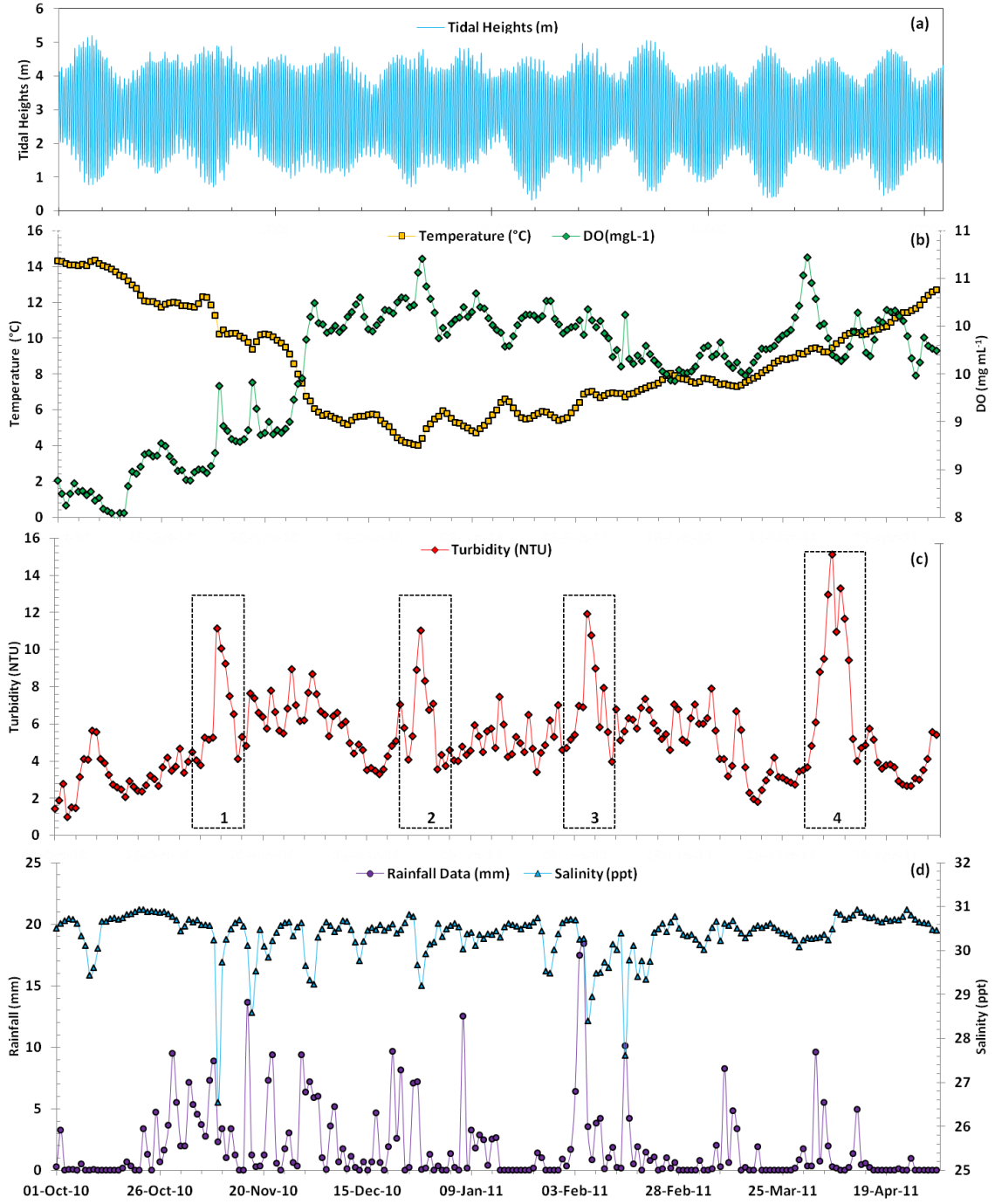

Figure 2-4 Time series of daily averaged data collected during the 7-month deployment period; a) Tidal heights illustrating neap and spring tides; b) Temperature and dissolved oxygen; c) Turbidity; d) Rainfall and salinity; 1,2,3,4 in c) highlight the 4 turbidity events identified during the deployment [112].

Averaged daily data indicated that four turbidity events occurred during the deployment period (Fig. 2-4c). Analysis of rainfall data (Fig. 2-4d) and tide height data (Fig. 2-4a) suggested that the first 3 of these events were caused by heavy rainfall accompanying a spring tide. Tidal amplitude at Poolbeg ranges from 0.5 m during neap tide periods up to 2.5 m during spring tides (Fig. 2-4a). Increased river flow during rainfall events combined with ebb flow periods during spring tides cause discernible changes in the stratification and mixing at the monitoring site. This is primarily attributed to changes in the location of the saltwater wedge, whereby increases in the percentage of freshwater in the water column causes a drop in salinity at 2.5 m from the water surface (Fig. 2-4d). The resulting brackish water has a lower salt concentration, and can retain higher dissolved gas concentrations, explaining the higher DO levels during the first 3 events (Fig. 2-4b). The input of organic matter, nutrients and suspended sediments associated with runoff and freshwater input explain the increased turbidity levels (Fig. 2-4c).

The signature and causes of the 4th event observed in April 2011 (Fig. 2-4) differs from the previous three events described. As this is the start of the increased primary production period owing to water warming at this latitude and season, it is likely that increased turbidity can be related to increased phytoplankton growth. Prior the measured sustained increased in turbidity, an increased level of DO is recorded, without a corresponding decrease in salinity levels as recorded in previous events (Fig. 2-4b). DO levels rise in the initial stage of this process owing to higher photosynthetic rates of autotrophs during daylight hours. In the latter stage, the decay of primary producers causes an increase in turbidity and a decrease in DO levels as a consequence of more organic material available for digestion by other micro-organisms. At the same time, day vs. night DO variations during the 4th event are higher than prior to or after the event (Fig. 2-5 a,b). To investigate this observation, four days of DO data were selected within the event (from 4th April until 8th April) and four days of DO data were selected before the event (March 20th until March 24th). The data is parametric and an independent t-test was performed to check the variance within the 2 groups. The difference between DO levels before the event and DO levels after the event is significant $t(766)=2.034$, $p<0.01$. Levene's test indicated unequal variances ($F=83.99$, $p < 0.01$). The observations in this event were substantiated by the reported occurrence of an algal bloom on the coast one week later (Fig. 2-5c).

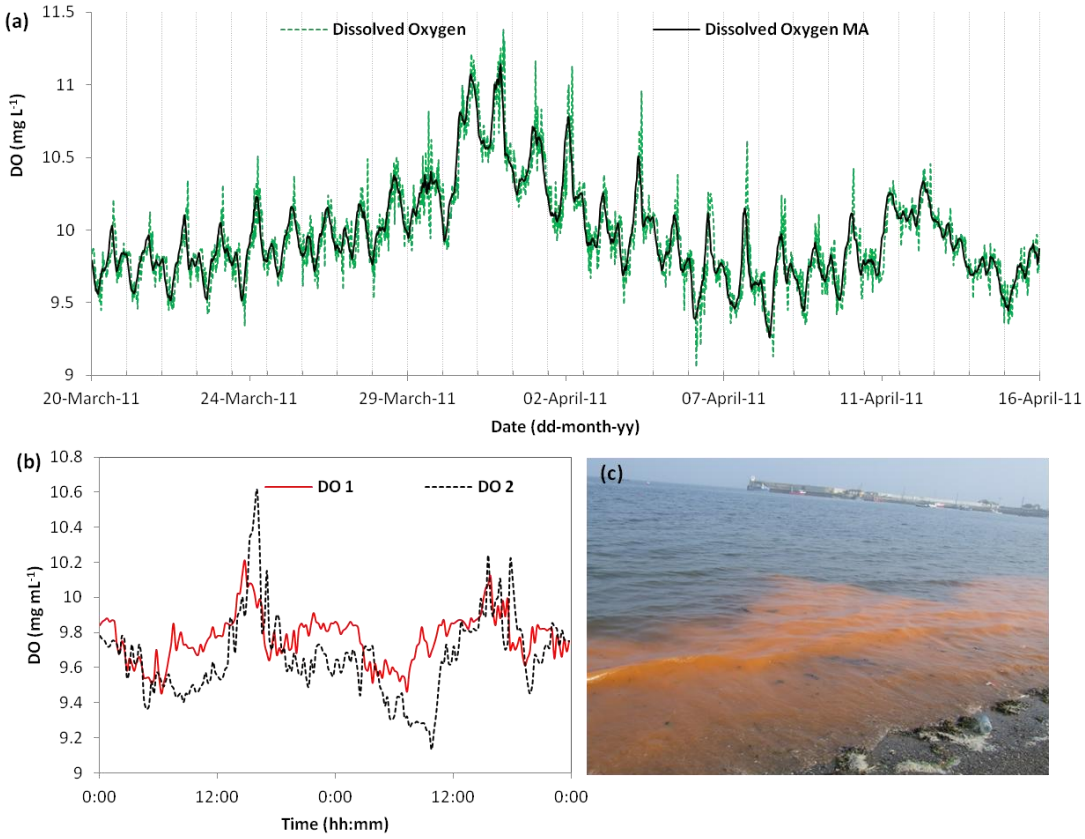

Figure 2-5 a) Time series of raw DO data from the 20th of March until 15th of April showing the diurnal DO cycle before, during and after the 4th event. Dissolved Oxygen MA represents the 3 h moving average for the DO data. Minor gridlines are set to show the daily cyclical DO variation; b) DO levels showing the diurnal DO cycle before the event and during the event. DO 1 represents the data collected on the 20th and 21st of March 2011 and DO 2 represent the data collected on the 7th and 8th of April 2011 c) Picture taken by the Skerries Coast Guard on 19th of April showing the impact of an algal bloom [112].

Results presented here indicate that *in-situ* physicochemical parameters like turbidity, DO, temperature and salinity, supported by meteorological data can be used to advance the understanding of such complex and dynamic environments.

2.3.2 Turbidity results and the influence of ship traffic

Initial results indicated that turbidity levels originating from vessels arriving was considerably higher than vessels departing from Dublin Port. This matter was further

investigated on site, and the manoeuvring patterns of vessels were recorded in detail over several days. Large conventional commercial craft are limited to speeds of between 8 to 15 knots whilst within the jurisdiction of Dublin Port. The lower limit varies with vessel type and is “as safe navigation permits”. Additionally, when docking, vessels usually have to undertake a turning manoeuvre in the channel, before coming alongside the dock (Fig. 2-6b). This manoeuvre frequently involves use of lateral propulsion systems (bow thrusters), resulting in further re-suspension of bed sediments. The impact of this intensive mixing and stirring has been observed visually and confirmed with *in-situ* sensor readings (Fig. 2-6a). Observation of the differences between turbidity readings associated with arrival and departure of one vessel, have led to the conclusion that the auxiliary systems used for this procedure have a higher impact on the re-suspension of sediments than those solely associated with direct vessel transit across the port. The sudden increase in turbidity co-occurred with increased DO and decrease in salinity and temperature (Fig. 2-6c). This results not only in re-suspension of riverbed material but also in artificial upwelling at this location, considered a negative effect of motorised aquatic traffic [121].

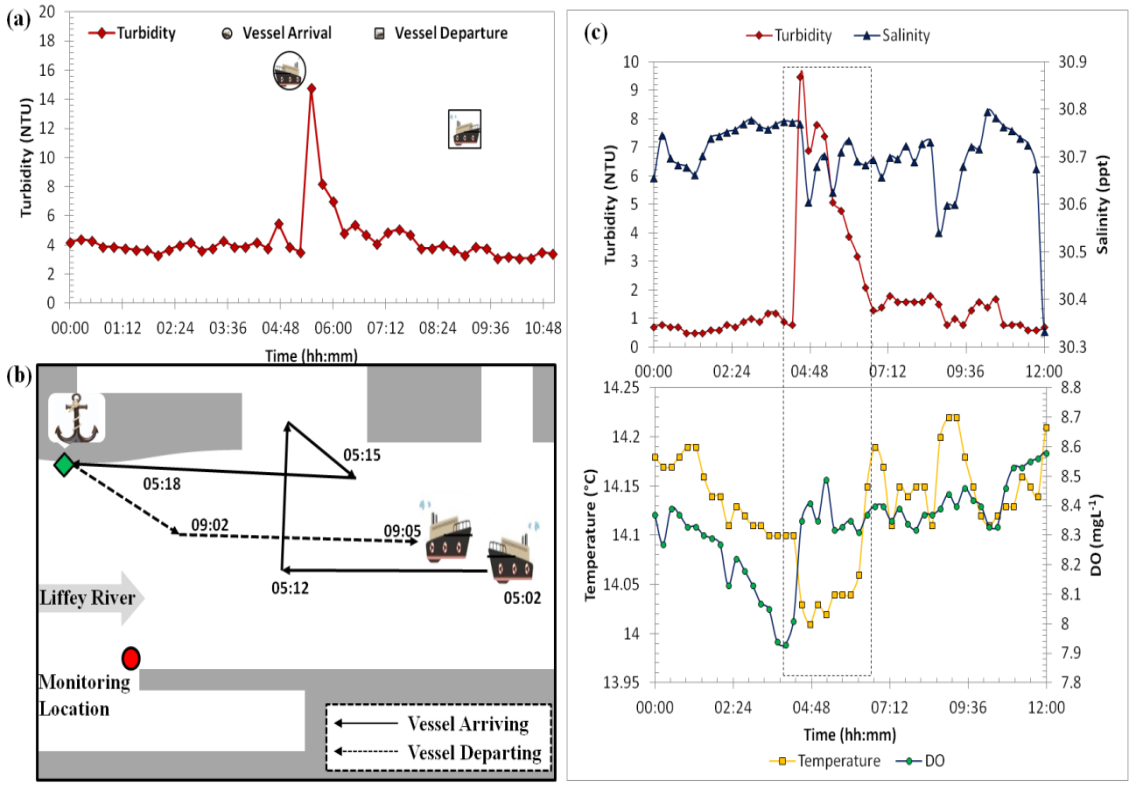

Figure 2-6 Different effects of arriving and departing vessels on turbidity (a) Time series of arriving and departing vessels (as recorded by Dublin Port Authority) and the turbidity sensor readings; (b) Graphical representation of a typical vessel docking manoeuvre pattern in Dublin Port and the associated time stages; (c) Example of vertical mixing at the site showing turbidity, temperature, DO and salinity data, due to vessel manoeuvring [112].

To further understand the long-term influence of ship traffic on re-suspension of sediments, the dataset containing turbidity readings was averaged for each time of the day when the measurement was recorded (Fig. 2-7b). It was found that means turbidity values increase in the morning from 04:30 and reach a maximum value around 06:00. This pattern is repeated in the evening, with slightly lower mean values, and is absent at midday. This origin of this pattern is explained in Fig. 2-7a, where three days with close or the same vessel arrival and departure times were selected. The turbidity data recorded for this period was plotted against arrival and departure times. This demonstrated that arriving ships have a pronounced effect on the collected turbidity data, particularly in the morning and in the evening. Vessel arrival coincided with sharp increases in turbidity, followed by a steady decrease in turbidity levels.

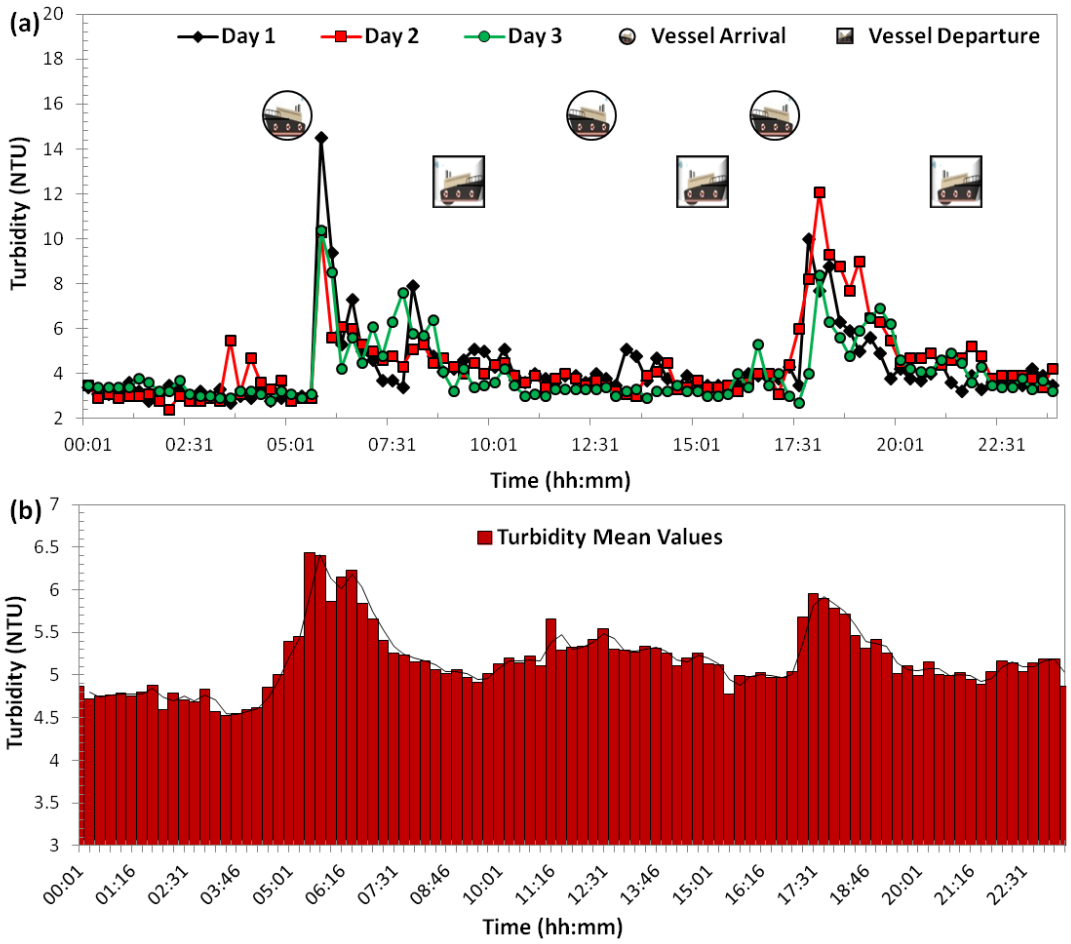

Figure 2-7 The impact of ship traffic in Dublin port on turbidity levels on short and long time scales showing similar patterns; (a) Time series of turbidity readings for 3 different days and time series of arriving and departing vessels. The 3 days were selected so that the arrival and departure times are similar (± 15 min). (b) Average turbidity values for the entire data set at each sampling time during the course of 24 hours [112].

High turbidity levels in the morning are surprising, (Fig. 2-7b) given that port activity is lower at this point than it is at midday or in the evening. This may be explained by re-suspension of fine sediments with lower critical shear stress accumulated during night [95]. Arrival of the first vessel is, in most of the cases, the first event that disturbs the environment after the night settling period. Fine particles and organic material accumulated during night will be mixed in the water column and eventually flushed downstream in the estuary. The arrival of the second vessel causes no visible effect on turbidity and in most cases arrival time cannot be identified from the turbidity values.

The mean turbidity values from the midday period are lower and the distribution peak is broad compared with morning and evening periods. There are two possible reasons for this pattern: easily re-suspended sediments with low critical shear stress from the top layer of the river bed were already flushed downstream or were already suspended by the previous ship passages; or the remaining sediments with a higher critical shear stress are not able to follow the same process resulting in a lower value of turbidity. Turbidity is not a volume dependent measurement, meaning that even if there is most likely a higher mass of suspended material in the water body attributed to intensive ship traffic, the concentration per unit volume of water is lower owing to advection and dispersion of the suspended material by the previous traffic activity. The 2nd reason for the pattern is the tidal cycle. Tidal cycle is one of the major driving forces governing re-suspension dynamics, controlling distance between riverbed and vessel propulsion systems. Erosion and re-suspension processes occur when bottom shear stress exceeds threshold critical values [122]. Small clearances between the ship and the riverbed generate higher energy events on bed sediments and higher amounts of sediments being re-suspended. Vessels arriving at low tide have a higher impact on the turbidity readings while vessels arriving on high tides have a lower impact. Fig. 2-8 shows two different tidal days and the impact of ship arrivals on the turbidity readings. These findings suggest that most of the re-suspension events recorded as sharp turbidity peaks above the baseline level are caused by vessels arriving in the port when the water level is relatively low. This is true most of the times but exceptions exist. Fig. 2-8b, shows that vessels arriving on high tide cause re-suspension as well (peak at 17:15), although the effect is smaller. Depending on the weather conditions, wind direction and speed, and how busy the port is, vessel manoeuvring time within the port is variable. Vessels need longer times to turn in the presence of high wind speeds, especially when the wind blows seawards. This prolonged effort generates higher energy events on the river bed sediments and eventually causes re-suspension even though the vessel arrives on high tide. The second explanation for the re-suspension is the flood tide, which slowly pushes upstream (towards the location of the sonde) the turbidity plume formed after the turning manoeuvre.

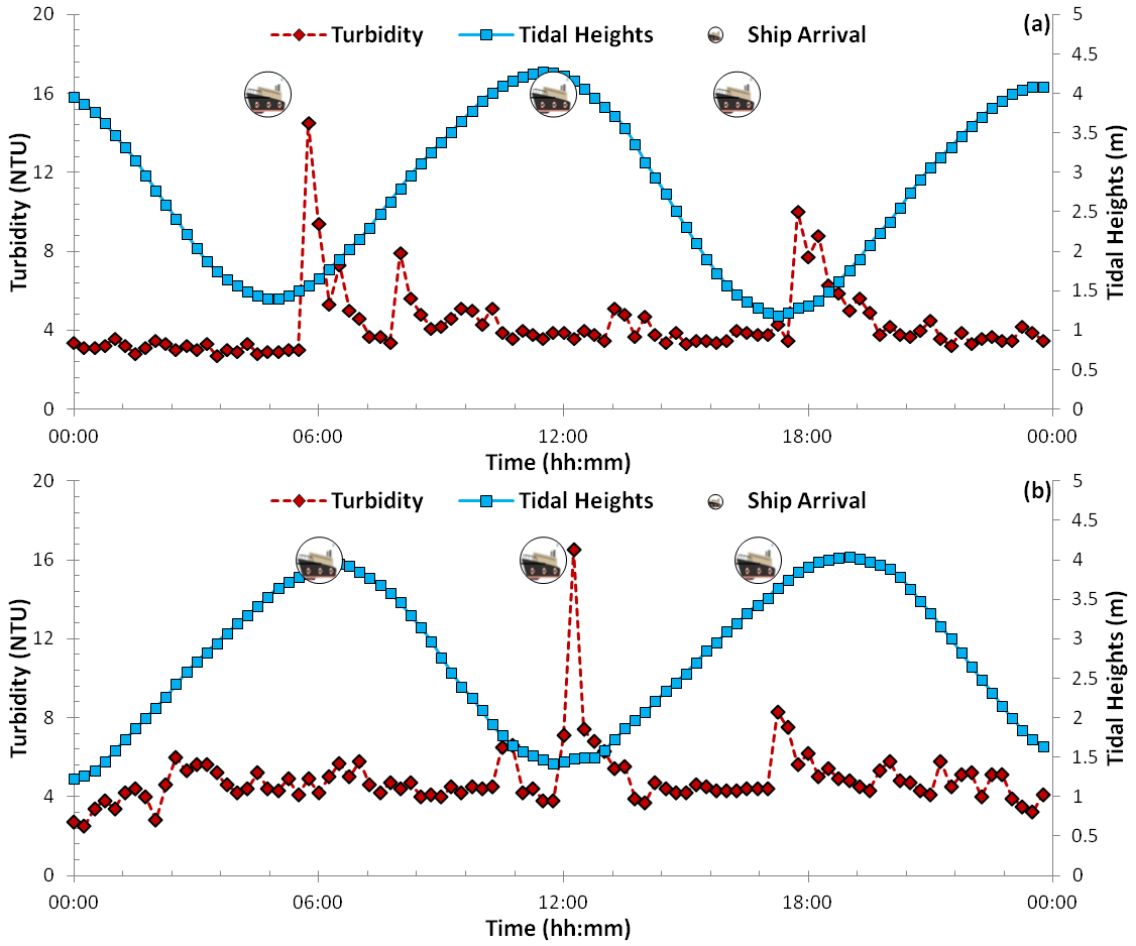

Figure 2-8 Effect of ship traffic on turbidity readings during flood and ebb flows in Dublin Port. (a) Time series of turbidity, tide height and vessel arrival times in a day with low tide in the morning and evening; (b) Time series of turbidity, tide height and vessel arrival times on a day with low tide at midday and midnight [112].

To further investigate the statistical relevance of ship traffic on water quality in Dublin Port, collected turbidity data were separated into seven groups based on time of day. Turbidity data were assigned to 7 groups (labelled 1:7), corresponding to a time period over the course of 24 h. Group 1 contained the turbidity data collected within 00:00 and 04:00 interval, group 2 (04:00-07:00), group 3 (07:00-10:00), group 4 (10:00-14:00), group 5 (14:00-16:00), group 6 (16:00-19:00) and group 7 (19:00-24:00). A Kruskal-Wallis statistical test was performed to determine significant differences between the turbidity readings from the seven groups. The test has revealed a significant difference ($X^2(6) = 92.842$, $p < 0.01$). Boxplots of all groups indicates that the 2nd, 4th and 6th

assigned groups have the highest medians. A further Mann-Whitney test for 2 independent variables was used as a post-hoc test. Group no.1 was selected as control for comparison as this group represents turbidity measurements obtained from 00:00-04:00 when vessel activity in Dublin Port is least. The Mann-Whitney test with Bonferroni correction showed the significant difference between group 1 and 2 ($p < 0.01$, $r= 0.21$), group 1 and 4 ($p < 0.01$, $r= 0.18$) and group 1 and 6 ($p < 0.01$, $r= 0.24$). This test was made assuming no large vessel traffic within the 00:00-04:00 interval, and the effect sizes of ship traffic on turbidity (r values) are calculated based on this assumption. In reality, this is not entirely true and the effect size values represent only a portion of the real effect of ship traffic on turbidity readings. Since it was not possible to split the turbidity data into more accurate time-based groups (relative to the vessel arrival times), this also limits the actual effect size, by decreasing the median values of each group. Nevertheless, it was found that ship traffic has a small-medium effect on the turbidity data within the time stages relative to the arrival of vessels.

2.3.3 Comparison between turbidity events associated with natural events and ship traffic.

Turbidity events caused by ship passage were usually short lived between 1 and 2 h, Fig. 2-7a. The turbidity spikes were characterized by a sharp increase, followed by a relatively quick decrease due to higher settling velocities of heavy particles. After this initial stage the turbidity decrease rate slows down as the concentration of suspended sediments approaches background levels. This behaviour is consistent with the findings of [123] in the Port of St. Petersburg, Florida.

Besides anthropogenic activity related to ship traffic within the estuary, turbidity levels were also influenced by heavy rainfall. Daily rainfall was found to be moderately correlated with average daily turbidity levels ($R = 0.387$, $p < 0.01$). Fig. 2-9a shows the impact of a heavy rainfall event on the turbidity levels at the site. A moving average of 10 data points was used to smooth the turbidity data set. In contrast to ship traffic, rainfall was found to generate long-term turbidity events, characterised by sustained background turbidity levels (Fig. 9a). This is due to the continuous freshwater input carrying debris and contaminants from urban runoff. The less dense freshwater sitting on the top moves seaward and slowly mixes with the seawater, giving rise to higher

turbidity values at the site. Rainfall events were also distinguished using the salinity data (Fig. 9b) which decreases and confirms the freshwater intrusion.

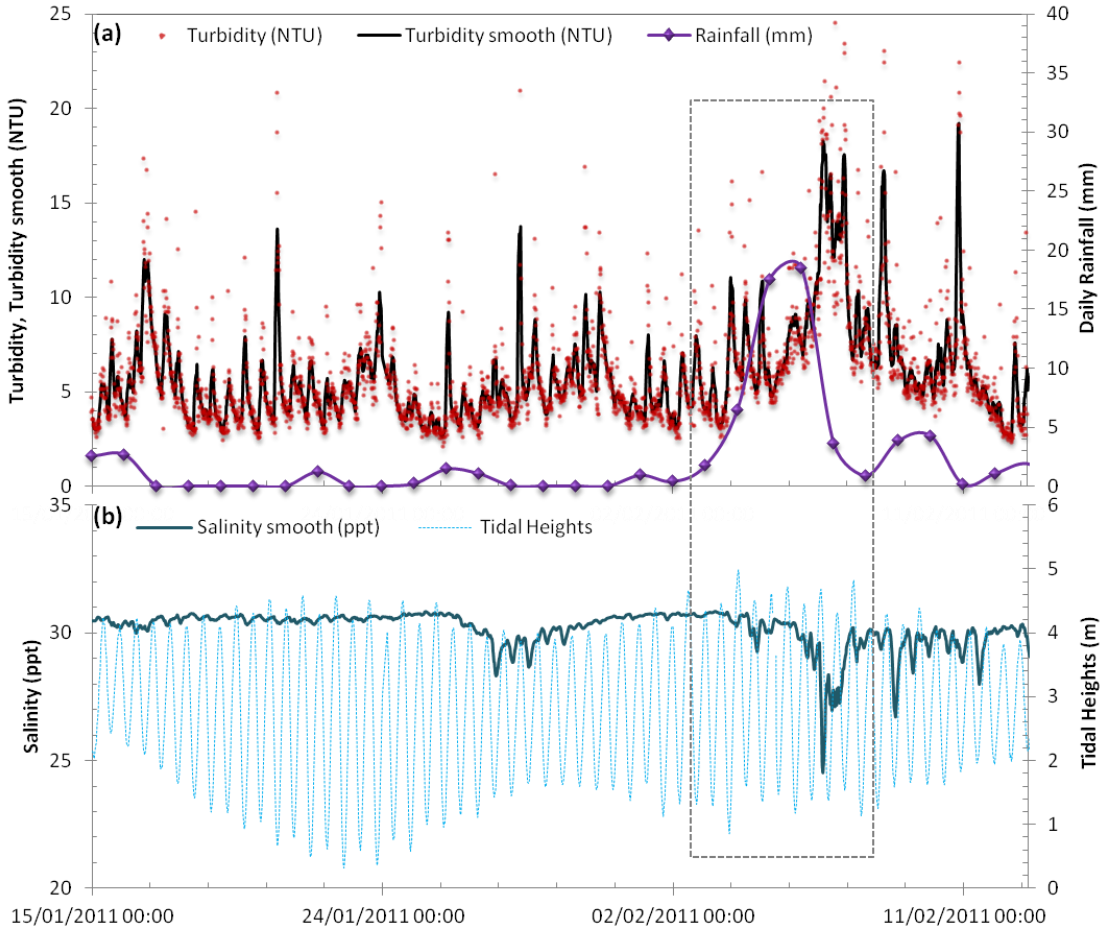

Figure 2-9 Time series showing the effect of a heavy rainfall event from 5th to 8th February 2011 on the *in-situ* turbidity readings (a) and *in-situ* salinity (b). Turbidity smooth data series was generated from Turbidity using a 10 data points moving average [112].

No significant correlation was found between tidal heights and turbidity data. Although in Fig. 2-8 we show that vessels arriving on low tide are more likely to cause re-suspension that the ones arriving on high tide, this effect is not visible when looking the two variables plotted against each other (Fig. 2-10a). This effect is expected due to background turbidity variability (seasonal, weather conditions) but also due to the fact that the number of data points generated during ship traffic events is much lower than the total number of data points. Fig. 2-10b shows that the shape of the relationship

between turbidity and tidal height (Fig. 2-10a) is mostly driven by the frequency distribution of tidal heights.

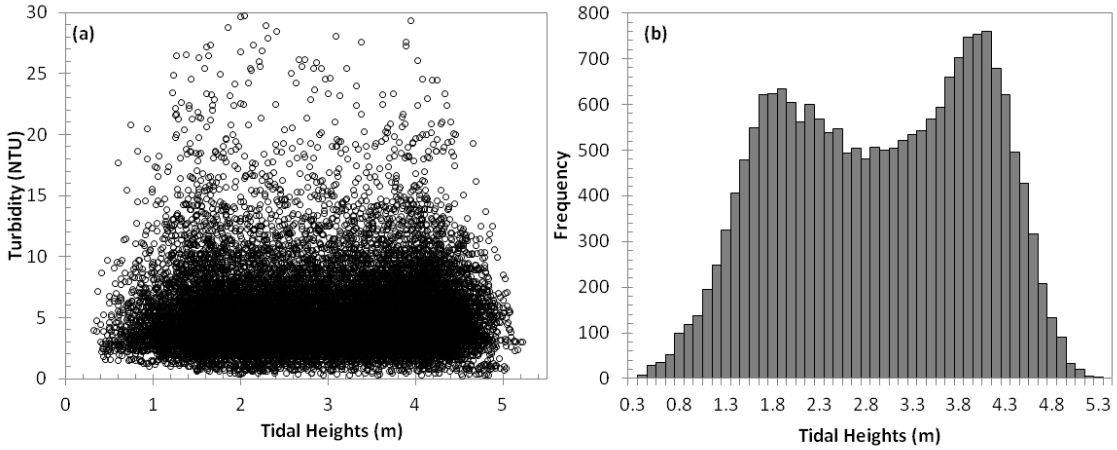

Figure 2-10 (a) Relationship between turbidity and tidal heights and (b) tidal heights frequency distribution over the deployment period [112].

2.3.4 Discrete sampling and ship traffic effect

The Bathing Water Directive (Directive 2006/7/EC) was implemented across all member states of the European Union from 2008-2013 [69]. Under this directive, classification of bathing water in "excellent", "good" and "sufficient" quality is based on the microbial indicators *E. coli* and intestinal Enterococci. Dublin Bay provides recreational opportunities for a third of Ireland's population, and is surrounded by three important recreational areas: Sandymount Strand, Merrion Strand and Dollymount Strand [124]. Therefore, it is essential to understand all the environmental conditions and factors that contribute to changing FIB concentrations in Dublin Bay.

For this purpose a sampling plan was designed to investigate for the possible effect of ship traffic on the *E. coli*, Enterococci and TSS loads. To account for vertical distribution along the water column, water samples were collected at different depths before and after the scheduled morning vessel arrival. Results from 2 sampling days, August 15th 2012 (Day 1) and September 7th 2012 (Day 2) are represented in Fig. 2-11 and 12. A concentration gradient in the water column for FIB data was noticed for the

samples collected before the arrival with higher bacteria densities recorded in the surface water layer (0.5m). This is expected since the bottom layer represents a mixture of fresh water input from the Liffey River and saline bay water. The fresh water contains higher levels of faecal indicators accumulated from runoff and diffuse point source pollution [125]. Bedri Z. *et al.* has used a hydro-environmental model to study the impact of the Ringsend Treatment Works discharges of *E. coli* on the water quality of Dublin Bay. Results from the model, which accounted for wind speed, tidal cycle, density differences within the water column and flow velocities indicate that *E. coli* levels at the deployment site in this study are not affected by the Ringsend Treatment Works discharges [111]. The second reason for the presence of the concentration gradient is the increase osmotic pressure bacteria are subjected to in the water column. Salt rich environments cause the water to leave the cell and permeate trough the cell wall leaving the bacteria dehydrated. This eventually leads to the death of bacteria. On both days (Fig. 2-11, 2-12) *E. coli* and Enterococci counts increase after vessel arrival, at all depths, suggesting the source of enrichment is not coming from mixing of the water column but rather from re-suspension of sediment associated microorganisms. The largest difference was recorded on Day 2 of this intensive sampling period, when *E. coli* and Enterococci levels were up to 9 times and 3 times higher respectively in samples collected after ship passage (data at 0.5 m Fig. 2-12). To further test this hypothesis, sediment samples were collected for microbial analysis on Day 2. The results recorded were as follows: Enterococci $18.9 \times 10^3 \pm 1.2 \times 10^3$ MPN GDW^{-1}; *E. coli* $13.2 \times 10^3 \pm 0.9 \times 10^3$ MPN GDW^{-1} and coliforms $89.3 \times 10^3 \pm 12.4 \times 10^3$ MPN GDW^{-1}. These results are consistent with results from other studies reviewed by Pacepsky and Shelton [106], demonstrating again that enrichment of the water column originated from bottom sediments and not from mixing of the buoyant top layer of fresh water with denser saline water underneath. The present findings are particularly pertinent because there is only one other study [126] that addresses re-suspension of sediment associated faecal indicators attributed to ship traffic in a river, but no study which addresses this matter in estuarine environments or ports. The implications of this work for the management of microbial water quality are important, since the presence of bottom sediments containing large reservoirs of faecal indicator bacteria can potentially introduce substantial uncertainty in monitoring and control. These bacteria should not be considered as indicators of recent faecal pollution, but still be regarded as risk-

associated indicators [106]. Evaluation of best management practices should include effects of sediment re-suspension on chemical and microbial water quality due to ship traffic and also incorporate these data into future predictive models.

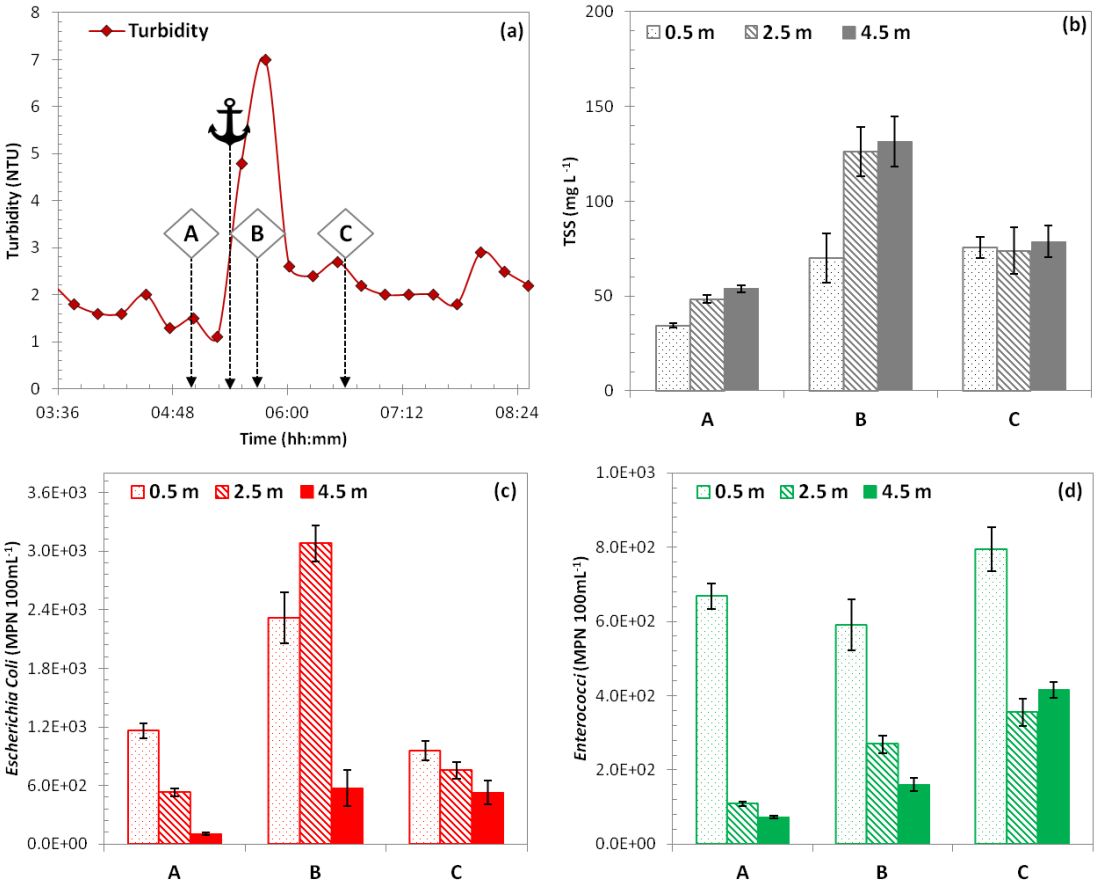

Figure 2-11 Analysis of discrete water samples collected on 15th August 2012. a) Time series of turbidity readings collected from the sonde; A,B,C represent the sampling times and the anchor represents the vessel docking times; b), c), d) TSS, *Escherichia coli* and Enterococci results from samples collected at times A,B,C and at different water depths: 0.5 m, 2.5 m and 4.5 m (Error bars represent SD, n = 3) [112].

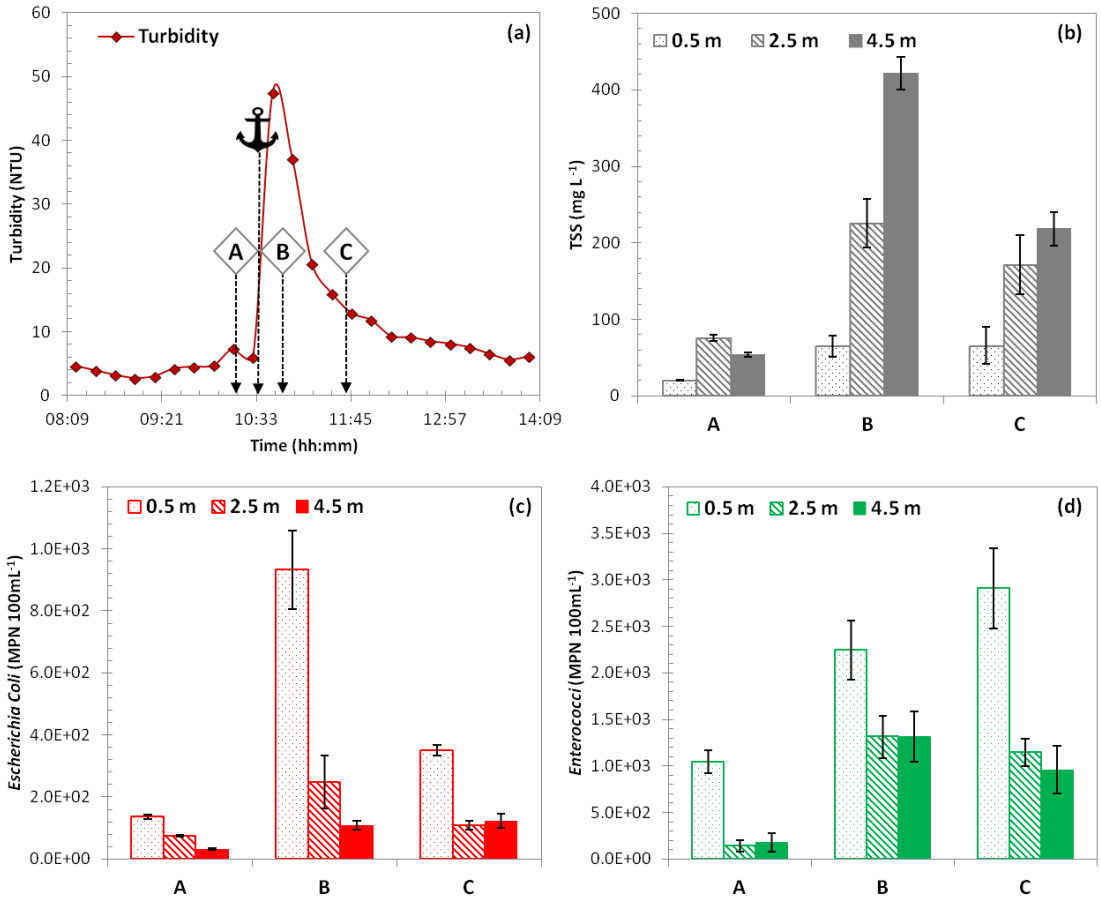

Figure 2-12 Analysis of discrete water samples collected on 9th September 2012. a) Time series of turbidity readings collected from the sonde; A, B, C represent the sampling times and the anchor represents the time at which the vessel has docked; b), c), d) TSS, *Escherichia coli* and Enterococci results from grab samples collected at times A, B, C and at different water depths: 0.5 m, 2.5 m and 4.5 m (Error bars represent SD, n = 3) [112].

2.4 Conclusions

The findings of this study advance understanding of estuarine environments and demonstrate the advantages of judicious use of continuous monitoring in such environments. Continuous monitoring of parameters like DO, turbidity, salinity and temperature have proven to be a valuable tool, providing far greater insight into the complexity and temporal heterogeneity than possible with discrete sampling regimes of areas such as Dublin Port,. This study has shown that such systems are powerful tools that can inform discrete sampling regimes and that these two approaches should be regarded as complementary. We have shown this by examining sporadic turbidity events, mostly attributed to vessel activity in Dublin Port resulting from re-suspension of sediments by vessel propulsion systems. We have shown that these events are an important driver of microbial contamination levels and characteristics of the water column at any particular instant in time. Such effects are strongly related to water level at vessel arrival times. Vessels turning around at high water levels appear to have little effect on *in-situ* turbidity in the reaches of Dublin Port. Statistical analysis indicates that shipping entering and exiting Dublin Port has a small-medium effect on the turbidity data.

Importantly, it has been demonstrated from this study that benthic sediments in Dublin Port are a reservoir for *E. coli* and Enterococci, to the extent that re-suspension of these pollutants is undesirable. *E. coli* levels associated with vessel arrival were increased up to nine fold, while Enterococci levels increased 3 times. Thus, sampling outside of re-suspension events associated with shipping can greatly underestimate microbial and pollutant contamination levels. Even short-term, high-frequency (sub-hourly) continuous monitoring of water column parameters can inform sampling regimes for such dynamic environments. In this study, both daily and averaged turbidity data show a similar pattern with the highest turbidity values recorded in the morning period between 05:00 and 07:00 after the arrival of the first vessel. This indicates that the water quality at the site is not homogeneous for the duration of 24 h. The most likely higher concentrations of pollutants will occur in this period than in any other time of the day as a consequence of the re-suspension of fine sediments and organic detritus accumulated during night. These findings have led to the conclusion that if relevant monitoring is to

be performed at the site, sampling times should take these daily variations into account, for a more representative estimation of the water quality.

3 CONTINUOUS FLUOROMETRIC METHOD FOR MEASURING Β-GLUCURONIDASE ACTIVITY: COMPARATIVE ANALYSIS OF THREE FLUOROGENIC SUBSTRATES

ABSTRACT

E. coli β-glucuronidase (GUS) activity assays are routinely used in fields such as plant molecular biology, applied microbiology and healthcare. Methods based on the optical detection of GUS using synthetic fluorogenic substrates are widely employed since they don't require expensive instrumentation and are easy to perform. In this study three fluorogenic substrates and their respective fluorophores were studied for the purpose of developing a continuous fluorometric method for GUS. The fluorescence intensity of 6-chloro-4-methyl-umbelliferone (6-CMU) at pH 6.8 was found to be 9.5 times higher than that of 4-methyl umbelliferone (4-MU) and 3.2 times higher than the fluorescence of 7-hydroxycoumarin-3-carboxylic acid (3-CU). Michaelis-Menten kinetic parameters of GUS catalysed hydrolysis of 6-chloro-4-methyl-umbelliferyl-β-D-glucuronide (6-CMUG) were determined experimentally (K_m = 0.11 mM, K_{cat} = 74 s^{-1}, K_{cat}/ K_m = 6.93 x 10^5 $s^{-1}M^{-1}$) and compared with the ones found for 4-methyl-umbelliferyl-β-D-glucuronide (4-MUG) (K_m = 0.07 mM, K_{cat} = 92 s^{-1}, K_{cat}/ K_m = 1.29 x 10^6 $s^{-1}M^{-1}$) and 3-carboxy-umbelliferyl-β-D-glucuronide (3-CUG) (K_m = 0.48 mM, K_{cat} = 35 s^{-1}, K_{cat}/ K_m = 7.40 x 10^4 $s^{-1}M^{-1}$) . Finally a continuous fluorometric method based on 6-CMUG as a fluorogenic substrate has been developed for measuring GUS activity. When compared with the highly used discontinuous method based on 4-MUG as a substrate it was found that the new method is more sensitive and reproducible (%RSD=4.88). Furthermore, the developed method is less laborious, faster and more economical and should provide an improved alternative for GUS assays and kinetic studies.

3.1 Introduction

β-glucuronidase (EC 3.2.1.31) enzymes catalyze the hydrolysis of β-D-glucopyranosiduronic derivatives into their corresponding aglycons and D-glucuronic acid sugar moieties. β-glucuronidase (GUS) is a globular protein, active as a homotetramer and made up of 603 amino acids [70]. The enzyme is active as a homotetramer because the active sites contain elements of two neighbouring monomers, as revealed by the crystal structure (Fig. 3-1) [127]. The active site residues of the enzyme are highly conserved. GUS enzyme retains the anomeric configuration of the glucuronic acid and is appropriately termed a retaining hydrolase [71]. The enzyme has three important residues that participate in the break-down of glucuronides. It breaks down the O-glycosyl bond by nucleophilic attack with the nucleophilic residue being Glu504 (equivalent to Glu540 in humans). The acid-base residue is Glu413 (equivalent to human Glu451) while the residue Tyr468 (Tyr504 in humans) has been proven important but its role is not clear [71, 72]. Matsumura and Ellington [73] modelled the *E. coli* GUS against the human crystal structure and proposed that seven conserved residues (Asp163, Tyr468, Glu504, Tyr549, Arg562, Asn566 and Lys568) form eight intermolecular hydrogen bonds with the substrate. This bonding is thought to confer the typical specificity of GUS to β-D-glucuronide based substrates. In a more recent study, Wallace *et al.* determined the crystal structure of bacterial GUS and when they aligned the sequence of *H. sapiens* GUS with the *E. coli* GUS they found a 45% sequence identity between the two. Furthermore they discovered the *E. coli* GUS contains a 17-residue "bacterial loop" which is not found in the human ortholog and they used this for selecting GUS inhibitors in the gastro intestinal tract [127].

GUS enzymes have been found in animals, plants and microbes and their function and characteristics are subject to intensive studies in fields such as human healthcare, biology, microbiology and environmental monitoring [128]. GUS *in-vitro* assays are extensively performed in various fields. In plant molecular biology, the GUS gene from *E. coli* is widely used as a reporter gene for the study of gene regulation in transformed plants [129] Gene expression in cells and tissue of transgenic plants is routinely studied using the GUS fusion system [130] GUS assays are routinely used for diagnostic purposes but also for specific detection of *E. coli* in water and food samples. When tested, GUS-positive reactions were observed in 94-96% of *E. coli* isolates [74-76] GUS

has been exploited as a marker enzyme for *E. coli* by the implementation of GUS targeted substrates into growth media [131]. In this approach, the target bacteria are selectively grown and GUS activity is used as a confirmatory step. Direct measurement of GUS activity, without the culturing of target bacteria has also been used [81] In this case, the detection relies on measuring *in-vitro* GUS activity and the procedure is much quicker (3-4 h) and relatively easy to perform [81] The numerous applications mentioned above demonstrate the importance of developing a simple, sensitive, reliable and high-throughput method for measuring GUS activity. Methods based on optical detection of GUS activity are particularly attractive since they don't require expensive instrumentation and they are easy to perform routinely. For this purpose synthetic substrates made up of glucuronides linked to a chromophore or fluorophore have been designed for GUS [34] Colour formation or fluorescence due to the hydrolysis of the synthetic substrates can be recorded. In general, chromogenic substrates are phenol-based, water soluble, heat stable and specific and occur in a wide range of different colours [34]. Although a few chromogenic substrates have been used for GUS, the use of fluorogenic substrates is more appealing. Fluorescence based techniques are usually 1000-fold more sensitive than absorbance based ones. The most common fluorogenic substrate is 4-methyl-umbelliferyl-β-D-glucuronide (4-MUG) which, upon hydrolysis, releases the fluorescent aglycon 4-methyl umbelliferone (4-MU) (Fig. 3-1) [132]. The major drawback of 4-MU is its high pKa value of 7.8, which causes only partial dissociation at pHs around the optimum pH for GUS activity. To overcome this issue, researchers have employed discontinuous enzyme assays which require the addition of alkali. This has the dual purpose of increasing the pH and of stopping the reaction due to GUS deactivation [129]. Discontinuous assays have certain limitations when compared to continuous ones. For example, the continuous methods offer a more straightforward approach, where instant visualisation of the kinetic data enables prompt evaluation of the assay. Also, reagent consumption is minimised together with sample manipulation. Continuous absorbance [133] and fluorescence [134] based methods for measuring GUS activity exist. However, they are limited and cannot be applied when only small quantities of GUS are available.

In recent years new synthetic substrates developed previously are becoming commercially available. Among them, 3-carboxy-umbelliferyl-β-D-glucuronide (3-

CUG) has been recently applied for the detection of *E. coli* GUS in a rugged *in-situ* optical sensor [135]. The author reports a higher fluorescence and solubility of the new fluorophore compared with 4-MU in cold water. Another substrate, 6-chloro-4-methyl-umbelliferyl-β-D-glucuronide (6-CMUG) which enabled higher sensitivity at physiological pH is reported in the literature [136] and it was evaluated for the detection of *E. coli* in a culture based assay [137].

In this context, we describe the development of an efficient continuous fluorometric method for measuring *E. coli* GUS activity. This has been achieved by comparing two relatively new fluorogenic substrates (6-CMUG, 3-CUG) and their aglycons with the universally used 4-MUG (Fig. 3-1). The spectroscopic characteristics of the three substrates and their corresponding aglycons are analysed and compared and eventually the emission/excitation wavelengths are tuned to maximise the performance of the method at physiological pHs. We then evaluate the performance of the newly developed method against the widely used discontinuous one described by Jefferson [129] and we show a better sensitivity and reproducibility can be achieved. Although the present work describes a continuous fluorometric method for measuring *E. coli* GUS activity, the current substrates and data may have application to analysis of GUS enzymes from various other sources.

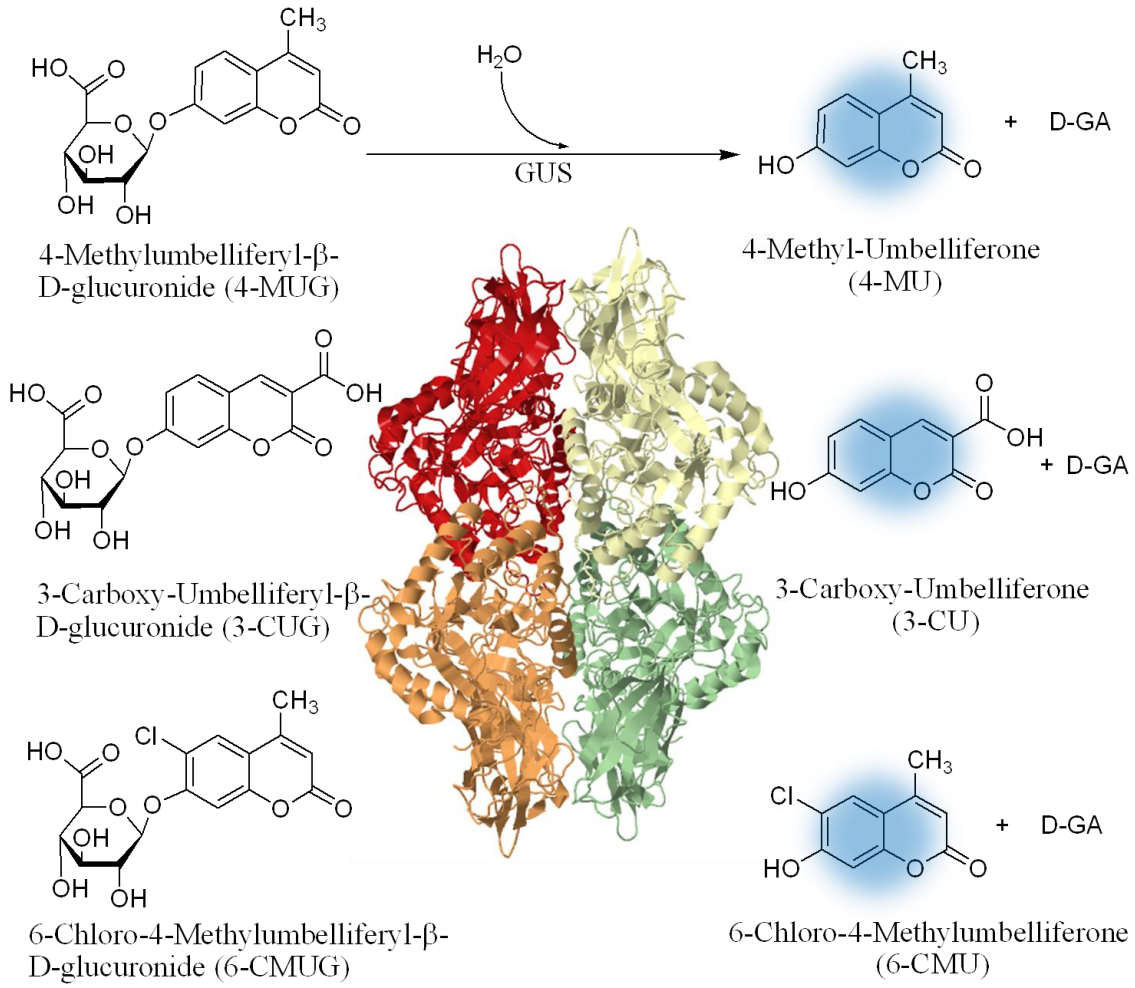

Figure 3-1 Fluorogenic synthetic substrates investigated in this study (left) and their respective fluorophores (right) as hydrolysed by GUS. Crystal structure of the *E. coli* GUS tetramer [127] (middle) rendered with PyMOL (PDB ID: 3k46); D-GA = D-Glucuronic Acid [138].

3.2 Materials and Methods

3.2.1 Materials

E. coli β-glucuronidase type VII-A (27% purity), sodium phosphate monobasic and dibasic, sodium carbonate, sodium bicarbonate, sodium citrate, citric acid, 1,4-dithiothreitol (DTT), 7-hydroxyxoumarin-3-carboxylic acid (3-CU) (99%), 4-methyl umbelliferone (4-MU) (99%) and 4-methyl-umbelliferyl-β-D-glucuronide (4-MUG) (99%) were all purchased from Sigma Aldrich Ireland. The other two fluorogenic

substrates 6-chloro-4-methyl-umbelliferyl-β-D-glucuronide (6-CMUG) (97%) and 3-carboxy-umbelliferyl-β-D-glucuronide (3-CUG) (99%) were ordered from Glycosynth Limited (UK) and Marker Gene Technologies (US), respectively. 6-chloro-4-methyl-umbelliferone (6-CMU) (97%) was ordered from Carbosynth Limited (UK). Water was passed through a Milli-Q water purification system.

Buffers were prepared fresh daily from stock solutions, sterilised by autoclaving at 115 °C (200 kPa) for 15 min. pH studies involving GUS reaction rates, pKa calculations and excitation/emission optimisation were performed in a range of buffers at 50 mM spanning from pH 3.0 to 10.6 (Table 3-1). Buffer pH was measured using a Hanna Instruments pH meter with an accuracy of ±0.01 pH units.

Stock solutions of fluorophores and substrates (100 mM) were prepared in 1 mL DMSO (99.5%) and kept at 4 °C. Further dilutions were prepared daily in buffer or deionised water with a final DMSO concentration in the working solution, ranging from 0.01% - 1%. GUS working solutions were kept on ice for the duration of the experiment and were prepared daily from stocks (1 mg mL^{-1} stored at -20 °C).

Table 3-1 Buffer systems used for pH studies.

Buffer System	pH Values (±0.01)
Sodium Citrate/- Citric Acid	3.0, 3.6, 4.0, 4.6, 5.0
Sodium Phosphate Monobasic/- Sodium Phosphate Dibasic	6.0, 6.2, 6.4, 6.6, 6.8, 7.0, 7.2, 7.4, 8.0
Sodium Carbonate - Sodium Bicarbonate	9.2, 10.0, 10.6, 11.4

3.2.2 Methods

3.2.2.1 UV/Vis Spectroscopy

UV/Vis absorption spectra were obtained using a Shimadzu UV-1800 spectrophotometer. All spectra were obtained in the wavelength region spanning from 280 to 700 nm, using a 1 nm data interval.

3.2.2.2 Fluorescence spectroscopy

Fluorescence measurements were performed using two instruments. The first was an LSB 50 luminescence spectrometer from Perkin-Elmer equipped with Monk-Gillieson type adjustable monochromators and a gated photomultiplier tube. The light source was pulsed Xe, producing an output of 9.9 watts. The spectrofluorometer provides automatic correction of excitation spectra for wavelength dependent variations in the exciting lamp intensity. The second instrument was a Jasco FP 8300 Spectrofluorometer equipped with a holographic concave grating in modified Rowland mount monochromator and a 150 watts Xe lamp. A Peltier thermostated single cell holder (ETC-273T) was used to maintain constant temperatures and for temperature studies. Sample cells were 3.5 mL (10x10 mm) and 1.4 mL (10x4 mm) UV quartz cuvettes, equipped with a Teflon stopper (Helma Analytics). Unless otherwise stated all the emission and excitation spectra were recorded using the accumulation mode as an average of 3 scans (with a scan speed of 200 nm min^{-1}). Most of the data presented was obtained using the Jasco FP 8300 instrument, unless otherwise stated in the legend.

3.2.2.3 Kinetic analysis (Michaelis-Menten Model)

Kinetic constants K_m and V_{max} were determined at pH of 6.8 ± 0.02. Reaction velocities were determined at substrate concentrations ranging below and above K_m for each of the substrates. Substrate solutions of varying concentrations were prepared in 50 mM sodium phosphate buffer (pH 6.8) and brought to 20 °C through incubation. Over the course of the experiments room temperature was recorded and it was maintained between 19.5-20 °C (± 0.1). Briefly 2.0 mL of the substrate solution was added to the cuvette, allowed to equilibrate and introduced into the fluorometer (set to time-drive acquisition mode). At this time a background reading of the fluorescence intensity was recorded, setting the excitation and emission maximum as determined for each of the substrates. A 10 µL buffered GUS enzyme solution (0.1 mg mL^{-1}), kept on ice for stability, was added and the cuvette was vigorously mixed. The reaction was monitored by recording the increase in fluorescence intensity with readings taken every 5 s. The conversion from FU to actual product released/time unit was carried out through the use of calibration curves prepared for each fluorophore at each substrate concentration.

3.2.2.4 Temperature optimisation

GUS activity was measured using 6-MUG (0.5 mM), 3-CUG (1 mM) and 4-MUG (0.5 mM) at different temperatures, spanning from 6 °C up to 70 °C. The enzyme concentration was kept constant for the duration of the study (0.2 μg mL^{-1}) and the measurement was performed in a continuous fashion. Briefly, 20 μL GUS (0.01 mg mL^{-1}) was injected into 1.4 mL quartz cuvette containing 0.98 mL buffered substrate solution (pH 6.8) initially warmed/chilled to the desired temperature. The solution was vigorously mixed and placed in the fluorometer where the fluorescence was monitored using the λ_{ex} and λ_{em} maximum of each fluorophore. Measurements were collected every second for 6 min. Reaction rates (FU min^{-1}) were determined using the slope of fluorescence formation after normalisation to 1 min. In the case of high temperatures (50-70 °C), where GUS denaturation was observed, slopes were determined only from the linear part of the data (1-4 min). To convert FU min^{-1} into μM min^{-1} calibration curves were constructed for each of the three fluorophores, at 20 °C using the same instrument settings and conditions as for the progress curves. Corrections to account for the fluorescence dependence on temperature were applied to the final data. An example on how the data was collected for the correction process is presented in Fig. 3-18 for 3-CU. The same methodology was used for 4-MU and 6-CMUG. For each temperature and substrate a control was run without GUS to correct for the auto-hydrolysis of substrate during the assay period.

3.2.2.5 pH optimisation

For pH optimisation, reaction rates were determined using a discontinuous method adapted from Jefferson [129]. Briefly 20 μL GUS (0.025 mg mL^{-1}) was mixed with 0.98 mL buffered substrate (various pH values, Table 3-1) at room temperature, into 1.5 mL Eppendorf test tubes. After mixing the reaction was allowed to equilibrate and achieve maximum velocity for 1 min, when the first 100 μL were collected into Eppendorf tubes containing 0.9 mL stop buffer (200 mM Na_2CO_3, pH 11.4). This was the "time=0" point, and successive 100 μL aliquots were removed at regular time intervals (3, 6, 9 and 12 min). GUS activity (μM min^{-1}) was determined through calibration curves of the three fluorophores in stop buffer and in the presence of substrate. All the experiments were performed in triplicate and a control without GUS was maintained.

3.2.2.6 Analytical performance of the continuous method

To assess the analytical performance of the continuous method described in this paper we used the widely known discontinuous method described by Jefferson [129] as a comparison standard. The same concentration of GUS (5 ng mL^{-1}) was run for 10 times using both methods. Temperature was kept constant at 37 °C and in both methods the reaction was allowed to proceed for 12 min. For the discontinuous method we used the same procedure as described above with the exception that the buffer pH was 6.8. In both methods the same settings were used on the fluorometer to facilitate direct comparison of the fluorescent signal.

3.3 Results and discussion

3.3.1 UV Vis characterisation of substrates and fluorophores

A preliminary study was carried out to investigate the absorption characteristics of substrates and fluorophores at different pH values in different buffers. Absorption spectra of substrates and fluorophores were recorded in acidic, neutral and alkaline conditions and are shown in Fig. 3-2. 4-MUG and 6-CMUG absorption spectra are not influenced by pH in the analysed range and are characterised by absorption bands centred at 318 nm for 4-MUG and 323 nm for 6-CMUG. On the other hand 3-CUG absorption band shifts from 329 nm (neutral and basic pH) to 342 nm (acidic pH). At pH 3.0, 3-CU shows the same absorption behaviour as 3-CUG (Fig. 3-2), with the same absorption band shift (13 nm) from 339 nm to 352 nm. This suggests that in both cases the same transition takes place which is the protonation of 3-carboxylate anion at pH values below 5 [139].

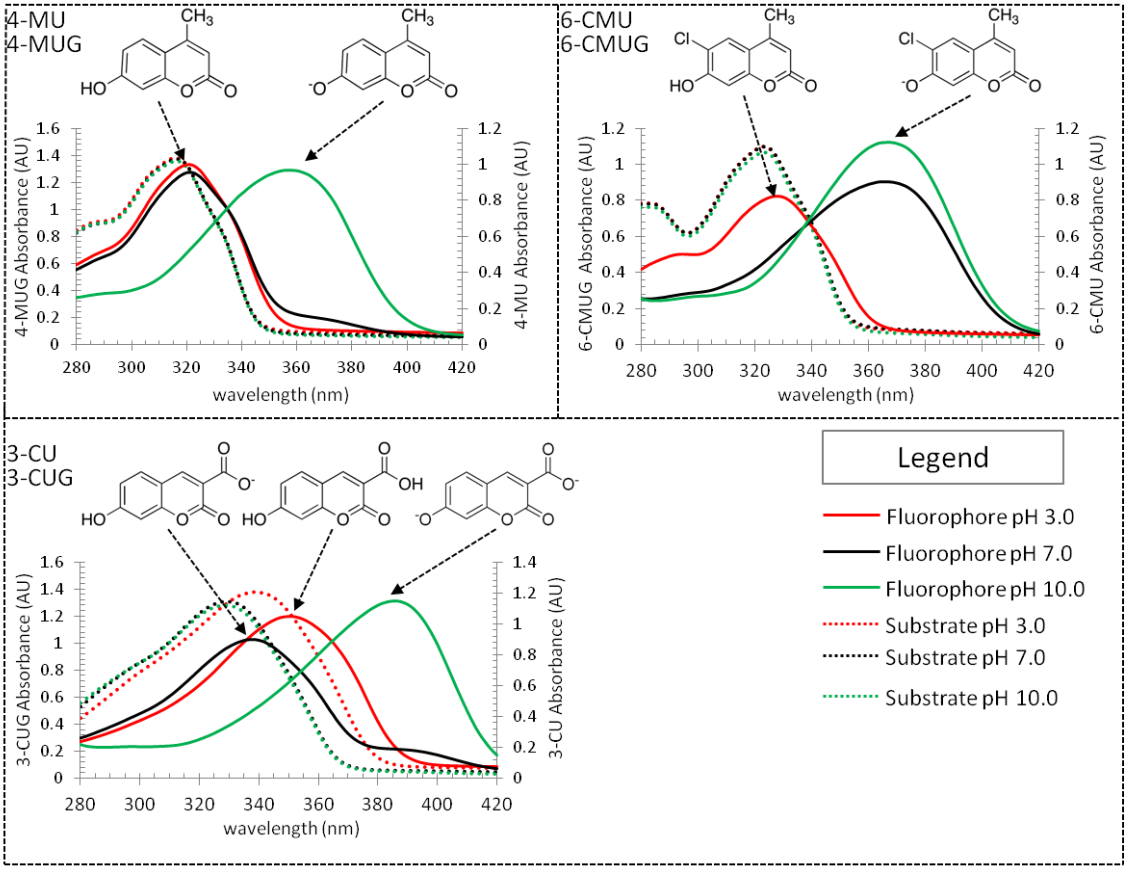

Figure 3-2 Absorbance spectra of substrates (100 µM) and fluorophores (50 µM) in acidic, neutral and alkaline conditions; 4-MU/4-MUG (top left), 6-CMU/6-CMUG (top right) and 3-CU/3-CUG (bottom left). Legend applies to all the 3 panels. Absorption bands assigned to the N, A- and A2- are highlighted by the black arrows [138].

Contrarily to substrates, the fluorophores have absorption spectra which are pH dependent. The change in the absorption spectra can be explained by acid-base equilibrium due to the transition from the undissociated (neutral, N) to dissociated (anionic, A^-) form with increasing pH (Fig. 3-2, 3-5).

Extensive studies have been carried out on 4-MU and other coumarin derivatives, to better understand their ground and excited state properties. The fluorescence behaviour of 4-MU has been studied previously in organic solvents and in neutral, acidic and alkaline aqueous solutions [140-144]. Moriya studied the ground and excited-state reactions of umbelliferone and 4-MU in acidic, neutral and alkaline conditions and

concluded that in the electronic ground-state only two molecular species are spectroscopically detectable [140]. One is a neutral species (N) and the other is an ionized species (A^-). If the pH is changed from acidic to basic the molecule is deprotonated at the 7-hydroxyl group. Later, the same author discovered the absorption band corresponding to the cationic species (C^+) by conducting studies in concentrated sulphuric acid (λ_{max}= 345 nm). The absorption λ_{max} is increased in the following order: $N < C^+ < A^-$ [145]. The results of this study are consistent with those previous results and in the pH range tested only the N (λ_{max}=321 nm) and A^- (λ_{max}=364 nm) forms were detected for 4-MU in acidic and alkaline conditions. For 6-CMU a similar behaviour is dictated by acid-base equilibrium with the 2 forms, N (λ_{max}=329 nm) and A^- (λ_{max}=369 nm) was observed. 3-CU on the other hand behaves slightly different in the pH the range tested (Fig. 3-2). Due to the 3-carboxylic group, two protonation steps occur from basic to acidic pH [139]. The band for the neutral form N is positioned at 352 nm. The A^- formed due to the deprotonation of the carboxy group appears at λ_{ex}= 339 nm, while the dianionic form (A^{2-}), after the second step deprotonation of the 7-hydroxy group is red shifted and appears at λ_{ex}= 385 nm (Fig. 3-2, 3-5).

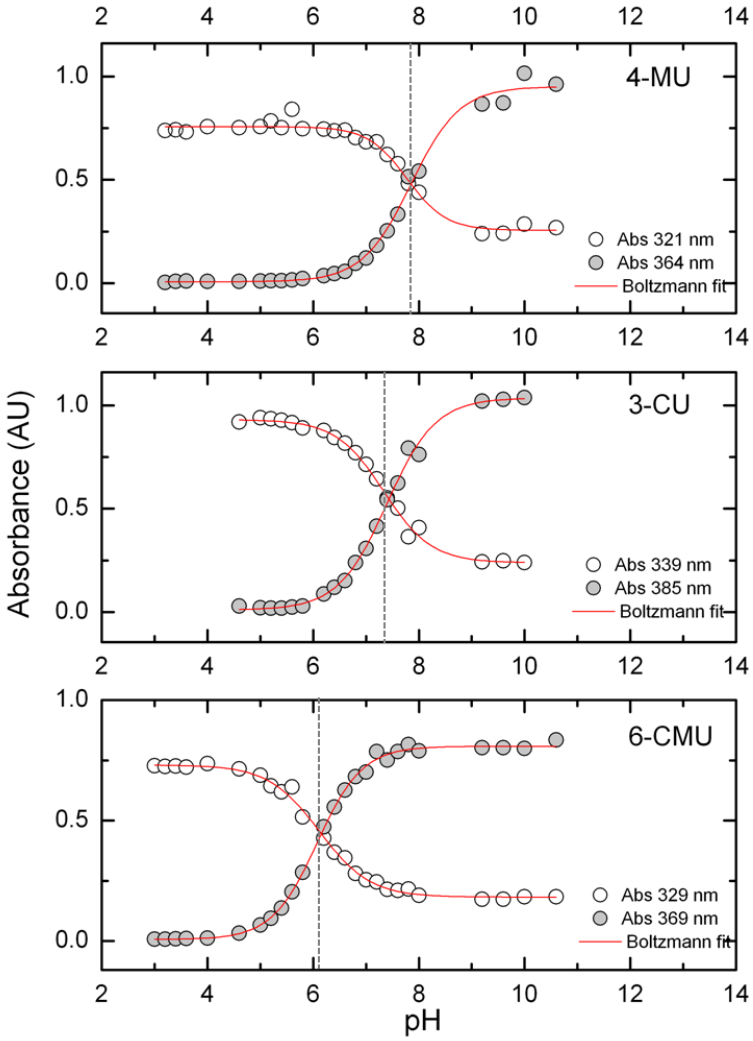

Figure 3-3 Spectrophotometric titration of the ground state equilibrium for 4-MU (top), 3-CU (middle) and 6-CMU (bottom), 50 μM. Drop lines highlight the pKa values inferred from the nonlinear regression fitting of the experimental data to the Boltzman Sigmoidal model. For 3-CU (middle panel) only the 5-10 pH range was used. Measurements were collected at the corresponding λmax (N, A-) for each fluorophore and are reported in the legend as Abs [138].

The pKa values for the ground state equilibrium were estimated using spectrophotometric titration followed by nonlinear regression fitting of the experimental data to the Boltzman Sigmoidal model (Fig. 3-3). Experimental pKa values were foundto be: 7.86 ± 0.6, R^2=0.993 (4-MU), 6.12 ± 0.3, R^2=0.996 (6-CMU) and 7.38 ± 0.6, R^2=0.993 (3-CU). These values are similar to the ones reported in the literature for 4-MU [146] and 3-CU [147] while for 6-CMU, no pKa value is reported. The low pKa

value of 6-CMU makes this fluorophore ideal for fluorometric assays at physiological pH values, as it is almost fully dissociated into the anion at this pH.

3.3.2 Fluorometric characterisation of substrates and fluorophores

As 3-CU [147, 148] and 6-CMU [136] have been synthesised more recently than 4-MU, there is a lack of literature on the behaviour of these two fluorophores in the ground and excited state. Excitation and emission 3D scans of 4-MU, 3-CU and 6-CMU in different buffers and at different pH values ranging from 3.0 up to 11.0 were collected. Analysis of the emission spectra over the pH range revealed that the shape of the emission spectrum is pH and excitation wavelength independent. The emission maximum (λ_{em}) was found to be 447 nm for 4-MU, 445 nm for 3-CU and 452 nm for 6-CMU, respectively (Fig. 3-4). Although in the ground state the studied fluorophores show two spectroscopically detectable species, in the excited state only one form was detected, corresponding to the λ_{em} for each. When excited at different wavelengths, the fluorophores yield the same emission spectrum over the pH range tested, regardless of which ground state species absorbs the excitation energy. Previous studies on 4-MU and umbelliferone conjugates have shown that there are actually 4 excited state possible species depending on pH and solvent: enol or neutral (N*), anion (A^-*), cation (C^-*) and a long-wave emitting keto-tautomeric form (K*) [145, 146, 149]. The tautomeric form is an excited state reaction product due to proton transfer between the spatially separated acidic (OH) and basic (C=O) groups. The fact that only the A^-* (4-MU, 6-CMU) and A^{2-}* (3-CU) were detected in the excited state is a consequence of a dissociative process in the excited state. Therefore the neutral excited molecule in the solution is converted in its lifetime into the anionic form and emits at the same wavelength as the anionic excited molecule [140]. This process is better known as the Kasha's rule.

Excitation spectra were collected by setting the emission wavelength at the λ_{em} for each of the three fluorophores and results are reported in Fig. 3-5. There is a striking similarity between the excitation and absorption spectra for each of the fluorescent molecules. The absorption and excitation spectra are practically superimposable. This allows for the assignment of the absorbing species in the ground state to the same species that absorb the excitation energy [150]. Upon increase of the pH from 3.0 to

11.5 the excitation band corresponding to the N form gradually decreases being replaced with a new excitation band corresponding to the A^- form. This is the case for 4-MU and 6-CMU, while for 3-CU there is a deviation from this model due to the two step dissociation of the hydroxy and carboxy groups. The isosbestic points at 347 nm (3-CU), 333 nm (4-MU) and 337 nm (6-CMU) indicate the ground state equilibrium between the A^{-2} and A^- form for 3-CU and the N and A^- form for 4-MU and 6-CMU (Fig. 3-5).

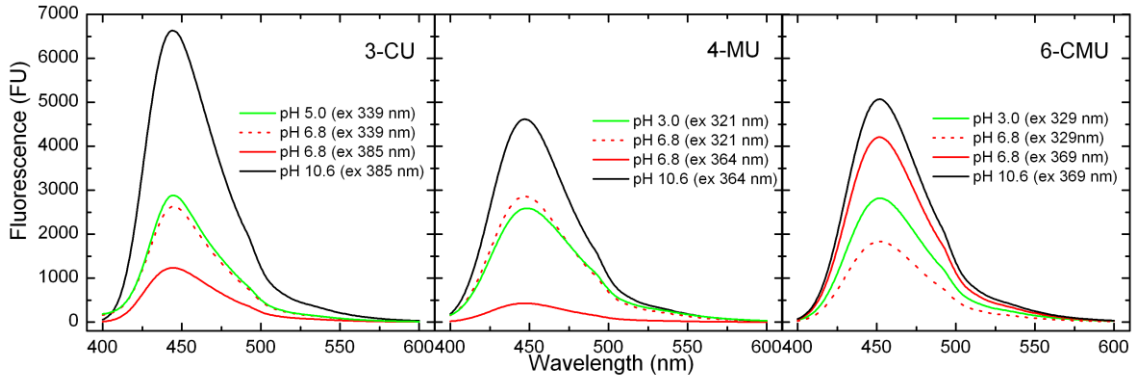

Figure 3-4 Emission spectra of 2.46 μM 3-CU (left), 4-MU (middle) and 6-CMU (right) in acidic, neutral and alkaline conditions at 20°C. λex denoted in the legend (in brackets) were used to collect the corresponding emission spectra. The same instrument configuration was used for all measurements [138].

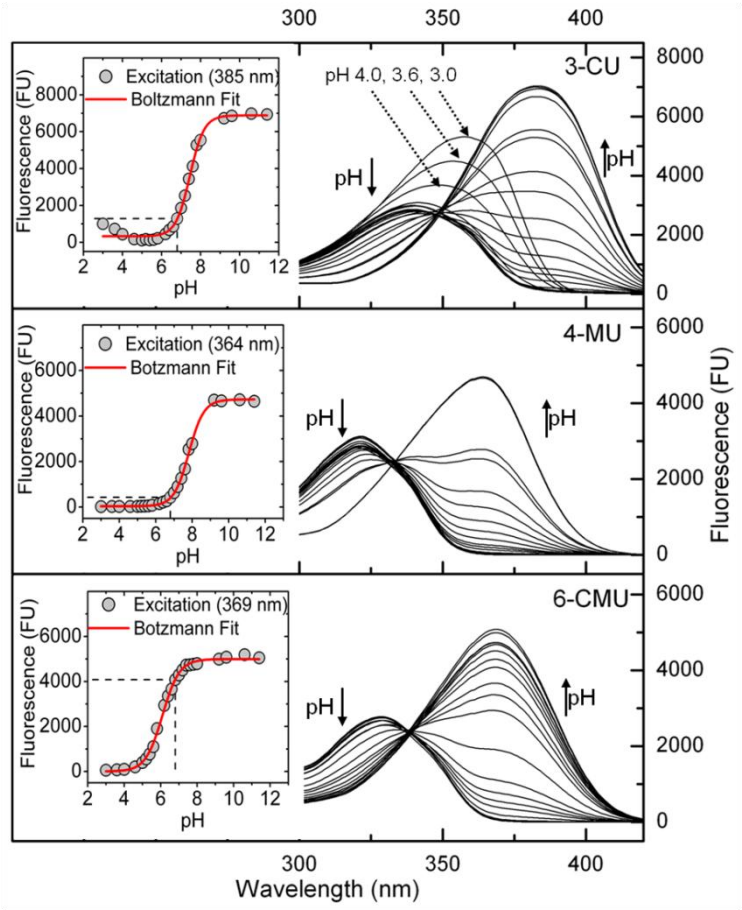

Figure 3-5 Excitation spectra of 2.46 μM 3-CU (3-CU), 4-MU (middle) and 6-CMU (bottom) at 20 °C in the 3.0- 11.5 pH range. λem used to collect the excitation spectra were 445 nm (3-CU), 447 nm (4-MU) and 452 nm (6-CMU). Dotted arrows in the top panel highlight the appearance of the A2- (pH 4.0, 3.6, 3.0) in the case of 3-CU. Insets show the pH dependent emission of 2.46 μM 3-CU (3-CU), 4-MU (middle) and 6-CMU (bottom) at 20 °C in the pH range tested while the dotted drop lines highlight the intensity at pH 6.8; λex used for each fluorophore are mentioned in the legend. The same instrument configuration was used for all the measurements [138].

Emission spectra were collected by setting the excitation wavelength corresponding to the maximum bands found for the A^- forms for 4-MU and 6-CMU and for the A^{2-} form for 3-CU. Fluorescence intensities recorded at the maximum emission wavelength for each fluorophore were plotted against pH. The fluorescence intensity of 6-CMU in the 6.8-7.0 pH range was found to be roughly 9.5 times higher than that of 4-MU and 3.2 times higher than the fluorescence of 3-CU (Fig. 3-5 inset). This further proves, that the

low pKa value of 6-CMU renders this fluorophore as a superior candidate for continuous measurements at physiological pH values. On the other hand, at pH values above 9 where full dissociation occurs, 3-CU emits a fluorescent signal 1.5 times higher than 4-MU and 1.3 times higher than 6-CMU, making 3-CU a better candidate for discontinuous measurements where the pH can be adjusted.

Continuous monitoring of GUS activity requires that changes in fluorescence intensity to be measured in the conditions of the reaction assay, where the fluorophore is produced in μM or nM concentration in a mM solution of substrate. Hence the effect of the presence of different substrate concentrations on the fluorescence spectra of fluorophores was investigated. It was found that the inner filter effect [151-153] has a substantial impact on the optimal excitation wavelength and consequently on the intensity of emitted fluorescent signal. When the same concentration of fluorophore was used in the presence of increasing concentrations of substrates (0-2 mM) at pH 6.8, a red shift of the maximum excitation wavelength (λ_{ex}) was noticed for 4-MU and 3-CU (Fig. 3-6). This shift is caused by the increasing absorbance of substrate with increasing concentration. As a consequence, 4-MU and 3-CU which at pH 6.8 have a maximum excitation wavelength at 321 nm and 339 nm due to the N form which is predominant were obstructed from absorbing incident light at shorter wavelengths. This is particularly important if enzyme assays are to be carried out at suboptimal substrate concentrations (around K_m value or lower) as the excitation wavelength can be chosen to maximise the fluorescent signal and by that the LOD and the sensitivity of the assay. When the same studies were performed for 6-CMU using different concentrations of 6-CMUG it was found that the substrate had no influence on the maximum excitation wavelength of the fluorophore. This is due to the lower pKa value of 6-CMU (6.18 ± 0.3). At pH 6.8, 6-CMU is almost fully dissociated and absorbs strongly at 369 nm (Fig. 3-6).

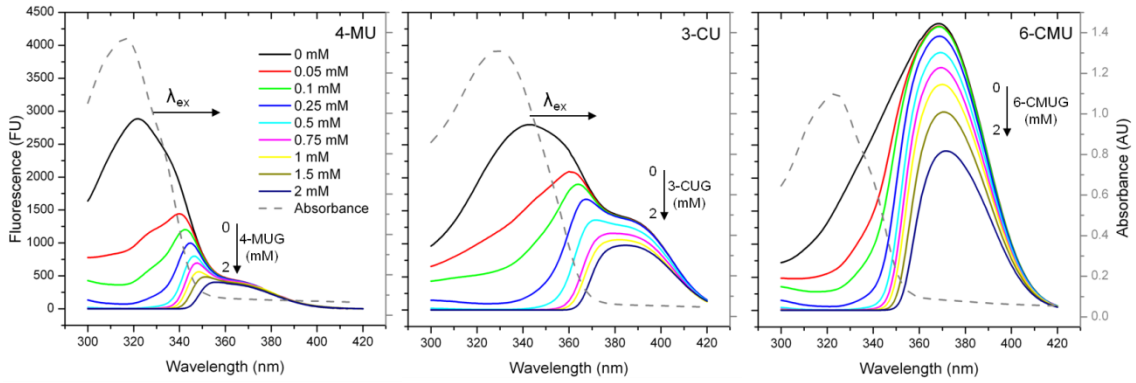

Figure 3-6 Excitation spectra of 2.5 µM 3-CU (left), 4-MU (middle) and 6-CMU (right) in the presence of 3-CUG, 4-MUG and 6-CMUG at pH 6.8 and 20 °C. Legend in the left panel applies to all the panels in the Fig. and it represents the molar concentrations of the substrates. Overlaid with dotted lines are the absorbance spectra of 3-CUG, 4-MUG and 6-CMUG at 100 µM at pH 6.8 and 20 °C. Horizontal arrows denote the λex shift while vertical arrows denote the substrate concentration increase. Each substrate + fluorophore spectrum was corrected by subtracting the spectrum of the respective substrate concentration [138].

A suitable method to continuously monitor GUS activity requires that the fluorescence of the fluorophore (reaction product) to be directly proportional to its concentration in the reaction medium. This also implies that the excitation wavelength for the fluorophore has to be chosen not only to confer linearity but also to maximise the LOD and the sensitivity of the method. For this purpose the concentration of substrate was kept constant at 0.5 mM and increasing concentrations of fluorophore were added. It was found that the presence of substrate does not influence the shape of the emission spectrum for any of the flurorophores, affecting only the intensity of the emitted fluorescence (Fig. 3-7, 3-8, 3-9).

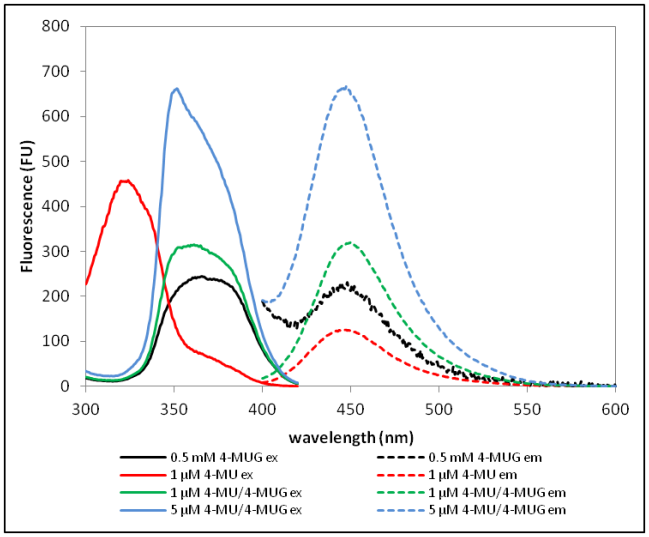

Figure 3-7 Excitation and emission spectra of 4-MUG and 4-MU; 4-MU em and 4-MU ex are the spectra of 4-MU; 4-MU/4-MUG ex and 4-MU/4-MUG em are spectra of 4-MU in the presence 0.5 mM 4-MUG; concentrations of 4-MU used are shown in the legend; emission wavelength: 446 nm; excitation wavelength: 351 nm; slit width: 5 nm (ex) and 2.5 nm (em). Measurements carried out using the LSB 50 fluorometer [138].

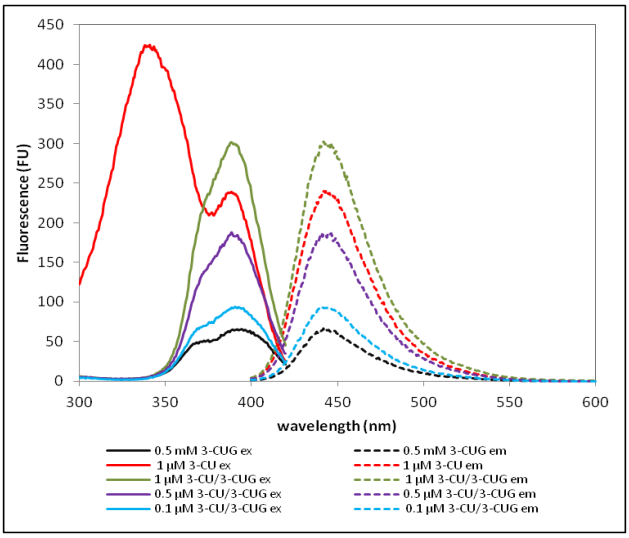

Figure 3-8 Excitation and emission spectra of 3-CUG and 3-CU; 3-CU em and 3-CU ex are the spectra of 3-CU; 3-CU /3-CUG ex and 3-CU /3-CUG em are spectra of 3-CU in the presence 0.5 mM 3-CUG; concentrations of 3-CU used are shown in the legend; emission wavelength : 446 nm; excitation wavelength: 351 nm; slit width: 5 nm (ex) and 2.5 nm (em). Measurements carried out using the LSB 50 fluorometer [138].

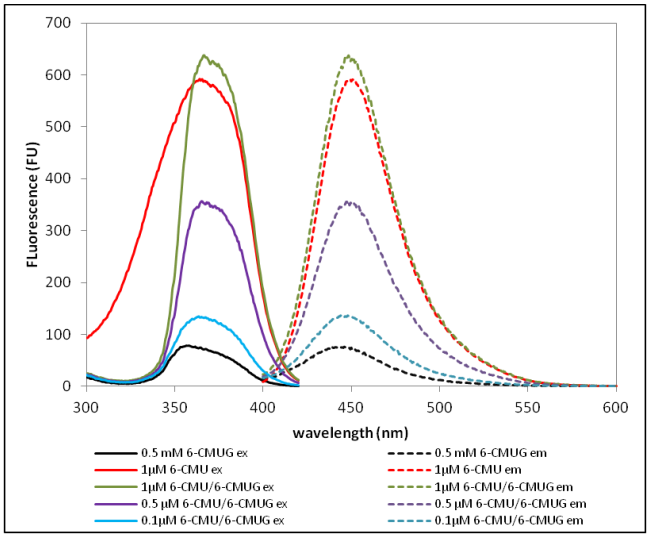

Figure 3-9 Excitation and emission spectra of 6-CMUG and 6-CMU; 6-CMU em and 6-CMU ex are the spectra of 6-CMU; 6-CMU/6-CMUG ex and 6-CMU/6-CMUG em are spectra of 6-CMU in the presence 0.5 mM 6-CMUG; concentrations of 6-CMU used are shown in the legend; emission wavelength: 446 nm; excitation wavelength: 351 nm; slit width: 5 nm (ex) and 2.5 nm (em). Measurements carried out using the LSB 50 fluorometer [138].

3.3.3 Kinetic analysis of GUS catalysed hydrolysis of the substrates

One way to investigate the interaction between GUS and the three substrates: 4-MUG, 3-CUG and 6-CMUG is through the use of Michaelis-Menten parameters: K_m and V_{max}. A comparison between these parameters for the three substrates can give insights into the enzyme's preferred molecule, catalysis rates and optimal substrate concentration. By conducting studies under the same conditions (pH, temperature and GUS concentration) a comparison and a decision can be made regarding which of these substrates is optimal for continuous GUS assay.

A study was conducted to investigate the Michaelis-Menten kinetic parameters between GUS and 4-MUG, 3-CUG and 6-CMUG. Fluorescence change is a convenient and sensitive approach to monitor kinetics of hydrolytic enzymes. Unfortunately, it loses linearity as the absorbance of the fluorogenic substrate increases with concentration increasing the IFE (inner filter effect). Decreases in fluorescence due to the inner filtering exceeds 10% once the sum of absorbance at excitation and emission wavelengths exceed 0.08 [154]. To overcome this issue, corrections for absorbance are

applied to the experimental data or calibration curves for the fluorophore are constructed in the presence of different substrate concentrations. The latter, although more laborious and time consuming than the former, will give more accurate estimations of the kinetic parameters. For this purpose calibration curves were performed for each substrate concentration using different fluorophore dilutions. Fig. 3-10, 3-11 and 3-12 show the calibration curves used to convert fluorescence units (FU) into μM concentration of product.

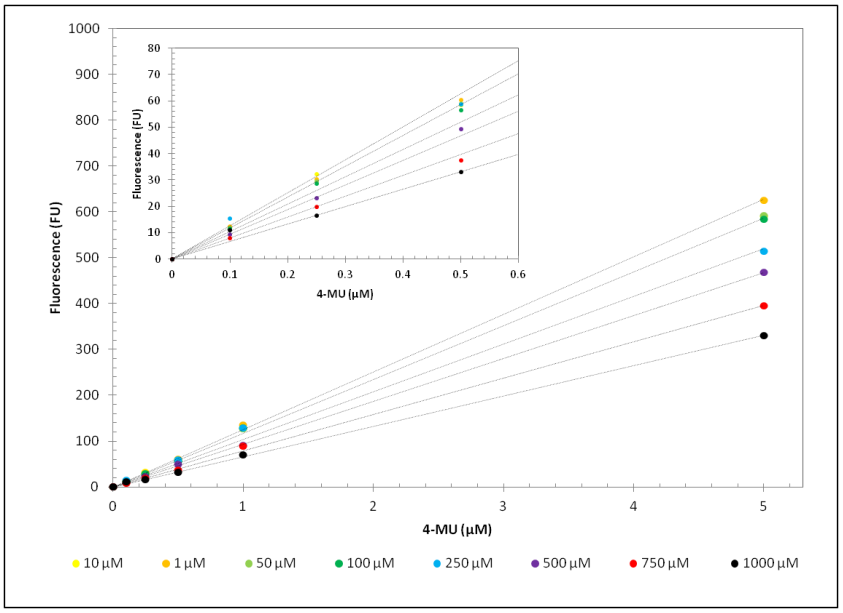

Figure 3-10 Calibration curves of 4-MU in the presence of different 4-MUG concentrations (shown in the legend); λex= 351 nm, λem 446 nm; slit widths: 5 nm (ex), 2.5 nm (em); dotted lines represent the trendlines of the linear regression model. Measurements carried out using the LSB 50 fluorometer [138].

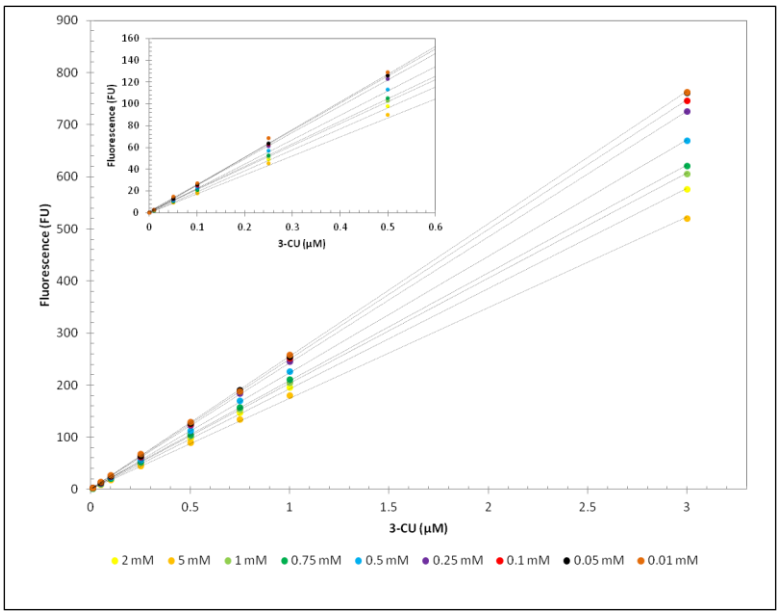

Figure 3-11 Calibration curves of 3-CU in the presence of different 3-CUG concentrations (shown in the legend); λex= 389 nm, λem 444 nm; slit widths: 5 nm (ex), 2.5 nm (em); the dotted lines represent the trendlines of the model. Measurements carried out using the LSB 50 fluorometer [138].

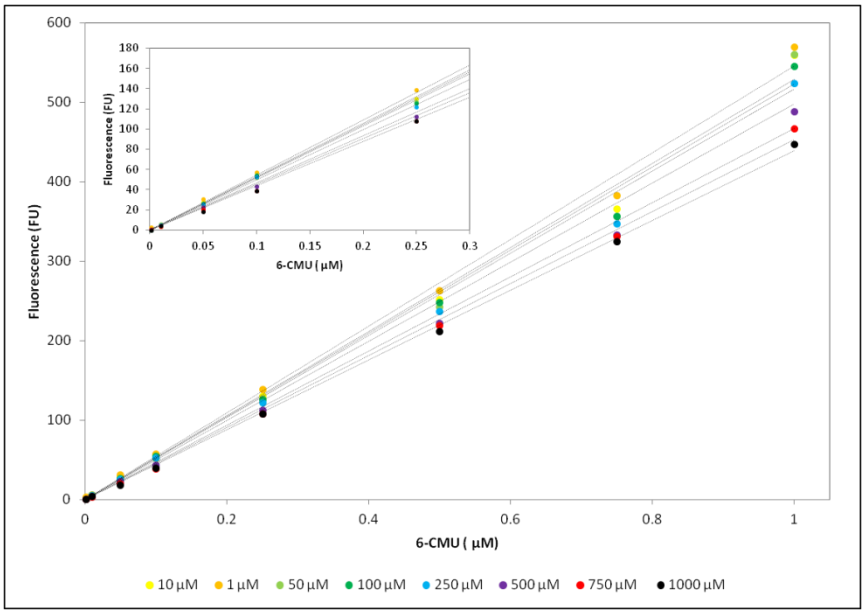

Figure 3-12 Calibration curves of 6-CMU in the presence of different 6-CMUG concentrations (shown in the legend); λex= 365 nm, λem 449 nm; slit widths: 5 nm (ex), 2.5 nm (em); the dotted lines represent the trendlines of the model. Measurements carried out using the LSB 50 fluorometer [138].

The highest signal loss due to IFE and probably fluorescence quenching was noticed in the case of 4-MU followed by 3-CU and 6-CMU. This loss in the fluorescence efficiency of the fluorophore with increasing substrate concentration can introduce errors into the determination of kinetic parameters if it is not taken into account. Progress curves of fluorescence accumulation as a function of time were measured for each of the 3 substrates in the presence of GUS and are shown in Fig. 3-13, 3-14 and 3-15. Equation (1) was used to calculate the initial velocities from the slope of the progress curves (Slope 2) and the slope of the fluorophores calibration curves (Slope 1).

Equation 1:

$$Initial\ velocity\ (\mu M\ min^{-1}) = \frac{\text{Slope 2 (FU s}^{-1}) * 60}{\text{Slope 1 (FU µM}^{-1})}$$

Equation 2:

$$V = \frac{V_{max}\,[S]}{K_m + [S]}$$

Initial reaction velocities were plotted against substrate concentration. Michaelis-Menten equation (2) was used to estimate the K_m and V_{max} using Solver. The model estimates the two parameters by minimising the sum of square residuals (SSR). A residual analysis was carried out for each of three models to determine if the model is a good fit for the data. Fig. 3-16 shows the best fit of the Michaelis-Menten model to the experimental data for 4-MUG, 3-CUG and 6-CMUG. K_m/V_{max} values derived from the 3 models are summarised in Table 3-2 together with the calculated K_{cat} values. As experiments were conducted under identical conditions and with similar enzyme concentrations, the Michaelis-Menten constants can be directly compared to identify possible binding preferences. The K_m value for 3-CUG is almost 7 times higher when compared with that obtained for 4-MUG and 4.5 times higher when compared to the K_m value for 6-CMUG. This suggests a preferential binding of GUS to 4-MUG and 6-CMUG which also suggests that a much lower concentration of 4-MUG and 6-CMUG is needed to maximise the reaction velocity. Maximum rate, V_{max} occurs when the intrinsic binding energy is used for the catalytic process rather than binding and is a result of the enzyme binding the substrate weakly but the transition state strongly. Maximum catalysis rates, K_{cat}/K_m, occur when the structure of the enzyme is complementary to the transition state of the substrate and the intrinsic binding energy is used to stabilise the transition state [155]. Our results show that 4- MUG has the highest first order catalysis rate (K_{cat}/K_m), followed by 6-CMUG and 3-CUG (Table 3-2). This suggests that the transition state structure of 4-MUG and 6-CMUG are more complementary to the enzyme binding site that the transition state of 3-CUG. Differences in binding preferences are commonly due to the steric differences or electronic hindrances at the enzyme binding site. Since the two catalytic residues in GUS are Glu413 and Glu504 [127], [156] it was proposed that the similarity between the active site and the 3-carboxyl group of the aglycon in 3-CUG might result in electronic repulsion, which translates into a lower affinity of the enzyme for the substrate and a higher Michaelis-Menten constant [157]. Using the K_m values derived from the Michaelis-Menten model one can calculate how much substrate is required to reach any desired level of saturation. For zero order reactions the substrate concentration is usually kept high (at least 3 times the K_m value) [158]. The kinetic parameters from Table 3-2 suggest that 4-MUG would be the preferred substrate of choice in assaying GUS activity, closely followed by 6-CMUG. On the other hand, the

progress curves in Fig. 3-13, 3-15 show that the same amount of GUS will produce a fluorescent signal 6 times higher in the presence of 6-CMUG as compared to 4-MUG.

Taking this into account it is clear that a method based on 6-CMUG will have an improved LOD and better response times. To our knowledge this is for the first time Michaelis-Menten catalytic parameters are reported for the GUS hydrolysis of 6-CMUG. These studies suggest 6-CMUG is a suitable candidate for measuring *E. coli* GUS activity using a continuous flurometric method.

Table 3-2 Kinetic parameters for GUS.

Substrate	K_m (mM)[a]	V_{max} (μM min^{-1}) [a]	k_{cat} (s^{-1}) [a]	k_{cat} (s^{-1}) [b]	k_{cat}/K_m (s^{-1} M^{-1}) [a]
4-MUG	0.07	2.56	92	222 ± 13.4	1.29×10^6
3-CUG	0.48	0.99	35	132 ± 9.3	7.40×10^4
6-CMUG	0.11	2.07	74	207 ± 8.5	6.93×10^5

[a] Measurements performed at 20 °C and pH 6.8 with 135 ng mL^{-1} GUS.

[b] Measurements performed at 37 °C and pH 6.8 with 1.35 ng mL^{-1} GUS.

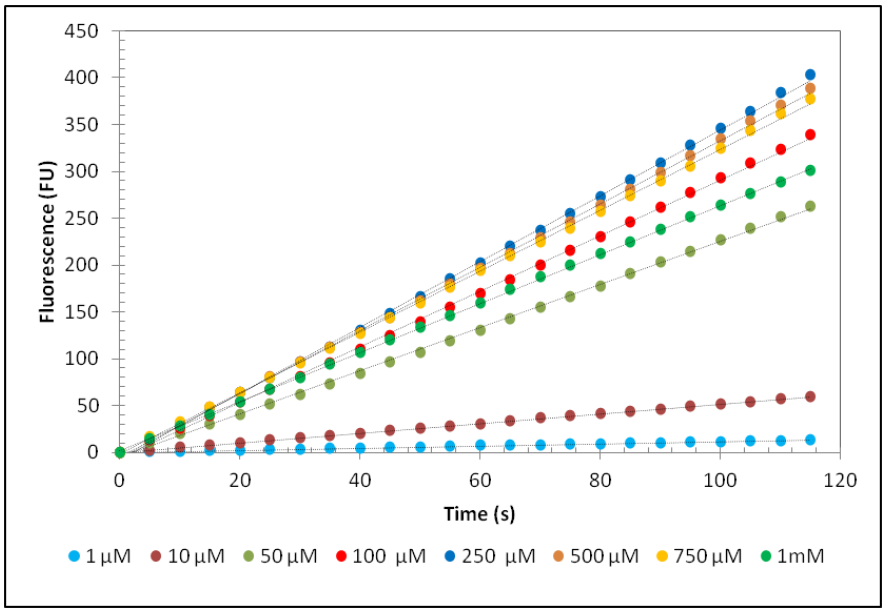

Figure 3-13 Progress curves for GUS catalysed hydrolysis of different 4-MUG concentrations (shown in the legend); λex= 351 nm, λem 446 nm; slit widths: 5 nm (ex), 2.5 nm (em); the dotted lines represent the trendlines of the model. GUS was added at a concentration of 135 ng mL^{-1}. Measurements carried out using the LSB 50 fluorometer [138].

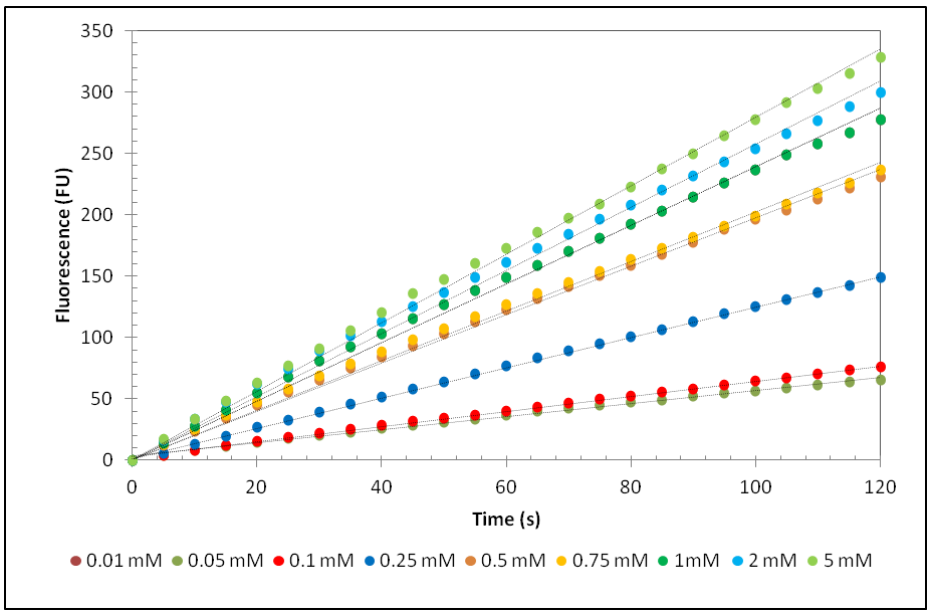

Figure 3-14 Progress curves for GUS catalysed hydrolysis of different 3-CUG concentrations (shown in the legend); λex= 389 nm, λem 444 nm; slit widths: 5 nm (ex), 2.5 nm (em); the dotted lines represent the trendlines of the model. GUS was added at a concentration of 135 ng mL^{-1}. Measurements carried out using the LSB 50 fluorometer [138].

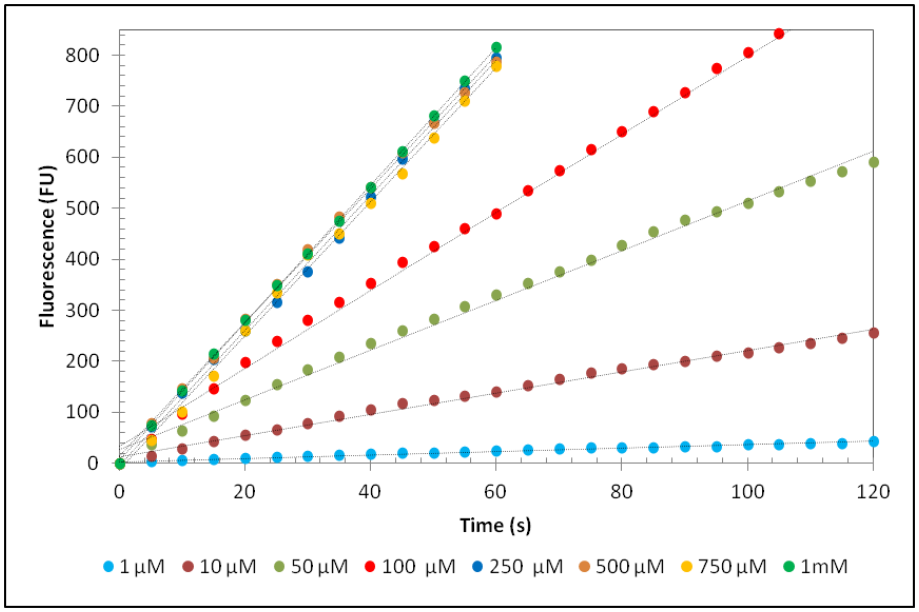

Figure 3-15 Progress curves for GUS catalysed hydrolysis of different 6-CMUG concentrations (shown in the legend); λex= 365 nm, λem 449 nm; slit widths: 5 nm (ex), 2.5 nm (em); the dotted lines represent the trendlines of the model. GUS was added at a concentration of 135 ng mL^{-1}. Measurements carried out using the LSB 50 fluorometer [138].

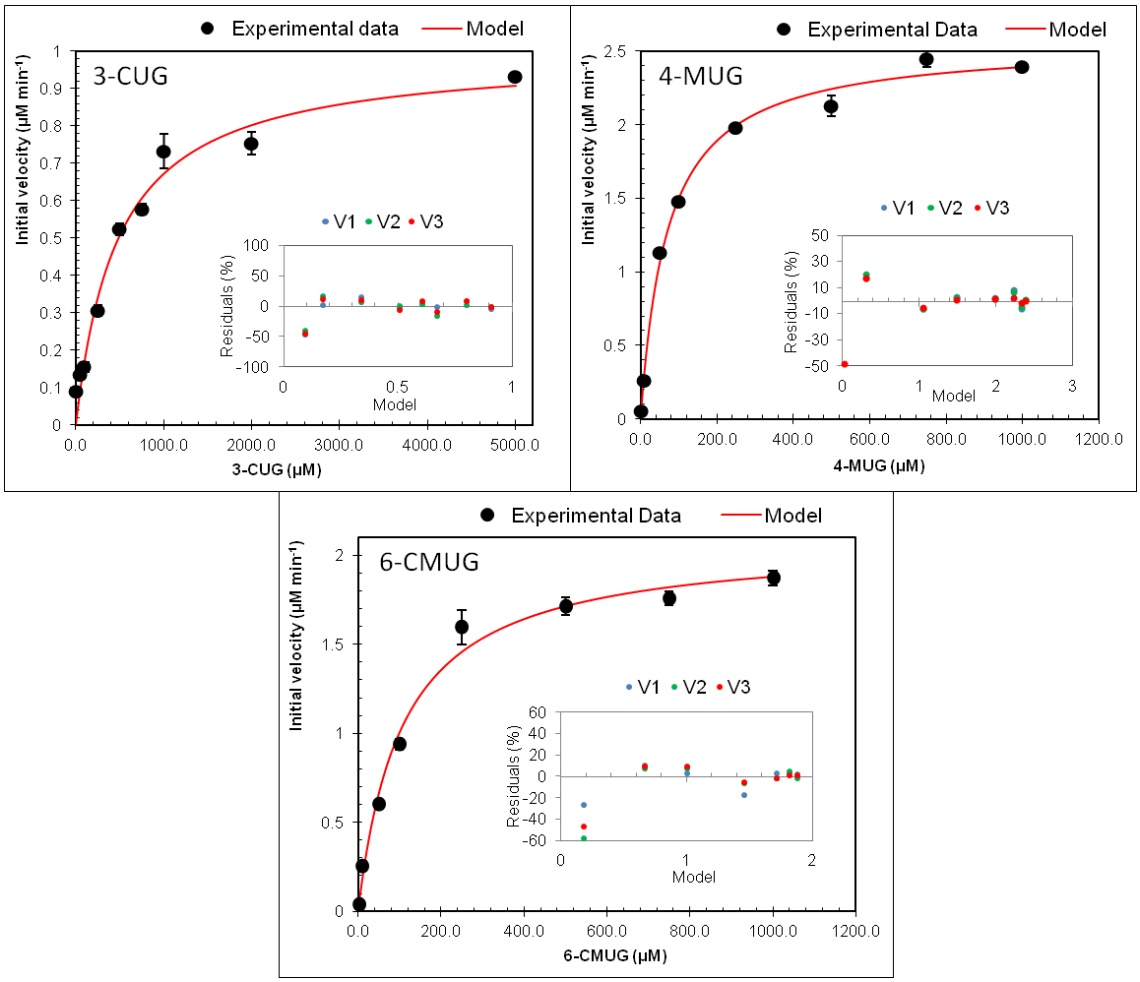

Figure 3-16 Kinetics of GUS (135 ng mL^{-1}) catalysed hydrolysis of 3-CUG (left) 4-MUG (middle) and 6-CMUG (right) and nonlinear regression fitting of the experimental data to the Michaelis-Menten model. Initial reaction velocities were determined at 20 °C and pH 6.8. The insets in each panel show the distribution of residuals for each run (V1, V2, and V3). Error bars represent the standard deviation of n=3 [138].

3.3.4 Temperature and pH optimisation

Enzyme assays are carried out in well defined conditions for consistent and reproducible results. Temperature and pH play an important role in both the development of enzyme assays but also on the study of enzyme structures. Temperature influences enzyme catalysed reactions in the same way it influences other chemical reactions. As a general rule, reaction rates increase with temperature by a factor of 2-3 for each 10 °C. Once the temperature exceeds a certain maximum value turnover rates start to decline due to

destabilisation and deactivation of the enzyme. Fig. 3-17 shows the temperature profile for GUS catalysed hydrolysis of 4-MUG, 6-CMUG and 3-CUG. Although maximum reaction rates were observed at 44 °C (3-CUG and 6-CMUG) and 50 °C (4-MUG) we chose to use 37 °C as the optimum temperature to make sure GUS denaturation doesn't occur [159]. Previous studies on wild type GUS using 4-nitrophenyl-β-D-glucuronide (4-NPG) and 4-MUG [160] as substrate [161],[162] and recombinant GUS using 3-CUG as substrate [157] report similar temperature profiles with a maximum activity between 40-50 °C. Between 10-40 °C GUS activity increased linearly with temperature, at a rate of 0.08, 0.07 and 0.05 μM min^{-1} $°C^{-1}$ for 4-MUG, 6-CMUG and 3-CUG respectively. Denaturation was observed after 50 °C while above 65 °C there was little or no activity left. Because a continuous method was used to determine GUS activity within the temperature range, a correction for the influence of temperature on the intensity of the three fluorophores was applied to calibration curves recorded at 20 °C in the assay buffer (Equation in Fig. 3-19). In this case only one calibration curve was needed for each substrate. We found that there is a 15% loss in 6-CMU fluorescence with temperature rise (from 2 °C to 70 °C) which is normal in such systems and is due to the thermal activation of non-radiative de-excitation pathways [163]. On the other hand, for 4-MU and 3-CU a 60% and 40% gain in fluorescence was noticed for the same temperature interval (Fig. 3-19). These two fluorophores have a higher pKa than 6-CMU and are just partially dissociated at pH 6.8. With increasing temperature the equilibrium is shifted to the right thus decreasing the pKa and favouring the dissociation process. This process is explained by excitation spectra collected for the three fluorophores in the 5-70 °C temperature range (Fig. 3-20) where the absorption bands corresponding to the A^- (4-MU) and A^{2-} (3-CU) are gradually increasing with temperature.

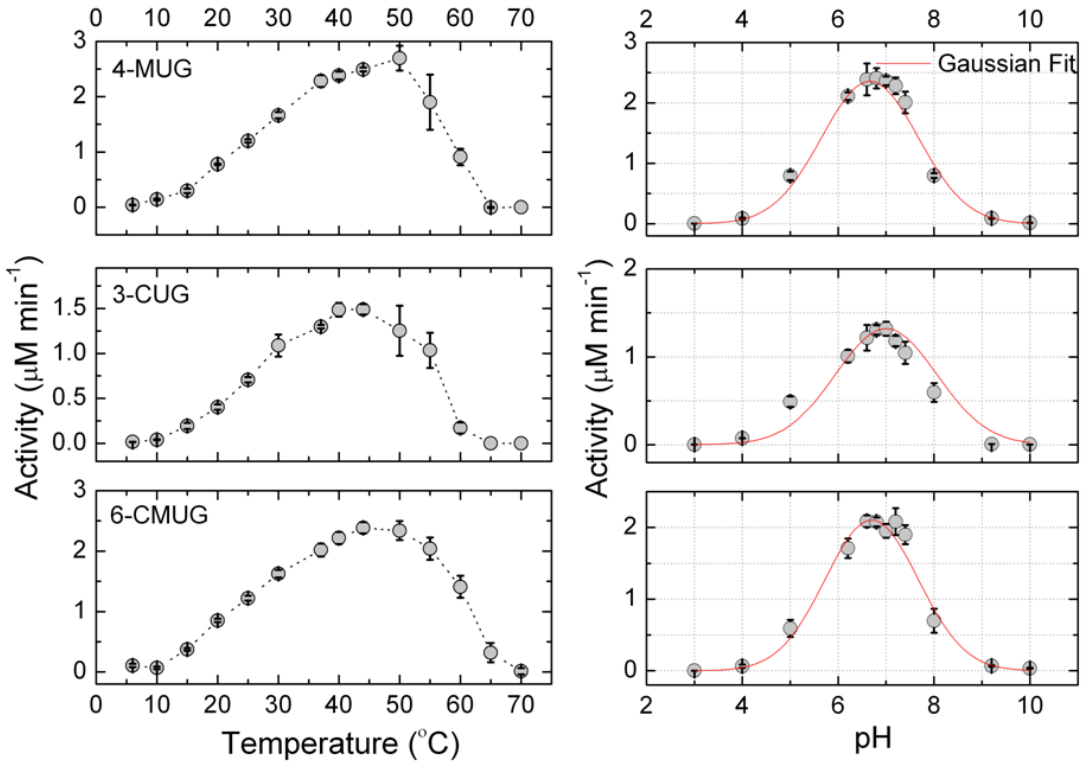

Figure 3-17 Temperature (left) and pH (right) profiles for GUS catalysed hydrolysis of 3-CUG (2 mM), 4-MUG (0.5 mM) and 6-CMUG (0.5 mM). pH profiles were recorded at 20 °C in the presence of 135 ng mL^{-1} GUS while temperature profiles were recorded at pH 6.8 in the presence of 54 ng mL^{-1} GUS. Error bars represent the standard deviation of n=3 [138].

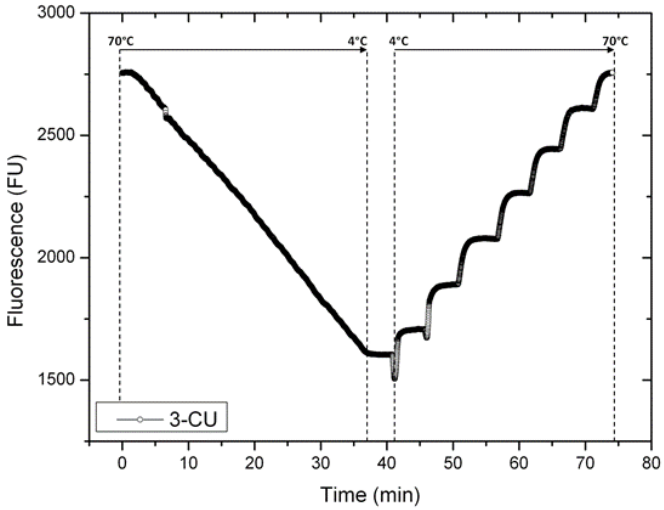

Figure 3-18 Temperature dependent fluorescence intensity of 3-CU at pH 6.8. Constant temperature decrease at a rate of 2 °C min^{-1} from 70 °C to 4 °C (left) and stepwise temperature increase from 4 °C to 70 °C with 5 min equilibrium steps (right); the first step used in this case was from 4°C to 10 °C after which all the subsequent steps were 10 °C each; λex= 385 nm, λem 445 nm [138].

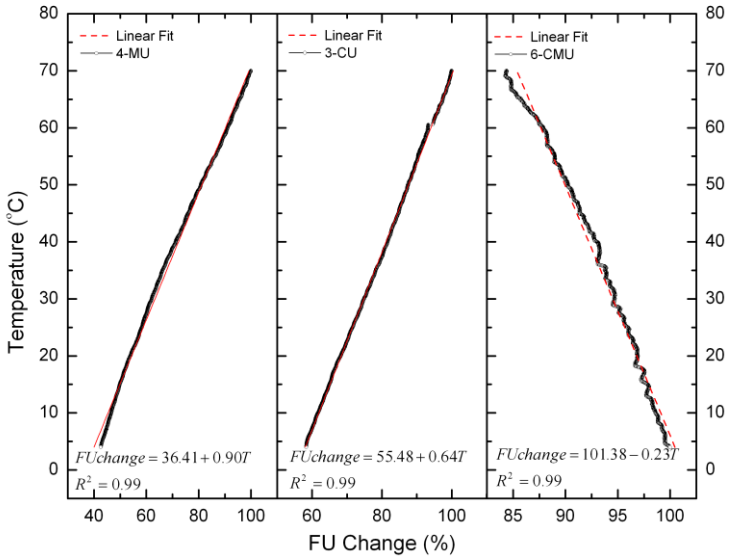

Figure 3-19 Temperature dependent fluorescence intensity of 4-MU, 3-CU and 6-CMU at pH 6.8. A constant temperature decrease rate of 2 °C min^{-1} from 70 °C to 4 °C was used to collect the data (example shown in Fig. 3-18). Equations corresponding to the linear fitting of the data are shown in each panel; λex / λem used were: 364 / 447 (4-MU), 385 / 445 (3-CU), 369 / 452 (6-CMU) [138].

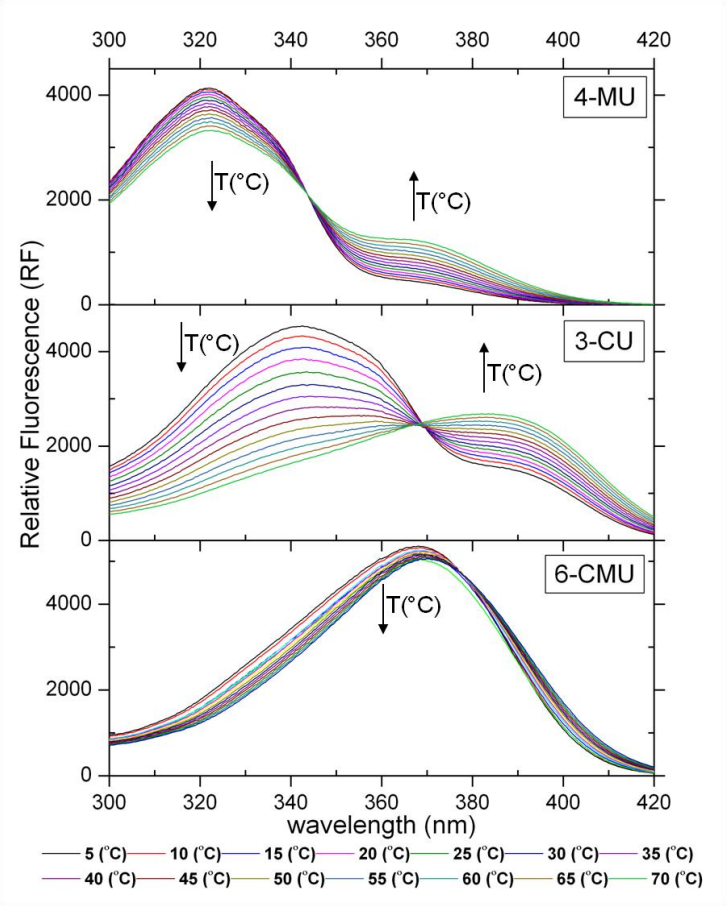

Figure 3-20 Temperature dependent excitation spectra of 4-MU, 3-CU and 6-CMU at pH 6.8; λem used were: 447 (4-MU), 445 (3-CU), 452 (6-CMU) [138].

The pH profile plays an important role in the activity of enzymes because it is responsible for the ionization of functional groups directly involved in catalysis and any charged groups involved in the stabilisation of the protein structure. As a consequence the pH dependence can offer insight into the catalytically active functional groups and potentially their chemical nature. In the case of GUS the activity increases with pH to a maximum (pH 6.6 -7.2) and drops to zero in the alkaline region following a bell shaped curve (Fig. 3-17). Similar pH optimum values for *E. coli* GUS activity are reported in the literature in the presence of various substrates and range from 6.5 up to 7.5 pH units [161], [160], [164] ,[165] ,[166] ,[167]. This behaviour is consistent with a simple diprotic system were the increase and decrease in activity on both sides of the optimum pH represents titration curves of active site residues. The midpoints on the curves

correspond to the pK values of these active groups in the enzyme substrate complex [159]. Our results suggest that there is no difference between the pH profiles with the three substrates (Fig. 3-17). This confirms that the shape of the pH curve is driven by functional groups in GUS and not by functional groups in the substrate.

3.3.5 Analytical performance of the continuous method

Results presented in the previous sections suggest that 6-CMUG is the preferred substrate for measuring GUS activity in a continuous fashion. To further test this, the continuous fluorometric method developed in this study was compared with the widely used discontinuous method [129] based on 4-MUG. The same GUS concentration was run 10 times using both methods (Fig. 3-21). The average activity was found to be 0.041 ± 0.0025 μM min^{-1} (4-MUG) and 0.058 ± 0.0028 μM min^{-1} (6-CMUG) with a %RSD of 6.20 and 4.88 respectively. The smaller %RSD for the continuous method is expected and is probably due to fewer random errors introduced during the experimental procedure. The discontinuous method is more susceptible to such errors due to the multiple handling steps required and this aspect is also noticeable from the linear fitting of the experimental data (Fig. 3-21). The difference in the two average activities is significant and is likely due to GUS loss during the process. Since, for this experiment, we used a relatively low GUS concentration, it is likely that the multiple pipetting steps required for the discontinuous method are the underlying cause of this observation. For the same GUS concentration the continuous method offers an almost 10 fold improvement in the fluorescent signal recorded (note the scale in Fig. 3-21). This is due to the inherent disadvantage of the discontinuous method which requires the measurement of fluorophore produced in a 10 fold dilution. Although 4-MU is slightly more fluorescent at pH 10.6 than 6-CMU at pH 6.8, the requirement for stopping the enzymatic reaction with concomitant pH adjustment and dilution results in an increase in the LOD of the discontinuous method. Besides the analytical capabilities, the continuous method offers other advantages such as time and labour savings and is more sustainable with regard to reagents and consumables used. As an example, for the experimental data collected in Fig. 3-21, both methods required between 5-6 h to generate results but the effective working time was approximately 5 h for the discontinuous method and approximately 30 min for the continuous one. Furthermore,

over 100 pipette tips and 76 test tubes were used, generating 55-60 mL of waste using the discontinuous method as opposed to 2 pipette tips and 11 mL of waste for the continuous method. When data are obtained in a discontinuous set-up, aliquots are removed at pre-determined times as the enzymatic reaction proceeds. The fluorescence is then measured and a progress curve is constructed ensuring the product formation proceeds linearly. This is not necessarily an easy task when it is considered that only a limited number of measurement points are available and deviations from linearity are often hard to identify. In a continuous set-up, once the enzymatic reaction has been initiated the product formation can be monitored at a higher rate. Deviations from linearity can be observed in real time and collected kinetic data is more accurate and offers a more detailed insight into the chemical process. GUS activity can be measured in less than 2 min as long as the linearity is checked and maintained. One disadvantage of the continuous method is that using a single cell holder bench fluorometer, only one sample can be analysed at any time while the discontinuous method allows for simultaneous analysis of multiple samples. This can be easily corrected if the 6-CMUG method is coupled with a plate reader. This set-up should also provide high-throughput screening of GUS activity.

Although we developed this method for diagnostic purposes and particularly for the detection of *E. coli* in environmental water samples its applicability can be easily extended to other areas. GUS activity measurements are performed and routinely used in plant molecular biology, human healthcare, biology, microbiology and environmental monitoring [128]. Furthermore, the method can be easily automated and can eventually be employed in a flow-through system for unattended sample analysis and sensing applications.

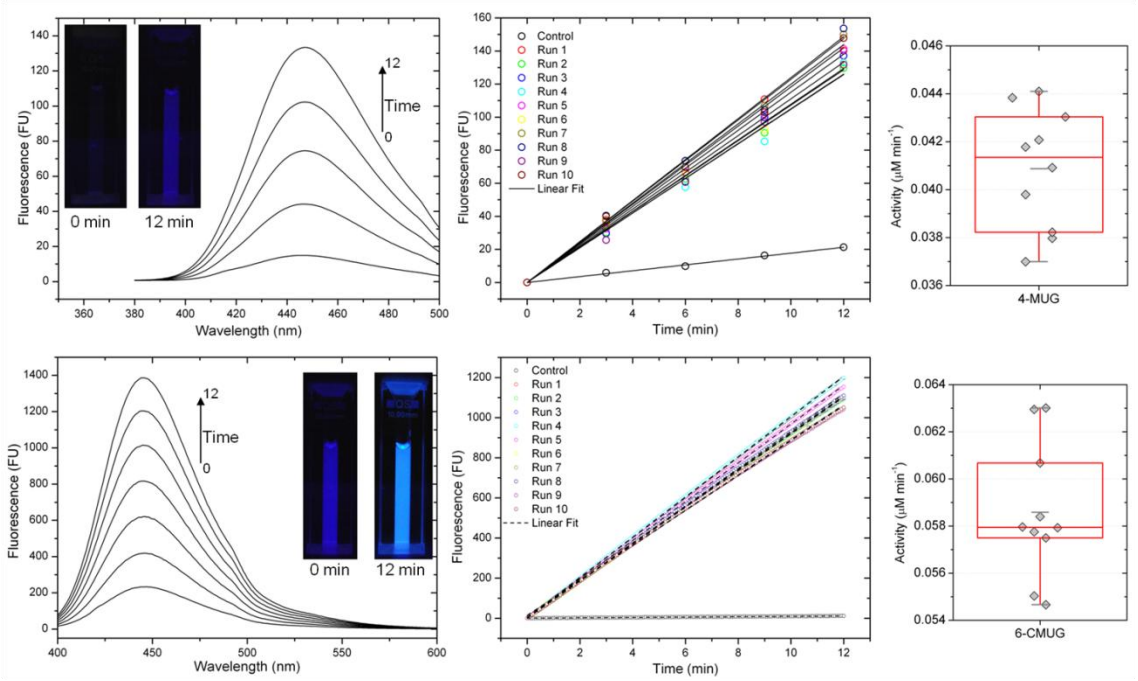

Figure 3-21 Comparison of the discontinuous (top) and continuous (bottom) method for measuring GUS activity. Progress curves (normalised to t=0 min) from running the same GUS concentration (1.35 ng mL^{-1}) 10 times with the two methods (middle), emission spectra as a function of time (left) and box plots after conversion (right). For the 4-MUG based method GUS activities were multiplied by 10 to account for the dilution factor. Emission spectra in the left panel were collected at 3 min intervals (discontinuous method) and at 2 min intervals (continuous method). Insets in the left panel show images collected for both methods before and 12 min after GUS addition. Experimental conditions are detailed in Methods section [138].

3.4 Conclusions

In summary, two lesser known fluorogenic substrates (6-CMUG and 3-CUG) were studied and compared with the widely used 4-MUG for measuring GUS activity in a continuous set-up. Spectrophotometric characterization using UV Vis and steady state fluorescence spectroscopy of fluorophores and substrates revealed that 6-CMUG is the substrate of choice for continuous measurements. This was found to be mainly due to the lower pKa value (6.12 ± 0.3) of its fluorophore 6-CMU. As a consequence, at pH 6.8 where GUS acitivity reaches its maximum this fluorophore is almost fully dissociated into its A^- form. When emission spectra were collected using the excitation bands for the ionised forms of 4-MU, 6-CMU and 3-CU, the fluorescence intensity of 6-CMU was found to be roughly 9.5 times higher than that of 4-MU and 3.2 times higher than the fluorescence of 3-CU. Michaelis-Menten kinetic parameters of GUS catalysed hydrolysis of 4-MUG, 3-CUG and 6-CMUG were determined experimentally and compared and are reported for the first time in case of 6-CMUG (K_m = 0.11 mM, K_{cat} = 74 s^{-1}, K_{cat}/ K_m = 6.93 x 10^5 $s^{-1}M^{-1}$ at pH 6.8 and 20 °C). Finally a continuous fluorometric method based on 6-CMUG as a fluorogenic substrate has been developed for measuring GUS activity. When compared with the highly used discontinuous method based on 4-MUG as a substrate it was found that the new method is more sensitive (almost 10 times) and more reproducible (%RSD=4.88). Furthermore, the developed method is less laborious, faster and more economical and should provide an improved alternative for GUS assays and GUS kinetic studies.

4 NOVEL PROTOCOL FOR THE RECOVERY AND DETECTION OF *ESCHERICHIA COLI* IN ENVIRONMENTAL WATER SAMPLES

ABSTRACT

To achieve active management of bathing areas and to reduce risk associated with the presence of faecal pollution, tests capable of rapid on-site assessment of microbiological water quality are required. A protocol for the recovery and detection of faecal pollution indicator bacteria, E. coli, using β-D-Glucuronidase (GUS) activity was developed. The developed protocol involves two main steps: sample preparation and GUS activity measurement. In the sample preparation step syringe filters were used with a dual purpose, for the recovery and pre-concentration of *E. coli* from the water matrix and also as µL reactors for bacteria lysis and GUS extraction. Subsequently, GUS activity was measured using a continuous fluorometric method developed previously. The optimum GUS recovery conditions for the sample preparation step were found to be 100 µL PELB (supplemented with 1 mg mL^{-1} lysozyme and 20 mM DTT) at 37 °C for 30 min. The protocol was evaluated on environmental samples (fresh and seawater) against an establish GUS assay method (Coliplage®). GUS activities corresponding to samples containing as low as 26.18 MPN E. coli 100 mL^{-1} were detected for the seawater sample and as low as 110.2 MPN E. coli 100 mL^{-1} for the freshwater samples. By comparison with the Coliplage® method, this protocol offered an improvement in the measured GUS activities of 3.08 fold for freshwater samples and 4.13 fold for seawater samples. Furthermore, the protocol developed here, has a time-to-result of 75 min, and successfully addresses the requirement for tests capable of rapid assessment of microbiological water quality.

4.1 Introduction

In Europe the water quality of recreational areas has major medical, environmental and economical implications. To limit the pollution in such areas a new European Directive for the management of bathing water quality was published in 2006 [69]. This directive brings a legal framework to these problems and increases the responsibility for monitoring and remediation of such sites. Furthermore, the Directive also introduces the concept of active management by assessing the contamination vulnerability of the water body and by routine monitoring of faecal indicators bacteria (FIB), *E. coli* and *enterococci*. Standards methods for *E. coli* detection rely on cultivation of the target organism which requires relatively long incubation periods (from 18h up to a few days).

In this context, a protocol for the recovery and detection of *E. coli* from environmental samples has been developed. The protocol is presented in Fig. 4-1 and consists of six steps. The first four steps represent the sample preparation procedure, while the remaining two steps are required for the detection. A continuous fluorometric method for measuring GUS activity has been previously developed in the group [138]. The key aspect of this work was the use of 6-chloro-4-methyl-umbelliferyl-β-D-glucuronide (6-CMUG) as a fluorogenic substrate instead of 4-methyl-umbelliferyl-β-D-glucuronide (4-MUG). For the sample preparation step syringe filters were used with a dual purpose, pre-concentration of bacteria from the water sample (step 1, Fig. 4-1) and also as μL reactors for cell lysis and GUS extraction (step 3, Fig. 4-1). Beside the pre-concentration of bacteria, the filtration (step 1) also removes the sample matrix, which can contain compounds that interfere with GUS assay. An example of such interferences are represented by dissolved free GUS or extracellular GUS[170],[186] and by dissolved free ions which can inhibit GUS activity or quench the fluorescent signal [187],[188]. Once the bacteria are captured, the lytic agent is added into the syringe filter and allowed to lyse the cells for 30 min, at 37 °C (steps 2, 3 Fig. 4-1). Subsequently, GUS is eluted into 2 mL of buffer (step 4, Fig. 4-1). This step also removes interferences like light scattering from particles or sediment present in the water samples as they are retained on the filter.

This work describes the optimisation of the sample preparation procedure to maximise the recovered GUS (steps 1-4, Fig. 4-1). Once coupled with the continuous fluorometric method, the performance of the protocol is evaluated on environmental water samples and by comparison with an established GUS assay method (Coliplage® method).

As a consequence this chapter aims to:

- Optimise the sample preparation procedure in order to maximise the recovered GUS activity (steps 1-4, Fig. 4-1);
- Couple the sample preparation with the continuous fluorometric method and evaluate the performance of the protocol in detecting *E. coli* from environmental water sample;
- Asses the performance of the developed protocol against an established GUS assay method (Coliplage® method).

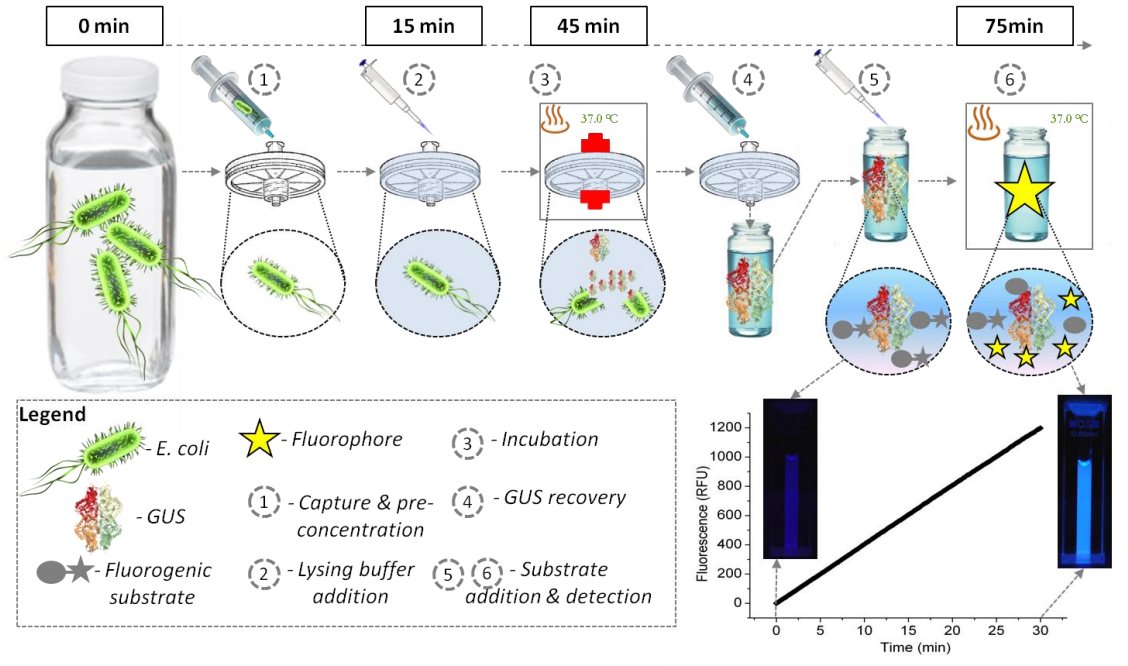

Figure 4-1 Graphical representation of the developed protocol for detecting *E. coli* in environmental waters using the marker enzyme GUS.

4.2 Materials and Methods

4.2.1 Materials

4.2.1.1 Reagents

E. coli β-glucuronidase type VII-A (27% purity), sodium phosphate monobasic and dibasic, sodium carbonate, sodium bicarbonate, 1,4-dithiothreitol (DTT), 4-methyl umbelliferone (4-MU) (99%) and 4-methyl-umbelliferyl-β-D-glucuronide (4-MUG) (99%) were all purchased from Sigma Aldrich Ireland. The other two fluorogenic substrates 6-chloro-4-methyl-umbelliferyl-β-D-glucuronide (6-CMUG) (97%) and 3-carboxy-umbelliferyl-β-D-glucuronide (3-CUG) (99%) were ordered from Glycosynth Limited (UK) and Marker Gene Technologies (US), respectively. 6-chloro-4-methyl-umbelliferone (6-CMU) (97%) was ordered from Carbosynth Limited (UK). Water was passed through a Milli-Q water purification system. Stock solutions of fluorophores and substrates (100 mM) were prepared in 1 mL DMSO (99.5%) and kept at 4 °C. Further dilutions were prepared daily in buffer or deionised water with a final DMSO concentration in the working solution, ranging from 0.01% -1%.

4.2.1.2 Detergents and lysis buffers

Triton® X-100, Triton® X-114, Tween® 20, Tween® 80, Nonidet® P-40 Substitute (P-40), Brij® 35, Brij® 58, CHAPS, Non Detergent Sulfobetaine 201 (NDSB) were all ordered from VWR Ireland. Bug Buster® protein extraction reagent (BB) was ordered from VWR. Bacterial PE LB™ (PELB) with PE LB™ Lysozyme was ordered from VWR. CellLytic™ B Cell Lysis Reagent (CL) was ordered from Sigma Aldrich Ireland.

4.2.1.3 Syringe Filters

Corning® syringe filters with cellulose acetate surfactant free membrane (SFCA), nylon membrane and polyethersulfonate membrane (PES) with pore sizes of 0.45 μm, were all ordered from Sigma Aldrich Ireland. Syringe filters caps, Combi-Cap male/female Luer were ordered from VWR Ireland.

4.2.1.4 *E. coli* tests

The Colilert-18®/Quanti-Tray 2000® system (IDEXX Laboratories) used for the enumeration of coliforms and *Escherichia coli* was ordered from Techno-Path Ireland.

4.2.2 Methods

4.2.2.1 Fluorescence spectroscopy

Fluorescence measurements were carried out using a Jasco FP 8300 Spectrofluorometer equipped with a holographic concave grating in modified Rowland mount monochromator and a 150 watts Xe lamp. A Peltier thermostatted single cell holder (ETC-273T) was used to maintain constant temperatures and for temperature studies. Sample cells were 3.5 mL (10x10 mm) and 1.4 mL (10x4 mm) UV quartz cuvettes, equipped with a Teflon stopper (Helma Analytics). Unless otherwise stated all the emission and excitation spectra were recorded using the accumulation mode as an average of 3 scans (with a scan speed of 200 nm min^{-1}).

4.2.2.2 Microbial analysis of water samples

Water samples were collected in sterile 500 mL or 2 L high density polypropylene (HDPP) bottles. Samples were transported to the lab on ice within 2 h and inoculated within 4 h after collection. The Colilert-18®/Quanti-Tray 2000® system (IDEXX Laboratories) was used for the enumeration of coliforms and *Escherichia coli* and Enterolert®/Quanti-Tray 2000® system (IDEXX Laboratories) was used for the enumeration of Enterococci. The enumeration protocol was followed in accordance with manufacturer's instructions. Aliquots of 10 mL from original water samples were diluted 1:10 with sterile deionised water into 100 mL bottles. After the addition of Colilert-18 samples were inoculated into Quanti-Trays and sealed. For *E. coli* and coliform enumeration, samples were incubated at 37.0 °C for 18 to 20 h. Following incubation the Quanti-Tray wells were read visually for yellow colour indicating the presence of coliforms and for blue fluorescence indicating the presence of *E. coli*. The number of positive wells was recorded for both tests and converted to most probable number (MPN) estimations using tables provided by the manufacturer. For quality control, replicates of positive controls of *E. coli* ATCC 11775, negative controls and laboratory reagent blank were analysed for each 20 samples.

4.2.2.3 Sample preparation for the recovery of GUS from environmental water samples

A sample preparation protocol for the capture and pre-concentration of *E .coli* followed by the recovery of GUS from environmental water samples is presented in Fig. 4-1 (steps 1 to 4) and a picture of the consumables used for the analysis of one water sample

is presented in Fig. 4-2. For step 1, after vigorously mixing the water sample, 50 mL sterile syringes with luer lock were used to collect 50 mL of sample and pass it through the syringe filter. This procedure was carried out twice for each measurement to account for 100 mL of sample. Following bacteria capture, each syringe filter was washed three times with 10 mL of deionised water using a 20 mL syringe and finally purged with air (3 to 5 cycles) to remove residual liquid. In the 2nd step, 100 μL of lytic agent was gently pipetted into to the syringe filter and allowed to flow inside. In step 3, the syringe filters were immediately sealed using screw caps, vigorously mixed for 5 s and placed in the incubator at 37 °C for 30 min facing upwards (Fig. 4-2 inset). In step 4, upon removal from the incubator, the caps were removed and a 2 mL sterile syringe was used to flush 1.9 mL of cold sodium phosphate buffer (pH 6.8) through the filter and a 2 mL glass vial was used to collect the filtrate. This was followed by a gentle step of air purge using the same syringe to recover the remaining residual liquid (2-3 drops) without excessive foaming.

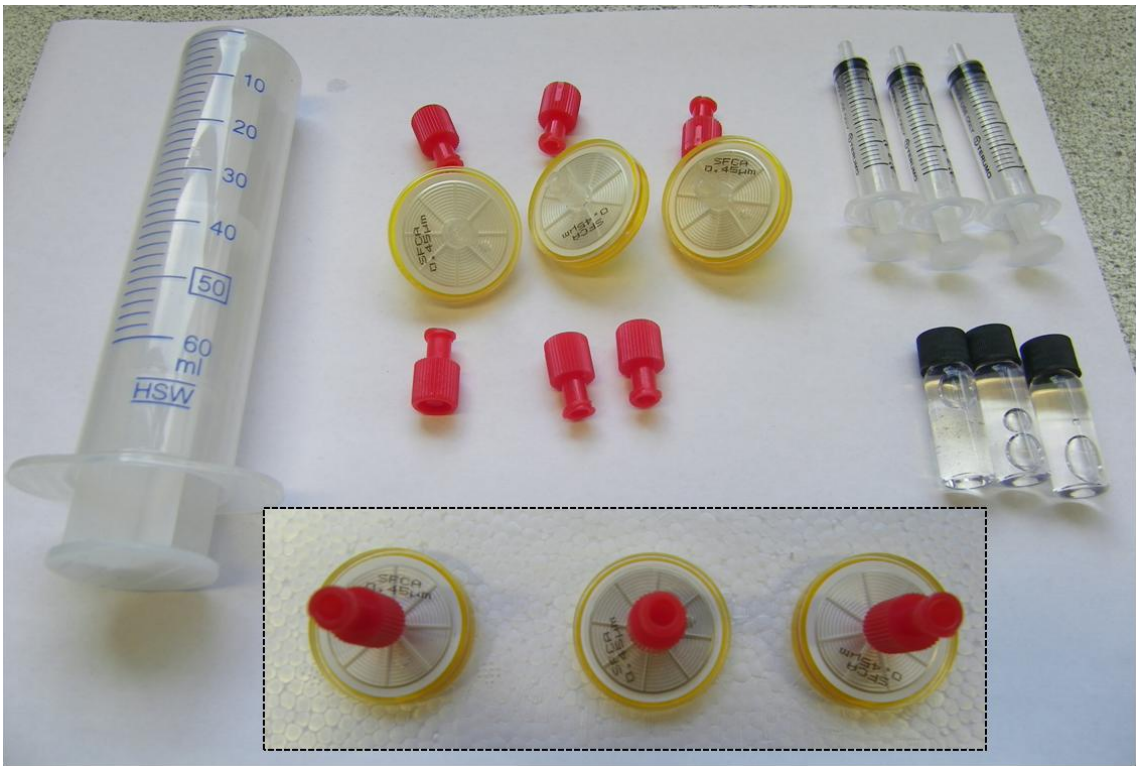

Figure 4-2 Picture showing the syringes, syringe filters, caps and glass vials required for the analysis of 1 water sample. Inset shows the capped syringe filters in a polystyrene holder before incubation.

4.2.2.4 GUS detection

Sample GUS activity measurement was carried out by the addition of fluorogenic substrate to the 2 mL of collected filtrate. The measurement can be carried out in a continuous or discontinuous fashion as detailed below.

4.2.2.4.1 Continuous set-up

A continuous fluorometric assay for measuring GUS activity as developed previously [138] was used. Briefly, the 2 mL of recovered GUS solution was transferred to a 3.5 mL quartz cuvette. This was placed in the fluorometer and allowed to reach 37 °C (2 min) after which 10 µL of 6-CMUG (100 mM) in DMSO was added to give a final 6-CMUG concentration of 0.5 mM. The solution was vigorously mixed and placed back in the fluorometer where the fluorescence was monitored using the λ_{ex} (369 nm) and λ_{em} (452 nm) maximum of 6-CMU. Measurements were collected every second for a time spawn between 10 and 30 min depending on the sample GUS activity. Reaction rates

(FU min^{-1}) were determined using the slope of fluorescence formation after normalisation to 1 min. To convert FU min^{-1} into μM min^{-1} calibration curves were constructed for 6-CMU in the presence of 0.5 mM 6-CMUG, at 37 °C in the assay buffer containing 100 μL PELB supplemented with 1 mg mL^{-1} lysozyme and 20 mM DTT.

4.2.2.4.2 Discontinuous set-up

A discontinuous method for measuring GUS activity was adapted from Jefferson [129]. Briefly, the 2 mL vials containing the recovered GUS were placed in the incubator and allowed to reach 37 °C (5 min). Upon removal 10 μL of 4-MUG (100 mM) in DMSO was added to give a final 4-MUG concentration of 0.5 mM. The vials were vigorously mixed and placed back in the incubator at 37 °C. After mixing the reaction was allowed to equilibrate and achieve maximum velocity for 5 min, when the first 200 μL were collected into Eppendorf tubes containing 1.8 mL stop buffer (200 mM Na_2CO_3, pH 11.4). This was the "time=0" point, and successive 200 μL aliquots were removed at regular time intervals (10, 20 and 30 min). The solutions were allowed to reach room temperature, and the fluorescent signal was measured in 3.5 mL quartz cuvettes. GUS activity (μM min^{-1}) was determined through calibration curves of 4-MU in stop buffer and in the presence of 0.5 mM 4-MUG. All the activities recorded were multiplied by 10 to account for the dilution factor.

4.2.2.4.3 Kinetic end-point set-up

Sample preparation was carried out as outlined in step 1 in section 4.2.2.3. Once the bacteria were captured inside the syringe filter, 100 μL of lytic agent containing 0.5 mM 4-MUG was added. The syringe filter was further capped and incubated at 37 °C for exactly 30 min. Upon removal from the incubator, the reaction was stopped by elution with 1.9 mL of stop buffer (200 mM Na_2CO_3, pH 11.4) into 2 mL glass vials. The solutions were further transferred into 3.5 mL quartz cuvettes and the fluorescence was recorded. A control sample was run using the same procedure, for 100 mL of deionised water. This also served as the black or time=0 point and the fluorescence was subtracted from the sample fluorescence. The result expressed in FU was converted into μM 4-MU

using calibration curves, and finally converted in activity (μM min^{-1}) by time derivatization.

4.2.2.5 Optimisation of sample preparation

4.2.2.5.1 Syringe filter selection

100 mL of water samples were filtered through the three types of syringe filters (PES, SFCA and nylon) and the filtrate was collected in sterile 100 mL containers. Both the sample and the filtrate were analysed for *E. coli* using the method described in section 4.2.2.2 and the % of captured bacteria was calculated for each syringe filter type. The % of captured *E. coli* was assessed for each filter for two types of samples, one with low sediment loads and one with high sediment loads. For the recovery of GUS from each filter, 100 μL of sodium phosphate buffer containing 250 ng mL^{-1} GUS was added to each syringe filter in triplicates. The filters were capped as described in section 4.2.2.3 and placed in the incubator for 30 min at 37 °C. Upon removal, GUS was eluted in 1.9 mL of sodium phosphate buffer and the residual activity measured. A control was carried out using the same procedure without the filtration step, by preparing 2 mL of GUS (25 ng mL^{-1}) in sodium phosphate buffer.

4.2.2.5.2 Lytic agent selection

A range of non-ionic and zwitterionic detergents (section 4.2.1.2) were evaluated for the recovery of GUS from *E. coli* contaminated environmental samples. With the exception of CHAPS and NDSB, all the detergents were received in 10% purified aqueous solutions from which 0.1%, 0.5%, 1%, 2% and 5% (v/v) dilutions were prepared in phosphate buffer (pH 6.8). CHAPS and NDSB were received as powders from which 10% (w/v) stocks were prepared in deionised water. The commercially available lytic agents were used at the received concentration or further diluted in phosphate buffer to give 10%, 20%, 50% and 75% (v/v) dilutions. For the determination of GUS activity, the sample preparation protocol (steps 1 to 4) was used as described in section 4.2.2.3, coupled with the discontinuous detection method described in section 4.2.2.4.2. For the initial screening a total of 8 environmental samples, collected over 3 months, were used. All the samples were collected from the Tolka River, in the vicinity of Dublin City University and analysed for *E. coli* and total coliforms. At the end of study, an optimum

concentration was chosen for each detergent/lytic agent, and a final sample was analysed with all the detergents/lytic agents at this concentration.

E. coli β-glucuronidase type VII-A was used to evaluate the inhibitory effect of each detergent/lytic agent on GUS. For this purpose, 10 µL of GUS (0.35 µg mL^{-1}) was added to 100 µL of detergent/lytic agent in a 2 mL glass vial. The vials were capped and incubated at 37 °C for 30 min to mimic the lysis protocol, after which 1.9 mL of sodium phosphate buffer with 0.5 mM 4-MUG was added. The activity was further measured using the discontinuous method described in section 4.2.2.4.2.

The impact of the detergents/lytic agents on the fluorescent efficiency of 4-MU and 6-CMU was also evaluated. For this purpose, 4-MU was added at a concentration of 100 nM into 2 mL vials containing 1.9 mL stop buffer and 100 µL detergent/lytic agent at various concentrations (detailed above). The fluorescence of each sample was recorded at 20 °C, and compared with a control sample without detergent. This data was further used to correct the fluorescence intensities recorded for each detergent/lytic agent concentration. For 6-CMU, the same experiment was carried out at pH 6.8 and 37 °C.

4.2.2.5.3 Protocol Optimisation

For all the optimisation steps described in this section samples were processed as described in section 4.2.2.3 and 4.2.2.4.2 unless otherwise stated. To optimise the six parameters, a total of three different water samples collected from the Tolka River were used. Activities are reported as % relative to the optimum condition found for each parameter.

4.2.2.5.3.1 Lysozyme concentration

Lysozyme was prepared from 40 mg mL^{-1} stock solutions to a final concentration of 0.1, 0.25, 0.5, 1, 1.25, 1.5, 2.0 and 5.0 mg mL^{-1} in PELB buffer. 100 µL aliquots were added into the syringe filter and the sample was processed as described in sections 4.2.2.3 and 4.2.2.4.2.

4.2.2.5.3.2 Volume of lytic agent

Lysozyme was added at a final concentration of 1 mg mL^{-1} in PELB buffer and from this solution, aliquots of 25, 50, 75, 100, 1.25, 150 and 200 µL were introduced into the syringe filter.

4.2.2.5.3.3 Temperature

Samples were incubated at 20, 25, 30, 37, 40, 44, 50 and 60 °C for 30 min. The volume of PELB buffer added into the filter was 100 µL supplemented with lysozyme (1 mg mL^{-1}).

4.2.2.5.3.4 Time

Samples were incubated at 37 °C for 5, 10, 15, 20, 25, 30, 45, 60, and 120 min. The volume of PELB buffer added into the filter was 100 µL supplemented with lysozyme (1 mg mL^{-1}).

4.2.2.5.3.5 Shaking speed

A Stuart SSL2 reciprocating shaker was used to evaluate the effect of shaking speed (RPM) on GUS recovery. Samples were processed at 20 °C with RPM values of 50, 100, 150, 200 and 250.

4.2.2.5.3.6 DTT Concentration

A 0.5 mL stock solution of DTT (100 mM) was prepared fresh in PELB buffer. Further dilutions were prepared in the same PELB buffer (containing 1mg mL^{-1} lysozyme) to a final concentration of 1, 2, 5, 10, 20, 30, 40 and 50 mM.

4.2.2.5.4 Recovery

This experiment was designed to evaluate the activity of GUS recovered from the syringe filter as a function of elution steps. A water sample highly contaminated with *E. coli* (8664 MPN) was collected from the Camac River and processed as described in section 4.2.2.3 and 4.2.2.4.2. This resulted in the activity recorded after the 1st elution step. To further check for residual GUS left in the syringe filters another three elution steps consisting of 2 mL of sodium phosphate buffer were carried out and GUS activity was measured. The same experiment was carried out with the commercially available GUS (*E. coli* β-glucuronidase type VII-A). As a detection method in this case we used the continuous one described in section 4.2.2.4.1

4.2.2.6 Evaluation of the kinetic end-point method

The kinetic end-point method described in section 4.2.2.4.3 was evaluated against the continuous method described in section 4.2.2.4.1. For comparison, two water samples were collected from Tolka River and dilutions were generated by filtering 5, 10, 25, 50, 75 and 100 mL from the original sample.

4.2.2.7 Analytical Performance

The analytical performance of the method was evaluated by comparison with a widely used method for rapid detection of *E. coli* using GUS [170-177],[180]. Fresh water samples were collected from Tolka River while seawater samples were collected from Dublin Bay. A total of 3 samples (2 freshwater, 1 seawater) were collected for this study over the course of two weeks. From each sample, dilutions of 1 %, 2 %, 4 %, 5 %, 10 %, 25 %, 50 % and 75 % sample were prepared in 1L sterile containers with deionised water. From this volume, 300 mL were used for the protocol developed here while 300 mL were used for the literature method. *E. coli* counts were determined as described in section 4.2.2.2, from the original sample and were estimated for the prepared samples from the dilution factor. For the literature method, 100 mL volumes were removed and filtered through 0.45 µm pore size, 47 mm diameter polycarbonate filters. The filters were washed three times with 10 mL aliquots of deionised water and placed in 50 mL Erlenmeyer flasks containing 10 mL assay buffer (50 mM sodium phosphate buffer pH 6.8, 0.5 mM 4-MUG and 0.1% Triton X-100). The flasks were incubated at 37 °C in a shaking water bath for 35 min. After the first 5 min 2 mL were removed and added to a 2 mL glass vial containing 40 µL of 1M NaOH. This point represented the time=0 point for the reaction progress. Every 10 min for the next 30 min a 2.0 mL aliquot was removed and mixed in the same manner with NaOH. The fluorescent signal was than measured and GUS activities determined as described in section 4.2.2.4.2 for the discontinuous method. A control containing deionised water instead of the sample was used to monitor the auto hydrolysis of the substrate during the process.

For the protocol developed here, we used the optimum conditions for both GUS recovery and detection. The lytic agent was prepared daily in 2.5 mL volumes using 62.5 µL lysozyme (40 mg mL^{-1}), 500 µL DTT (100 mM) in PELB, and 2 mL PELB.

The syringe filters were incubated at 37 °C for 30 min, and GUS activity measured with the continuous method as described in section 4.2.2.4.1.

4.3 Results and Discussion

4.3.1 Filter selection

The ideal filter for this application should provide sufficient capabilities in terms of *E. coli* recovery from the water sample, very low binding affinity with GUS and full compatibility with the chemical characteristics of the lytic agent and sample to be filtered. Furthermore, the filter should be able to provide sufficient flow rates and be robust enough to withstand filtration of large volumes (100 mL or more) of environmental water samples without clogging or damaging the membrane. Based on these characteristics three types of material were selected for the filter: polyethersulfonate membrane, nylon membrane and cellulose acetate membrane. The filter testing was carried out in terms *E. coli* capture efficiency from fixed volumes of water sample and in terms GUS binding affinity. All the three filters offered a good % *E. coli* capturing efficiency with values of over 99.5%. A low turbidity sample (low sediment load) and a high turbidity sample (high sediment load) were used in this experiment and the results are summarised in Table 4-1. The high turbidity sample was collected briefly after a rainfall event which also explains the higher *E. coli* counts.

Table 4-1 *E. coli* capturing efficiency for the three types of syringe filters tested.

	Low Sediment load (2.13 ± 0.46 mg L^{-1})			High Sediment load (32.53 ± 2.01 mg L^{-1})		
Filter type	Sample (MPN)	Filtrate (MPN)	% Captured	Sample (MPN)	Filtrate (MPN)	% Captured
PES	1081	0	100	7556	5.1	99.93
SFCA	1081	2.0	99.81	7556	2.0	99.97
Nylon	1081	3.0	99.72	7556	3.1	99.95

In terms of GUS binding affinity, we performed a GUS recovery test from the syringe filters. The results are presented in Fig. 4-3, and suggest that there is a certain level of GUS activity loss for all the three materials. The highest % recovery was obtained from the SFCA filter followed by the PES filter and nylon filter. Further assessment of the syringe filters was done in terms of robustness, flow rates and the manual pressure

required for filtering various volumes of sample. Overall the SFCA filter showed optimal performance and it was chosen for this application.

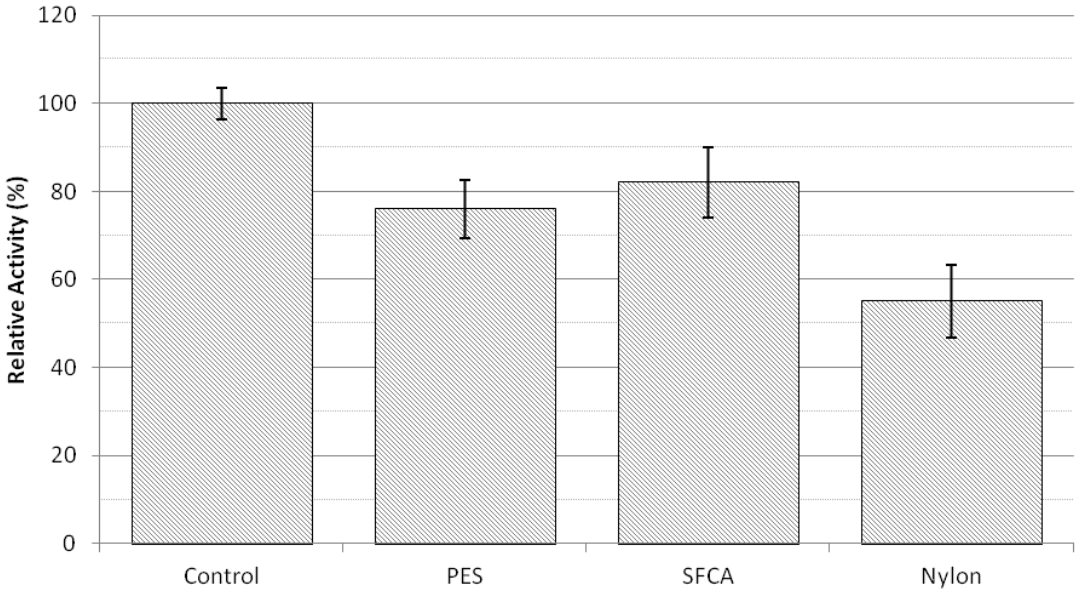

Figure 4-3 GUS activities recovered from the syringe filters. The activities are expressed as % relative to the control. Experimental details are described in Methods. Error bars represent the STD of three runs from three filters for each material

4.3.2 Fluorophore calibration curves

The excitation/emission behaviour of these two fluorophores 6-CMU and 4-MU has been discussed in detail previously [138]. The optimum λ_{ex} / λ_{em} wavelengths were found to be 369/452 and 364/447 for 6-CMU and 4-MU respectively. Calibration curves prepared for the two fluorophores at medium and high sensitivity setting on the fluorometer are presented in Fig. 4-4. The two different sensitivity settings were used to avoid problems arising from detector saturation in samples with high GUS activity. As the calibration curves were performed using the same fluorometer settings, the slopes can be readily compared between 4-MU and 6-CMU as a function of sensitivity. For the high sensitivity setting, the slope of 4-MU is slightly higher than the slope of 6-CMU (1858.7 as opposed to 2018.1) while for the medium sensitivity setting, the two slopes are very similar (24194 as opposed to 24390). This further confirms the analysis done

previously, which showed that the fluorescence efficiency of 6-CMU at pH 6.8 is similar with the fluorescence of 4-MU at pH 11.4 [138].

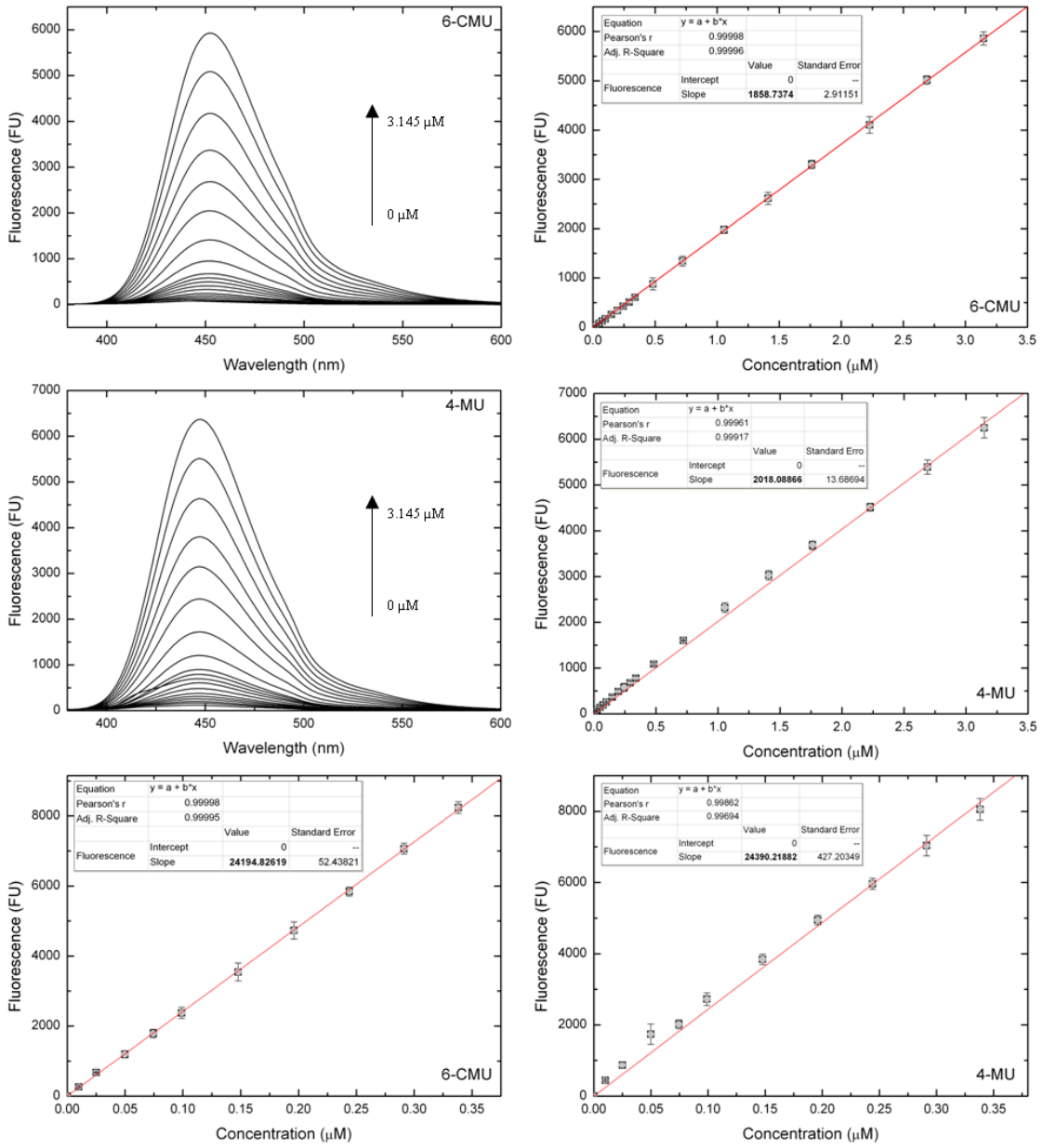

Figure 4-4 Calibration curves of 6-CMU and 4-MU for two fluorometer sensitivity settings. Emission spectra and calibration curve recorded for 6-CMU using medium sensitivity (top) and high sensitivity (bottom left). Emission spectra and calibration curve recorded for 4-MU using medium sensitivity (middle) and high sensitivity (bottom right). Experimental conditions are detailed in methods. The error bars represent the SD of three individually prepared solutions.

4.3.3 Lytic agent selection

A range of non-ionic and zwitterionic detergents together with three commercially available lytic agents were evaluated for the recovery of GUS from river water samples. In the initial stage, a total of 8 samples were used for screening various concentrations of detergents/lytic agents. The *E. coli* counts found over the course of this study varied from 1112 (MPN 100 mL^{-1}) up to 8704 (MPN 100 mL^{-1}). To facilitate direct comparison between the GUS activities recorded for water samples with varying *E. coli* concentrations, all the recorded GUS activities were adjusted to represent the activity of 2500 MPN *E. coli* 100 mL^{-1} using the following equation:

$$GUS\ 2500 = \frac{GUS}{\frac{E.coli}{2500}}$$

Where

- GUS 2500 -represents the calculated GUS activity for 2500 MPN *E. coli*
- GUS - represents the activity measured from the water sample
- *E. coli* - represents the *E. coli* (MPN 100 mL^{-1}) found in the sample

In addition to this, GUS activities were further corrected for each detergent/lytic agent concentration to account for the influence of these compounds on the fluorescence efficiency of the fluorophores. It was found that higher detergent/lytic concentrations have a higher fluorescence quenching effect. At 0.005 % (v/v) detergent concentration and 1/20 lytic agent dilution no quenching effect was noticed. In the case of detergents, accelerated quenching was noticed once the concentration of detergent exceeded 0.05% (v/v). Using this information, GUS activity data was further corrected to account for the loss in fluorescence signal using the following formula:

$$GUS_{cor} = GUS + [GUS \times (\%FU_B - \%FU_D)]$$

Where

- GUS_{cor} - represents the corrected GUS activity (nM min^{-1})
- GUS - represent GUS activity (nM min^{-1})
- $\%FU_B$ - represents the fluorescence intensity of the blank expressed as 100%

- $\%FU_D$ - represents the fluorescence intensity in the presence of detergent/lytic agent expressed in % relative to the blank.

For both 4-MUG and 6-CMUG the highest fluorescence quenching effect was noted in the case of NDSB (Fig. 4-5). The lytic agents had no significant effect on 4-MU and 6-CMU fluorescence with the exception of CL, where a 9.6% loss was observed (Fig. 4-5).

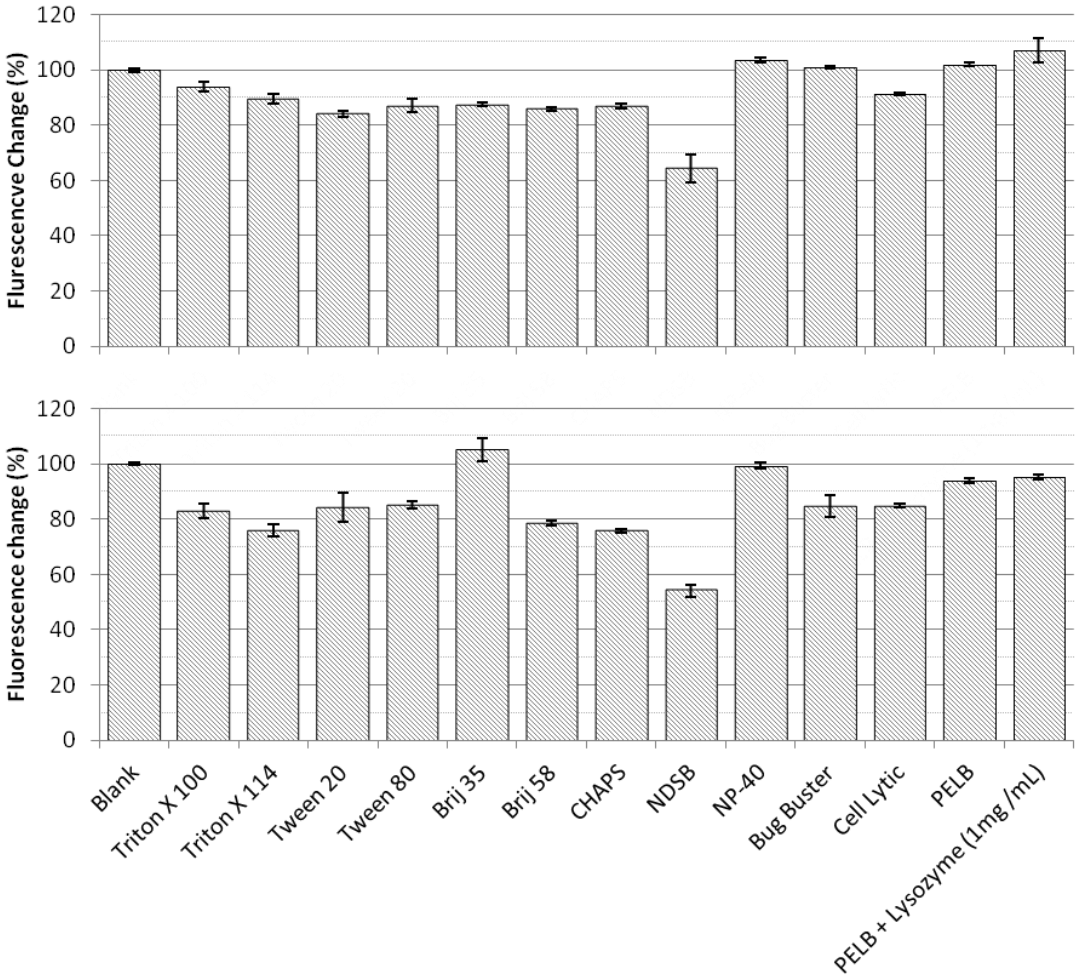

Figure 4-5 Fluorescence of 100 nM 4-MU (top) and 100 nM 6-CMU (bottom) in the presence of detergents (0.05% (v/v)) and lytic agents (5% (v/v)). Fluorescence intensity is expressed as relative to the fluorescence intensity of the blanks which was 2232 ± 57 for 6-CMU and 2417 ± 68 for 4-MU. Experimental conditions are detailed in the Methods Section.

GUS activities recorded at detergent concentrations ranging from 0.1% to 5% are presented in Fig. 4-6. For all the detergents GUS activity increased with increasing detergent concentration in the 0.1% - 1% range with the exception of Triton X114 and NDSB. After the 1% threshold activities either decreased (denoting GUS inhibition or GUS denaturation) or remained constant. Triton X100, Tween 20, Brij 35 and NP 40 generated the highest GUS activities at 1% and 2% concentration.

The lytic agents performed best in terms of GUS activity at the received concentration with the exception of CL which was more effective at 75% (Fig. 4-7). The highest GUS activity was measured using the PELB buffer as received, supplemented with 1 mg mL^{-1} lysozyme. The activity recorded in this set-up was 1.6 times higher than BB, 2.1 times higher than CL and 3.8 times higher than the activity recorded for Triton X100.

Overall these results suggested that the lytic agents were more effective in recovering GUS from environmental water samples than the detergents. To further test if this assumption stands, the same water sample was analysed with all the detergents and lytic agents at the optimum concentrations found previously. Although the exact same methodology was used as in the previous experiment (Fig. 4-6, 4-7) the GUS activities recorded for one sample (Fig. 4-8) were found to be slightly different. This difference was noticed in the ratios of GUS activities recorded in the various conditions. Although the best GUS recovery was still obtained using the PELB lysozyme combination, the improvement over the recovery with 1% Triton X100 was only 1.7 higher this time as opposed to 3.8. We also found a 2.1 and 2.5 improvement over BB and CL as opposed to 1.6 and 2.1 found previously. It is clear that the variability recorded between the two analyses is driven by the sample characteristics. For the screening experiment multiple samples were used, collected over a relatively long period of time. The difference noticed might be in this case due to variations in the amount of GUS / culturable cell. Previous work has shown that indeed the culture-based methods used to enumerate *E. coli* do not detect viable but not culturable (VBNC) bacteria and so they underestimate the number of GUS active cells [180]. The VBNC is defined as the state in which bacteria still maintain a certain level of metabolic activity but no longer grow when supplemented with growth medium. The major inducer of VBNC state is the environmental stress, which could be due to lack of nutrients, salinity, temperature or UV radiation among others [189, 190]. Another reason for the difference might be due

to the presence of particle associated bacteria [112], [106]. These bacteria form clusters or attach to suspended sediments and when cultured their number is being underestimated. Our results suggest that the later might be the case for some of the noticed discrepancies. For the experiments in Fig. 4-7 the samples were collected after a rainy period. The sediment load in the sample was higher and as consequence it is possible the bacteria numbers were underestimated by the culture based method. However in both experiments (Fig. 4-7 and Fig. 4-8) the PELB lysozyme combination recovered the highest amount of GUS and was chosen as the optimum method.

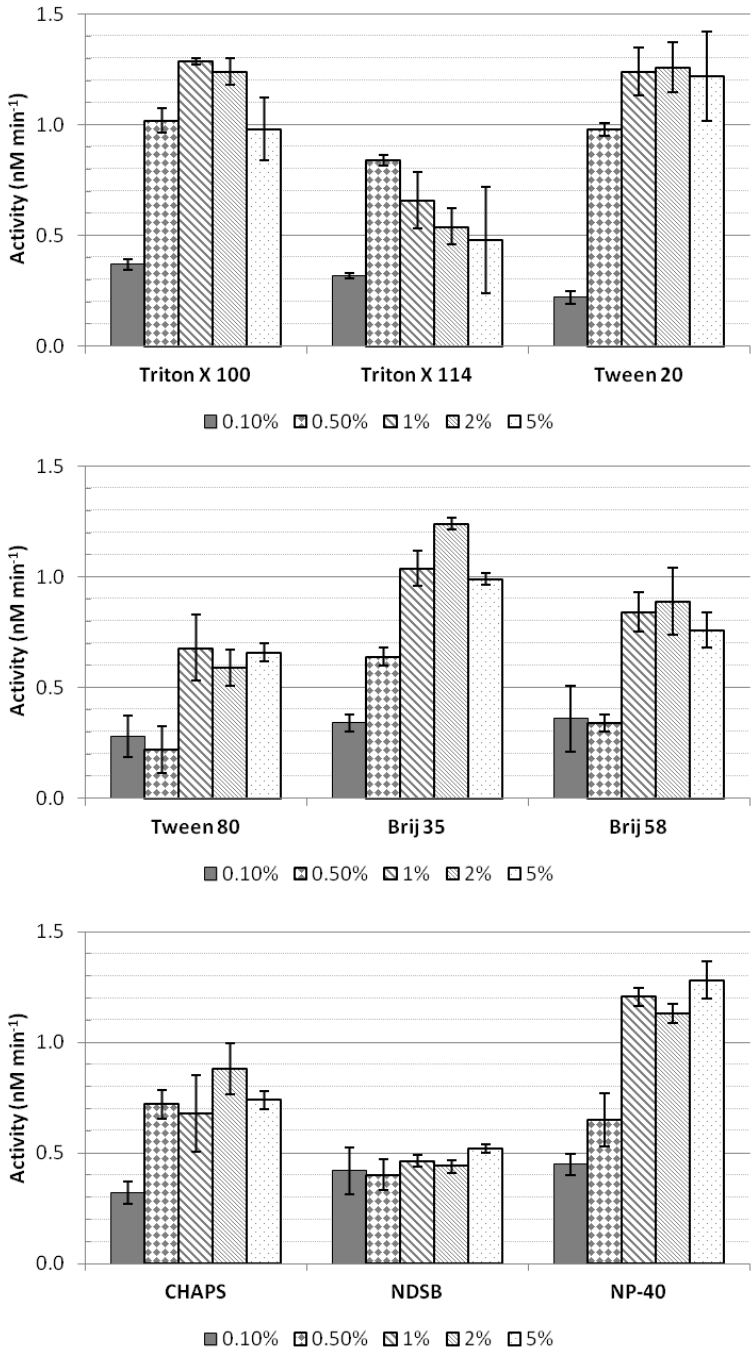

Figure 4-6 GUS activities measured from environmental water samples at different detergent concentrations (shown in the legend). Experimental details are described in methods. Error bars represent the STD of three measurements.

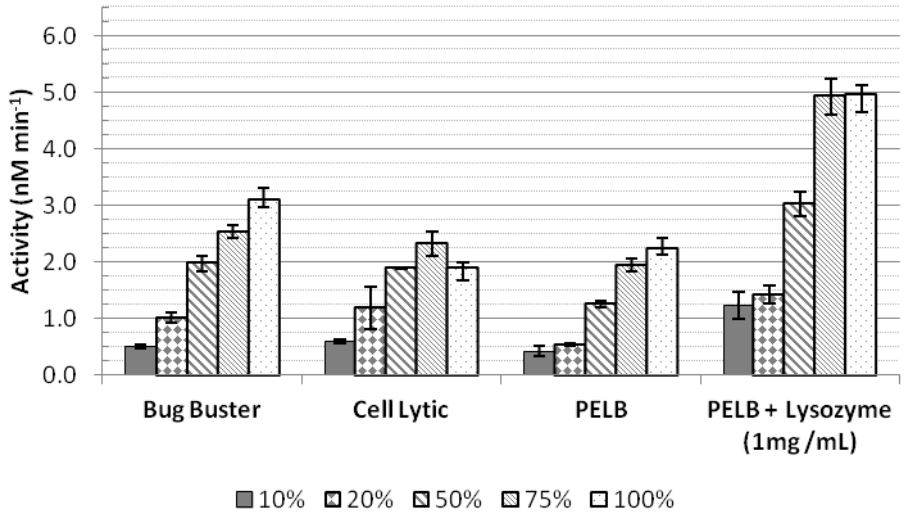

Figure 4-7 GUS activities measured from environmental water samples at different lytic concentrations (shown in the legend). Experimental details are described in methods. Error bars represent the STD of three measurements.

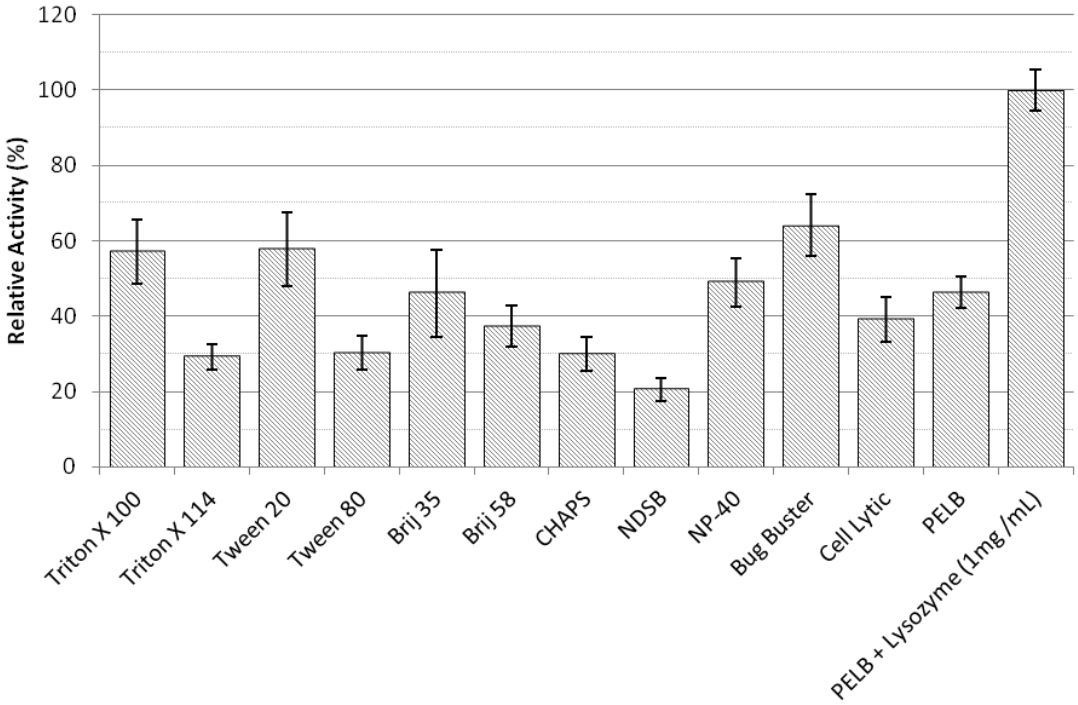

Figure 4-8 GUS activities measured for the same environmental sample using the different detergents/lytic agents. Experimental details are described in methods. Error bars represent the STD of three measurements.

The measured GUS activity once the sample is eluted from the syringe filter can be dictated by a range of parameters. Among them, the lysis efficiency, permeabilisation rate, GUS solubility and GUS stability seem to be the most important. In an attempt to get further insight into this process, pure GUS was passed through the same process as the water samples (Fig. 4-9). The highest activities in this case were recorded for PELB and PELB lysozyme mixture and were found to be 38% and 28% higher than the control (sodium phosphate buffer 50 mM, pH 6.8). This is somehow surprising, but it can be due to the presence of NaCl (50mM) in the PELB buffer. Past research has shown that the presence of NaCl in the GUS assay buffer can enhance the activity of GUS [191]. The lowest activity and hence the highest GUS inhibition was observed in the presence of BB. In this case GUS activity was 61% lower than in the control. As this lytic agent offered the 2nd best GUS recovery from the environmental samples (Fig. 4-7, 4-8) this result suggests that BB is the most potent in terms of cell lysis efficiency, out of the lytic agents tested.

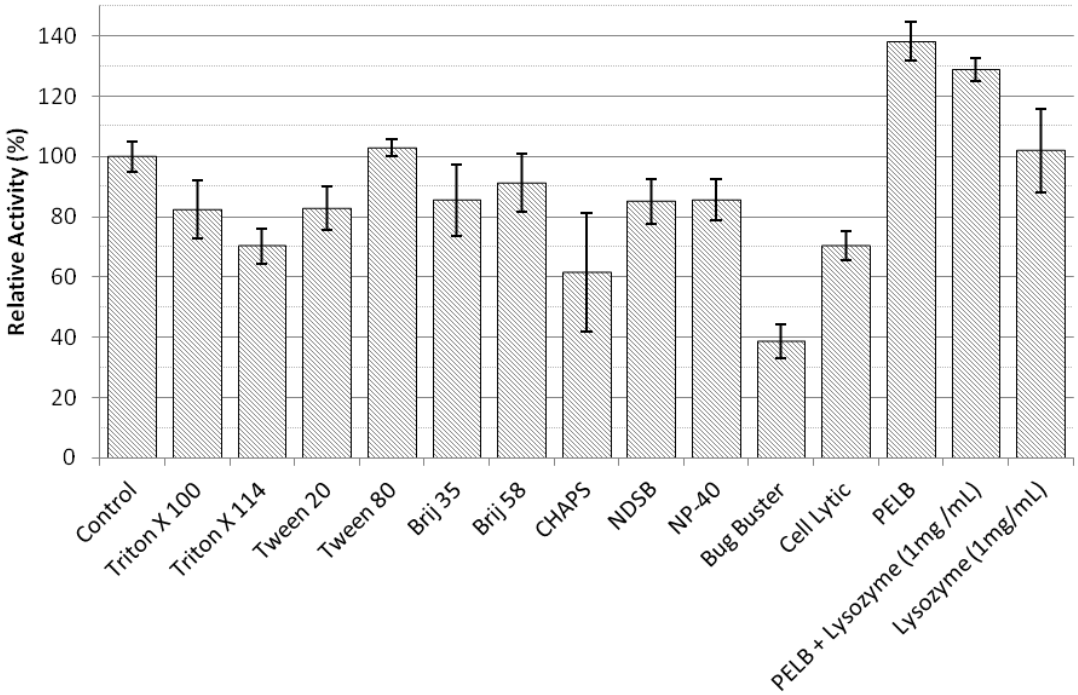

Figure 4-9 GUS activities measured for *E. coli* β-glucuronidase type VII-A in the presence of detergents/lytic agents. Activities are expressed as % relative the control. Experimental details are described in methods. Error bars represent the STD of three measurements.

4.3.4 Protocol Optimisation

Using the optimum GUS recovery conditions found in the previous section, the protocol was further optimised for best results and analytical performance. In this regard a series of parameters including lysozyme concentration, lytic agent volume, temperature, time, shaking and DTT concentration were investigated.

The optimum lysozyme concentration in terms of GUS activity was found to be 1 mg mL^{-1}. Results suggest higher concentrations had an inhibitory effect on the recovered activities and did not improve the protocol (Fig 4-10). The optimum lytic agent volume in terms of GUS activity was found to be 200 µL and this was also the maximum volume that could be introduced into the syringe filter (Fig 4-11). Starting with 50µL the GUS activity increases linearly with volume added. This effect can be explained by the increasing availability of lytic agent to the trapped bacteria. When using smaller volumes of liquid, the available space in the syringe filter is filled with air and it is possible not all the trapped bacteria have access to the lytic agent. When working with samples which had a high sediment load we found it challenging to introduce 200 µL into the syringe filter. We noticed the dead volume (available volume) in the syringe filter was taken up by the trapped sediments and as such there was no space left for the addition of 200 µL lytic agent. Since no difficulties were encountered with the addition of 100 µL to the syringe filter and because minimal variability in sample preparation is desired, the 100 µL volume was chosen for further experiments. The optimum temperature for GUS recovery was found to be 37 °C (Fig 4-12). This offered a 37 % improvement over the room temperature (20 ± 2 °C). The temperature profile recoded is similar with the temperature profile found previously for recombinant GUS; at higher temperatures GUS activity declines drastically [138]. In this case, the observed GUS activity is not just a function of GUS catalytic rate with temperature, but it also depends on other chemical processes. Among them, the catalytic rate of lysozyme, the rate of GUS solubilisation and the rate of GUS denaturation are also important. Previous studies on wild type GUS using 4-nitrophenyl-β-D-glucuronide (4-NPG) [160] and 4-MUG [161],[162] as substrate report temperature profiles with a maximum GUS activity between 40-50 °C. This suggests the wild type GUS is more resistant to temperature stress than the recombinant GUS which losses some activity after 37 °C due to

temperature denaturation [138]. In our case a 44 % and 71 % drop in GUS activity was noticed when temperature was increased from 37 °C to 44 °C and 50 °C respectively. This suggests the rate of lysozyme activity dictates this process and as such the lysis efficiency decreases drastically with temperature.

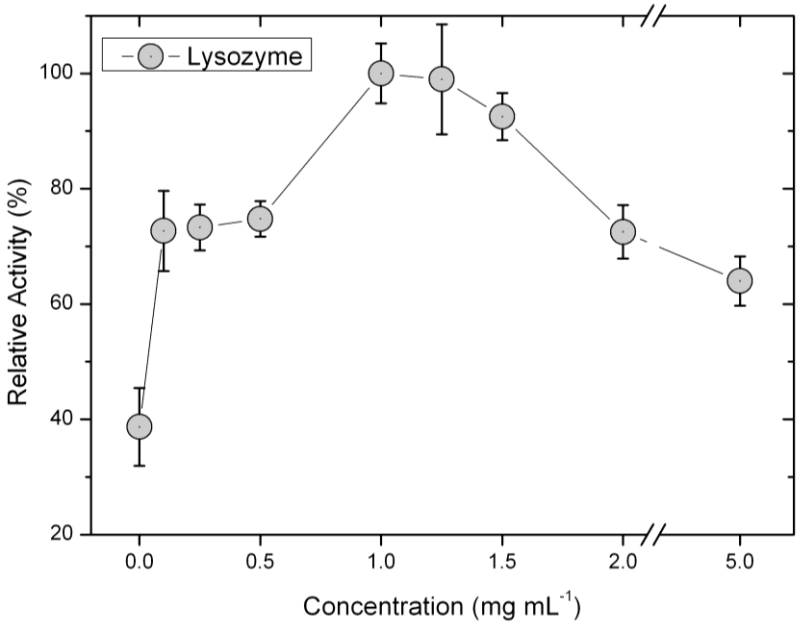

Figure 4-10 Optimisation of lysozyme concentration. Activities are expressed as % relative to the highest activity recorded (1 mg mL^{-1} lysozyme). Experimental details are described in methods. Error bars represent the STD of three measurements.

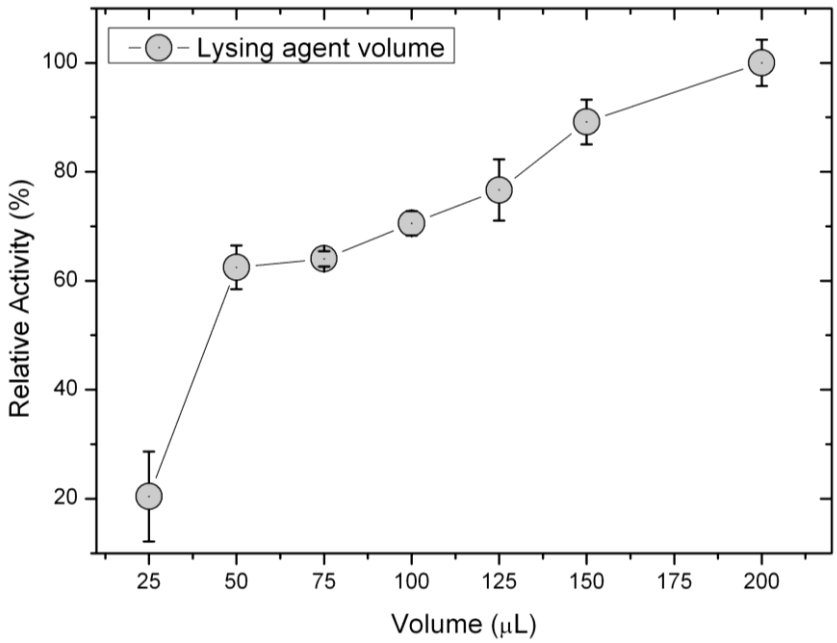

Figure 4-11 Optimisation of lytic agent volume. Activities are expressed as % relative to the highest activity recorded (200 μL). Experimental details are described in methods. Error bars represent the STD of three measurements.

The optimum lysing time for the recovery of GUS was found to be 30 min (Fig. 4-13). From 5 to 30 min a linear increase in GUS activity was noticed. From 30 min to 45 min, 60 min and 120 min, a 7.5 %, 34 % and 39% drop in GUS activity was recorded. Because the extracted GUS (in the syringe filter) increases with time this drop in the measured activity is not due to a lower amount of GUS present, but possibly due to GUS denaturation. During this experiment an increase in the viscosity of the lytic agent inside the filter for samples incubated for 60 and 120 min was noticed. Since the filter is transparent, the movement of liquid inside can be followed with gentle swirling. As the filters were tightly capped and there was no solvent evaporation during the process, the viscosity build-up is most likely due to an increase in the amount of cell debris. It is possible that GUS suffers some irreversible structural changes in these high viscosity conditions which cause it to unfold and become catalytically inactive once recovered in buffer.

For the shaking speed optimisation, the highest activity was recorded when samples were processed at 250 RPM although only a slight improvement (2.2 %) was observed

from 100 RPM to 250 RPM (Fig 4-14). The highest activity increase was noticed between 0 RPM and 50 RPM and 100 RPM after which the activity reached a plateau. Overall, the shaking did improve the recovered GUS activity with 21.8 %. The noticed effect is probably due to a better mixing regime in the syringe filter and improved accessibility of lytic agent to trapped bacteria.

Addition of DTT into the PELB buffer showed to significantly improve the GUS activities recorded (Fig. 4-15). At 20mM DTT a 70% improvement into the GUS activity was observed and this was also the optimum DTT concentration. Further increase in the DTT concentration to 30 mM, 40 mM and 50 mM did not improve the results. DTT is used in protein assays to reduce the disulfide bonds in cysteine residues. This prevents intramolecular and intermolecular bond formation between cysteine residues of proteins and so it prevents structural changes in the protein conformation. In the case of enzymes, DTT helps by maintaining them into a catalytically active conformation. Our results suggest a certain level GUS unfolding occurs in the extracellular environment and the presence of DTT helps with stabilising the enzyme and keeping it active.

Further work was carried out to investigate the efficiency of one step elution with 1.9 mL of sodium phosphate buffer in recovering GUS from the syringe filter (Fig. 4-16). For the *E. coli* contaminated samples, the 1st elution step recovered 84.7% of the total GUS activity (the sum of all the 4 elution steps). The 2nd step recovered 11.66% of the total activity, while the 3rd step recovered the remaining of 3.61%. After the 4th elution no GUS activity was detected. In the case of recombinant GUS, the recovery was higher in the 1st step (89.7 %) while the 2nd and 3rd step yielded GUS activities of 8.64 % and 1.63 %. No residual activity was detected after the 4th elution step. The slight difference between the 1st step recoveries for the sample and GUS is probably due to the presence of sediments and bacteria debris in the syringe filter. This can hinder the elution of GUS, by trapping GUS molecules. Overall, for the purpose of this study only 1 elution step was used.

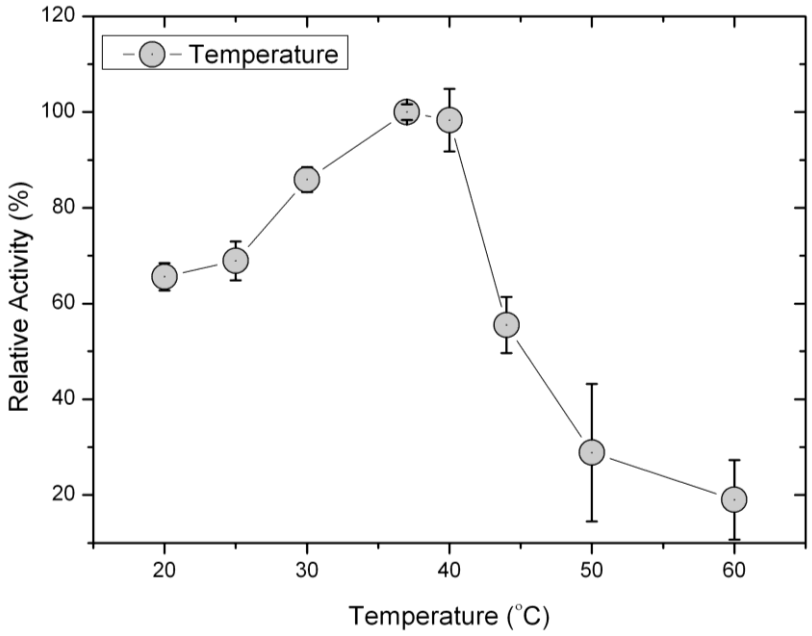

Figure 4-12 Optimisation of temperature. Activities are expressed as % relative to the highest activity recorded (37 °C). Experimental details are described in methods. Error bars represent the STD of three measurements.

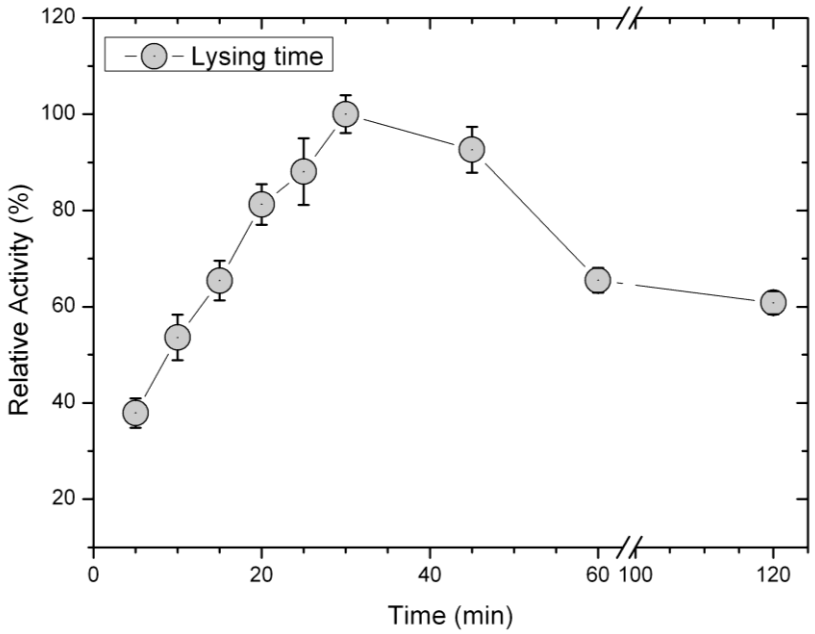

Figure 4-13 Optimisation of lysing time. Activities are expressed as % relative to the highest activity recorded (30 min). Experimental details are described in methods. Error bars represent the STD of three measurements.

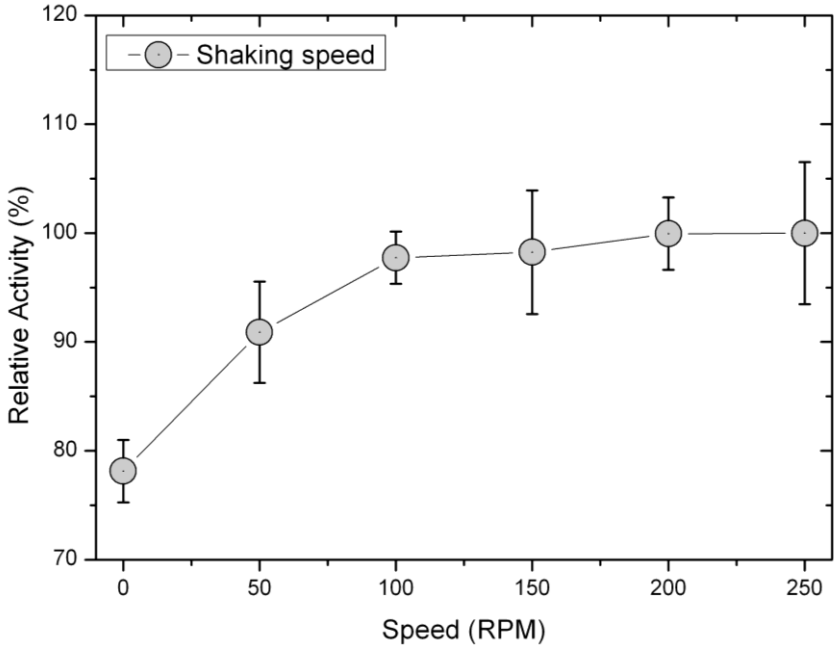

Figure 4-14 Optimisation of shaking speed. Activities are expressed as % relative to the highest activity recorded (250 RPM). Experimental details are described in methods. Error bars represent the STD of three measurements.

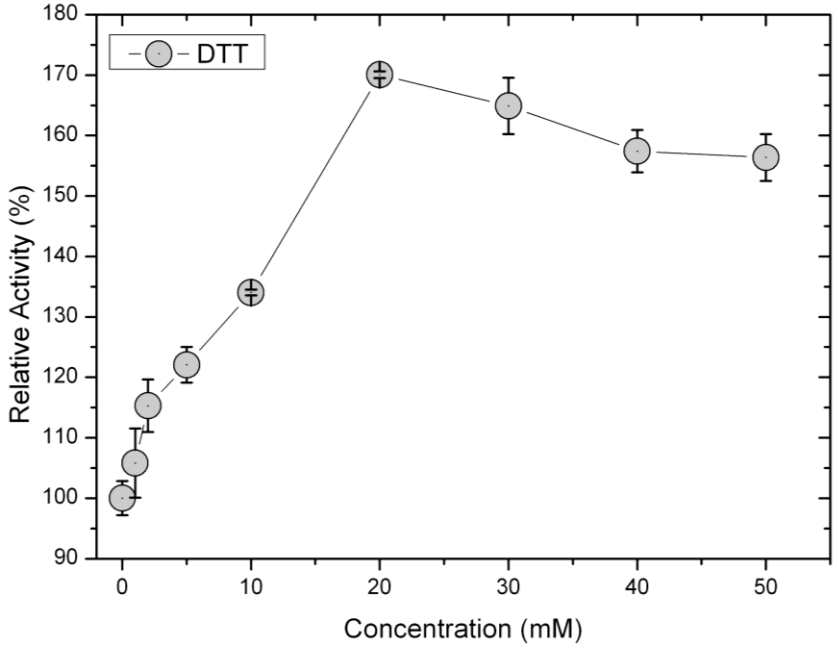

Figure 4-15 Optimisation of DTT concentration. Activities are expressed as % relative to the blank (no DTT added). Experimental details are described in methods. Error bars represent the STD of three measurements.

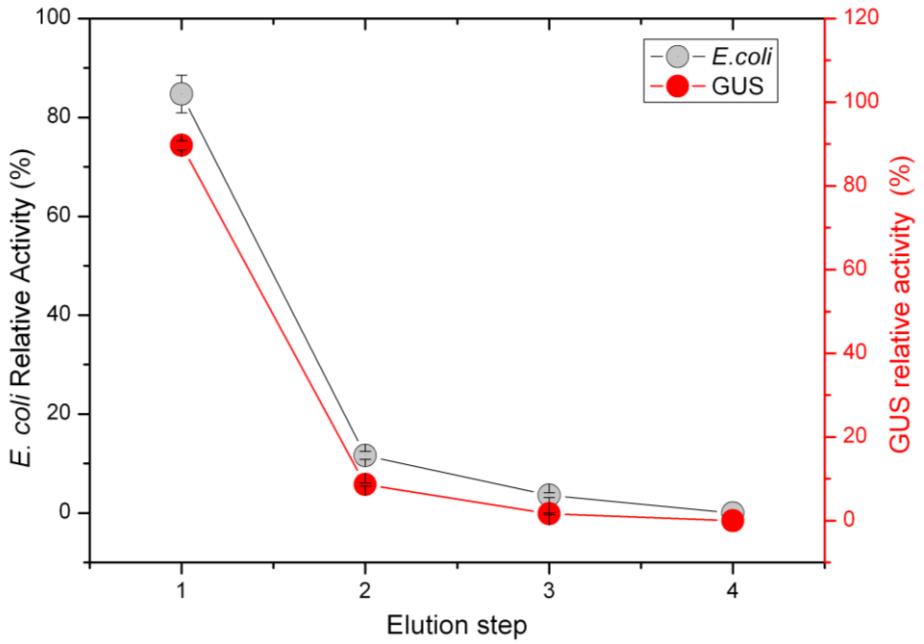

Figure 4-16 Residual activity after the 1st, 2nd, 3rd and 4th elution step with sodium phosphate buffer for an *E. coli* (8664 MPN) contaminated water sample (left axis) and a known GUS concentration (25 ng mL^{-1})(right axis). % activities are expressed as relative to the total activity detected after the 4 elution steps. Error bars represent the standard deviation of N=3 runs. Details of the experimental procedure are given in Methods section.

4.3.5 Evaluation of the kinetic end-point method

The kinetic end-point method is slightly different from the developed protocol, as the GUS-based catalytic reaction takes place in the syringe filter. Furthermore, instead of recovering the enzyme and measuring its activity over a certain period of time, the kinetic end-point method relies on measuring the fluorescent signal in the reaction mixture after a fixed period of time-in this case 30 min. As a consequence the end-point method is more similar with the Coliplage® method [169], initially developed by Fiksdal *et al.* [171].

Both methods performed well in terms of linearity achieved between the *E. coli* counts in the sample and the measured GUS activity. R^2 values higher than 0.98 were obtained for all the samples (Fig. 4-17, 4-18). In terms of activity detected (nM min^{-1}) the kinetic end-point method performed better. Activities were on average 1.6 times higher for the

kineti-end point method – this can be noticed from the slopes of the linear fit models (insets in Fig. 4-17, 4-18). As the two methods rely on different processes, the noted difference can be due to a multitude of reasons. In the kinetic end-point set-up, the substrate is added into the syringe filter at the same time with the lytic agent. At this point only a small amount of GUS is available to bind with the substrate and the reaction rates are limited by the amount of GUS present which is in turn limited by the lysis rate. As more GUS is being released, reaction rates increase drastically. In addition, permeabilisation of substrate through the cellular wall can also account for more fluorophore being released in the kinetic end-point method. Finally, for the continuous protocol there is a 15.3% loss in GUS activity as shown in Fig. 4-16 due to elution limitations. All of the above could account for the noted difference in GUS activities between the two methods. In terms of variably, the continuous method performed better than the kinetic end-point. Overall we found higher STDs of three replicates for the kinetic end-point method. This uncertainty is expected, since the later method relies on a rough estimation that the kinetic rates proceed linearly between time=0 (blank=initial fluorescence + substrate auto-hydrolysis over 30 min) and time=30 (reaction end-point).

Overall, the kinetic end-point method proved to be quite versatile and much easier to use. It requires less labour and processing time / sample and recorded GUS activities are higher. This also means a lower LOD can be potentially achieved. On the other side, the intra-sample variability was higher and it is not possible to follow the reaction rates in a real-time manner. Furthermore, the GUS activity relies only on two measurements and as such the confidence in the results is lower.

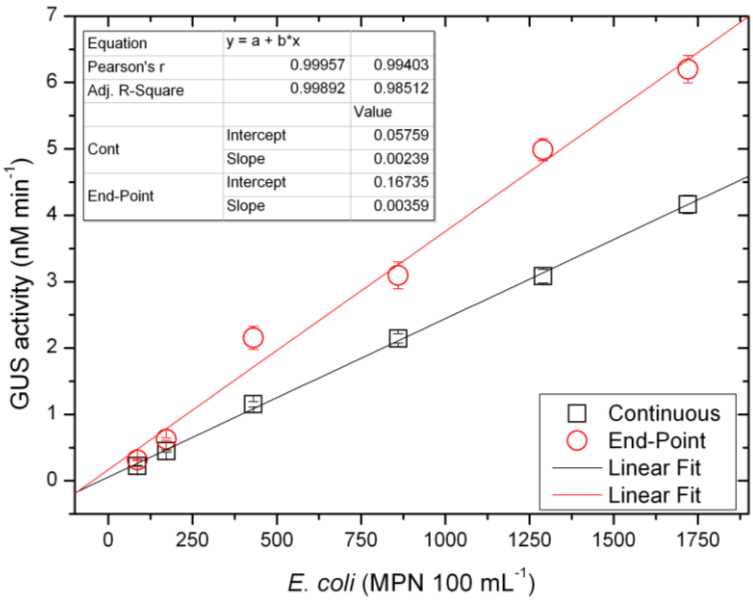

Figure 4-17 GUS activities recorded from dilutions of the same sample with the kinetic end-point method and the protocol developed here (continuous) on a sample contaminated with 1720 MPN *E. coli* 100 mL^{-1}. Experimental details are described in methods. Error bars represent the STD of three measurements.

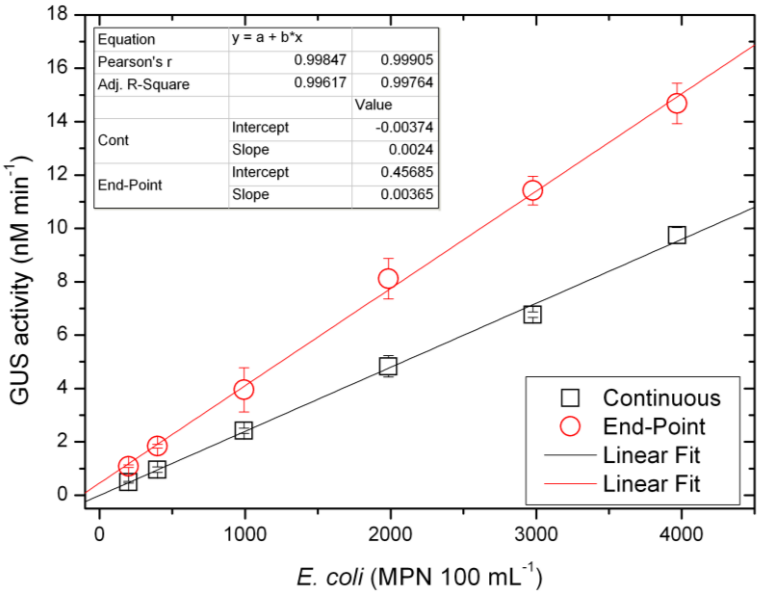

Figure 4-18 GUS activities recorded from dilutions of the same sample with the kinetic end-point method and the protocol developed here (continuous) on a sample contaminated with 3968 MPN *E. coli* 100 mL^{-1}. Experimental details are described in methods. Error bars represent the STD of three measurements.

4.3.6 Analytical Performance

The analytical performance of the protocol developed here was determined by comparison with the Coliplage® method [169]. Since 2006 the Coliplage® method has received great interest as it has the potential to offer real-time active management of recreational bathing areas and has been already evaluated against reference methods (ISO 9308-3) [192]. This protocol was evaluated both against a standard culture based-method (Colilert-18®) and against Coliplage®.

Results collected for the two fresh water samples are presented in Fig. 4-19, 4-20. For both methods a good linear fit ($R^2 \geq 0.974$) was found between the *E. coli* counts in the sample and the measured GUS activity (Fig. 4-19). The protocol developed here was more sensitive and a lower limit of detection was achieved. Using the Coliplage® a LOD of 275.5 *E. coli* 100 mL^{-1} was found. When a further dilution of 137.75 *E. coli* 100 mL^{-1} was run the signal could not be differentiated with certainty from the control sample. Using our protocol a LOD of 110.2 *E. coli* 100 mL^{-1} was found. This sample was the 4% dilution from the original water sample as explained in methods. GUS activities measured with this protocol were 3.08 times higher than the GUS activities measured with Coliplage® (see inset, slope in Fig. 4-20). This difference can be attributed primarily to a dilution factor. In our protocol the sample is concentrated from 100 mL and GUS is recovered in 2 mL with subsequent activity measurement. In the Coliplage®, the sample is concentrated in 10 mL. This suggests our protocol should generate GUS activities 5 times higher. Since only a 3.08 fold improvement was found, the difference can be attributed to the distinct nature of the two protocols. In terms of enzyme kinetics our method is more accurate, since the signal is recorded as a function of extracted GUS, in the absence of *E. coli* and other bacteria and particles –although it is possible cell debris is present. In the Coliplage® method, the signal is measured as a function of a few processes going on simultaneously. The mild conditions used (0.1% Triton X100) in the assay buffer do not ensure lysis of bacteria, but rather weaken the cellular wall and allow a better permeabilisation of substrate. The signal is also recorded as a function of substrate uptake by *E. coli*. Furthermore, over the 30 min required in the assay, it is possible the ratio of extracellular GUS/intracellular GUS changes. Although recorded signals show linearity over time it is not clear which of this processes accounts

for most of the increase in fluorescence and how the proportion of signal from each process changes with time.

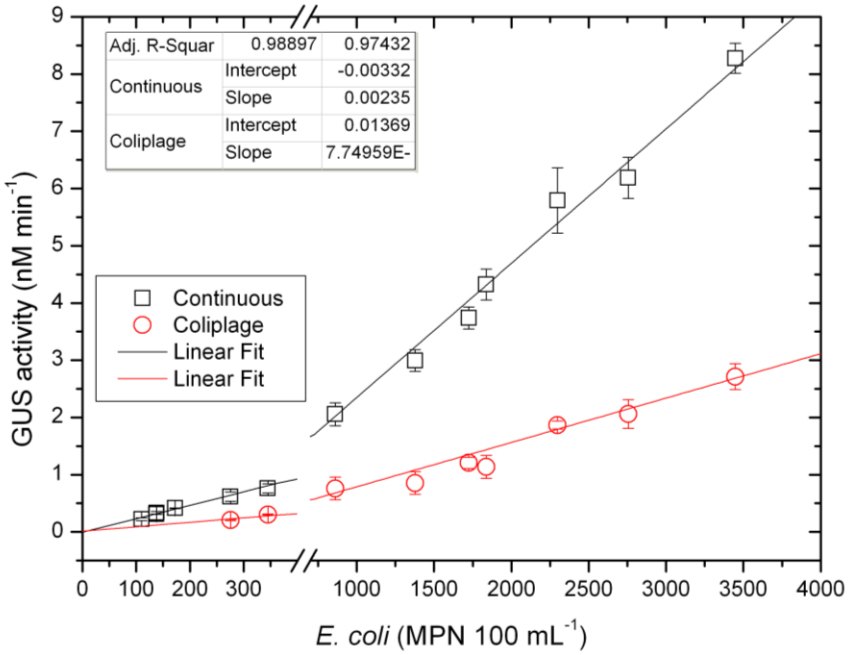

Figure 4-19 GUS activities recorded from dilutions of two freshwater samples with this protocol and the Coliplage method. Axis break inserted between 400-700 to highlight the lower range. Insets show R^2, and slope values (nM min^{-1} *E. coli*$^{-1}$) for the two methods. Experimental details are described in methods. Error bars represent the STD of three measurements.

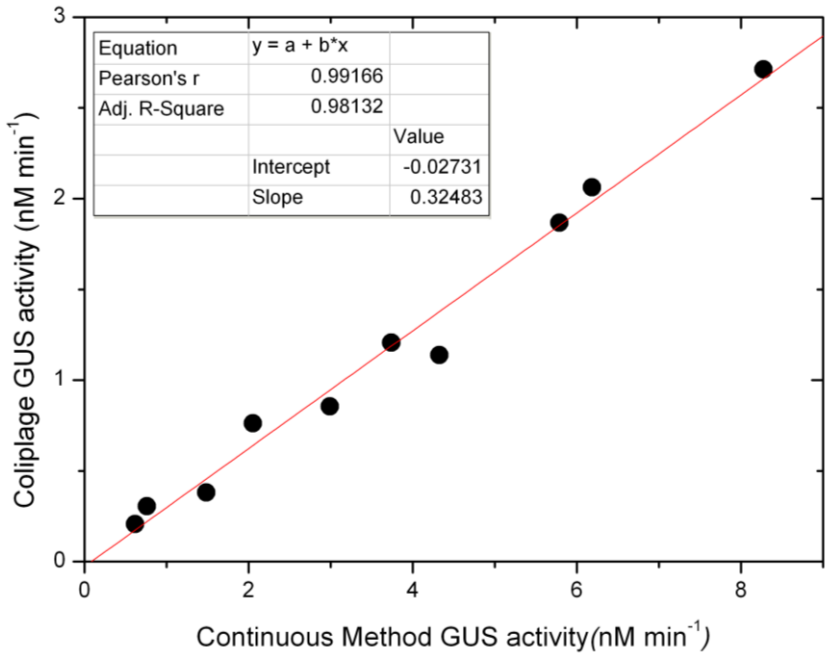

Figure 4-20 Correlation between this protocol and Coliplage method for freshwater samples.

Results collected for the seawater samples are presented in Fig. 4-21, 4-22. Similar with the freshwater samples, a good linear fit ($R^2 \geq 0.99$) was found between the *E. coli* counts in the sample and the measured GUS activity (Fig. 4-21). Using the Coliplage® a LOD of 130.1 *E. coli* 100 mL^{-1} was found while our protocol had a LOD of 26.18 *E. coli* 100 mL^{-1}. GUS activities measured with this method were 4.13 times higher than the GUS activities measured with Coliplage® (see inset, slope in Fig. 4-22). This value is higher than the one recorded for freshwater samples of 3.08 and suggests that for seawater samples our method recovers higher GUS activities. The different environmental stressors bacteria are susceptible too in the freshwater and marine ecosystems might be the cause of this observation [81][192]. In the marine environment, bacteria are also exposed to salinity gradient stress and as such higher ratios of VBNC to viable culturable bacteria were found [193], [194], [169]. The two methods rely on different GUS detection principles and the results suggest this protocol is more effective in recovering GUS from VBNC cells.

Both methods detected significantly higher GUS activities/cell in the seawater sample (see slopes in the insets of Fig. 4-19 and Fig. 4-21) as opposed to the freshwater samples. This has been discussed previously and our results are in concordance with

that. GUS activities between 1.67 – 1.88 times higher were found in seawater [169] than in freshwater [180], [175], [170]. In this study, GUS activities of 2.93 time higher (this protocol) and 2.16 time higher (Coliplage®) between the two water types. This difference can be attributed as explained above to higher ratios of VBNC to viable culturable cells, but also due to the presence of more GUS positive non-target bacteria [195], [196] or the presence of GUS positive marine biomass [197]. Overall this method showed a better performance in terms of GUS activity detected (LOD) and a good correlation with the Coliplage® method (Fig. 4-20, 4-22).

The analytical performance of the protocol was also assessed in terms of %RSD of replicates from the same sample. This was carried out at a low concentration (110 MPN *E. coli* 100 mL^{-1}) close to the LOD of the method and at a medium concentration (688 MPN *E. coli* 100 mL^{-1}). Raw data expressed as fluorescence increase over time and box plots after the conversion into GUS activity are shown in Fig. 4-23, 4-24. The method shows good reproducibility with a %RSD of 11.21 for the low concentration and a %RSD of 5.56 for the medium concentration.

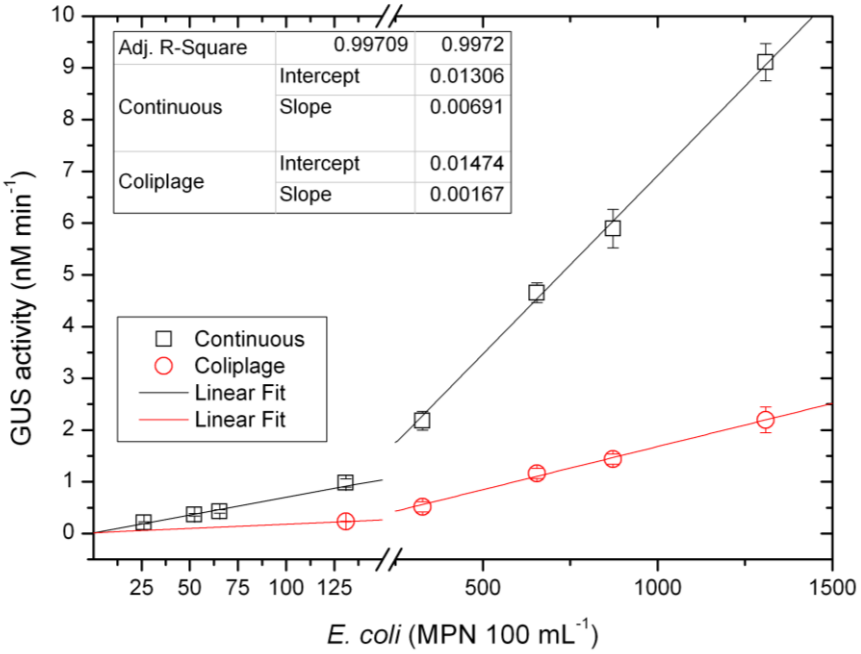

Figure 4-21 GUS activities recorded from dilutions of a seawater sample with this protocol and the Coliplage method. Axis break inserted between 150-200 to highlight lower range. Insets show R^2, and slope values (nM min^{-1} *E. coli*$^{-1}$) for the two methods. Experimental details are described in methods. Error bars represent the STD of three measurements.

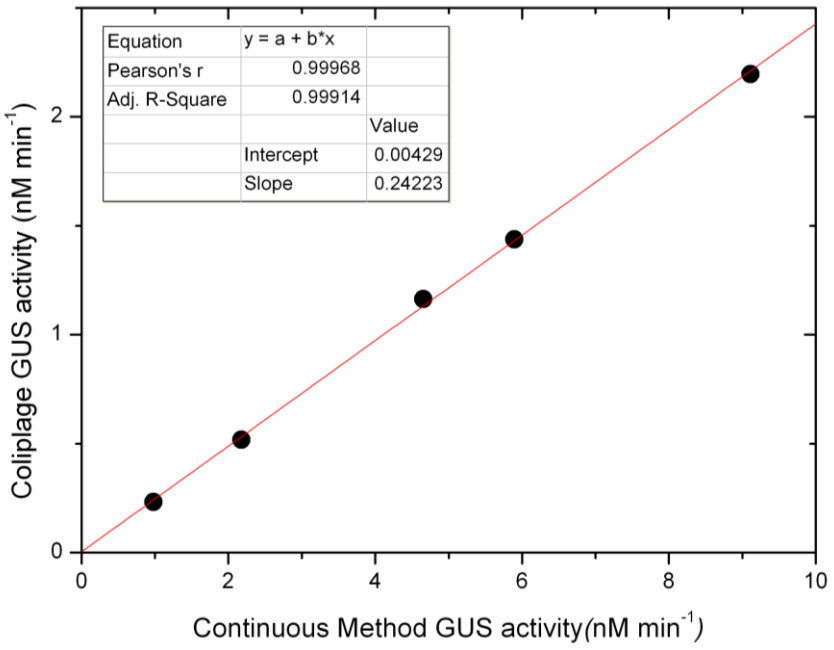

Figure 4-22 Correlation between this protocol and Coliplage method for seawater samples.

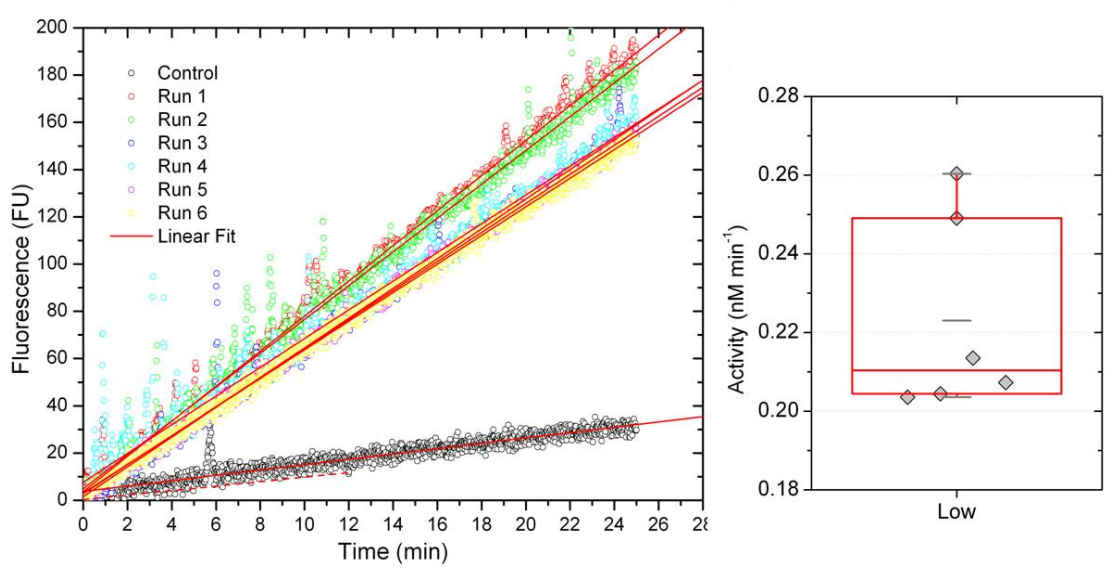

Figure 4-23 Progress curves (FU min^{-1}) from running the same sample (110 MPN *E. coli* 100 mL^{-1}) 6 times with this protocol (left) and box plots after conversion to GUS activity (nM min^{-1})(right). Experimental conditions are detailed in Methods section.

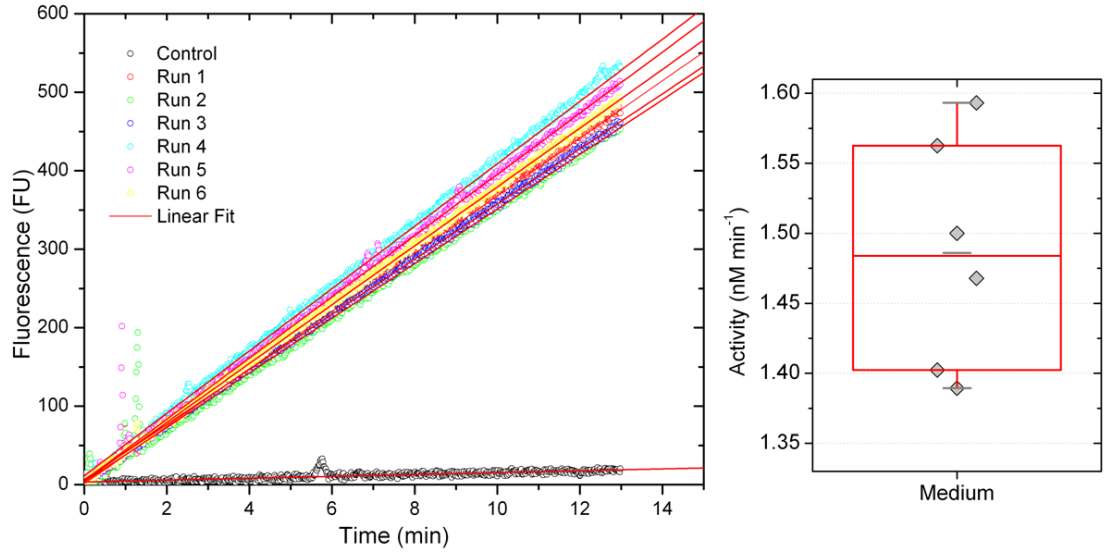

Figure 4-24 Progress curves (FU min^{-1}) from running the same sample (688 MPN *E. coli* 100 mL^{-1}) 6 times with this protocol (left) and box plots after conversion to GUS activity (nM min^{-1})(right). Experimental conditions are detailed in Methods section.

The method presented here is easy to perform and does not require specialised training or equipment. The syringe filtration for the recovery of GUS proved to be a versatile, easy to use and robust alternative to the bench-top vacuum filtration. No issues were encountered in filtering 100 mL volumes of river through the syringe filter. Although for the data presented here 100 mL of seawater were filtered with ease, however on different occasions we found this to be a bit challenging. In such circumstances, a smaller volume can be filtered and the GUS activity adjusted accordingly. When GUS is recovered from the filter by elution with buffer a certain level of foaming is present, especially after the air purge step which recovers the last 2-3 residual drops. This foam is easily solubilised by the addition of substrate in DMOS.

Finally, the protocol developed here shows a good potential for on-site measurement of *E. coli*. The syringe filtration and recovery of bacteria can be carried out in the field. For the lysing procedure (syringe filter incubation) a portable miniaturised incubator can be used. As it stands, the method is limited by the use of a bench top fluorometer for the detection of GUS activity. Hand-held portable miniaturised fluorometers exist and have been used previously for on-site measurements [179]. In the research group, a portable miniaturised fluorometer (ColiSense) with incubation capabilities was tailor designed for the protocol presented here. The system successfully delivered results on-site within a 75 min period [198]. Furthermore, due to the continuous nature in which GUS activity is monitored, the method has the potential to be automated into a flow-through system.

4.4 Conclusions

In summary, a protocol for the recovery and detection of faecal pollution indicator bacteria, *E. coli*, using GUS activity was developed. The developed protocol involves two main steps: sample preparation and GUS activity measurement. In the sample preparation step syringe filters were used with a dual purpose, for the recovery and pre-concentration of *E. coli* from the water matrix but also as μL reactors for bacteria lysis and GUS extraction. Subsequently, GUS activity was measured using a continuous fluorometric method developed previously. The optimum GUS recovery conditions for the sample preparation step were found to be: 100 μL PELB (supplemented with 1 mg mL^{-1} lysozyme and 20 mM DTT), at 37 °C for 30 min.

The aim of this work was to address the need for tests capable of rapid on-site assessment of microbiological water quality. To achieve an active management of bathing areas and to reduce the risk associated with the presence of faecal pollution, such tests are essential. The protocol developed here, has a time-to-result of 75 min, and as such successfully addresses this requirement. Additionally the kinetic end-point method presented can further reduce this time to 45 min, although the variability of replicates was higher.

The protocol was evaluated on environmental samples (fresh and seawater) against an establish GUS assay method (Coliplage®). GUS activities corresponding to samples containing as low as 26.18 MPN *E. coli* 100 mL^{-1} were detected for the seawater sample and as low as 110.2 MPN *E. coli* 100 mL^{-1} for the freshwater samples. By comparison with the Coliplage® method, this protocol offered an improvement in the measured GUS activities of 3.08 fold for freshwater samples and 4.13 fold for seawater samples.

The main advantages of this technology are: the short time required for analysis (45 min, sample preparation + 30 min, detection time), minimal sample manipulation, minimal reagent consumption and the potential for on-site measurements; As such, this method could aid stakeholders in meeting early warning requirements and water safety plans for bathing areas.

5 APPLICATION OF ENZYME BASED METHODS FOR RAPID ASSESSMENT OF FAECAL POLLUTION INDICATORS IN SURFACE WATERS

ABSTRACT

A previously protocol for the recovery and detection of *E. coli* was couple with a miniaturised fluorometer (ColiSense) and the system was assessed for the rapid detection of FIBs in environmental samples. The system successfully detected *E. coli* in all of the 45 grab samples tested. A positive correlation was found between the log transformed GUS activities and the log transformed *E. coli* counts (r^2=0.53) and log transformed Enterococci counts (r^2=0.66) respectively. This suggests the protocol developed here can be applied successfully for the rapid assessment of faecal pollution in bathing areas.

5.1 Introduction

The need for rapid assays and methods that provide real-time or nearly real-time quantification of indicators of faecal water contamination is recognised among different levels of government [199], [81]. Methods for the removal, tagging or amplification of the target microorganism or some of their components were reviewed by Noble and Weisberg [168]. These methods include: molecular whole cell and surface recognition methods (including for example immunoassays), nucleic acid detection methods and enzyme-substrate based methods (including selective growth of the target microorganism). The first two groups are not yet routinely used due to the fact that they are not sensitive enough, the equipment is expensive or they detect total rather than viable cells. Assays based on the determination of enzyme activity can be done *in-vivo* or *in-vitro*. *In-vivo* assays rely on the measurement of enzyme activity as a function of substrate uptake by the cell while *in-vitro* assays rely on extracting the enzyme and measuring its activity as a function of substrate breakdown. Assays based on the direct determination of activity by extracting the enzyme provide relatively quick results (between 30 min and 4 h). These assays avoid the cultivation step and exploit GUS's activity extracted from *E. coli* cells. They are simple to perform and do not require expensive instrumentation. The assays are based on the GUS catalysed hydrolysis of added fluorogenic or chromogenic substrates. GUS activity can be determined directly in the water sample after the addition of substrate or after a pre-concentration step. This is usually achieved by collecting the cells by filtration and transfer of the filtered cells into an assay solution containing the substrate [169].

5.1.1 Specificity and detection limits of direct GUS based methods to predict *E. coli* concentrations.

The applications of rapid enzyme assays techniques and the use of GUS and GAL for monitoring microbial water quality and predicting faecal pollution contamination have been discussed previously [81]. The author concluded that rapid assays can be useful for early warning of faecal contamination in water, and represent an alternative indicator concept since the GAL and GUS activities are more persistent to environmental stress than the culturability of coliforms and *E. coli*. Several researchers have investigated the relationship between these enzymes activities and *E. coli*, faecal coliforms and total coliforms abundance in different water bodies [170-177], [178, 179]. All the field trials

have shown regression straight lines with a slope less than 1 when plotting log GAL activity or log GUS activity versus log culturable target bacteria [171]. This suggested that enzyme activity calculated per culturable indicator bacteria decreases when their number increases. One hypothesis for this trend is the fact that the enzyme assay detects both culturable and viable but not culturable (VBNC) bacteria. Garcia-Arminsen *et al*. [180] analysed highly contaminated river water samples using DVC-FISH (direct viable count coupled with fluorescence *in-situ* hybridisation) and GUS activity. The author found a value of 0.994 for the log-log regression line between the results obtained with the 2 methods, concluding that the GUS based method also detects VBNC bacteria. *E. coli* are known to maintain their virulence although they enter a VBNC state [181], [182] as a consequence their presence is important from a public health point of view [183]. This suggests GUS assay might be a better indicator for determining the infection risk associated with certain water bodies.

Various limits of detection are reported in the literature for the quantification of *E. coli* concentrations using the fluorometric detection of 4-MUG. Georges *et al.* reported a LOD of 20 CFU 100 mL^{-1} for faecal coliforms when assaying GUS activity after pre-concentration of fresh water samples [176]. Lebaron *et al.* [169] reported a LOD of 5 CFU 100 mL^{-1} for *E. coli* in seawater samples. When fresh water samples were analysed using a hand held fluorimeter the LOD was 7 CFU mL^{-1} [179]. GUS is accepted as a biomarker for *E. coli* detection in microbiological water quality controls [131]. GUS activity is prevalent among *E. coli* strains. For example 92.4% of *E. coli* strains were found to be GUS positive when they were isolated from treated and raw water [184] while when *E. coli* were isolated from human faecal samples, a lower percentage GUS positive was found [185]. Although GUS is activity is also present in other members of the *Enterobacteriaceae,* like *Shigella* and *Yersinia* but with lower prevalence [131] this shouldn't strongly interfere with the assay, unless they are present at similar or higher concentrations than *E. coli*.

5.2 Materials and Methods

5.2.1 Materials

Sodium phosphate monobasic and dibasic and 1,4-dithiothreitol (DTT), were all purchased from Sigma Aldrich Ireland. The fluorogenic substrate 6-chloro-4-methyl-umbelliferyl-β-D-glucuronide (6-CMUG) (97%) was ordered from Glycosynth Limited (UK), 6-chloro-4-methyl-umbelliferone (6-CMU) (97%) was ordered from Carbosynth Limited (UK). Water was passed through a Milli-Q water purification system. Stock solutions of fluorophores and substrates (100 mM) were prepared in 1 mL DMSO (99.5%) and kept at 4°C. Further dilutions were prepared daily in buffer or deionised water with a final DMSO concentration in the working solution, ranging from 0.01% - 1%. Bacterial PE LB™ (PELB) with PE LB™ Lysozyme were ordered from VWR.

Corning® syringe filters with cellulose acetate surfactant free membrane (SFCA) with pore sizes of 0.45 µm and Whatman™ glass microfibre filters (pore size: 1.2 µm and 47 mm diameter) were all ordered from Sigma Aldrich Ireland. Syringe filters caps, Combi-Cap male/female Luer were ordered from VWR Ireland.

The Colilert-18®/Quanti-Tray 2000® system (IDEXX Laboratories) used for the enumeration of coliforms and *Escherichia coli* and the Enterolert®/Quanti-Tray 2000® system (IDEXX Laboratories) used for the enumeration of Enterococci were ordered from Techno-Path Ireland. Positive controls of *E. coli* ATCC 11775 and *Enterococcus faecalis* ATCC 19433 were ordered Techno-Path Ireland.

5.2.2 Methods

5.2.2.1 Sample collection and site description

Water samples were collected over a five day period in the month of August 2015 from five rivers in the Dublin area (Liffey, Tolka, Camac, Poddle and Dodder), Fig. 5-1. For each day the sampling plan was designed to allow sample collection for baseline measurements from each river, followed by sample collection for profile measurements from one of the rivers.

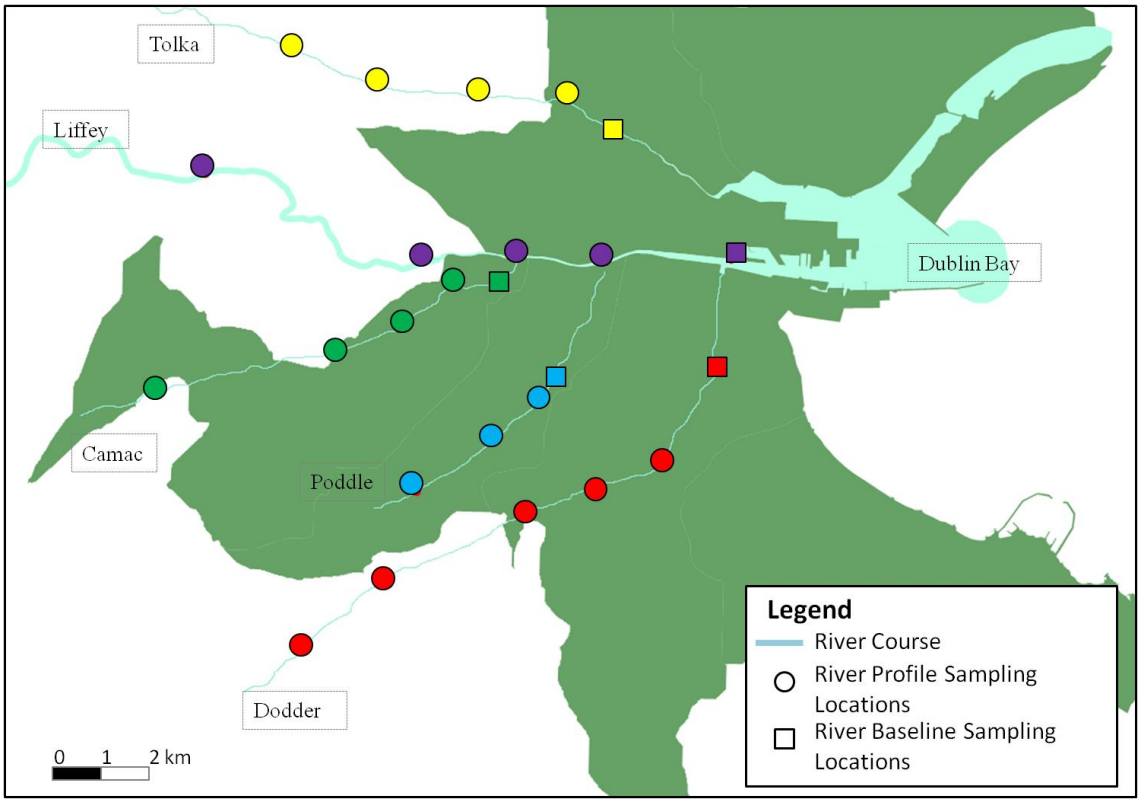

5-1 Map of Dublin area showing the location of collected water samples (colour coded for each river). With the exception of River Liffey, river courses are shown for illustrative purposes and do not represent the natural river course. Sampling locations for profile and baseline measurements are detailed in the legend.

Between eight and ten sampling locations were visited for each sampling day. Briefly, for baseline measurements samples were collected in the morning (between 5:00 a.m. and 7:00 a.m) from each river giving a total of five samples. For profile measurements,

samples were collected from the river sampled that day between 07:00 a.m. and 11:00 a.m. This sampling design aimed to provide a snap-shot of the riverine water quality in the Dublin area by reducing the variability associated with different sampling times.

5.2.2.2 On-site water quality analysis

A multi-parameter sonde (YSI 6600EDS V2-2), equipped with sensor probes for turbidity (NTU), dissolved oxygen saturation (%), temperature (°C), conductivity (mS cm^{-1}), pH and depth, purchased from YSI Hydrodata UK, was used for on-site measurements. The system was maintained and calibrated as described previously [114], [112]. Sensor function and power status were reviewed before each sampling day. On arrival to the site, the sonde was placed in an insulated bucket containing approximately 10 L of sample and allowed to stabilise for 5 to 10 min. Measurements were collected each 15 s for 5 min. Each parameter is reported as the average of 20 consecutive readings.

5.2.2.3 Microbial analysis of water samples

Water samples were collected in sterile 1L high density polypropylene (HDPP) bottles. Samples were transported to the lab on ice within 4 h and inoculated within 8 h after collection. The Colilert-18®/Quanti-Tray 2000® system (IDEXX Laboratories) was used for the enumeration of coliforms and *Escherichia coli* and Enterolert®/Quanti-Tray 2000® system (IDEXX Laboratories) was used for the enumeration of Enterococci. The enumeration protocol was followed in accordance with manufacturer's instructions. Aliquots of 10 mL from original water samples were diluted 1:10 with sterile deionised water into 100 mL bottles. After the addition of Colilert-18 and Enterolert, samples were inoculated into Quanti-Trays and sealed. For *E. coli* and coliform enumeration, samples were incubated at 37.0 °C for 18 to 20 h. Following incubation the Quanti-Tray wells were read visually for yellow colour indicating the presence of coliforms and for blue fluorescence indicating the presence of *E. coli.* For Enterococci enumeration samples were incubated at 41.0 °C for 24 to 28 h after which the blue fluorescent wells were counted as positive. The number of positive wells was recorded for both tests and converted to most probable number (MPN) estimations using tables provided by the manufacturer. For quality control, replicates of positive controls of *E. coli* ATCC 11775 and *Enterococcus faecalis* ATCC 19433, negative controls and laboratory reagent blank were analysed for each sample batch.

5.2.2.4 GUS activity measurement

5.2.2.4.1 Sample preparation

A sample preparation protocol for the capture and pre-concentration of *E .coli* followed by the recovery of GUS from environmental water samples was used as described in Chapter 4. Briefly, after vigorously mixing the water sample, 50 mL sterile syringes with luer lock were used to collect 50 mL of sample and pass it through the syringe filter. This procedure was carried out twice for each measurement to account for 100 mL of sample. In total 300 mL were used for each sample analysis. Following bacteria capture, each syringe filter was washed three times with 10 mL of deionised water using a 20 mL syringe and finally purged with air (3 to 5 cycles) to remove residual liquid. Subsequently, 100 µL of lytic agent (consisting of 100 µL PELB supplemented with 1 mg mL^{-1} lysozyme and 20 mM DTT) was gently pipetted into to the syringe filter and allowed to flow inside. The syringe filters were immediately sealed using screw caps, vigorously mixed for 5 s and placed in the incubator at 37° for 30 min facing upwards. Upon removal from the incubator, the caps were removed and a 2 mL sterile syringe was used to flush 1.9 mL of cold sodium phosphate buffer (pH 6.8) through the filter and a 2 mL glass vial was used to collect the filtrate. This was followed by a gentle step of air purge using the same syringe to recover the remaining residual liquid (2-3 drops) without excessive foaming.

5.2.2.4.2 GUS detection

For the detection of GUS activity in a continuous set-up, a miniaturised fluorometer (ColiSense) was design and built in-house by Brendan Heery [198].The specifications of the system were tailored to target the requirements of the GUS based method developed previously [138]. Fig. 5-2a shows the normalised absorbance and emission spectra for the chemical components of the enzyme assay at neutral pH (pH 6.8) and shows the characteristic spectra of the optical components of the system. Fig. 5-2b shows a schematic of the detection and incubation system. The system can accommodate three sample chambers for measuring the fluorescent signal (Fig. 5-2c). Each chamber can maintain a constant temperature of 44 ± 0.5°C. A fluorescence detection system incorporating an excitation light source (362) nm and emission detector (445) nm was integrated into each chamber. The system uses an LED with peak

emission at 361 nm and spectral width of 20 nm was selected to excite the 6-CMU molecule close to its maximum while exciting the 6-CMUG as little as possible. A photodiode with peak sensitivity at 570 nm and enhanced sensitivity in the blue region (65 % of max at 445 nm) was selected as the detector. A high pass optical filter with 420 nm cut-off was selected to reduce any interference from substrate fluorescence and block the excitation light from the detector. Glass sample vials (2 mL) were used as cuvettes due to their disposable nature and low cost. Data was collected and visualised on the PC via the USB port communication (Fig. 5-2d) and plotted in real-time using a Java developed graphical user interface (GUI) (Fig. 5-3).

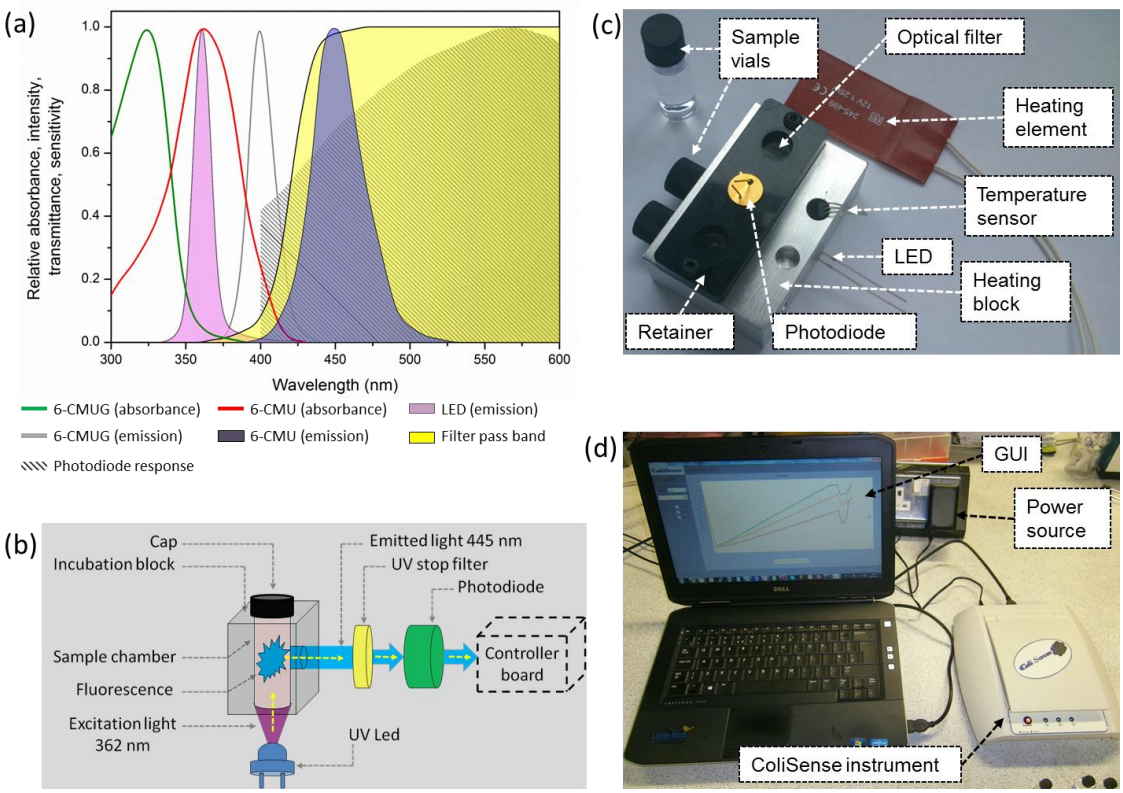

Figure 5-2 ColiSense system design and construction. (A) Normalised spectra of chemical components of the assay and optical components of the fluorescence detection system. (B) Schematic of the incubation and fluorescence detection system. (C) Physical realisation of key system components. (D) ColiSense instrument with power source and Graphical user interface (GUI) [198].

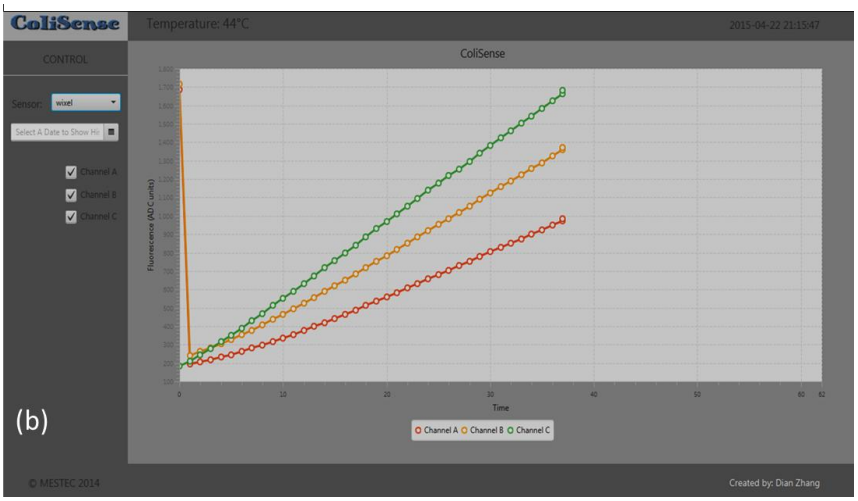

Figure 5-3 Graphical user interface (GUI) showing real-time data collection of fluorescent signal as a function of time [198].

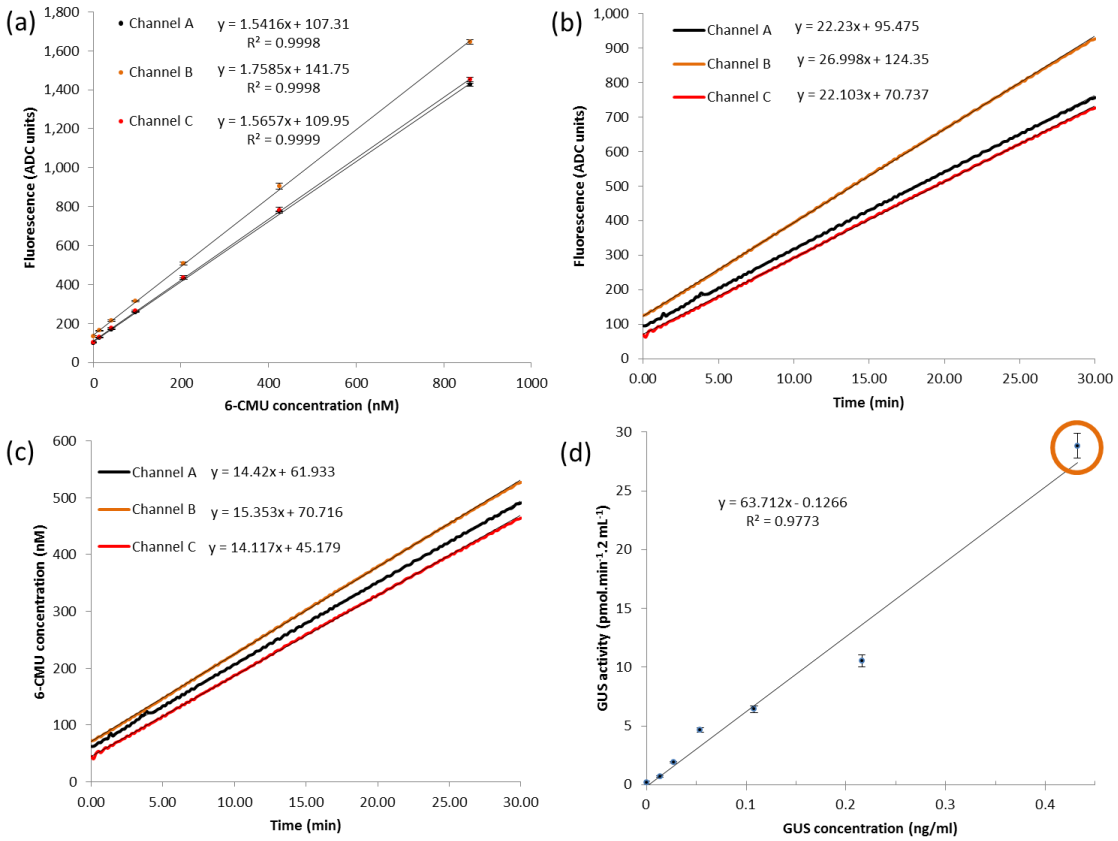

Figure 5-4 System characterisation. (A) Calibration of fluorescence response of ColiSense channels A, B, C with concentrations of 6-CMU up to 1,000 nM in pH 6.8 phosphate buffer with 500 µM 6-CMUG and PELB (n = 3). Error bars show SD of triplicate measurements. (B) Progress curves for 0.43 ng L^{-1} GUS added to 500 µM 6-CMUG in pH 6.8 phosphate buffer with PELB in ColiSense Channels A,B,C . (C) Progress curves from panel B expressed as 6-CMU concentration. (D) Enzyme activity per 100 mL recorded by ColiSense for concentrations of GUS up to 1 ng L^{-1} (n = 3). Error bars show SD of triplicate measurements [198].

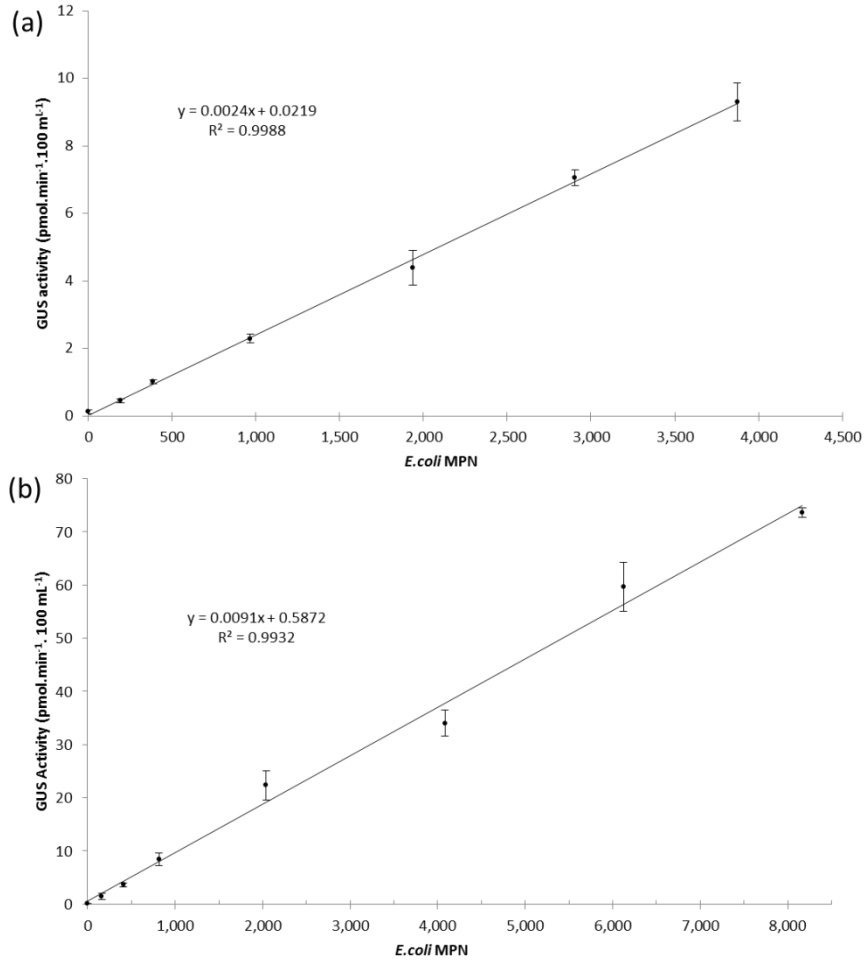

Figure 5-5 Target analyte testing. (A) Enzyme activity per 100 mL sample vs *E. coli* concentration in River Water (Salinity = 4 ppt) (n = 3), Error bars show SD of triplicate measurements. (B) Enzyme activity per 100 mL sample vs *E. coli* concentration in sea water (Salinity = 32 ppt) (n = 3), Error bars show SD of triplicate measurements [198].

5.2.2.5 Total suspended solids (TSS) analysis

Samples for TSS determination were collected in 500 mL HDPP bottles, transported to the lab on ice and analysed on the same day. Samples were processed as described in Standard Method 2540 D [116]. Briefly, glass microfibre filters (pore size: 1.2 µm and 47 mm diameter) were washed in DI water, placed in aluminium dishes and dried at 103-105 °C in the oven. After removal dishes were weighed and labelled. Aliquots consisting of 250 mL of water sample were vacuum filtered after which the filters were dried at 103-105 °C for 1 h and re-weighed.

5.2.2.6 Nutrient analysis

All river samples were analysed quantitatively for phosphate, nitrate and nitrite. This was done using the DR 900 Colorimeter from Hach®. Nitrate was measured using the chromotropic acid Test 'N Tube method, nitrite was measured using the diazotization Test 'N Tube method and phosphate was measured using the molybdovanadate Test 'N Tube. All Test 'N Tube kits were purchased from Hach®.

5.2.2.7 Rainfall and daily sunshine hours data

Hourly average rainfall measurements were collected from the Irish Meteorological Service (Met Éireann) from three meteorological stations in Dublin area: Dublin Airport (53°25'40" N, 6°14'27" W, 71 m above sea level), Casement Aerodrome (53°18'20" N, 6°26'20" W, 94 m above sea level) and Phoenix Park (53°21'50" N, 06°20'00'' W, 48 m above mean sea level). Hourly average sunshine data was available only from the Dublin Airport station.

5.2.2.8 Tide data

The Marine Institute, responsible for the Irish National Tide Gauge Network, supplied tidal height data for Dublin Port.

5.2.2.9 Water level data

Water level data for the Camac, Dodder, Poddle and Tolka rivers was obtained from Dublin City Council (DCC). Received data (Fig. 5-2) representing water levels (m) was converted into % water level change, relative to the maximum recorded for each river for the month of August. This conversion allowed inclusion of this data into the statistical analysis and facilitated direct comparison with the other water quality parameters.

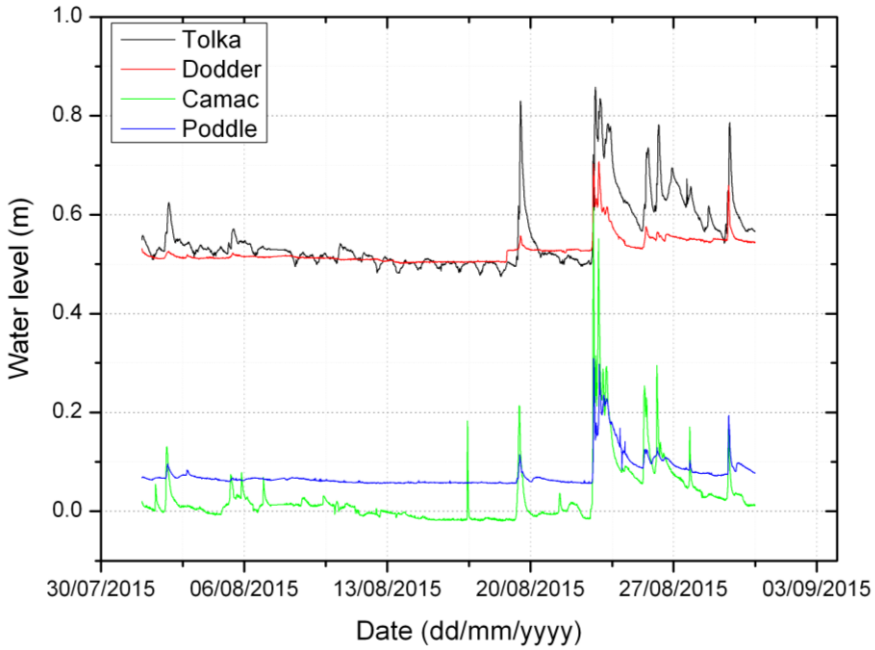

Figure 5-6 Raw water level data received from DCC. Rivers are specified in the legend.

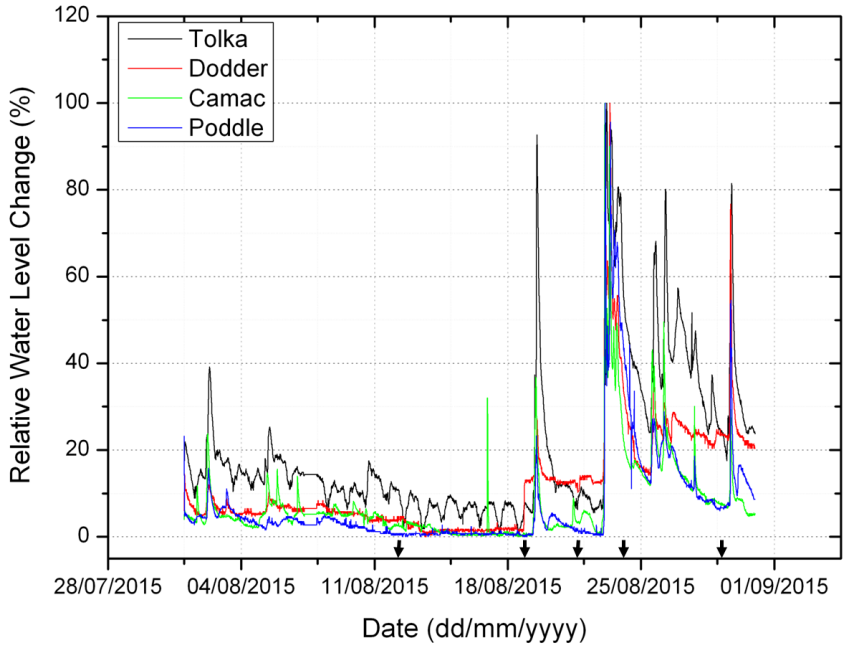

Figure 5-7 Water level data as % relative water level change. The small black arrows on the x axis represent the sampling days.

5.2.2.10 Data management and Statistical Analysis

Data was processed and analysed using SPSS® (SPSS Statistics 17.0, SPSS Inc., Chicago, IL, USA), Origin® and Excel 2007®.

5.3 Results and Discussion

5.3.1 Statistical analysis of the data

Descriptive statistics of the entire data set are presented in Table 5-1. To verify if the collected data is parametric, the measured variables were tested for the assumption of normal distribution and homogeneity of variance [118]. For the assumption of normally distributed data the Shapiro-Wilkinson test [118] was used coupled with visual inspection of frequency histograms, stem-and-leaf plots and Q-Q plots. TSS, turbidity, nitrite and phosphate were found to violate the assumption of normally distributed data and the assumption of parametrical statistical analysis.

Bivariate correlation analysis measures the inter-relationship between 2 variables in terms of correlation coefficient [119]. Spearmen's correlation coefficient, R, is a non-parametric statistic test, and so can be used when the data have violated the parametric assumption. Table 5-2 and Table 5-3 present the Spearmen's correlation coefficients matrix for all the measured parameters. The strongest correlation was found between turbidity and TSS ($R=0.942$, $p < 0.01$) followed by temperature and daily sunshine ($R=-0.894$, $p < 0.01$). Log (*E. coli*) it was found to correlate strongly with log (Enterococci) ($R=0.784$, $p < 0.01$), log (lyse GUS) ($R=0.773$, $p < 0.01$), log (extra GUS) ($R=0.726$, $p < 0.01$), log (raw GUS) ($R= 0.609$, $p < 0.01$) and moderately with daily sunshine ($R=-0.323$, $p<0.05$). Log (Enterococci) was found to correlate strongly with log (extra GUS) ($R=0.792$, $p < 0.01$), log (lyse GUS) ($R=0.773$), log (raw GUS) ($R=0.598$, $p < 0.01$) and moderately with turbidity ($R=0.313$, $p < 0.05$), DO% ($R=0.334$, $p < 0.05$) and daily sunshine ($R=0.0501$, $p < 0.01$).

Table 5-1 Descriptive statistics of the measured parameters; N = sample size, STD=standard deviation.

Parameter	**Units**	**N**	**Min**	**Max**	**Mean**	**STD**
E. coli	MPN 100 mL^{-1}	45	201	24196	3993.73	4584.36
Enterococci	MPN 100 mL^{-1}	45	85	19863	1195	2946
TSS	mg L^{-1}	45	.400	70.53	19.38	19.25
Turbidity	NTU	45	.733	54.90	10.50	12.41
Nitrate	mg L^{-1} N -NO^{3-}	45	.100	2.90	1.528	.621
Nitrite	mg L^{-1} N -NO^{2-}	45	.002	.060	.0128	.009
Phosphate	mg L^{-1} P-PO_4	45	.070	.490	.204	.085
Lyse	pmol min^{-1}	45	1.03	144.07	8.32	21.27
Raw	pmol min^{-1}	45	16.49	135.354	43.63	25.02
Extra	pmol min^{-1}	24	13.26	105.29	37.33	23.20
Temperature	°C	45	13.07	17.011	15.12	1.00
Cond	mS cm^{-1}	45	.160	26.633	3.08785	7.17
pH		45	8.02	8.694	8.359	.160
DO	%	45	80.21	108.31	94.12	5.55
Water Level Change	%	39	.395	26.77	10.95	7.91

Table 5-2 Spearman's correlation coefficient matrix for the collected data.

	log (*E. coli*)	log (enterococci)	TSS (mg L^{-1})	Turbidity	NO_3^-	NO_2^-	PO_4^{-2}	log (Lyse GUS)	log (Raw GUS)
log (*E. coli*)	1.000	.784**	.155	.257	-.076	.162	.083	.773**	.609**
		.000	.311	.088	.619	.287	.590	.000	.000
log (enterococci)		1.000	.234	.313*	-.152	.045	-.019	.777**	.598**
			.121	.036	.320	.769	.902	.000	.000
TSS (mg L^{-1})			1.000	.942**	-.276	-.177	-.398**	.267	.174
				.000	.066	.246	.007	.076	.252
Turbidity				1.000	-.272	-.013	-.281	.386**	.314*
					.070	.933	.062	.009	.036
NO_3^-					1.000	.293	.299*	-.279	-.127
						.051	.046	.063	.405
NO_2^-						1.000	.567**	.142	.520**
							.000	.353	.000
PO_4^{-2}							1.000	.137	.255
								.369	.091
log (Lyse GUS)								1.000	.653**
									.000
log (Raw GUS)									1.000

Significant correlations are bolded.

*Significant at p<0.05 level, **Significant at p<0.01 level

Table 5-3 Spearman's correlation coefficient matrix for the collected data.

	log (Extra GUS)	Temperature	Conductivity	pH	DO (%)	Water Level Change (%)	Daily sunshine
log (*E. coli*)	.726**	.151	-.078	.161	.171	-.108	-.323*
	.000	.322	.609	.291	.262	.531	.030
log (Enterococci)	.792**	.289	-.283	.114	.334*	.149	-.501**
	.000	.054	.060	.455	.025	.384	.000
TSS (mg L^{-1})	.211	.407**	-.260	.188	.427**	.441**	-.460**
	.321	.006	.085	.216	.003	.007	.001
Turbidity	.274	.342*	-.265	.224	.342*	.422*	-.415**
	.195	.021	.078	.139	.022	.010	.005
NO_3^-	.034	-.333*	.088	.187	-.321*	-.530**	.456**
	.874	.025	.565	.219	.032	.001	.002
NO_2^-	.368	-.352*	-.015	.161	-.242	-.318	.321*
	.077	.018	.923	.290	.109	.059	.031
PO_4^{-2}	.459*	-.373*	.201	-.236	-.503**	-.360*	.350*
	.024	.012	.184	.118	.000	.031	.018
log (Lyse GUS)	.881**	.131	-.007	-.009	.156	.087	-.318*
	.000	.392	.962	.951	.305	.613	.033
log (Raw GUS)	.867**	.042	-.148	.153	.132	.065	-.205
	.000	.784	.333	.316	.389	.706	.177
log (Extra GUS)	1.000	.083	-.506*	.235	.248	.005	-.307
		.698	.012	.269	.243	.982	.144
Temperature		1.000	-.351*	-.248	.196	.462**	-.894**
			.018	.101	.198	.005	.000
Conductivity			1.000	-.331*	-.373*	-.212	.398**
				.026	.012	.214	.007
pH				1.000	.484**	-.202	.125
					.001	.237	.415
DO (%)					1.000	.313	-.311*
						.063	.038
Water Level Change (%)						1.000	-.564**
							.000
Daily sunshine							1.000

Significant correlations are bolded.

*Significant at p<0.05 level, **Significant at p<0.01 level

5.3.2 River level comparison

Recorded parameters were used to compare the five rivers in Dublin area. For this purpose, collected data was split into baseline data (collected at the most downstream point for each river) and longitudinal river profile data.

5.3.2.1 Baseline

The highest average *E. coli* levels were found in the River Camac, followed by River Tolka, River Poddle, River Dodder and River Liffey respectively (Fig. 5-5). Enterococci levels were found to vary in the same way although slightly higher levels were found in River Poddle as opposed to River Tolka. GUS activities determined from the three sample fractions followed the same pattern as the *E. coli* levels, while the highest TSS levels were found in River Camac and River Tolka. In terms of nutrients levels, the highest phosphate concentration was found in River Poddle followed by River Tolka and River Camac, with the lowest levels found in River Dodder (Fig 5-6). The highest nitrate levels were found in River Camac and the lowest in River Liffey (Fig 5-6).

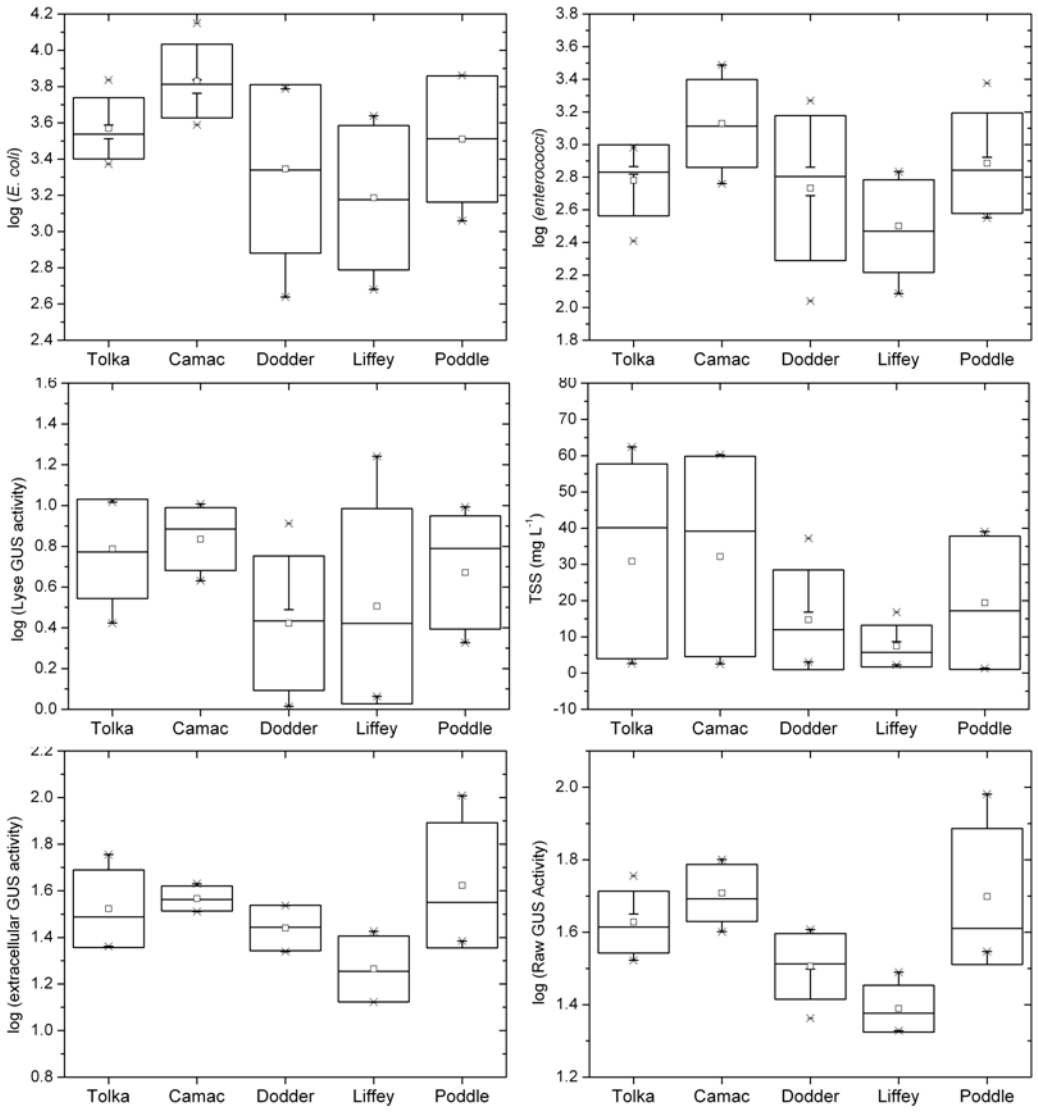

Figure 5-8 Box plots showing baseline variation of E. coli, enterococci, GUS activity (for different water sample fractions) and TSS levels, for the sampled rivers; Box plots represent the median (horizontal line in the box), STD (bottom and top box lines), mean (small square in the box), and the range (*); N=5.

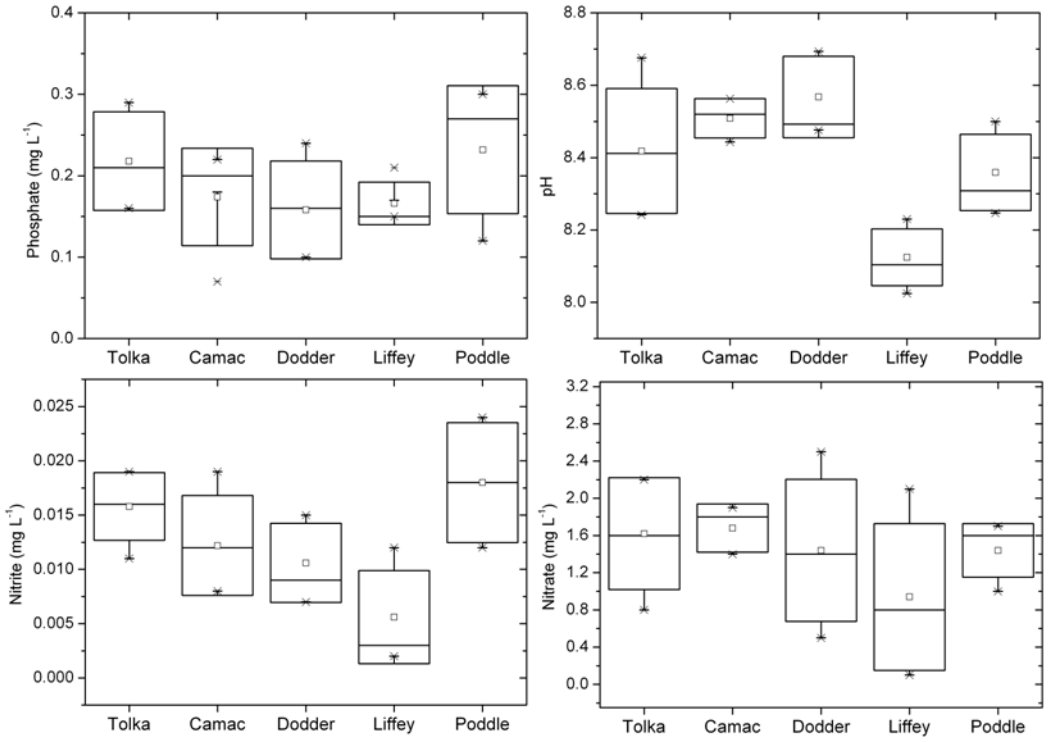

5-9 Box plots showing baseline variation of pH, phosphate, nitrate and nitrite levels for the sampled rivers; Box plots represent the median (horizontal line in the box), STD (bottom and top box lines), mean (small square in the box), and the range (*); N=5

5.3.2.2 Longitudinal Profiles

In general pollution levels followed an upward linear trend with increase contamination at the downstream sampling points (Fig. 5-9, Fig. 5-10). However a few exceptions to this exist. River Liffey was sampled both on its tidal (sampling points 1, 2 and 3) and non-tidal zones (sampling points 4, 5). Although the sampling was performed at low tide on ebb flow, there is still a high proportion of sea water mixed with the fresh water and a dilution effect on the tidal zone. This can be seen most easily from conductivity or salinity measurements (data not shown). Although relatively medium *E. coli* levels were recorded during the profile the GUS activities were found to be much higher than expected (Fig 5-7), especially for the sampling points in the tidal zone. This suggests a higher ratio of viable but not culturable (VBNC) to viable culturable (VC) bacteria might be present [169]. It is also possible samples collected at this points had a higher number of particle attached (associated) bacteria. Work published previously in our group found sediments in River Liffey to be highly contaminated with faecal indicator

bacteria (FIBs) [112]. Other exceptions to the upward trend were observed for River Camac. This river was sampled on a day with moderate rainfall (19th August 2015, Fig. 5-4). On the longitudinal profile, a pollution spot was identified at sampling point no 4. Sample collected from at this location had the highest levels of *E. coli*, Enterococci, nitrate, phosphate, nitrite and TSS recorded along the river and the lowest DO and pH values. GUS activities at this location were also very high by comparison and the highest GUS lyse activity (144.1 pmol min^{-1} $100mL^{-1}$) found in the study originates from this sample. As both the pH and DO levels dropped considerably at this location it is likely the pollution is caused by a non-point source, like an overflowing or damaged sewer. Furthermore because the water contamination was much lower upstream (sampling point 5), the source is located somewhere between this two sampling points. Another slight deviation from linearity was observed in the case of River Dodder at the sampling point 3 in terms of TSS levels. This was due to maintenance work on the channel for flood prevention and as such TSS levels were above normal.

Overall these upstream-downstream trends in the levels of contamination can be explained by the considerable urbanization and agriculture activities in the watershed and by the presence of various non-point pollution sources. In some rivers, such as Camac quality improvement can be observed from upstream to downstream, demonstrating that in some stretches the decay processes (mortality and settling) overtake the input of FIBs in the river.

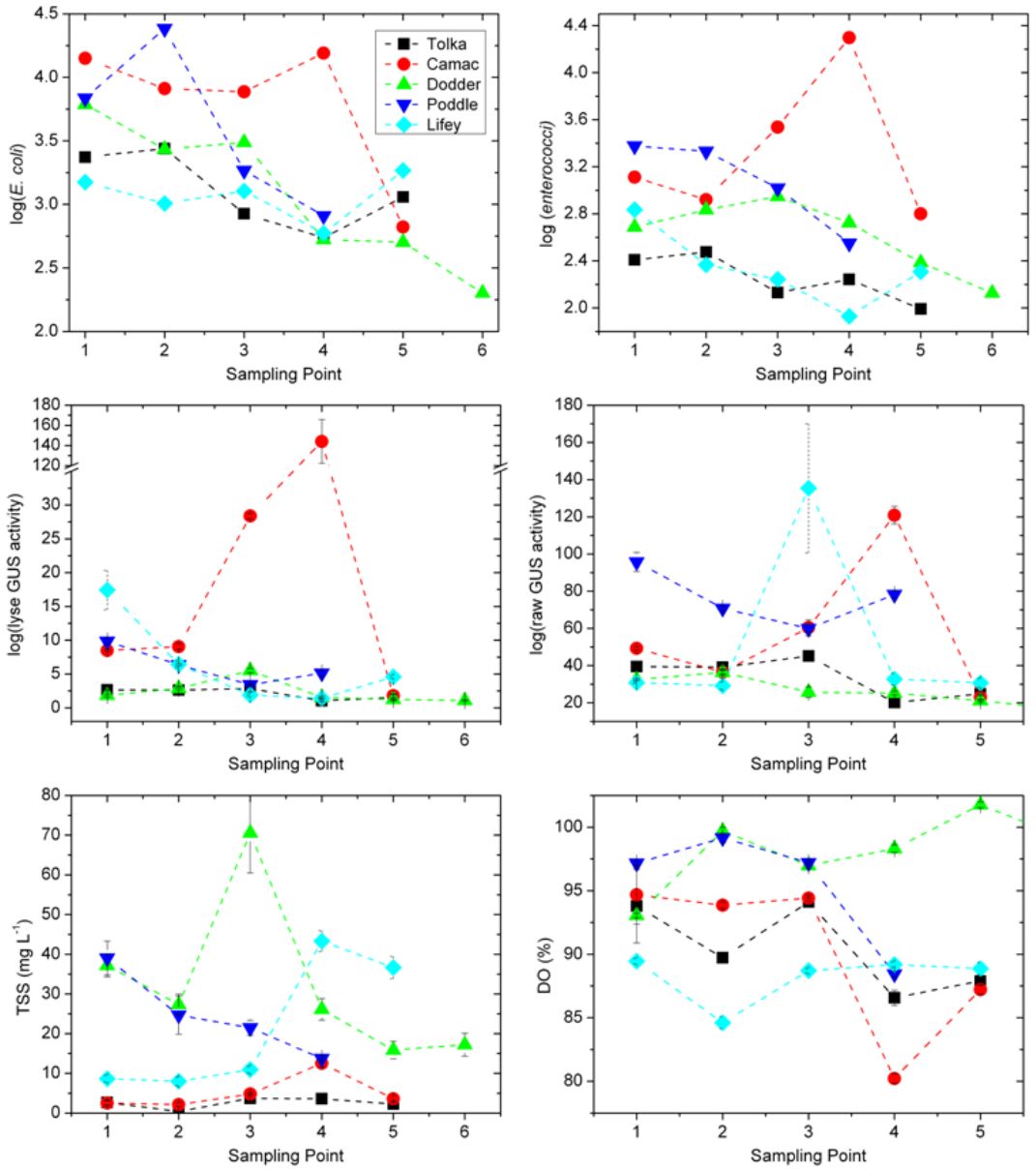

Figure 5-10 Longitudinal river profiles showing fluctuations in E. coli, enterococci, GUS activity (for different water sample fractions),TSS and DO% levels along the river. Sampling was carried out for each river from downstream (sampling point 1) to upstream (sampling point 1).

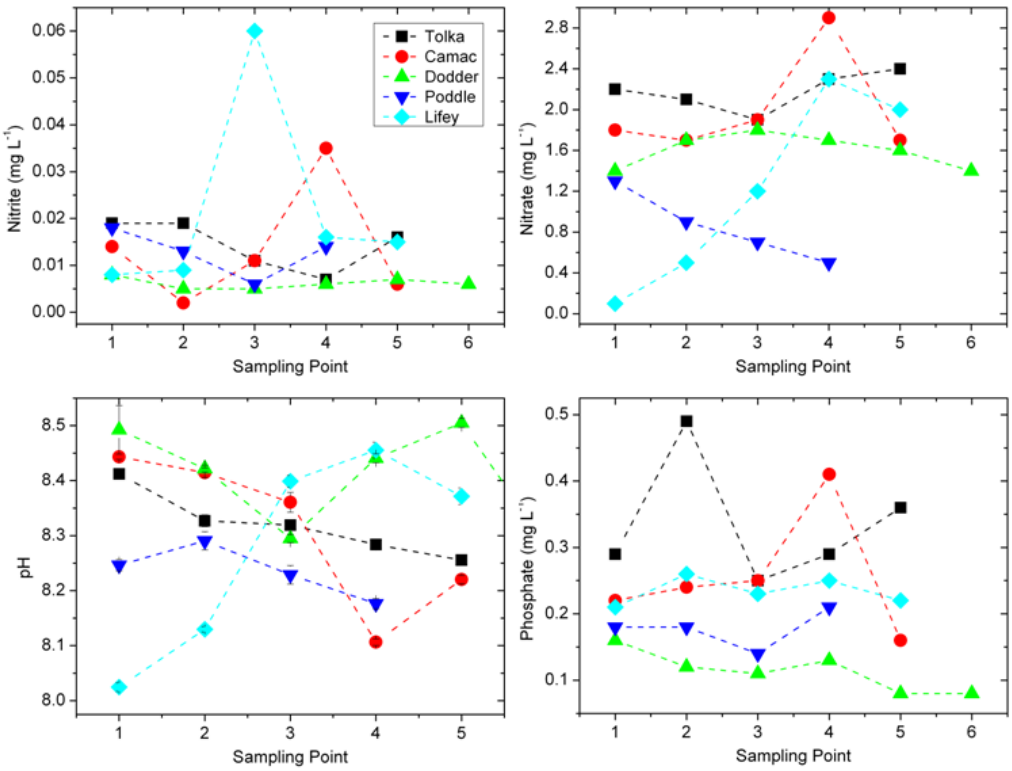

5-11 Longitudinal river profiles showing fluctuations in nitrate, nitrite and phosphate levels and pH along the river. Sampling was carried out for each river from downstream (sampling point 1) to upstream (sampling point 1)

5.3.3 Relationship between GUS and faecal indicators

The relanshionship between the GUS activities determined from the various water fractions are reported in Fig 5-13. The linear correlation between *E. coli* and lyse GUS activity in log units was significant (r^2=0.53, N=45, p<0.001). The highest r^2 value was obtained for the correlation between Enterococci and lyse GUS activities (r^2=0.66, N=45,p<0.001). This suggests GUS activity which is a marker enzyme for *E. coli* is more succesfull in predicting Enterococci levels. The reason for this might the difference in the survival rates between the two FIBs. Enterococci are known to be able to maintain culturability for longer time when expossed to environmental stress. As such it is possible the ratio between the VBNC to VC *E. coli* was relatively high and the culture-based method underestimated the real bacteria numbers. The ratio of

Escherichia coli to Enterococci found in those studies to reflect equal risk was between 2 and 3 (EU Directive 2002/0254).

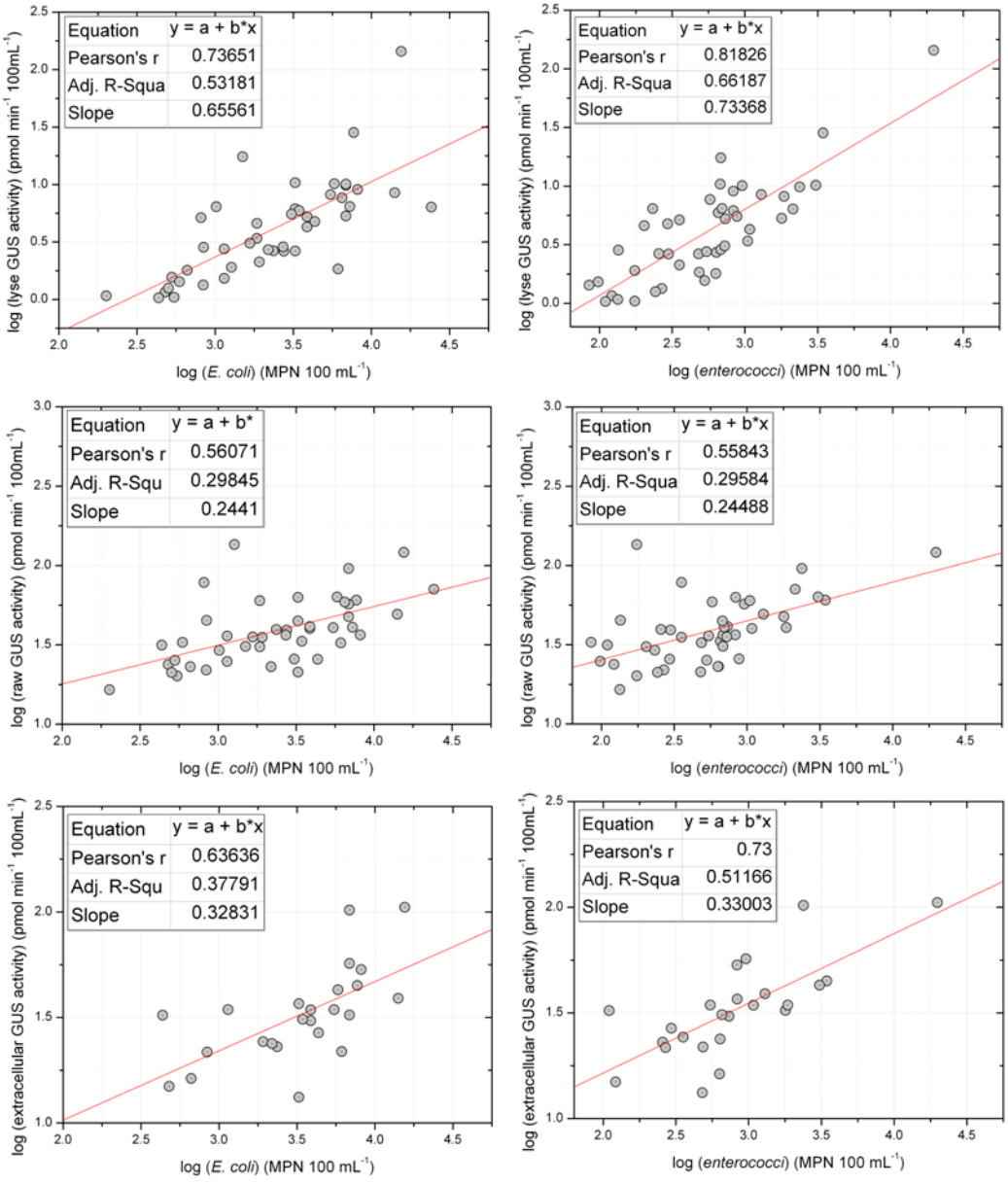

Figure 5-12 Log-log linear regressions between *E. coli* and Enterococci (X axis) counts and the GUS activity measured from various water fractions (Y axis) (detailed in Methods). Insets show the slope, adjusted R^2 and Pearson's correlation coefficient for each linear fit. Sample size N=45 (top and middle regressions) and N=24 (bottom regressions).

Table 5-4 Slope of the regression straight lines between log-transformed GUS activity and log-transformed concentrations of *E. coli* and faecal coliforms (FC) published in the literature. The culture based methods used for the enumeration of culturable *E. coli* and FC are also mentioned.

Organism Detected	**Methods**	**Type of water**	**Sample size (N)**	**R^2**	**Slope**	**References**
FC	MacConkey agar	Estuarine and wastewater	24	0.88	0.68	[171]
FC	Tergitol TCC agar	River	163	0.83	0.61	[176]
FC	Tergitol TCC agar	River	132	0.56	0.55	[172]
FC	m-FC-agar	Seawater	34	0.34	0.31	[174]
FC	m-FC-agar	River	98	0.90	0.83	[175]
FC	Tergitol TCC agar	River and wastewater	152	0.72	0.480	
E. coli	m-FC-agar	River	98	0.83	0.82	[170]
E. coli	Chromocult coliform agar	River	98	0.87	0.82	[175]
E. coli	MPN microplates	River and wastewater	41	0.92	0.73	[180]
E. coli	MPN microplates	Seawater	256	0.81	0.44	[169]
E. coli	MPN microplates	River and wastewater	166	0.76	0.52	[200]

The log-log relationships found in this study between *E. coli*, Enterococci and GUS activities are compared with previously reported relationships (Table 5-4). The slope reported for this study is found to be in the same range as the slopes reported in the literature for river and wastewater samples, although some better r^2 values were obtained in the literature. This can be due to a few reasons like sample size, variability in the source of the water samples analysed and also some variability in the analytical procedure used for sample processing. For example, in this study water samples were processed after vigorous mixing and as such the culture based method might have underestimated the real counts due to particle attached bacteria. Our samples contained a mix of five rivers with both freshwater and brackish sea water. This also introduced a level of variability in terms of VBNC to VC ratios. Furthermore samples were collected in both heavy rainfall and sunny conditions and this might account for variability in terms of pollution source. Overall the study presented here demonstrates the capabilities

of the developed *E. coli* protocol coupled with the ColiSense system to detect faecal pollution of fresh water.

5.4 Conclusions

A previously developed protocol for the recovery and detection of *E. coli* was couple with a miniaturised fluorometer (ColiSense) and the system was assessed for the rapid detection of FIBs in environmental samples. The system successfully detected *E. coli* in all of the 45 grab samples tested. A positive correlation was found between the log transformed GUS activities and the log transformed *E. coli* counts (r^2=0.53) and log transformed Enterococci counts (r^2=0.66) respectively. This suggests the protocol developed here can be applied successfully for the rapid assessment of faecal pollution in bathing areas.

6 CONCLUSIONS

In this thesis the requirement for rapid methods capable of assessing the risk of contamination with faecal pollution of bathing areas are identified. The European Directive for the management of bathing water quality brings a legal framework to these problems and increases the responsibility for monitoring and remediation of such sites [1]. Furthermore, the Directive also introduces the concept of active management by assessing the contamination vulnerability of the water body and by routine monitoring. of faecal indicators bacteria (FIB), *E. coli* and Enterococci. Standards methods for *E. coli* detection rely on cultivation of the target organism which requires long incubation periods (from 18h up to a few days). This time frame is too long and does not allow for immediate action to be taken, putting the users of the recreational area at risk. As a consequence this thesis investigates the use of alternative/surrogate faecal indicators for rapid assessment of faecal pollution in environmental waters. To pursue this aim the thesis has examined the use of turbidity (Chapter 2) and GUS (Chapter 3, 4, 5) as rapid faecal pollution indicators.

In Chapter 2, it is shown that commercially available sensors can be used for continuous monitoring of water quality as a decision support tool. Furthermore the findings of this study advance understanding of estuarine environments and demonstrate the advantages of high frequency monitoring. Continuous monitoring of parameters like DO, turbidity, salinity and temperature have proven to be a valuable tool, providing far greater insight into the complexity and temporal heterogeneity than possible with discrete sampling regimes. In Dublin Port, short-term turbidity events are largely related to vessel activity caused by re-suspension of sediments by vessel propulsion systems. The magnitude of such events is strongly related to water level and tidal state at vessel arrival times. Measurements of *Escherichia coli* and Enterococci contamination from discrete samples collected at key periods related to detected turbidity events were up to 9 times higher after vessel arrival than prior to disturbance. Benthic sediments in Dublin Port are reservoirs for *E. coli* and Enterococci, to the extent that re-suspension of these pollutants is undesirable. Daily *in-situ* turbidity patterns revealed time-dependent water quality “hot spots” during a 24 h period. As such if representative assessment of water quality is to be performed at such sites, sampling times, informed by continuous monitoring data, should take into account these daily variations. This work outlines the

potential of sensor technologies and continuous monitoring, to act as a decision support tool in both environmental and port management.

In Chapter 3, a continuous fluorometric method based on 6-CMUG as a fluorogenic substrate has been developed for measuring GUS activity. This has been achieved by comparing and studying two lesser known fluorogenic substrates (6-CMUG and 3-CUG) with the widely used 4-MUG for measuring GUS activity in a continuous set-up. Spectrophotometric characterization using UV Vis and steady state fluorescence spectroscopy of fluorophores and substrates revealed that 6-CMUG is the substrate of choice for continuous measurements. This was found to be mainly due to the lower pKa value (6.12 ± 0.3) of its fluorophore 6-CMU. As a consequence, at pH 6.8 where GUS acitivity reaches its maximum this fluorophore is almost fully dissociated into its A^- form. When emission spectra were collected using the excitation bands for the ionised forms of 4-MU, 6-CMU and 3-CU, the fluorescence intensity of 6-CMU was found to be roughly 9.5 times higher than that of 4-MU and 3.2 times higher than the fluorescence of 3-CU. Michaelis-Menten kinetic parameters of GUS catalysed hydrolysis of 4-MUG, 3-CUG and 6-CMUG were determined experimentally and compared and are reported for the first time in case of 6-CMUG (K_m = 0.11 mM, K_{cat} = 74 s^{-1}, K_{cat}/ K_m = 6.93 x 10^5 $s^{-1}M^{-1}$ at pH 6.8 and 20 °C). When compared with the highly used discontinuous method based on 4-MUG as a substrate it was found that the new method is more sensitive (almost 10 times) and more reproducible (%RSD=4.88). Furthermore, the developed method is less laborious, faster and more economical and should provide an improved alternative for GUS assays and GUS kinetic studies.

In Chapter 4, a protocol for the recovery and detection of faecal pollution indicator bacteria, E. coli, using β-D-Glucuronidase (GUS) activity was developed. The developed protocol involves two main steps: sample preparation and GUS activity measurement. In the sample preparation step syringe filters were used with a dual purpose, for the recovery and pre-concentration of *E. coli* from the water matrix and also as µL reactors for bacteria lysis and GUS extraction. Subsequently, GUS activity was measured using a continuous fluorometric method developed previously. The optimum GUS recovery conditions for the sample preparation step were found to be 100 µL PELB (supplemented with 1 mg mL^{-1} lysozyme and 20 mM DTT) at 37 °C for 30 min. The protocol was evaluated on environmental samples (fresh and seawater) against

an established GUS assay method (Coliplage®). GUS activities corresponding to samples containing as low as 26.18 MPN E. coli 100 mL^{-1} were detected for the seawater sample and as low as 110.2 MPN E. coli 100 mL^{-1} for the freshwater samples. By comparison with the Coliplage® method, this protocol offered an improvement in the measured GUS activities of 3.08 fold for freshwater samples and 4.13 fold for seawater samples. Furthermore, the protocol developed here, has a time-to-result of 75 min, and successfully addresses the requirement for tests capable of rapid assessment of microbiological water quality.

In Chapter 5, the developed protocol for the recovery and detection of *E. coli* was coupled with a miniaturised fluorometer (ColiSense) and the system was assessed for the rapid detection of FIBs in environmental samples. ColiSense is a tailor designed portable miniaturised fluorometer, with incubation capabilities developed in the group by Brendan Heery. The system successfully detected *E. coli* in all of the 45 grab samples tested. A positive correlation was found between the log transformed GUS activities and the log transformed *E. coli* counts (r^2=0.53) and log transformed Enterococci counts (r^2=0.66) respectively. This suggests the protocol developed here can be applied successfully for the rapid assessment of faecal pollution in bathing areas.

To conclude, a novel protocol for detecting *E. coli* in environmental samples has been developed and used in conjunction with ColiSense for *on-site* detection of *E. coli* in less than 45 min. The LOD of the system is below the threshold for ‘excellent quality’ as set by the EU and it can be successfully used as an early warning system for faecal pollution. Furthermore, the system can be easily implemented as a resource for real time active management of bathing areas and aid in ensuring the safety of users.

7 REFERENCES

[1] O. Savichtcheva, S. Okabe, Water Res., 40 (2006) 2463-2476.

[2] C.J. Hurst, R.L. Crawford, J. Garland, D.A. Lipson, A.L. Mills, L.D. Stetzenbach, Manual of environmental microbiology, ASM press, (2007).

[3] A. Rompré, P. Servais, J. Baudart, M. de-Roubin, P. Laurent, J. Microbiol. Methods, 49 (2002) 31-54.

[4] S. Seurinck, W. Verstraete, S.D. Siciliano, Appl. Environ. Microbiol., 69 (2003) 4942-4950.

[5] J.D. Berg, L. Fiksdal, Appl. Environ. Microbiol., 54 (1988) 2118-2122.

[6] D. Ivnitski, I. Abdel-Hamid, P. Atanasov, E. Wilkins, Biosensors and Bioelectronics, 14 (1999) 599-624.

[7] P.H. Gleick, Dirty-water: Estimated Deaths from Water-related Diseases 2000-2020, Pacific Institute for Studies in Development, Environment, and Security, (2002).

[8] D. Sartory, J. Watkins, J. Appl. Microbiol., 85 (1998) 225S-233S.

[9] T. Taguchi, H. Takeyama, T. Matsunaga, Biosensors and Bioelectronics, 20 (2005) 2276-2282.

[10] V.J. Cabelli, A.P. Dufour, L. McCabe, M. Levin, Journal (Water Pollution Control Federation) (1983) 1306-1314.

[11] A.P. Dufour, Health effects criteria for fresh recreational waters, (1984).

[12] W. Grabow, Water S. A., 22 (1996) 193-202.

[13] P. Tallon, B. Magajna, C. Lofranco, K.T. Leung, Water, Air, & Soil Pollution, 166 (2005) 139-166.

[14] R. Fujioka, C. Sian-Denton, M. Borja, J. Castro, K. Morphew, J. Appl. Microbiol., 85 (1998) 83S-89S.

[15] W. Ryan, P. Collier, L. Loredo, J. Pope, R. Sachdev, Biotechnol. Prog., 12 (2008) 596-601.

[16] M.T. Madigan, J.M. Martinko, J. Parker, Pearson Education (2003).

[17] J. Cohen, H.I. Shuval, Water, Air, & Soil Pollution, 2 (1973) 85-95.

[18] E.E. Geldreich, B.A. Kenner, Journal (Water Pollution Control Federation) (1969) 336-352.

[19] D. Mara, N.J. Horan, Handbook of water and wastewater microbiology, Academic press, (2003).

[20] C. Gleeson, N. Gray, The coliform index and waterborne disease: problems of microbial drinking water assessment, London, England: E & FN Spon (1997).

[21] K. Lemarchand, P. Lebaron, FEMS Microbiol. Lett., 218 (2003) 203-209.

[22] B. Dutka, A. Chau, J. Coburn, Water Res., 8 (1974) 1047-1055.

[23] K.O. Isobe, M. Tarao, M.P. Zakaria, N.H. Chiem, L.Y. Minh, H. Takada, Environ. Sci. Technol., 36 (2002) 4497-4507.

[24] K.O. Isobe, M. Tarao, N.H. Chiem, L.Y. Minh, H. Takada, Appl. Environ. Microbiol., 70 (2004) 814-821.

[25] R. Leeming, P. Nichols, Water Res., 30 (1996) 2997-3006.

[26] N. Hirulkar, D. Tambekar, African Journal of Biotechnology, 5 (2009).

[27] M.D. Sobsey, F.K. Pfaender, Evaluation of the H2S method for detection of fecal contamination of drinking water, (2003).

[28] G.W. Pettibone, K.N. Irvine, K.M. Monahan, Water Res., 30 (1996) 2517-2521.

[29] I.D. Bull, M.J. Lockheart, M.M. Elhmmali, D.J. Roberts, R.P. Evershed, Environ. Int., 27 (2002) 647-654.

[30] M.F. Fitzsimons, M.K. Abdul Rashid, J.P. Riley, G.A. Wolff, Mar. Pollut. Bull., 30 (1995) 306-312.

[31] T.T. Truong, P.J. Marriott, N.A. Porter, R. Leeming, Journal of Chromatography A, 1019 (2003) 197-210.

[32] D.S. Francy, R.A. Darner, C. County, Procedures for developing models to predict exceedances of recreational water-quality standards at coastal beaches, US Department of the Interior, US Geological Survey, (2006).

[33] A. Brady, R. Bushon, M. Plona, Cuyahoga Valley National Park, Ohio, 7 (2004).

[34] E. Frampton, L. Restaino, J. Appl. Microbiol., 74 (2008) 223-233.

[35] I. George, P. Crop, P. Servais, Water Res., 36 (2002) 2607-2617.

[36] E. de Boer, R.R. Beumer, Int. J. Food Microbiol., 50 (1999) 119-130.

[37] I.N. Rivera, E.K. Lipp, A. Gil, N. Choopun, A. Huq, R.R. Colwell, Environ. Microbiol., 5 (2003) 599-606.

[38] W.J. le Roux, D. Masoabi, C.M. de Wet, S.N. Venter, Water Sci. Technol., 50 (2004) 229-232.

[39] J.R. Crowther, ELISA: theory and practice, Springer, (1995).

[40] A.G. Gehring, D.M. Albin, P.L. Irwin, S.A. Reed, S. Tu, J. Microbiol. Methods, 67 (2006) 527-533.

[41] D. Ivnitski, I. Abdel-Hamid, P. Atanasov, E. Wilkins, Biosensors and Bioelectronics, 14 (1999) 599-624.

[42] J.M. Song, T. Vo-Dinh, Anal. Chim. Acta, 507 (2004) 115-121.

[43] Y. Liang, J. Song, J. Pharm. Biomed. Anal., 38 (2005) 100-106.

[44] I. Abdel-Hamid, D. Ivnitski, P. Atanasov, E. Wilkins, Anal. Chim. Acta, 399 (1999) 99-108.

[45] S. Levasseur, M. Husson, R. Leitz, F. Merlin, F. Laurent, F. Peladan, J. Drocourt, H. Leclerc, M. Van Hoegaerden, Appl. Environ. Microbiol., 58 (1992) 1524-1529.

[46] I. Hübner, I. Steinmetz, U. Obst, D. Giebel, D. Bitter-Suermann, Appl. Environ. Microbiol., 58 (1992) 3187-3191.

[47] P. Leonard, S. Hearty, J. Brennan, L. Dunne, J. Quinn, T. Chakraborty, R. O'Kennedy, Enzyme Microb. Technol., 32 (2003) 3-13.

[48] P. Vanouse, http://www.paulvanouse.com/dwpcr.html, (2013).

[49] P. Feng, R. Lum, G.W. Chang, Appl. Environ. Microbiol., 57 (1991) 320-323.

[50] E. Fricker, C. Fricker, Lett. Appl. Microbiol., 19 (2008) 44-46.

[51] S.R. Monday, T.S. Whittam, P.C. Feng, J. Infect. Dis., 184 (2001) 918-921.

[52] A.K. Bej, S.C. McCarty, R. Atlas, Appl. Environ. Microbiol., 57 (1991) 2429-2432.

[53] A.K. Bej, R.J. Steffan, J. DiCesare, L. Haff, R.M. Atlas, Appl. Environ. Microbiol., 56 (1990) 307-314.

[54] L.J. Gilissen, P.L. Metz, W.J. Stiekema, J. Nap, Transgenic Res., 7 (1998) 157-163.

[55] T. Garcia-Armisen, P. Lebaron, P. Servais, Lett. Appl. Microbiol., 40 (2005) 278-282.

[56] M. Farré, L. Kantiani, S. Pérez, D. Barceló, TrAC Trends in Analytical Chemistry, 28 (2009) 170-185.

[57] www.nnin.org, (2013)

[58] R. Jamieson, R. Gordon, D. Joy, H. Lee, Agric. Water Manage., 70 (2004) 1-17.

[59] S.M. Dorner, W.B. Anderson, R.M. Slawson, N. Kouwen, P.M. Huck, Environ. Sci. Technol., 40 (2006) 4746-4753.

[60] G. Jiang, M.J. Noonan, G.D. Buchan, N. Smith, J. Contam. Hydrol., 93 (2007) 2-20.

[61] G.A. Olyphant, Water Res., 39 (2005) 4953-4960.

[62] M.B. Nevers, R.L. Whitman, Water Res., 39 (2005) 5250-5260.

[63] T.M. Zimmerman, Modeling to predict escherichia coli at presque isle beach 2, city of erie, erie county, pennsylvania (2008) .

[64] D.S. Francy, E.A. Stelzer, J.W. Duris, A.M. Brady, J.H. Harrison, H.E. Johnson, M.W. Ware, Appl. Environ. Microbiol., 79 (2013) 1676-1688.

[65] T. Shibata, H.M. Solo-Gabriele, C.D. Sinigalliano, M.L. Gidley, L.R. Plano, J.M. Fleisher, J.D. Wang, S.M. Elmir, G. He, M.E. Wright, Environ. Sci. Technol., 44 (2010) 8175.

[66] L.L. He, Z. He, Water Res., 42 (2008) 2563-2573.

[67] D.S. Francy, Aquat. Ecosyst. Health Manage., 12 (2009) 177-182.

[68] W.F. Directive, EC of the European Parliament and of the Council of, 23 (2000) 1.

[69] EU, Official J.European Union, 64 (2006) 37-51.

[70] B. Henrissat, Biochem. J., 280 (1991) 309.

[71] M.R. Islam, S. Tomatsu, G.N. Shah, J.H. Grubb, S. Jain, W.S. Sly, J. Biol. Chem., 274 (1999) 23451.

[72] A.W. Wong, S. He, J.H. Grubb, W.S. Sly, S.G. Withers, J. Biol. Chem., 273 (1998) 34057-34062.

[73] I. Matsumura, A.D. Ellington, J. Mol. Biol., 305 (2001) 331-339.

[74] P. Feng, P.A. Hartman, Appl. Environ. Microbiol., 43 (1982) 1320-1329.

[75] S.C. Edberg, C.M. Kontnick, J. Clin. Microbiol., 24 (1986) 368-371.

[76] C.W. Kaspar, P.A. Hartman, A.K. Benson, Appl. Environ. Microbiol., 53 (1987) 1073-1077.

[77] J.R. Lakowicz, Principles of fluorescence spectroscopy, Springer, (2006).

[78] M. Abramowitz, http://micro.magnet.fsu.edu/primer/java/jablonski/lightandcolor/, (1998).

[79] C. Parker, W. Rees, Analyst, 87 (1962) 83-111.

[80] L.D. Lavis, R.T. Raines, ACS chemical biology, 3 (2008) 142-155.

[81] L. Fiksdal, I. Tryland, Curr. Opin. Biotechnol., 19 (2008) 289-294.

[82] J. Boissonnas, N. Connolly, F. Mantoura, L. d'Ozouville, J. Marks, J.F. Minster, M. Ruivo, S. Vallerga, ESF Marine Board Position Paper, 5 (2002).

[83] DPW, Dublin Port Company Website, http://www.dublinport.ie/., (2012), Accessed 22/06/2012.

[84] T. Soomere, Environmental Fluid Mechanics, 5 (2005) 293-323.

[85] K.S. Johnson, J.A. Needoba, S.C. Riser, W.J. Showers, Chem. Rev., 107 (2007) 623-640.

[86] H.W. Jannasch, L.J. Coletti, K.S. Johnson, S.E. Fitzwater, J.A. Needoba, J.N. Plant, Limnol.Oceanogr.Methods, 6 (2008) 263-276.

[87] M. Elliott, D.S. McLusky, Estuar. Coast. Shelf Sci., 55 (2002) 815-827.

[88] R.L. Ohrel, K.M. Register, Volunteer Estuary Monitoring: A Methods Manual. Ocean Conservancy, (2006).

[89] F. Regan, A. Lawlor, B.O. Flynn, J. Torres, R. Martinez-Catala, C. O'Mathuna, J. Wallace, (2009) 819-825.

[90] J.K. Hart, K. Martinez, Earth-Sci. Rev., 78 (2006) 177-191.

[91] A. Lawlor, J. Torres, B. O'Flynn, J. Wallace, F. Regan, Sens Rev, 32 (2012) 29-38.

[92] H.B. Glasgow, J.M. Burkholder, R.E. Reed, A.J. Lewitus, J.E. Kleinman, J. Exp. Mar. Biol. Ecol., 300 (2004) 409-448.

[93] T.A. Mastran, A.M. Dietrich, D.L. Gallagher, T.J. Grizzard, Water Res., 28 (1994) 2353-2366.

[94] A.R. Knowlton, F. Korsmeyer, J. Kerwin, H. Wu, B. Hynes, Final report to NOAA Fisheries for Contract (1995) 81.

[95] D.H. Schoellhamer, Estuar. Coast. Shelf Sci., 43 (1996) 533-548.

[96] V. Lesage, C. Barrette, M. Kingsley, B. Sjare, Mar. Mamm. Sci., 15 (1999) 65-84.

[97] Y.A. Yousef, Assessing effects on water quality by boating activity, (1974).

[98] P. Garrad, R. Hey, Journal of Hydrology, 95 (1987) 289-297.

[99] E. Hayes, W. Landis, Hum. Ecol. Risk Assess., 10 (2004) 299-325.

[100] C.P. Newcombe, D.D. MacDonald, N. Am. J. Fish. Manage., 11 (1991) 72-82.

[101] W. Henley, M. Patterson, R. Neves, A.D. Lemly, Rev. Fish. Sci., 8 (2000) 125-139.

[102] H. Hong, L. Xu, L. Zhang, J. Chen, Y. Wong, T. Wan, Mar. Pollut. Bull., 31 (1995) 229-236.

[103] L.W. Perelo, J. Hazard. Mater., 177 (2010) 81-89.

[104] G. Bryan, W. Langston, Environmental Pollution, 76 (1992) 89-131.

[105] Y.A. Yousef, W.M. McLellon, H.H. Zebuth, Water Res., 14 (1980) 841-852.

[106] Y. Pachepsky, D. Shelton, Crit. Rev. Environ. Sci. Technol., 41 (2011) 1067-1110.

[107] P. Roslev, S. Bastholm, N. Iversen, Water, Air, & Soil Pollution, 194 (2008) 13-21.

[108] S. Roth, J.G. Wilson, J. Exp. Mar. Biol. Ecol., 222 (1998) 195-217.

[109] J. Wilson, Estuar. Coast. Shelf Sci., 55 (2002) 953-967.

[110] DCC, Dublin waste to energy project environmental impact statement. Dublin City Council, Chapter 12, (2006), 48.

[111] Z. Bedri, M. Bruen, A. Dowley, B. Masterson, Mar. Pollut. Bull. (2013).

[112] C. Briciu-Burghina, T. Sullivan, J. Chapman, F. Regan, Environ. Monit. Assess., 186 (2014) 5561-5580.

[113] V. Choiseul, J. Wilson, E. Nixon, (1998) 75-86.

[114] R.J. Wagner, Geological Survey (US), Guidelines and standard procedures for continuous water-quality monitors: Site selection, field operation, calibration, record computation, and reporting, US Dept. of the Interior, US Geological Survey, (2000).

[115] M. Byappanahalli, M. Fowler, D. Shively, R. Whitman, Appl. Environ. Microbiol., 69 (2003) 4549-4555.

[116] APHA-AWWA-WEF, Standard methods for the examination of water and wastewater, 18th Ed edition, American Public Health Association, America Water Works Association and Water Environment Federation, Washington DC, 1992.

[117] J.S. Horsburgh, A. Spackman Jones, D.K. Stevens, D.G. Tarboton, N.O. Mesner, Environmental Modelling & Software, 25 (2010) 1031-1044.

[118] A. Field, Discovering Statistics Using SPSS Second Edition SAGE Publication, London, (2005).

[119] J.F. Healey, Statistics: A tool for social research, Wadsworth Pub Co, (2011).

[120] D. Preston, P. Protopapas, C. Brodley, Arxiv preprint arXiv:0901.3329, (2009).

[121] T. Lindholm, M. Svartström, L. Spoof, J. Meriluoto, Hydrobiologia, 444 (2001) 217-225.

[122] R. Verney, J. Deloffre, J. Brun-Cottan, R. Lafite, Cont. Shelf Res., 27 (2007) 594-612.

[123] D.H. Schoellhamer, Resuspension of bottom sediments, sedimentation, and tributary storm discharge at Bayboro Harbor and the Port of St. Petersburg, Florida, US Geological Survey, (1993).

[124] Z. Bedri, M. Bruen, A. Dowley, B. Masterson, Environmental Modeling and Assessment, 16 (2011) 369-384.

[125] B. Steets, P. Holden, Water Res., 37 (2003) 589-608.

[126] G.W. Pettibone, K.N. Irvine, K.M. Monahan, Water Res., 30 (1996) 2517-2521.

[127] B.D. Wallace, H. Wang, K.T. Lane, J.E. Scott, J. Orans, J.S. Koo, M. Venkatesh, C. Jobin, L.A. Yeh, S. Mani, M.R. Redinbo, Science, 330 (2010) 831-835.

[128] L.J. Gilissen, P.L. Metz, W.J. Stiekema, J. Nap, Transgenic Res., 7 (1998) 157-163.

[129] R.A. Jefferson, Plant Mol. Biol. Rep., 5 (1987) 387-405.

[130] R.A. Jefferson, S.M. Burgess, D. Hirsh, Proc. Natl. Acad. Sci. U. S. A., 83 (1986) 8447-8451.

[131] A. Rompré, P. Servais, J. Baudart, M. de-Roubin, P. Laurent, J. Microbiol. Methods, 49 (2002) 31-54.

[132] M. Manafi, Int. J. Food Microbiol., 60 (2000) 205-218.

[133] S. Aich, BioTechniques, 30 (2001) 846-851.

[134] S. Fior, A. Vianelli, P.D. Gerola, Plant science, 176 (2009) 130-135.

[135] J.R. Geary, G.M. Nijak, S.L. Larson, J.W. Talley, Enzyme Microb. Technol., 49 (2011) 6-10.

[136] K. Chilvers, J. Perry, A. James, R. Reed, J. Appl. Microbiol., 91 (2002) 1118-1130.

[137] J.D. Perry, A. James, K. Morris, M. Oliver, K. Chilvers, R. Reed, F. Gould, J. Appl. Microbiol., 101 (2006) 977-985.

[138] C. Briciu-Burghina, B. Heery, F. Regan, Analyst, 140 (2015) 5953-5964.

[139] K.K. Sadhu, S. Mizukami, A. Yoshimura, K. Kikuchi, Organic & biomolecular chemistry, 11 (2013) 563-568.

[140] T. Moriya, Bull. Chem. Soc. Jpn., 56 (1983) 6-14.

[141] D. Jacquemin, E.A. Perpète, G. Scalmani, M.J. Frisch, X. Assfeld, I. Ciofini, C. Adamo, J. Chem. Phys., 125 (2006) 164324.

[142] J.P. Cerón-Carrasco, M. Fanuel, A. Charaf-Eddin, D. Jacquemin, Chemical Physics Letters, 556 (2013) 122-126.

[143] J. Seixas de Melo, P. Fernandes, J. Mol. Struct., 565 (2001) 69-78.

[144] B. Cohen, D. Huppert, The Journal of Physical Chemistry A, 105 (2001) 7157-7164.

[145] T. Moriya, Bull. Chem. Soc. Jpn., 61 (1988) 1873-1886.

[146] S.G. Schulman, L.S. Rosenberg, J. Phys. Chem., 83 (1979) 447-451.

[147] W. Sun, K.R. Gee, R.P. Haugland, Bioorg. Med. Chem. Lett., 8 (1998) 3107-3110.

[148] J. Chalom, C. Griffoul, M. Tod, S. Reveilleau, Hydrosoluble coumarin derivatives, their preparation and their use as an enzyme substrate or for the preparation of such substrates, (1994).

[149] I. Georgieva, N. Trendafilova, A. Aquino, H. Lischka, The Journal of Physical Chemistry A, 109 (2005) 11860-11869.

[150] D.W. Fink, W.R. Koehler, Anal. Chem., 42 (1970) 990-993.

[151] M. Kubista, R. Sjöback, S. Eriksson, B. Albinsson, Analyst, 119 (1994) 417-419.

[152] M.O. Palmier, S.R. Van Doren, Anal. Biochem., 371 (2007) 43-51.

[153] Q. Gu, J.E. Kenny, Anal. Chem., 81 (2008) 420-426.

[154] E.D. Matayoshi, G.T. Wang, G.A. Krafft, J. Erickson, Science (New York, NY), 247 (1990) 954.

[155] A. Fersht, Proceedings of the Royal Society of London.Series B.Biological Sciences, 187 (1974) 397-407.

[156] S. Jain, W.B. Drendel, Z. Chen, F.S. Mathews, W.S. Sly, J.H. Grubb, Nature Structural & Molecular Biology, 3 (1996) 375-381.

[157] J.R. Geary, G.M. Nijak Jr, S.L. Larson, J.W. Talley, Enzyme Microb. Technol., 49 (2011) 6-10.

[158] J. Markwell, Biochemistry and Molecular Biology Education, 37 (2009) 317-318.

[159] A. Cornish-Bowden, Fundamentals of enzyme kinetics, John Wiley & Sons, (2013).

[160] I. George, M. Petit, P. Servais, J. Appl. Microbiol., 88 (2000) 404-413.

[161] A.S. Xiong, R.H. Peng, Z.M. Cheng, Y. Li, J.G. Liu, J. Zhuang, F. Gao, F. Xu, Y.S. Qiao, Z. Zhang, J.M. Chen, Q.H. Yao, Protein Eng. Des. Sel., 20 (2007) 319-325.

[162] H. Flores, A.D. Ellington, J. Mol. Biol., 315 (2002) 325-337.

[163] X. Wang, O.S. Wolfbeis, R.J. Meier, Chem. Soc. Rev., 42 (2013) 7834-7869.

[164] D.H. Kim, Y.H. Jin, E.A. Jung, M.J. Han, K. Kobashi, Biol. Pharm. Bull., 18 (1995) 1184-1188.

[165] D.R. Witcher, E.E. Hood, D. Peterson, M. Bailey, D. Bond, A. Kusnadi, R. Evangelista, Z. Nikolov, C. Wooge, R. Mehigh, Mol. Breed., 4 (1998) 301-312.

[166] S. Aich, L.T. Delbaere, R. Chen, Protein Expr. Purif., 22 (2001) 75-81.

[167] J.R. Geary, G.M. Nijak, S.L. Larson, J.W. Talley, Enzyme Microb. Technol., 49 (2011) 6-10.

[168] R. Noble, R. Weisberg, J Water Health, 3 (2005) 381-392.

[169] P. Lebaron, A. Henry, A. Lepeuple, G. Pena, P. Servais, Mar. Pollut. Bull., 50 (2005) 652-659.

[170] A.H. Farnleitner, L. Hocke, C. Beiwl, G. Kavka, R.L. Mach, Water Res., 36 (2002) 975-981.

[171] L. Fiksdal, M. Pommepuy, M. Caprais, I. Midttun, Appl. Environ. Microbiol., 60 (1994) 1581-1584.

[172] I. George, A. Anzil, P. Servais, Water Res., 38 (2004) 611-618.

[173] A. Morikawa, I. Hirashiki, S. Furukawa, Water Sci. Technol., 53 (2006) 523-532.

[174] G. Caruso, E. Crisafi, M. Mancuso, J. Appl. Microbiol., 93 (2002) 548-556.

[175] A. Farnleitner, L. Hocke, C. Beiwl, G. Kavka, T. Zechmeister, A. Kirschner, R. Mach, Lett. Appl. Microbiol., 33 (2001) 246-250.

[176] I. George, M. Petit, P. Servais, J. Appl. Microbiol., 88 (2001) 404-413.

[177] I. George, P. Crop, P. Servais, Can. J. Microbiol., 47 (2001) 670-675.

[178] M. Nikaeen, A. Pejhan, M. Jalali, Iranian Journal of Environmental Health Science & Engineering, 6 (2009).

[179] D. Wildeboer, L. Amirat, R.G. Price, R.A. Abuknesha, Water Res., 44 (2010) 2621-2628.

[180] T. Garcia-Armisen, P. Lebaron, P. Servais, Lett. Appl. Microbiol., 40 (2005) 278-282.

[181] M. Pommepuy, M. Butin, A. Derrien, M. Gourmelon, R. Colwell, M. Cormier, Appl. Environ. Microbiol., 62 (1996) 4621-4626.

[182] Y. Liu, A. Gilchrist, J. Zhang, X. Li, Appl. Environ. Microbiol., 74 (2008) 1502-1507.

[183] D. Grimes, R. Colwell, FEMS Microbiol. Lett., 34 (1986) 161-165.

[184] M. Martins, I. Rivera, D. Clark, M. Stewart, R. Wolfe, B. Olson, Appl. Environ. Microbiol., 59 (1993) 2271-2276.

[185] G.W. Chang, J. Brill, R. Lum, Appl. Environ. Microbiol., 55 (1989) 335-339.

[186] C. Davies, S. Apte, Lett. Appl. Microbiol., 30 (2000) 99-104.

[187] V. Wutor, C. Togo, B. Pletschke, Chemosphere, 68 (2007) 622-627.

[188] C.A. Togo, V.C. Wutor, B.I. Pletschke, African Journal of Biotechnology, 5 (2010).

[189] A. Villarino, M. Rager, P.A. Grimont, O.M. Bouvet, European Journal of Biochemistry, 270 (2003) 2689-2695.

[190] A. Villarino, A.L. Toribio, B.M. Brena, P. Grimont, O.M. Bouvet, Biotechnol. Lett., 25 (2003) 1329-1334.

[191] T. Fujisawa, K. Aikawa, T. Takahashi, S. Yamai, Lett. Appl. Microbiol., 31 (2000) 255-258.

[192] A. Henry, G. Scherpereel, R. Brown, J. Baudart, P. Servais, N.C.B. Tabassi, (2012) .

[193] I.C. Anderson, M. Rhodes, H. Kator, Appl. Environ. Microbiol., 38 (1979) 1147-1152.

[194] J.D. Oliver, J. Microbiol., 43 (2005) 93-100.

[195] J.M. Pisciotta, D.F. Rath, P.A. Stanek, D.M. Flanery, V.J. Harwood, Appl. Environ. Microbiol., 68 (2002) 539-544.

[196] J. Baudart, P. Servais, H. De Paoli, A. Henry, P. Lebaron, J. Appl. Microbiol., 107 (2009) 2054-2062.

[197] C.M. Davies, S.C. Apte, S.M. Peterson, J.L. Stauber, Appl. Environ. Microbiol., 60 (1994) 3959-3964.

[198] B. Heery, C. Briciu-Burghina, D. Zhang, G. Duffy, D. Brabazon, N. O'Connor, F. Regan, Talanta, 148 (2016) 75-83.

[199] A. Center, V. Warrenton, Report Of The Experts Scientific Workshop On Critical Research Needs For The Development Of New Or Revised Recreational Water Quality Criteria, (2007).

[200] P. Servais, T. Garcia-Armisen, A.S. Lepeuple, P. Lebaron, Annals of microbiology, 55 (2005) 151-156.

8 APPENDICES

8.1 List of peer reviewed publications

8.1.1 Journal articles

- Heery, B., Briciu-Burghina, C., Zhang, D., Duffy, G., Brabazon, D., O'Connor, N. & Regan, F. 2016, "ColiSense, today's sample today: A rapid *on-site* detection of β-glucuronidase activity in surface water as a surrogate for *E. coli*", *Talanta*, vol. 148, pp. 75-83.
- Briciu-Burghina, C., Heery, B. & Regan, F. 2015, "Continuous fluorometric method for measuring β-glucuronidase activity: comparative analysis of three fluorogenic substrates", *Analyst*, vol. 140, no. 17, pp. 5953-5964.
- Briciu-Burghina, C., Sullivan, T., Chapman, J. & Regan, F. 2014, "Continuous high-frequency monitoring of estuarine water quality as a decision support tool: a Dublin Port case study", *Environmental monitoring and assessment*, vol. 186, no. 9, pp. 5561-5580.
- Zhang, D., Sullivan, T., Briciu-Burghina, C., Murphy, K., McGuinness, K., O'Connor, N.E., Smeaton, A.F. & Regan, F. 2014, "Detection and classification of anomalous events in water quality datasets within a smart city-smart bay project", *International Journal on Advances in Intelligent Systems*, vol. 7, no. 1&2, pp. 167-178.

8.1.2 Conference Proceedings

- Regan, F., Sullivan, T., Zhang, D., Briciu-Burghina, C., O'Connor, E., Murphy, K., Cooney, H., O'Connor, N.E. & Smeaton, A.F. 2013, "A smart city-smart bay project-establishing an integrated water monitoring system for decision support in Dublin Bay", *SENSORCOMM 2013, The Seventh International Conference on Sensor Technologies and Applications*, 25-31 August 2013, pp. 75-82.
- Sullivan, T., Zhang, J., O'Connor, E., Briciu-Burghina, C., Heery, B., Gualano, L., Smeaton, A.F., O'Connor, N.E. & Regan, F. 2013, "Improving data driven decision making through integration of environmental sensing technologies", *Ocean 13*, 10-13 June 2013.

8.2 Conference contributions

- 6 - 8 June 2011 – FIPS 2011 (Faecal Indicators Problems or Solutions?), Edinburgh Conference Centre, Scotland, UK. "Towards the development and design of in-situ faecal matter sensing platforms for aquatic environments." - Poster presentation.
- 19th November 2011- AAMG 2011 Monitoring the Aquatic Environment using Sensor Technologies, Library, The Royal Society of Chemistry, London, UK. "Does continuous monitoring have a place in port management?" - Oral presentation.
- 7-9 March 2012- ENVIRON 2012, University College Dublin (UCD), Dublin, Ireland. "High frequency turbidity data as a decision support tool to aid effective monitoring programs in challenging environments" - Oral presentation.
- 22-27 April 2012: EGU 2012 (European Geosciences Union), Congress Centre, Vienna, Austria. "The role of continuous monitoring as a decision support tool"- Poster presentation.
- 20-25 August 2012: SESEH 2012 (Sino-European Symposium on Environment and Health), National University of Ireland (NUI), Galway, Ireland. "Continuous real-time monitoring of estuarine environments in Dublin" - Poster presentation.
- 14-16 May 2013: ATWARM 2013 (Water-The Greatest Global Challenge), Dublin City University (DCU), Dublin, Ireland. "Faecal indicator sensing-toward a faster method for marine and freshwater" – Oral Presentation
- 8-10 April 2015: ENVIRON 2015, Intitute of Technology Sligo (IT Sligo), Ireland. "A novel analytical protocol for detecting *E. coli* in environmental water samples using β-glucuronidase" – Oral Presentation